01357-13-T

Observations and Analyses of Cavitating Flow in Venturi Systems

DAVID MARTIN ERICSON, Jr.

Approved by
FREDERICK G. HAMMITT

July 1969

Financial Support Provided by:

National Science Foundation
Grant No. GK-1889

Department of Mechanical Engineering
Cavitation and Multiphase Flow Laboratory

OBSERVATIONS AND ANALYSES OF CAVITATING FLOW IN VENTURI SYSTEMS

David Martin Ericson, Jr.

A dissertation submitted in partial fulfillment
of the requirements for the degree of
Doctor of Philosophy in the
University of Michigan
1969

Doctoral Committee:
Professor Federick G. Hammitt, Chairman
Professor William Kerr
Professor George L. West
Assistant Professor Robert E. Barry

ABSTRACT

OBSERVATIONS AND ANALYSES OF CAVITATING FLOW IN VENTURI SYSTEMS

by

David Martin Ericson, Jr.

Chairman: Frederick G. Hammitt

The objective of this study was to determine the cavitation number for incipient cavitation in a set of geometrically similar venturis and then to correlate this cavitation number with the measurable properties of the system through "conventional" fluid flow parameters. Using water and mercury as the working fluids cavitation was observed in plastic and stainless steel venturis with throat diameters 1/8 to 3/4 inch, a throat length to diameter ratio of 4.6, and 6° included angle inlet and diffuser sections. Complete wall static pressure profiles were obtained and the cavitation number calculated from the relation $\sigma_c = (p_{min} - p_v)/\frac{1}{2}\rho V^2$. It was postulated that Reynolds number, Weber number, a thermodynamic parameter, and a gas content parameter (i.e., inertial, surface tension, and thermodynamics effects plus the availability of cavitation nuclei) would be the controlling parameters.

The data was treated using a linear regression analysis which permits a wide latitude in the form of the independent variable. Within the present data it was impossible to generate a predicting equation based simply on measurement of the physical parameters of the system. Nevertheless, the work shows that water and mercury cavitation are heavily influenced by the permanent gas present and that both Reynolds number and Weber number effects must be included. Thermodynamic effects were much less important over the temperature ranges available to the study. Further, it is deduced from the present work that local flow disturbances triggered

by surface imperfections have a strong impact upon the cavitation characteristics of the venturis. Presumably this will also hold true for other hydraulic systems. Although a complete predicting equation could not be generated, it was shown that for water, the results from a reference system could be scaled to another system. That is:

$$\frac{\sigma}{\sigma_{c_{ref}}} = \frac{(Vol\,\%\,Gas)}{(Vol\,\%\,Gas)_{ref}} \cdot \frac{D}{D_{ref}} \cdot \left(\frac{V_{ref}}{V}\right)^{n} \cdot \left(\frac{B}{B_{ref}}\right)^{1/4}$$

where n = 2 and B is a thermodynamic parameter.

Further, it was shown that gas content plays such a dominant role that the cavitation index may be expressed as:

$$\sigma_c = \sigma_{gas} + \sigma_{no\ gas}$$

Also, under the assumption that the partial pressure of gas within the permanent bubbles (cavitation nuclei) is proportional to the total gas content, one may say:

$$\sigma_c \cong \frac{k\alpha}{\frac{1}{2}\rho V^2} + f(D, V, B)$$

Finally, based upon the present results it is concluded that considerable study remains in the area of bubble growth and collapse in turbulent flowing systems. In particular, detailed knowledge of the nature and size distribution of potential cavity nuclei should provide needed insight into the inception process.

ACKNOWLEDGEMENTS

The author acknowledges the financial support of the National Aeronautics and Space Administration under Grant NsG-39-60, and the National Science Foundation under Grant GK-1889, that provided the bulk of the equipment for this work. The author is also deeply indebted to the United States Air Force for the opportunity to pursue this program under the sponsorship of the Air Force Institute of Technology.

The guidance, counsel and patience of Professor F. G. Hammitt during the term of the investigation is gratefully appreciated. His questions and comments frequently enabled the author to retrieve data and understanding from apparent chaos.

The author would be remiss if he did not also acknowledge the assistance and suggestions of numerous fellow candidates and research assistants who worked on the grant. Special thanks are due Dr. M. John Robinson for his assistance on equipment design and fabrication, Dr. James F. Lafferty for his suggestions on data interpretation, and Miss Marie T. Smith of the Air Force Weapons Laboratory for her aid in adapting the regression analysis program to the CDC-6600 computer.

Finally, thanks are due my wonderful family; to my wife, Ruth, for her continuing patience and encouragement during the experimentation and analysis, and to my daughters, Lisa, Kristina, and Edith for giving up family times while the dissertation was in final preparation.

TABLE OF CONTENTS

LIST OF TABLES

LIST OF FIGURES

Figure Page

Figure Page

Figure Page

NOMENCLATURE

C_p	Pressure coefficient
D	Diameter
L	Length
V	Velocity
V_t	Velocity in venturi throat
a_o	Pure material sonic velocity
c_p	Heat capacity
f_v	Fraction of liquid converted to vapor
g	Gravitational constant
h_{fg}	Latent heat of vaporization
k	Thermal conductivity
l	Subscript denoting liquid properties
p	Static pressure
p_a	Partial pressure of air
p_m	Minimum observed wall static pressure
p_v	Vapor pressure
r	Bubble radius
t	Fluid temperature or time
ΔT	Temperature difference
ΔH	Differential head
vp	Volume percent of gas
α	Gas concentration
β	Henry's Law constant
μ	Viscosity

NOMENCLATURE (Con't)

ρ	Density
σ_c	Cavitation number
σ_{st}	Surface tension

CHAPTER I

INTRODUCTION AND LITERATURE SURVEY

The broad question of cavitation has intrigued and plagued investigators for many years. The earliest references go back into the 18th century[1], although the "modern" references date from the 1890's, beginning with a paper by Thronycroft and Barnaby[2] on trials of a new naval propeller, followed by a paper on boiling phenomena by Reynolds[3]. In many instances, the interest has been essentially the scholarly or academic one of explaining the phenomena in analytical terms; for example, the treatises of Besant[4] and Rayleigh[5] on the mechanisms of cavitation bubble collapse. For many years there were no particular attempts beyond these to understand or analyze the phenomena, rather its existence was acknowledged and fluid systems were designed and engineered empirically to avoid the conditions that could produce cavitation. If such design was impossible, then allowances were made for cavitation in terms of performance margins and materials properties. The more recent emphasis on cavitation has received its impetus from several quarters. On the one hand, those involved in the design and employment of naval vessels and weapons established in the early 1940's that the cavitation produced by high performance marine propellers not only degrades performance, but because of its acoustic nature provides an excellent means for sonic tracking of submarines and undersea weapons by surface vessels and vice versa. Complimentary to this, and yet in contrast, we have the increased demand, especially in the past 15 years for compact, highly

reliable, and efficient turbo-machinery for the nation's space and nuclear programs.

In the more "conventional" fluid systems applications, it is relatively easy to include design factors to account for possibilities of damage, loss of efficiency, or both, in the equipment; and, if repair is required, it may generally be accomplished with comparative ease. But in nuclear power plants where repairs are increasingly more costly, difficult, and hazardous, and most especially in weight restricted space systems where repairs are essentially out of the question, equipment must be designed to operate reliably for a long period of time at maximum efficiency without large damage safety margins. Thus, the space age has given impetus to studies of cavitation damage to materials of interest to the machinery designer and to the study of cavitation in general. Concurrently, the demand for increased thermal efficiencies in nuclear power systems for space necessitated consideration of new heat transfer media and fostered a complete new technology on liquid metal properties and behavior. Along this line, extensive studies are being conducted at the University of Michigan and other locations to examine experimentally the resistance of a wide variety of materials to cavitation damage[6,7,8]. In general, the damage to the test specimens is assessed in terms of the degree of cavitation to which they were exposed (determined visually), the temperature and flow velocity of the system, and the duration of the test in a given fluid. Although this is adequate for the comparison of one material with another in a given facility, it is difficult to make comparisons with the results of other experimenters. If the nature of the cavitation could be established in terms of a single

correlatable parameter or set of parameters, obviously the usefulness of the damage data would be increased. The major factor complicating the establishment of such a correlation is that cavitation has not been observed[9,10,11] to scale classically. If cavitation scaled classically then a cavitation index described by

$$\sigma_c \equiv \frac{p - p_v}{\frac{1}{2}\rho V^2}$$

would be sufficient to insure equivalent cavitation. Here σ_c is the cavitation index or cavitation number, V the linear fluid velocity, p the absolute static pressure when cavitation occurs and p_v is the vapor pressure. Thus, under the laws of classical similarity, in geometrically and dynamically similar systems assuming cavitation occurs when the liquid vapor pressure is reached, an equal index means equivalent cavitation. It has been observed that this does not hold universally. This concept is explored further in Chapter II. In the cavitation literature these departures from the classical similarity relations with changes in the geometry, dynamics or state of a cavitation system are generally referred to as "scale effects". For the current work, this includes cavitating venturis or cavitating bodies in water tunnels. In addition to damage studies, scale effects also become significant due to the desirability (both for economic and experimental reasons) of using models when investigating the flow and cavitation characteristics of real fluids. However, unless cavitation can be characterized by a number or function which can be correlated through modified classical similarity laws, or new correlations, model tests cannot be confidently extrapolated to full-scale equipment and

may thereby lose a substantial portion of their validity and usefulness. Furthermore, unless some clearly explainable correlations can be developed in terms of the basic fluid and system parameters, meaningful comparisons of tests in different facilities are nearly impossible.

Although there have been and continue to be repeated references in the literature to the problem of scale effects, there have been few, if any, direct efforts to solve the total problem and establish the necessary theoretical and experimental correlations. A "working group" which is chaired by the thesis chairman, Dr. Hammitt, has now been established in the International Association for Hydraulic Research (IAHR) to attempt to correlate and coordinate world-wide investigations of this overall problem. In the past, Holl and Wislicenus[9] and Oshima[11] have outlined some significant problems and possible explanations in this regard, the former in a stated attempt to stimulate discussion and investigation of the problem, but the question still remains open. Hammitt[10], Jekat[12] and Kermeen[13] have suggested some degree of correlation of the cavitation parameter with Reynolds number and have presented some experimental data, while others have examined various specific items, i.e., gas content[14,15], surface roughness[16], etc., and their effect on the cavitation number. In addition to providing some insight into cavitating mechanisms in simple hydraulic systems, a study of scale effects may also have potential application to the problem of sub-cooled boiling, or heat transfer superheat problems. Such heat transfer problems are being vigorously pursued in connection with safety studies on Sodium Cooled Fast Reactors.

Part of the difficulty encountered in cavitation studies is clearly self-evident if one examines the definition of cavitation. Generally, cavitation is defined as the adiabatic formation of a cavity or void within a liquid volume. This cavitation may be one of two types or a mixture of them. "Gaseous" cavitation is presumed to occur when the liquid pressure is reduced to the point at which dissolved gas begins to come out of solution and form discreet bubbles, or when already formed micro-bubbles of entrained gas grow to visible size by adiabatic expansion under reduced pressure. "Vaporous" cavitation, in contrast, occurs when the fluid pressure is reduced to the point at which the vapor pressure exceeds the liquid pressure and the fluid "boils". The actual pressure at which cavitation occurs is a function of the liquid, its pressure history and its present condition, such as turbulence level, available nucleation sites, etc. As a general rule, gaseous cavitation will occur at liquid pressures greater than the vapor pressure. Although one might expect that vaporous cavitation would result whenever $p_L = p_V$, it has in fact been observed[17,18] and calculated[18] that a pure liquid, i.e., one free from possible sites for nucleation of the cavities, can withstand liquid pressures much less than the vapor pressure (perhaps even < 0) without cavitating. That is, the liquid exhibits a tensile strength. So even though the foregoing definitions categorized cavitation as to types, in most real liquids the situation is not nearly so concise. Both types of cavitation may and often do occur simultaneously with variable relative importance, and it is impossible to distinguish between them by simple visual observations. This is in itself one of the sources

of difficulty.

Even though classical similarity may not occur, the nature of flow relevant to cavitation may still be expressed in nondimensional terms by the cavitation number or index σ_c , given by

$$\sigma_c \equiv \frac{p - p_v}{\frac{1}{2}\rho V^2}$$

For the cavitating venturis used in this work and allied studies at the University of Michigan, p is defined as the minimum observed absolute static wall pressure (based on a complete static wall pressure profile) and V as the linear fluid velocity (V_t) in the venturi throat (computed from the mass flow rates) or:

$$\sigma_c = \frac{p_m - p_v}{\frac{1}{2}\rho V_t^2}$$

As we have stated, if classical scaling were sufficient for analysis of cavitation studies the parameter σ_c would define the flow; but it does not, thus additional correlations are required.

The objective of this present work was to examine the scale effects problem experimentally to obtain empirical correlations between the cavitation number defined above and the physical observables of the system; then, insofar as possible, to provide a theoretical explanation or justification for the effects in terms of the mechanisms involved. Holl and Wislicenus[9] have summarized some of the characteristics they believe are of importance, as has Hammitt[10]. In general, these may be grouped as follows:

a) Hydrodynamic scale effects on fluid pressure;

b) Thermodynamic scale effects;

c) Molecular or microscopic effects.

Group a) may include such things as viscosity, compressibility, gravity and surface condition effects, i.e., Reynolds number, Mach number and Froude number parameters; Group b) vapor pressure, density, heat capacity, and heat transfer effects; Group c) surface tension, i.e., Weber number, and fluid condition parameters such as gas content, number of nucleation sites, etc. These various possibilities are discussed in detail in Part II of the present work and the experimental results and correlations in Parts IV and V.

The venturis used in the experimental program had nominal diameters of 1/8 in., 1/4 in., 1/2 in., and 3/4 in. for the cylindrical throat section with the length to diameter rates (L/D) of the throat approximately 4.6. The inlet and diffuser were conical with 6° included angle in all cases so that geometric similarity could be assumed. The axial static pressure profile at the wall was determined and the pressure minimum thus obtained was used to calculate σ_c . These profiles were determined for various combinations of flow rates, temperature, gas content and degree of cavitation using water and mercury as the working fluids. The experimental apparatus and techniques are described in Part III.

CHAPTER II

ANALYSIS OF VARIABLES

It was pointed out in the introductory remarks that the phenomena of cavitation does not follow the usual classical laws of scaling and that this deviation has been observed by all those working in the field of cavitating flows. In this chapter, the physical variables that may enter into or influence these deviations from the classical case are examined. Likewise, the formulations of the physical relationships between the system variables that may be used to correlate the cavitation number with the observable or measurable properties of the system are explored and analyzed.

A. The Possible Variables

It has frequently been pointed out that there are a variety of reasons for choosing experimental or research systems that do not exactly duplicate the real world situations; reasons of economy, simplicity of fabrication, ease of operation, and so forth. In various research programs at the University of Michigan[6,7,10] the closed loop venturi system has been selected as being reasonably representative of modern turbomachinery for certain hydrodynamic studies. That is, it is a recirculating system, as are most power-generating facilities, it has reasonably steep pressure gradients during portions of the flow path, and it can be operated over a range of pressures and temperatures with a number of test fluids. In these systems, as with actual turbomachinery, there are a variety of variables that the test designer can

control or prescribe. Such controllable variables include, obviously; the system geometry, size, and working fluid (within certain limits); the test conditions of temperature, pressure, fluid velocity, gas content (again within certain limits) and the degree or kind of cavitation to be studied.

On the other hand, as soon as the limits or values of the above variables to be considered in any given test are established, there are immediately involved additional uncontrollable or dependent variables that must also be considered in any subsequent analysis. Selecting a particular fluid and temperature fixes physical properties such as density, viscosity, surface tension, heat capacity, thermal conductivity, and so on. Therefore, it is completely obvious that there may well be a variety of competing or complementary effects occurring simultaneously in the test system. If, for the purposes of analysis and discussion, a single geometrical configuration is established, then from the previous discussions the following list of variables of possible interest may be inferred.

TABLE 1

THE PHYSICAL VARIABLES

A characteristic length	D or L
Fluid temperature	t
Pressure	p
Fluid velocity	V
Viscosity	μ
Surface tension	σ_π
Thermal conductivity	k
Heat capacity	c_p
Vapor pressure	p_v
Sonic velocity (pure material)	a_o
Density (liquid and vapor)	ρ_l and ρ_v
Gas concentration	α

Certainly the techniques of dimensional analysis could be applied to this situation and thereby reduce the foregoing list to a set of nondimensional functions. However, simply by inspection it is possible to ascertain a number of such functions that are "standard" to a variety of fluid flow problems and considerations. These are:

$$\text{Reynolds Number} \quad Re = \frac{\rho V L}{\mu}$$

$$\text{Prandtl Number} \quad Pr = \frac{\mu c_p}{k}$$

$$\text{Weber Number} \quad We = \frac{\rho V^2 L}{\sigma_{ST}}$$

$$\text{Froude Number} \quad Fr = \frac{V}{\sqrt{gL}}$$

Moreover, because of our particular concern here with cavitation the cavitation parameter may be included.

$$\text{Cavitation Number} \quad \sigma_c = \frac{p - p_v}{\frac{1}{2}\rho V^2}$$

As we noted above, the importance of these five ratios is essentially obvious in a fluid system because of much prior research. At this point a number of the physical properties of the system have still not been considered. Once again however, prior cavitation research affords us some guidance for selecting additional nondimensional factors. Cavitation involves a two-phase system, therefore, a system

in which compressible flow can occur. This suggests the possibility of sonic velocity effects, so that the Mach number may be introduced into our consideration.

$$\text{Mach number} \qquad M = \frac{V}{a_o}$$

There is a considerable volume of data in the literature on gas content effects in fluid cavitation, such as that by Ripken[15] and Ruggeri and Gelder[19]. Holl[14] has suggested that the cavitation characteristics may be related to the gas content by the dimensionless parameter $\alpha\beta/\frac{1}{2}\rho V^2$. Therefore, this will be included in the compilation of possible variables for correlation.

A number of investigators[14,20,21] have reported cavitation numbers that vary depending upon whether the total static pressure is being increased or decreased, that is, cavitation disappearing or appearing, or, more commonly, "desinent cavitation" or "incipient cavitation" as suggested by Holl[14]. This suggests the possibility of the exposure time having some influence on the observed cavitation. A dimensionless time parameter may be established:

$$\tau = t/\tau_o = L/V\tau_o$$

In this instance τ_o is a fluid molecular relaxation time that can be derived from the kinetic theory of liquids[22]. A further discussion appears in Section I of this chapter.

In these proceeding arguments, the Prandtl number is the only one that can supply any information on the thermal state or characteristic

of the system. Stahl and Stepanoff[23] were the first to draw attention to the thermal cavitation effects in centrifugal pumps. The cited work defines a thermodynamic parameter, B, that was rearranged into the following form in a paper by Hammitt[24].

$$B = \frac{\rho_L C_p \, \Delta T/\Delta H}{\rho_v \, h_{fg}}$$

This may be normalized by multiplication with V^2/g to give:

$$B^* = \frac{\rho_L C_p \, \Delta T/\Delta H}{\rho_v \, h_{fg}} \cdot \frac{V^2}{g}$$

The foregoing has simply suggested some possible variables and non-dimensional parameters without any attempt to assess their influence or significance. This will be done in the following sections.

B. Scale Effects and Similarity

Because it has been observed that cavitating flows deviate from classical similarity it is appropriate to restate and further examine the assumptions that underlie classical similarity. These may be stated as follows[24,25,26]:

1. Geometric similarity is total, that is, even such things as surface roughness and finish maintain proportionality;

2. Inertia forces are the only forces active in the system so that all pressure differences are proportional to ρV^2 or, dynamic pressures at corresponding points must be constant.

For the case of cavitating flows, the following may be added:[9]

3. The pressure at which cavitation occurs is the equilibrium vapor pressure of the test fluid. This parameter is assumed to be known and a constant for the particular flow field under consideration.

4. Cavitation takes place instantaneously whenever the vapor pressure is reached. That is, the liquid can support no tension and there are no time effects.

If we examine these assumptions, we can see almost "a priori" that they are not valid without considerable qualification and therefore it is not at all surprising that "classical similarity" is not sufficient to explain cavitation. For instance, surface roughness in machined parts is in large measure a function of the materials and cutting tools used rather than part size "per se", so unless special precautions are taken surface roughness will not be scaled. The second assumption is of course simply that of a frictionless, incompressible fluid neglecting gravity or other body forces; that is, the flow outside the cavities is assumed to have these attributes. The third and fourth assumptions deal with the actual mechanism of cavity formation. This situation allows consideration of two categories or types of scale effects. First, there may be scale effects on the flow outside of, and irrespective of the presence of cavities, that influence the minimum pressure fields. Second, there may be effects on the cavitation process as such, so that the pressure at the cavitation voids is caused to depart from the equilibrium vapor pressure at liquid bulk temperature and which may subsequently cause tension and time effects.

C. Reynolds Number Considerations

For steady, incompressible, single-phase flow in absence of free surfaces, only viscous and inertial forces are of consequence, therefore, with geometric similarity a constant Reynolds number between model and prototype provides the necessary dynamic similarity. Obviously, situations in which the same working fluid is used in both instances, that is, density and viscosity are constant, require that the product of velocity and diameter (V*D) must be constant. Because local under-pressures in the fluid, necessary to cause the growth of cavitation bubbles from small nuclei according to the usual concept, are a function of the degree of turbulence, it is expected that the cavitation number should correlate at least to some extent with Reynolds number. Oshima[11] has developed a correlation between incipient cavitation number and Reynolds number for axially symmetric bodies considering only a balance between surface tension and inertia. This analysis predicts that the cavitation number increases with Reynold number. The available experimental evidence supports at least a partial correlation of the cavitation number and Reynolds number, but with contrasting results. The data of Rouse and McNown[27], Parkin and Holl[28], Parkin[29], Holl[16], and Kermeen and Parkin[21], as summarized by Holl and Wislicenus[9] indicate an increasing cavitation number with Reynolds number. More precisely, for ogives and 12% Joukowski hydrofoils, for a given size, σ_c increases with Re if the change is brought about by velocity changes, while for a given Re, σ_c decreases slightly with size. On the other hand, Gilehuff and Wislicenus[30] indicate that σ_c decreases with Re for a given size (i.e., σ_c decreases with

increasing velocity) and that σ_c increases with size at a given Reynolds number. Some of the most striking data in this regard are those of Kermeen and Parkin[21] for cavitation on sharp-edged disks. In this instance, σ_c increases with Re approximately as the fourth root, that is, $\sigma_c \simeq$ Constant x $Re^{1/4}$. Earlier work done at the University of Michigan[10] exhibits the same characteristics as NACA 16012 hydrofoils in the foreging references, σ_c decreasing with increasing Re. Similar characteristics have been observed in cavitation studies on centrifugal pumps. Hammitt[10] reports that for relatively low Reynolds numbers the cavitation number (Thoma coefficient) decreases with speed. Jekat[12] working over a large range on Reynolds numbers in axial inducers reports a cavitation number that passes through a minimum as the Reynolds number increases and then increases with further increases in Reynolds number. In light of the strong evidence thus available for a correlation of σ_c with Reynolds number, such a correlation will be attempted here.

D. Froude Number Considerations

The Froude number, or the ratio of inertial forces to gravitational forces, is of particular concern in open channel flow structures such as spillways, settling pools, weirs, etc., where liquid elevation changes can produce gravity and inertial forces that far exceed viscous and turbulent shear forces. This can also occur in large pump or marine propeller test facilities, that frequently have very large vertically oriented passages where elevation differences are important.

However, in the relatively compact, closed circuit turbomachinery applications exemplified by the test facilities used in this study, the net gravity forces are negligible so that Froude number correlations are not really pertinent. Therefore, they will be dropped from further consideration.

E. Weber Number Considerations

The Weber number, or ratio of inertial forces to surface tension forces is suggested by an examination of the basic equations governing the growth of a bubble. Plesset[31] was probably the first to modify the original Rayleigh analysis to show that the differential equation governing bubble growth may be written:

$$r\frac{d^2r}{dt^2} + \frac{3}{2}\left(\frac{dr}{dt}\right)^2 = \frac{1}{\rho_L}\left(p_v - p - \frac{2\sigma}{r}\right)$$

where the internal pressure of the bubble is determined in part by surface tension considerations. If the postulate of cavitation nuclei first attributed to Harvey[32] is accepted, then the surface tension effects must be presumed to be operating on a scale commensurate with the size of the cavitation nuclei. That is, in the expression:

$$We = \rho V^2 L/\sigma_{ST}$$

The characteristic length must be related in some way to a dimension typical of the nuclei. Because cavitation has been observed to occur quite readily even in systems where there are no visible nuclei, it is reasonable to assume in convential engineering systems typical nuclei diameters are less than 1 mil (0.001 in.). Unfortunately,

no prior attempts at correlation of the Weber number and the cavitation number have achieved much success. In all probability this can be attributed to the fact that for water (which is the fluid whose cavitation characteristics have received the most study) the surface tension is relatively insensitive (value of surface tension decreases by about 12 percent) to temperature over the range from 40° to 150°F where the bulk of the data has been obtained. Therefore the correlations have essentially been against V^2L. Kermeen and Parkin[21] did attempt to include surface tension effects and report a relationship:

$$\sigma = A - B/We_{r_o}$$

where We_{r_o} is a Weber number based upon an initial bubble radius r_o and free stream velocity, B is a factor depending upon air content and A is a factor depending upon the several pressure coefficients. This A factor may be dependent upon Reynolds number, although such a relationship has not been clearly established. With these considerations in mind, the correlations attempted here will use three Weber numbers defined as follows:

$$We_n = \frac{\rho V^2 D_n}{\sigma_{ST}}$$

where n = 1, 2, or 3 such that:

D_1 - Initial bubble nuclei diameter is assumed to be a linear function of the total gas content.

D_2 - A constant bubble diameter of 1 mil is assumed.

D_3 - The venturi throat diameter is assumed, i.e., nuclei diameter is assumed proportional to throat diameter.

The rule of variation chosen for D_1 is based upon the simple observation that for water, as the total gas content increases, a bubble cloud does become visible, implying larger nuclei. The dimension chosen for D_2 is arbitrary, but is based upon the argument that there may be some approximately fixed diameter of nucleus required within the range of the tests in order for the bubble to grow. This critical diameter is not yet known, although it appears to be a strong function of the fluid history. The 1 mil value was selected because with the lighting and camera techniques available smaller bubbles could not be observed visually, while those greater than 1 mil usually could be seen. The dimension chosen for D_3 is predicated upon the argument that as the venturi size changes - particularly as it is made smaller it may influence the nuclei size. Also, this provides a Weber number that is system-oriented and readily obtainable.

F. Gas Content Considerations

As was indicated earlier, there is a fairly extensive volume of literature dealing with the effects of gas content upon the cavitation characteristics of fluids. Olson[33] discusses work done at the St. Anthony Falls Hydraulic Laboratory and concludes that the measurement of total air content is not a satisfactory basis for evaluating the cavitation susceptibility of tunnel water, and, that even when total gas content and temperature of the water were controlled, the non-reproducibility of tests indicates that some other factor has strong

influence upon the cavitation. Harvey[32] has suggested that gas bubbles trapped in crevices of a hydrophobic solid may be the source of nuclei. This represents a source term that cannot be quantitatively related to the measured gas content and therefore is a theory difficult to verify experimentally. In later work at St. Anthony Falls, Ripken[34] arrives at the following conclusions, among others: (1) Cavitation inception numbers using water with a high concentration of air nuclei are significantly different from those with low concentrations; (2) Cavitation inception in the form of steady-state cavities (i.e., cavities that persist at a given point on the body) of abrupt appearance and disappearance as the pressure is lowered or raised tends to occur in water having a relatively low nuclei concentration. Conversely, cavitation inception in the form of transient bubbles tends to occur in water having a relatively high nuclei concentration; (3) the portion of the total gas content (for water) that is in the form of nuclei (entrained) is probably much more influential in cavitation inception processes than the portion in the dissolved form. Unfortunately, entrained gas is only a small percentage of the total gas content and it is only the total gas content that can easily be measured.

Ripken and Killen[15] have investigated the mechanisms of bubble growth and the influence of gas bubbles on the cavitation characteristics of water. They have argued that the entrained gas is the key factor and have shown that by slowly approaching the cavitation pressure the free gas concentration is stabilized. Under these conditions the cavity is transient and cavitation numbers are relatively high.

This suggests that it is "gaseous" cavitation which has been reported by others investigating similar effects. They also present data, taken under the above conditions, which indicate a strong dependance of cavitation number on gas content. A portion of this work was also devoted to examining vorticity effects on bubble growth, with these conclusions: 1) Boundary layer vorticity is capable of substantially increasing the size of stabilized gas bubbles present in water and such larger bubbles may directly serve as nuclei for cavitation. 2) Gas bubble size distribution is a desirable research index for the cavitation susceptibility of test water in preference to volume measurement of free or total gas content. They also noted that water velocities as low as 10 feet per second produced vorticity sufficient to grow large gas bubbles, thus indicating that most prototype turbomachinery will normally be supplied with a water that will readily cavitate. Narayanan[35] has also presented centrifugal pump data indicating that increasing the gas content significantly increases the cavitation tendency of the pump. In related work dealing with the cavitation characteristics of ship propellers, Silverleaf and Berry[36] have concluded that for tip vortex cavitation, the inception cavitation index increases with air content. Ruggeri and Gelder[19] have investigated cavitation in a verturi flow system and report data that indicate that the cavitation number increases with air content for incipient or just initiated cavitation; while for more fully developed cavitation, gas content appears to have little effect. Perhaps the most striking arguments pertaining to gas content effects are those presented by Holl[14] in a reanalysis of data reported earlier by Calehuff and Wislicenus[30]. In his paper, Holl makes a

distinction between "gaseous" and "vaporous" cavitation and develops the following argument. The static equilibrium equation for a bubble is given by:

$$p_a + p_v = p_c + \frac{2\sigma_{st}}{r}$$

where: p_a = partial pressure of air

p_c = liquid pressure outside the bubble

p_v = liquid vapor pressure

σ_{st} = surface tension

r = bubble radius

Now if the bubble is "saturated" with air, or more precisely, if the air pressure in the bubble equals the total partial pressure in the liquid, the air pressure becomes $\alpha\beta$ where α is the dissolved air content and β is the Henry's Law constant. These conditions will determine an upper limit to p_a. So, for this condition one can write:

$$\alpha\beta + p_v = p_c + \frac{2\sigma_{st}}{r}$$

or solving and multiplying by -1,

$$-p_v = -p_c + \alpha\beta - \frac{2\sigma_{st}}{r}$$

Now adding free stream minimum pressure and normalizing by division

with $\rho V^2/2$ gives,

$$\frac{p_m - p_v}{\frac{1}{2}\rho V^2} = \frac{p_m - p_c}{\frac{1}{2}\rho V^2} + \frac{\alpha\beta}{\frac{1}{2}\rho V^2} - \frac{2\sigma_{st}/r}{\frac{1}{2}\rho V^2}$$

where the left hand side is simply the cavitation number, and the first term on the right is a pressure coefficient, so that:

$$\sigma_c = C_p + \frac{\alpha\beta}{\frac{1}{2}\rho V^2} - \frac{2\sigma_{st}/r}{\frac{1}{2}\rho V^2}$$

Now it has been stated earlier the r is on the order of 0.5 mil or larger so that for the minimum velocities available in the current work (approximately 60 ft/sec in water) and at temperatures on the order of 60°F (r = 0.0005 in., σ_{st} = 0.0005 pounds/ft, γ = 62.09 pounds/ft^3) the surface tension factor is on the order of 7×10^{-3} and may be neglected in comparison with the gas content term, that will have values on the order of 0.06. Therefore we are left with the relationship:

$$\sigma_c = C_p + \frac{\alpha\beta}{\frac{1}{2}\rho V^2}$$

Because the exact pressure coefficient is a function of the shape involved it is sufficient for our purposes to say that:

$$\sigma_c \approx f\left(\alpha\beta/\tfrac{1}{2}\rho V^2\right)$$

and such a term will be used in subsequent analyses. This approach was used with a portion of these data and reported earlier[37]. In addition, Holl also concluded that: 1) Differences between desinent

cavitation numbers for gaseous and vaporous cavitation are directly proportional to the dissolved air content; 2) Gaseous cavitation can occur at very high ambient pressures; and 3) To minimize the effects of air content and thus avoid possible confusion of vaporous and gaseous cavitation, tests should be run at low dissolved air contents and high velocities. Clearly then, gas content effects are important, therefore in the current work we have included a consideration of gas content effects.

G. Mach Number Considerations

Whenever fluid dynamic problems are considered the fluid velocity is important and frequently is the controlling variable. For instance, the fluid velocity can determine head losses. Likewise, the fluid velocity may also be important in relationships to particular geometrical or fluid properties. The Mach Number is defined:

$$M = V/a_o$$

where V is the fluid velocity and a_o is a reference sonic velocity. For venturi flows, such considerations are important because a normally subsonic nozzle may become a supersonic diffuser. Shock waves occur in supersonic flows but do not appear in subsonic flows. This could lead to a choking or limitation of the mass flow rate as Mach numbers approach unity. Because sonic velocity in water is on the order of 5000 feet per second and most flows do not approach anywhere near that velocity, it seems of little concern. However, Karplus[38] has shown that the sonic velocity in water-air mixtures can drop by several orders of magnitude as air content approaches 50% by volume

when the gas is in the entrained state. This means that for gas concentrations as low as 10%, significant changes have occurred and the mixture sonic velocity may be on the order of the flow velocities. Although total gas contents in the present work do approach 2 to 3% by volume of air in water, a significant portion of this is dissolved. Furthermore, the point of concern in this work is cavitation inception, or that condition when bubbles just begin to appear, so that we can assume that there is no significant alteration of the flow field. Thus, although Mach number effects could have serious consequence in very well developed cavitating flows, and it has been shown[39] that one can compute the pressures in a cavitating venturi diffuser using a choked flow analogy, Mach number effects will be omitted from the current analysis.

H. Prandtl Number Considerations

The Prandtl number is of concern in convective heat processes and it is a material property relating viscous and thermal diffusivities. It has been included here because we are testing two dissimilar fluids (mercury and water) so the Prandtl number offers one potential means of correlation, since convective heat processes can influence the rate of growth and collapse of the bubbles[24,40]. On the other hand, because the Prandtl number is a material property with moderate sensitivity to temperature changes (factor of 3 variation for water over 50 to 150°F and about an order of magnitude over 70 to 400°F for mercury), it is not expected that it will provide a significant correlation within either the water or mercury data alone. This is based on the fact

that in neither case is the data taken at temperatures sufficiently high for thermal effects to be important[11,40].

I. Exposure Time Parameter

The classical assumption in regard to cavitation initiation is that whenever the fluid is subjected to conditions where the local pressure is equal to or less than vapor pressure, cavitation occurs instantaneously. Nearly, all the investigators in the field have demonstrated that this does not occur. In fact, in many facilities, if one approaches cavitation from a condition of no cavitation, as contrasted to approaching cavitation from a point of fully developed cavitation, two distinctly different cavitation pressures are observed. Following Holl's introduction of the second term, these are generally called incipient and desient cavitation. Such behavior certainly suggests the presence of exposure time effects and Holl and Treaster[41], among others, have labeled this hysteresis. Although this difference has not been observed in the test facilities at the University of Michigan, an exposure time parameter is included in this present work to see if it provides any insight into the mechanism of cavitation. An estimate of the actual time of exposure to the low pressure region in the venturi throat may be determined as simply the venturi throat length divided by the throat velocity. This leaves us with a term which must be made dimensionless to fit into our analysis scheme. The first approach that may be considered, based upon the work of Van Wyngaarden[42] is to divide by the time it takes a bubble to grow from some nuclei with radius r_o to a final bubble with radius, r. Unfortunately, this time of growth is not a unique or single valued function.

It is a function of the initial size assumed and the final size specified. Furthermore, in flowing systems such as that used here, this growth time may be a function of the average turbulence level or the Reynolds number of the flow or even the details of local turbulence. At this point we are forced to seek another avenue of approach. If we turn to the kinetic theory of liquids, we find that Frenkel[22] presents arguments concerning the molecular relaxation time of fluids, that is, the time for a disturbance in the "lattice" to be absorbed. If we argue that such a property may also be involved in the growth of nuclei then we can use this in our nondimensionalizing process, recognizing of course that this is a qualitative argument. Such molecular relaxation times are reported to be on the order of 10^{-13} seconds. Therefore, a dimensionless parameter may be established.

$$\tau_{au} = t/\tau_o = \frac{L/V_T}{\tau_o}$$

Correlations with such a parameter will be attempted with the current data.

J. Thermodynamic Parameter Considerations

One of the first attempts to theoretically examine the "thermodynamic effects" in cavitation is that of Stahl and Stepanoff[23]. In this work, they point out that as fluid moves into regions of low pressure where local total pressure is below the liquid vapor pressure, a temperature difference is created inducing heat flow from the bulk liquid to supply the latent heat of vaporization required in the cavitation process. Therefore, in the analysis, the degree of cavitation

is controlled by the temperature difference (ΔT) associated with the pressure differential between local pressure and the vapor pressure, the latent heat of vaporization, specific heat and thermal conductivity of the fluid, the size of the bubbles and the time the liquid spends in the low pressure area. It is also pointed out in the paper that a given amount of pressure depression results in a greater ΔT below thermal equilibrium at lower bulk temperatures and pressures than at higher temperatures for a given fluid. Or, in other words, more heat is available in the close vicinity, and thus more fluid could be vaporized at the lower fluid bulk temperatures. Because of the low vapor density under such conditions, the vapor volume created would be relatively large. This analysis has also been discussed by Stepanoff[43] who has shown that if sufficient time is allowed, then some ΔH_f in BTU/pound of liquid passing through the low-pressure zone will be available for vaporization of liquid. The value of ΔH_f is simply the difference between liquid enthalpy at the original equilibrium conditions and at the new conditions of reduced pressure. An equilibrium heat balance may be written:

$$\Delta H_f = c_p \Delta T \qquad (1)$$

Assuming thermal equilibrium, then per pound of liquid passing through the low pressure zone the heat balance equation may be written:

$$1 \times \Delta H_f = f_v h_{fg} \qquad (2)$$

where f_v is the fraction of each pound of liquid boiled per pound of liquid. Now if we let $f_v = \frac{V_v}{v_v}$ and $V_l = v_l$ x1 and substitute these into (2) we obtain the relationship:

$$\frac{V_l}{v_l} \Delta H_f = \frac{V_v}{v_v} h_{fg} \qquad (3)$$

or:

$$\frac{v_v}{v_l} \cdot \frac{\Delta H_f}{h_{fg}} = \frac{V_v}{V_l} = B \qquad (4)$$

where: V represents volume, v is specific volume, and subscripts l and v are for liquid and vapor respectively. This analysis can be modified by using some of the arguments of Salemann[44] and Hammitt[24] to a form that allows one to more easily determine ΔH_f. As has been noted,

$$\Delta H_f = C_{p_l} \Delta T \qquad (1)$$

Now since the temperature difference ΔT must arise from the superheating from pressure reduction, then we can use the slope of the saturated vapor pressure line to determine $\Delta T/\Delta H$ or the temperature change per unit head change. With this argument, the thermodynamic parameter may be written:

$$B = \frac{v_v}{v_l} \cdot \frac{C_{p_l}}{h_{fg}} \cdot \left(\Delta T/\Delta H\right) \qquad (5)$$

or to use densities:

$$B = \frac{\rho_\ell \, c_{p\ell} \, (\Delta T/\Delta H)}{\rho_v \, h_{fg}} \qquad (6)$$

It must be noted of course that in this form the thermodynamic parameter is no longer nondimensional but has the units of inverse feet. For the purposes of our correlation B can be multiplied by the kinetic head $\frac{1}{2}\rho V^2$, which then gives us the dimensionless parameter.

$$B = \frac{\rho_\ell \, c_{p\ell} \, (\Delta T/\Delta H)}{\rho_v \, h_{fg}} \cdot \frac{1}{2}\rho_\ell V^2 \qquad (7)$$

The thermodynamic parameter thus defined has a shortcoming however in that it does not account for heat transfer rates near the bubble wall. This is important in studies involving the collapse of cavitation bubbles and subsequent damage to the surrounding surfaces. If a bubble containing vapor enters a high-pressure region and begins to collapse and the heat conduction rates in the liquid are small enough, the vapor is forced to act essentially as a noncondensible gas, inhibiting collapse and presumably damage. Conversely, if the heat conduction is large, the collapse will be accelerated. Florschuetz and Chao[45] have examined this problem and in their treatment a revised thermodynamic parameter B_{eff} is defined:

$$B_{eff} = \left(\frac{\rho_\ell \, c_{p\ell} \, \Delta T}{\rho_v \, h_{fg}}\right)^2 \frac{k_\ell}{R_o} \left(\frac{\rho_\ell}{\Delta p}\right)^{1/2} \qquad (8)$$

Florschuetz and Chao show that for small B_{eff}, bubble growth and collapse are heat transfer controlled, i.e., thermodynamic effects are important, and that for large B_{eff} the bubble processes are inertia controlled. The difficulty in using such a definition in this present study is the problem encountered in defining the equilibrium bubble radius R_o in a flowing, multipressure, gas containing liquid. This relationship has been modified by Garcia and Hammitt[40] to correlate observed damage effects in a still more complex fashion. Because of this difficulty with establishing R_o the present work uses the original simplified relationship presented in Equation 7.

K. Analysis Summary

In this chapter we have established the important physical variables of the venturi system and have discussed their possible influences on the cavitation characteristics. To the extent possible these variables have been developed in terms of "conventional" fluid flow parameters. In this treatment no attempt was made to evaluate the relative importance of these various parameters. Instead, the data correlation techniques outlined in Chapter V and Appendices H and I will be used to determine the impact of the individual parameters in a given flow situation. However, as a result of this discussion we have a set of dimensionless terms against which the correlations with cavitation number may be attempted. The parameters selected are:

Reynolds number

Weber number

Prandtl number

Gas content parameter

Exposure time parameter

Thermodynamic parameter

CHAPTER III

EXPERIMENTAL FACILITIES AND TECHNIQUES

A. General Facility Description

The experimental studies were conducted in the venturi tunnel facilities of the Nuclear Engineering Department of the University of Michigan. Only a brief description of the two tunnel facilities (water and liquid metal) are presented here. The various construction details, etc., are omitted because they have been reported elsewhere[46].

The water tunnel facility is a multiple venturi system (maximum of four parallel loops) originally designed for cavitation damage studies. Figure 1 is a simplified schematic of this system. The flow rate and concurrently the extent of cavitation are controlled by means of a variable speed centrifugal pump and the total static pressure maintained on the "low pressure tank", into which all loops discharge. The latter control is accomplished by gas pressure loading of an attached surge tank. Fluid velocities from approximately 50 to 225 feet per second may be obtained in the smaller venturi throats; however, the 3/4 inch venturi has an upper velocity limit of about 180 feet per second because of the drooping head-flow characteristic curve of the pump. The gas content of the water can be varied from about 3.5 to 0.5 volume percent (based on standard temperature and pressure, STP, valves) by means of a cold-water vacuum deaerator in a bypass stream from the loop. The temperature is controlled by varying the flow rate of cooling water in coils in the low pressure

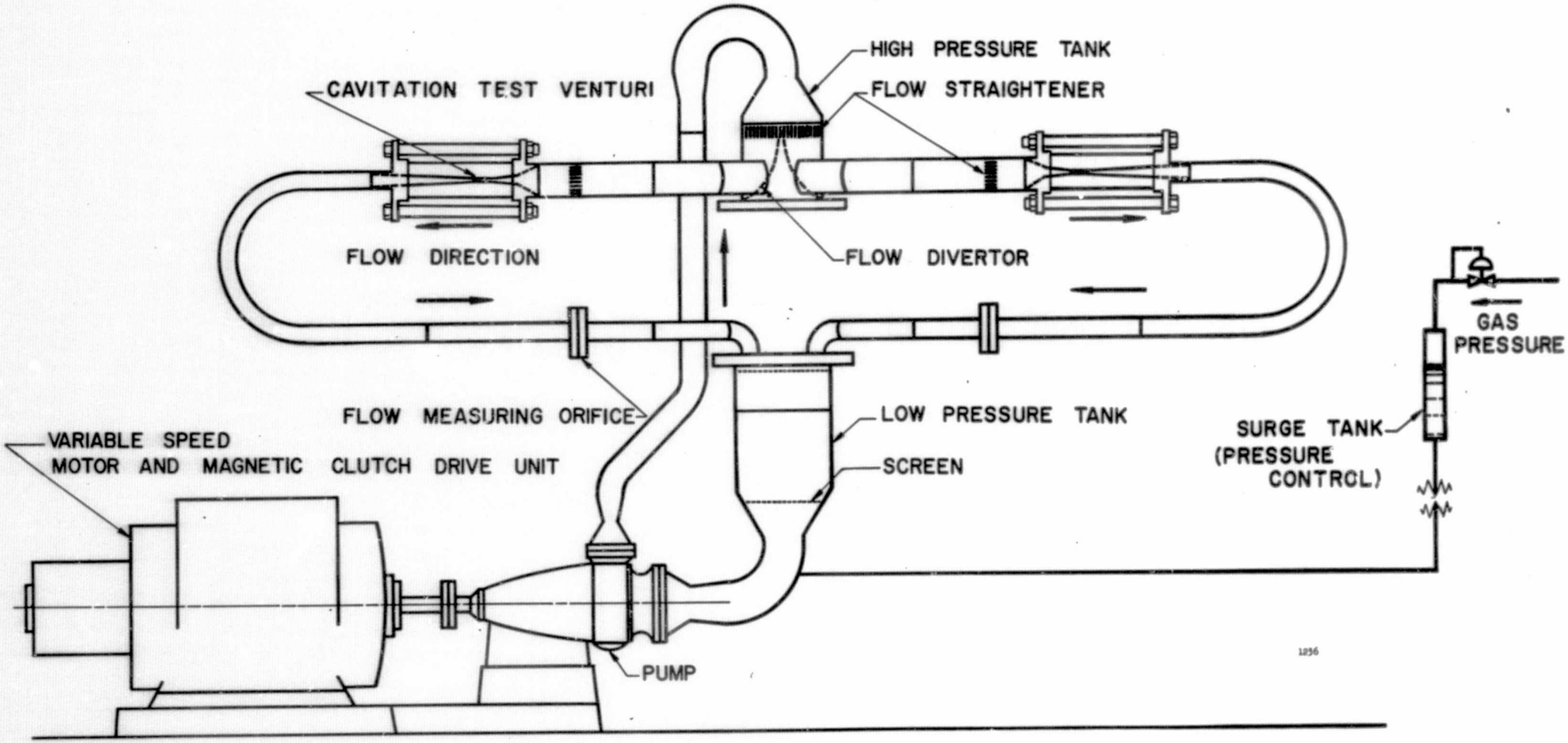

Figure 1. Water Damage Facility (Only two of the four loops are shown).

tank. With the plastic venturis, operation is limited to a temperature range from 50 to 150°F in order to prevent "crazing" or softening of the venturis. A general view of the water facility as used for damage studies is shown on Figure 2. A typical installation for one of the scale-effects venturis is shown in Figure 3.

The liquid metal tunnel facility is a single loop system currently using mercury as the working fluid. A schematic of this facility is shown on Figure 4. (The gas injection and sampling system are discussed in detail in a subsequent section.) The flow rate is controlled by means of variable-speed centrifugal sump pump, while the static pressure (and thus the degree of cavitation) is controlled by the two throttling valves (upstream and downstream of the test section). Flow velocities from 10 to 65 feet per second are attainable in this system from 1/8, 1/2, and 1/4 inch venturis. The 3/4 inch venturi was not run in this system. The gas content of the mercury was varied by injection of Argon or Hydrogen at the pump discharge (when the naturally entrained air was incorrect for the desired test) and levels from 0.1 to greater than 2.5 ppm by mass have been achieved (roughly 2.5 volume percent at STP). Temperature is controlled by varying the cooling waterflow when the plastic venturis are used (temperature less than 150°F) and by electrical clamshell heaters when the stainless steel venturis are used (temperatures to about 600°F can be obtained). Figure 5 shows the mercury loop with the upper clamshell heater removed and without pressure instrumentation, Figure 6 shows the 1/2 inch scale-effects venturi installed in the mercury loop.

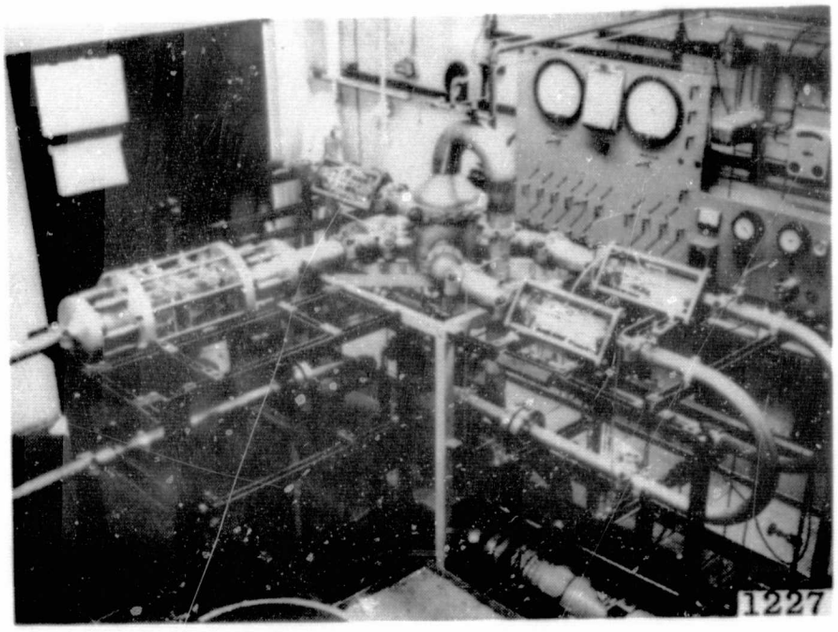

Figure 2. Water Cavitation, Closed Loop, Venturi Facility

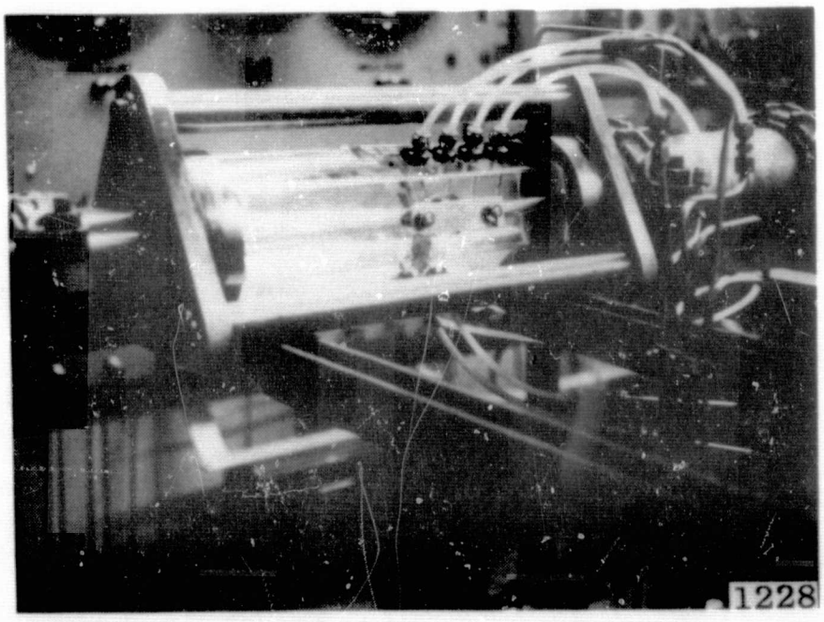

Figure 3. Scale Effects Venturi Installed in the Water Cavitation Facility (1/2 inch Throat).

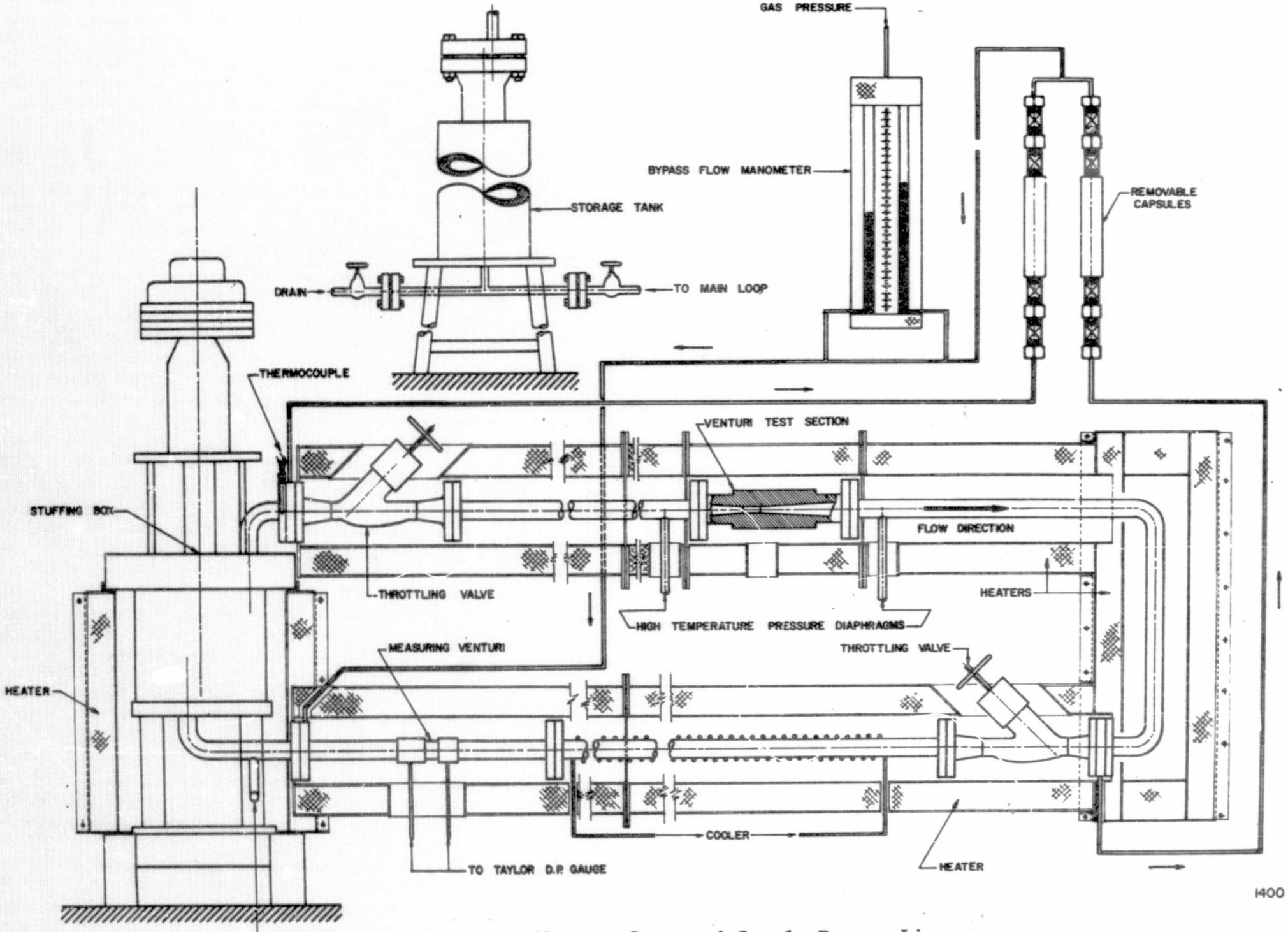

Figure 4. Mercury Loop and Sample Bypass Lines

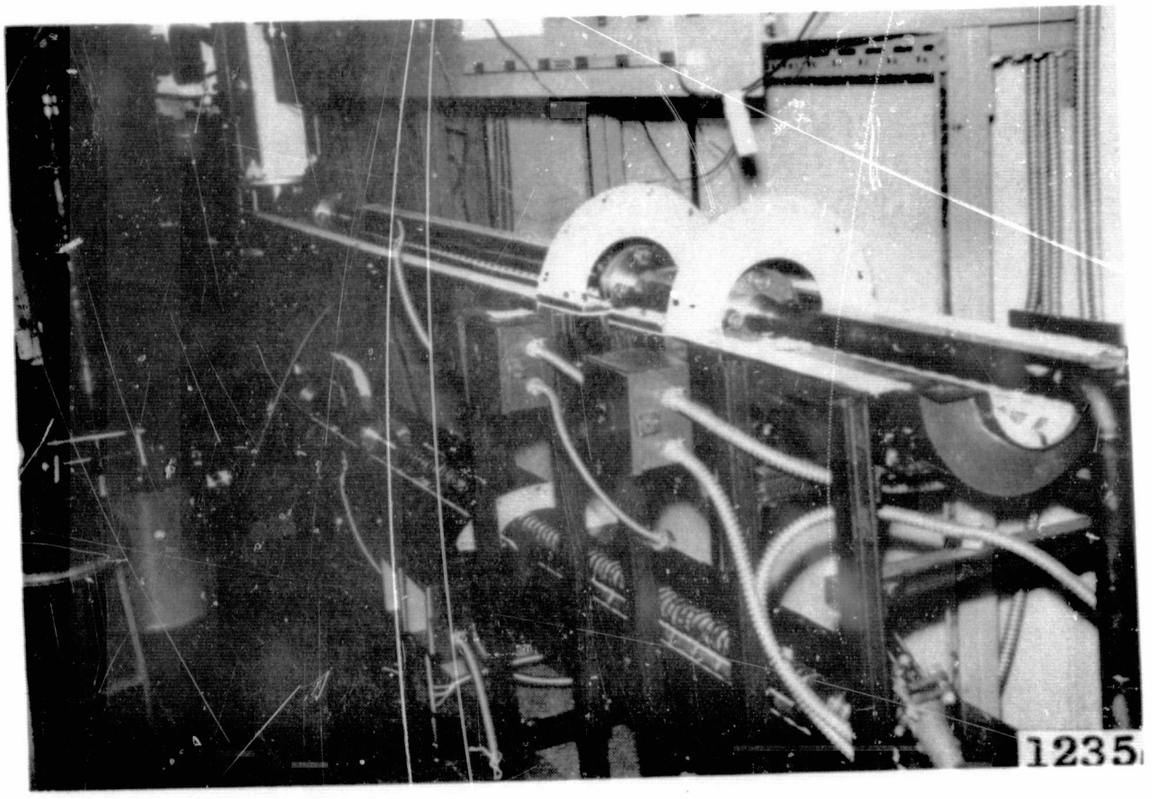

Figure 5. Mercury Facility with Top Half of Heater Section Removed.

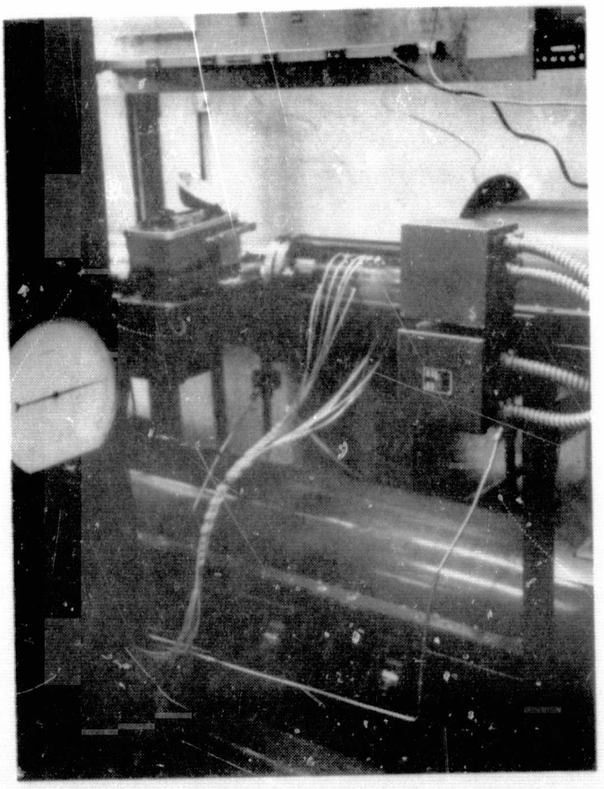

Figure 6. Scale Effects Venturi Installed on Mercury Loop (1/2 inch Throat).

B. Venturis and Pressure Manifold Description, Pressure Measuring Techniques

The venturis used for this work were based upon the designs of the damage test venturis used in earlier work in this laboratory. These venturis have conical inlets and diffusers with a 6° included angle, and a cylindrical throat with an L/D ratio of approximately 4.6. The basic geometry is shown in Figure 7. Overall length is 14.5 inches. The four transparent plastic venturis used in the work are shown in Figures 8 through 11 and Figures 12 through 15 are simplified cross-sections for the same venturis showing the basic flow path design. Although external configurations vary because of fabrication considerations the flow paths are geometrically similar. Also, in the case of the 1/2 inch and 3/4 inch venturis, the actual design was influenced by the availability of partially finished venturis that were adaptable to the present study. In all cases, the pressure taps were placed so that the centerline of the tap is normal to the venturi wall. For the 1/2 inch and 3/4 inch venturis the tap diameters were 40 mils, and for the 1/8 inch and 1/4 inch venturis, 20 mils.

The tap locations projected to the venturi centerline for the four plastic venturis are also shown in Figure 12 through 15 and for the 1/2 inch and 1/8 inch stainless steel in Figures 16 and 17. In these figures the distance from throat entrance to the tap centerline is indicated. For the 1/2 inch plastic venturi, which was the first used, the selection of the tap locations was somewhat arbitrary although guided by the requirement for good pressure data for the entire range of cavitation conditions to be studied. The cavitation conditions

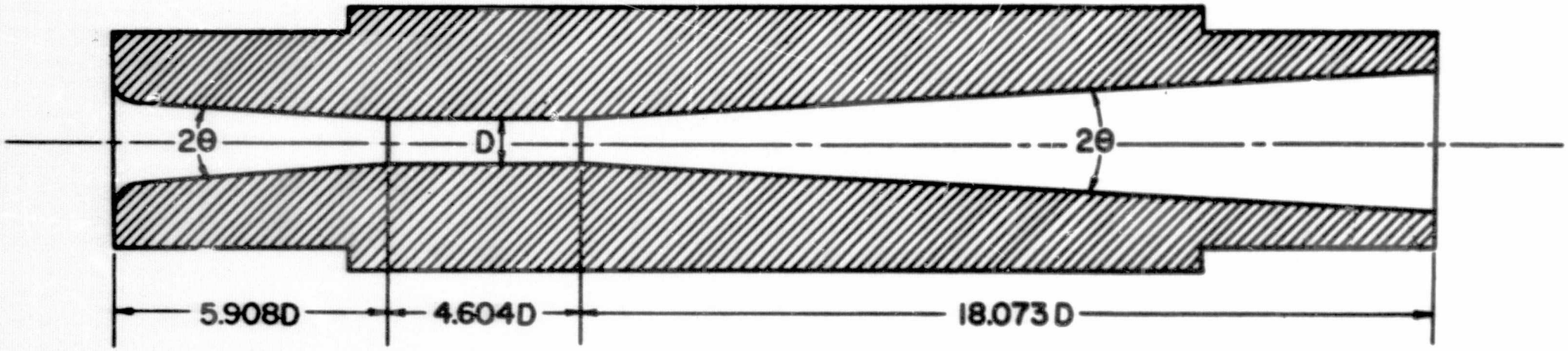

$$2\theta = \frac{5^\circ 54'}{6^\circ 04'}$$

D = 1/2 - INCH

1849

Figure 7. Basic Venturi Flow Path Dimensions

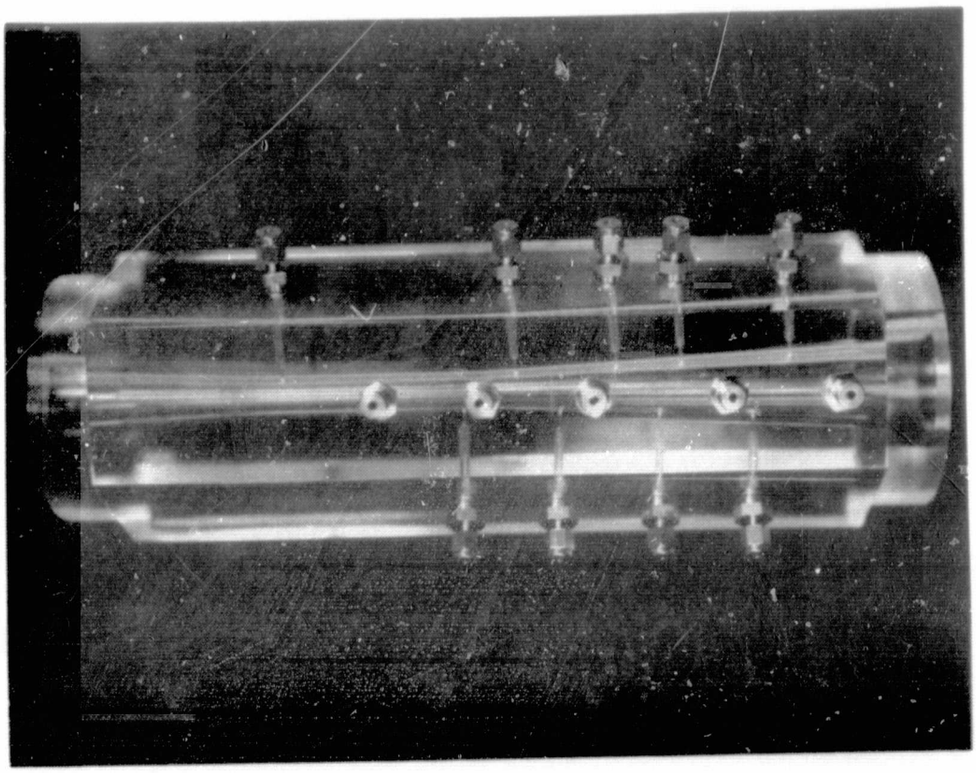

Figure 8. 3/4 Inch Plastic Scale-Effects Venturi, (534).

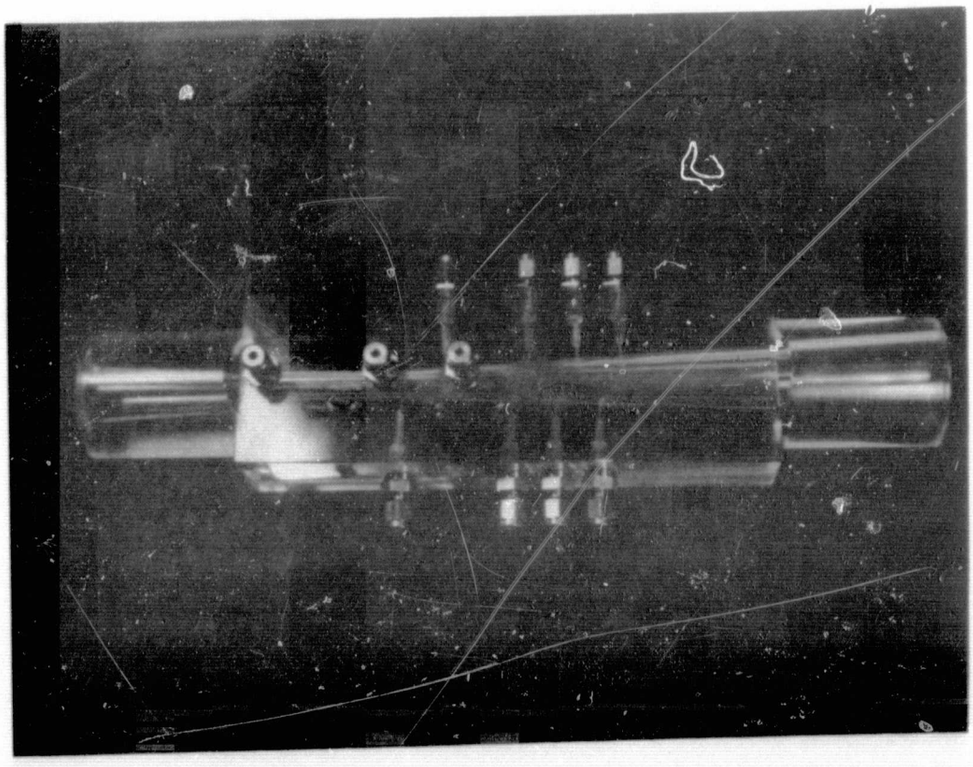

Figure 9. 1/2 Inch Plastic Scale-Effects Venturi, (412).

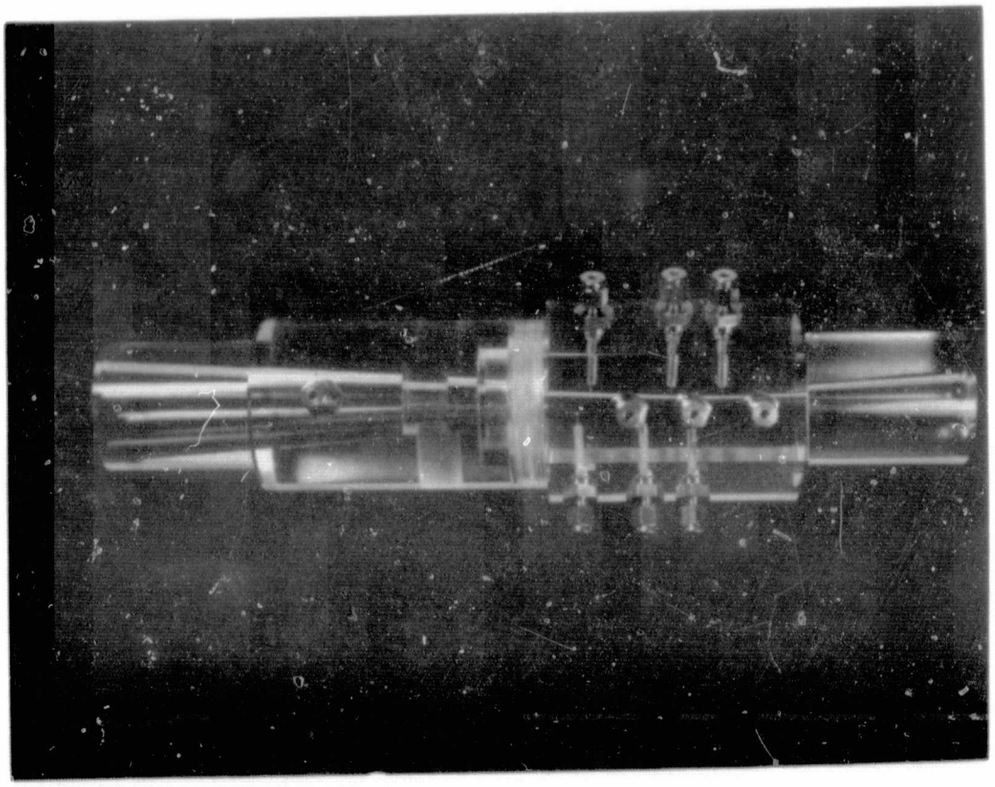

Figure 10. 1/4 Inch Plastic Scale-Effects Venturi, (614).

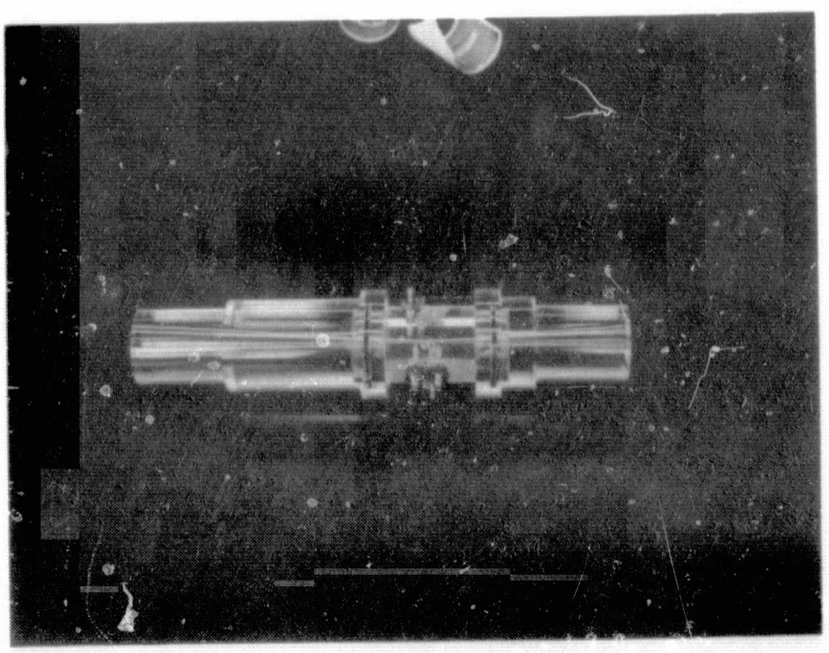

Figure 11. 1/8 Inch Plastic Scale-Effects Venturi, (818).

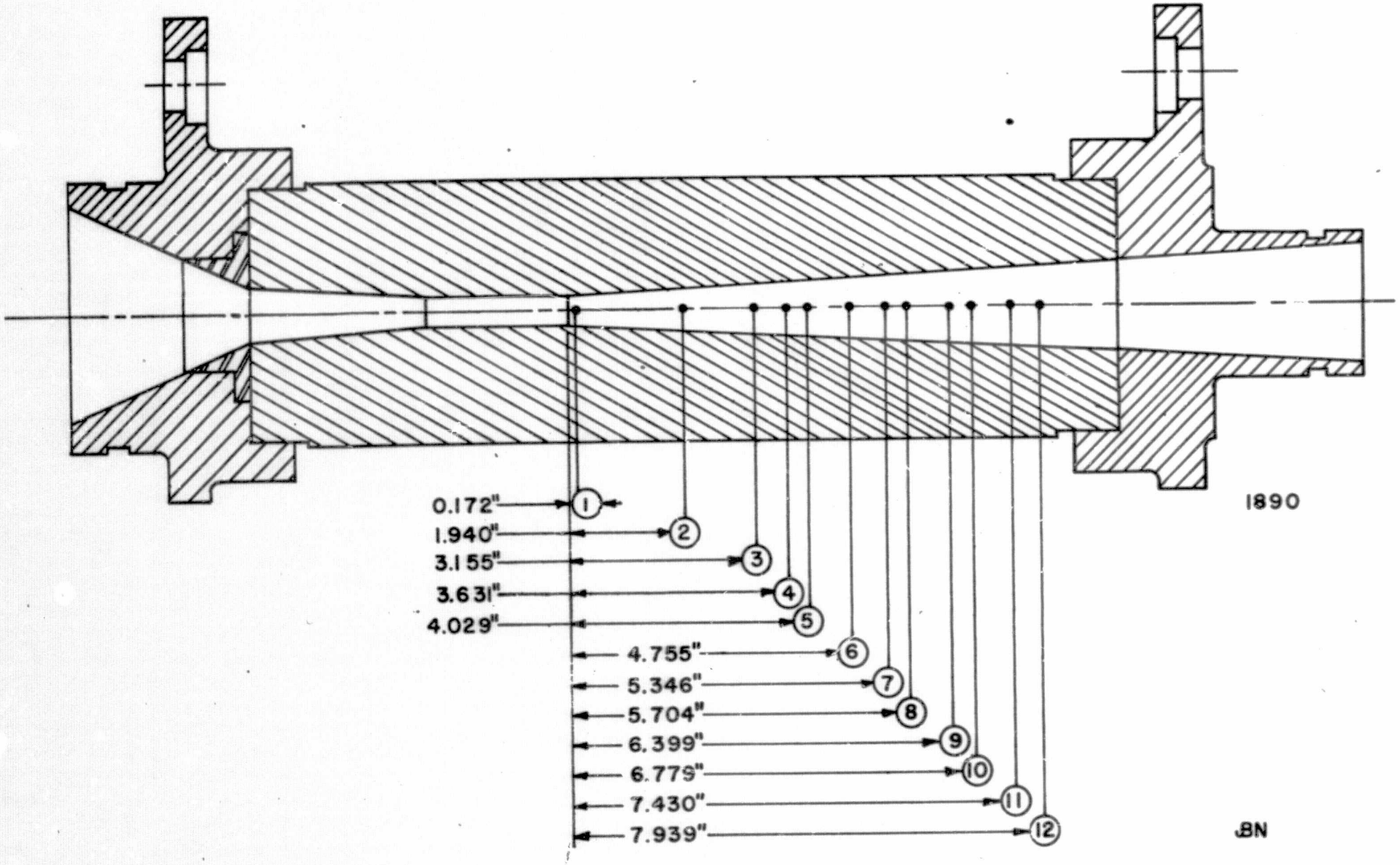

Figure 12. Pressure Tap Locations and Water Loop Installation Geometry for 3/4 Inch Plastic Venturi.

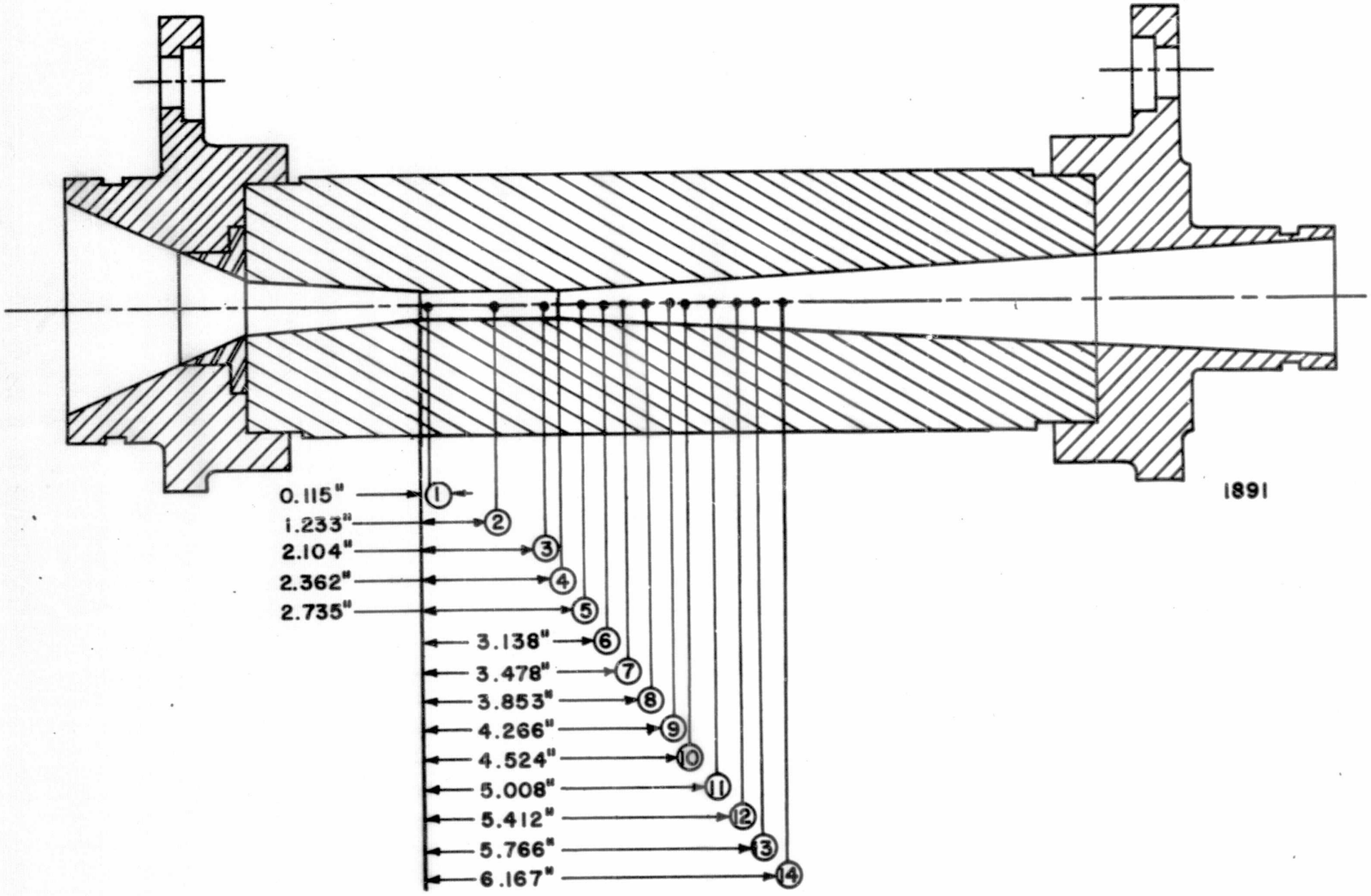

Figure 13. Pressure Tap Locations and Water Loop Installation Geometry for 1/2 Inch Plastic Venturi.

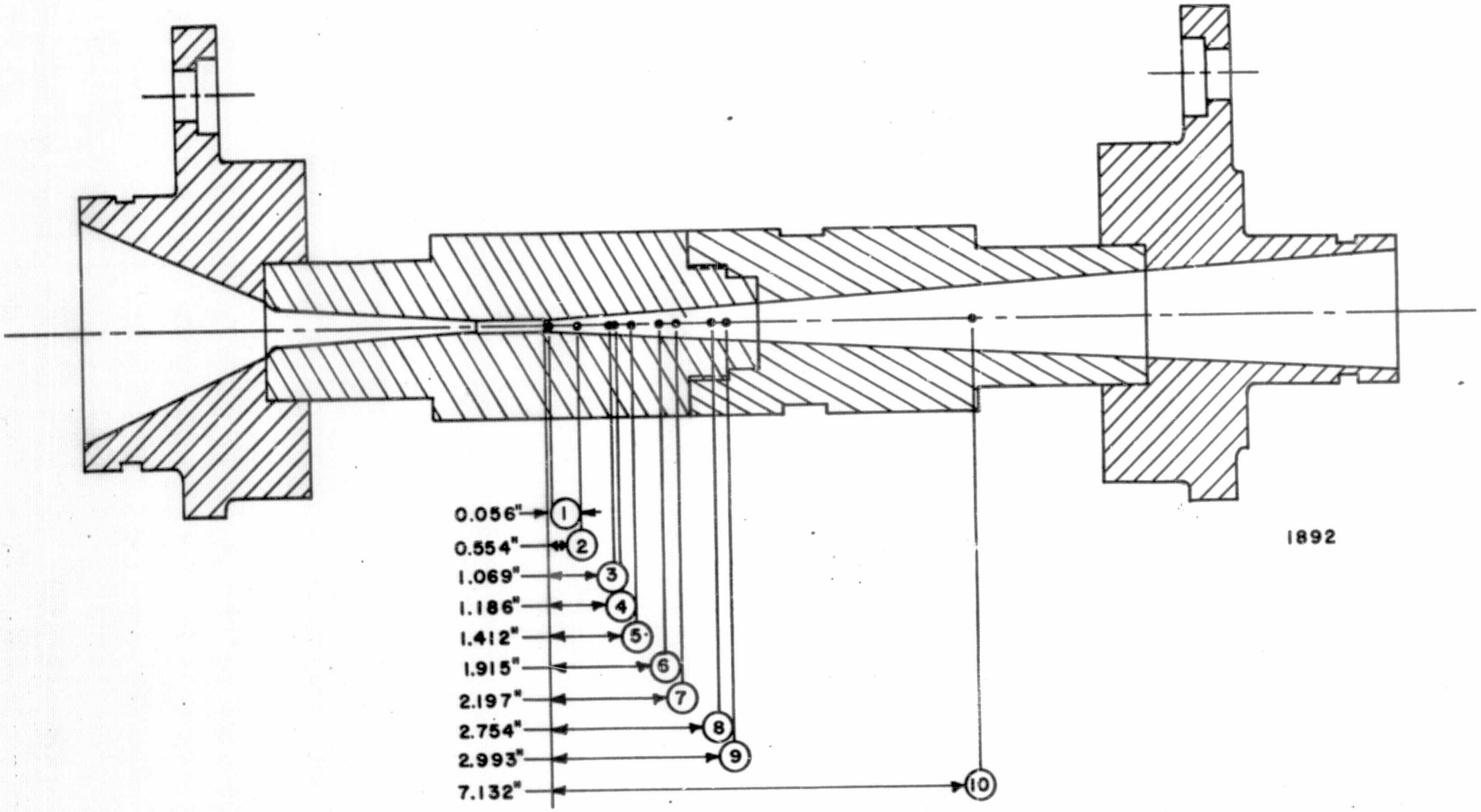

Figure 14. Pressure Tap Locations and Water Loop Installation Geometry for 1/4 Inch Plastic Venturi.

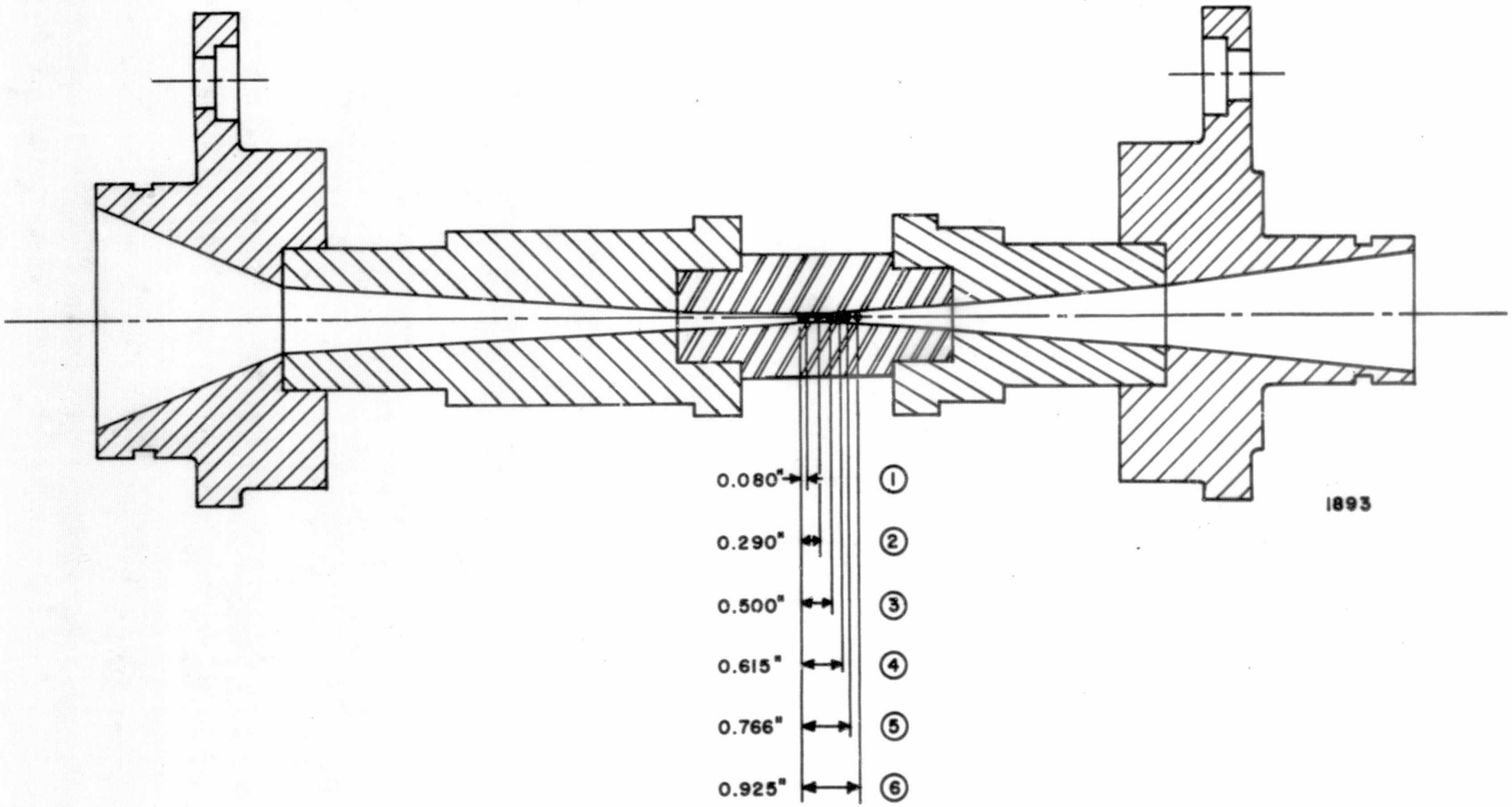

Figure 15. Pressure Tap Locations and Water Loop Installation Geometry for 1/8 Inch Plastic Venturi.

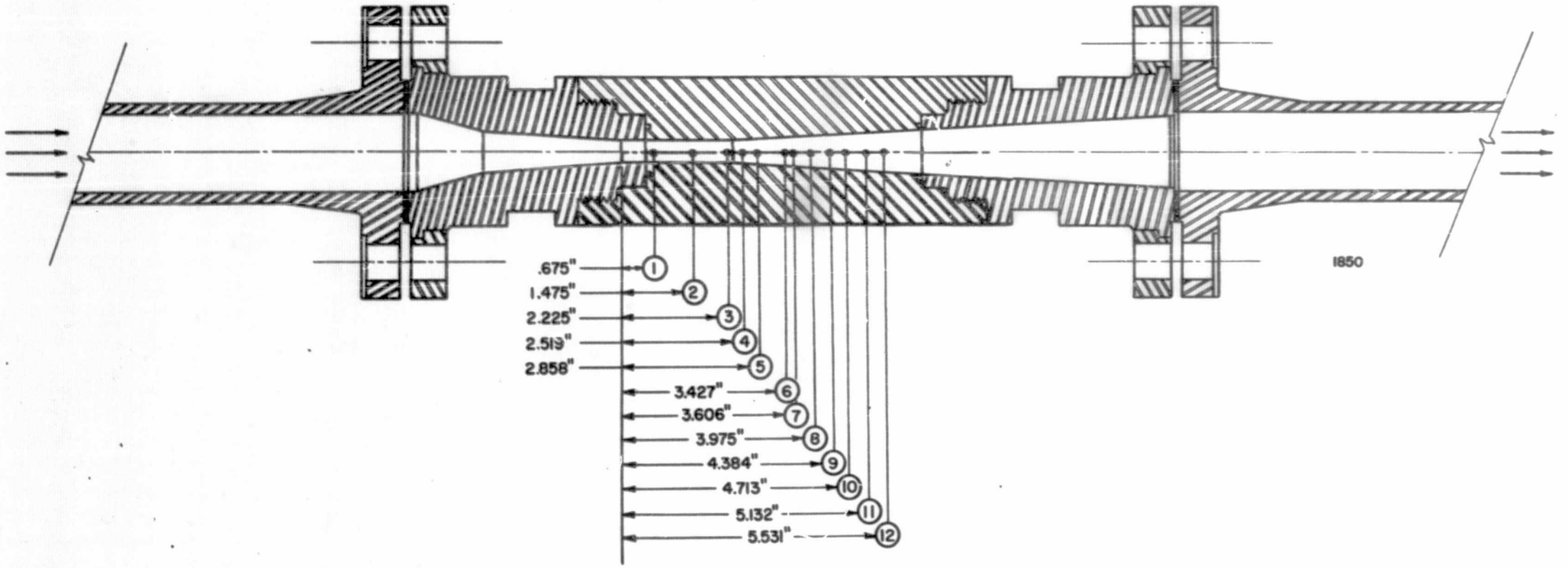

Figure 16. Pressure Tap Locations and Mercury Loop Installation Geometry for 1/2 Inch Stainless-Steel Venturi.

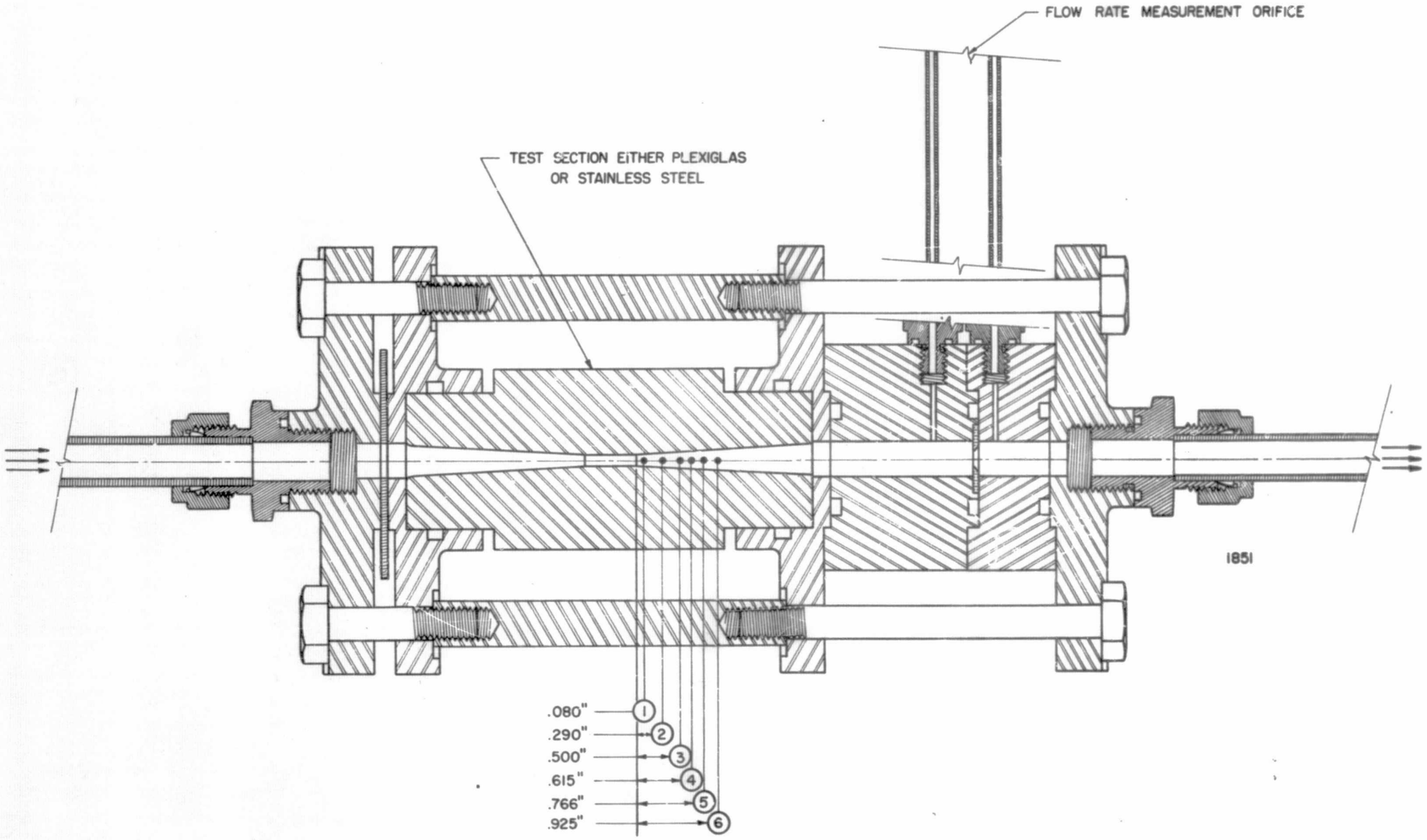

Figure 17. Pressure Tap Locations and Mercury Loop Installation Geometry for 1/8 Inch Stainless-Steel Venturi.

examined are discussed elsewhere (Appendix A) including definitions, significance and basis for particular choices. When the other venturis were designed an attempt was made to maintain geometric similarity of the tap locations, but in the case of the two smaller venturis (particularly the 1/8 inch) this was impossible primarily because there was insufficient room on the exterior surfaces for the necessary fittings. This lack of exact similarity is not considered to be detrimental, however, because the shape of the pressure profile and the minimum point are still adequately defined.

The pressure tap manifolding used in this work was quite simple. The flexible lines from the tap fittings on the venturi were joined through suitable unions to 1/4 inch stainless steel tubing and quick acting toggle valves. The output side of the valves was then connected to a manifold. The manifold in turn was connected through toggle valves to two precision Bourdon gages (Heise Gages) one covering the range -15 to + 45 psi and the other 0 to 600 psi. Thus by suitable selection of valves all pressures in the system could be read. Figures 18 and 19 show the manifold installed at the mercury tunnel facility. The low pressure gage and valves are visible on the cabinet, as is the line which connects the manifold to the high pressure gage which is installed and used in the regular loop control system also.

The procedure used to determine the pressure profiles was as follows. The pump speed, cooling rates, and gas contents were adjusted to provide the desired conditions i.e., flow, temperature and gas content, in the loop. Then the static pressure on the low pressure tank (in water loop) was set (or the throttling valve in the case of the mercury

examined are discussed elsewhere (Appendix A) including definitions, significance and basis for particular choices. When the other venturis were designed an attempt was made to maintain geometric similarity of the tap locations, but in the case of the two smaller venturis (particularly the 1/8 inch) this was impossible primarily because there was insufficient room on the exterior surfaces for the necessary fittings. This lack of exact similarity is not considered to be detrimental, however, because the shape of the pressure profile and the minimum point are still adequately defined.

The pressure tap manifolding used in this work was quite simple. The flexible lines from the tap fittings on the venturi were joined through suitable unions to 1/4 inch stainless steel tubing and quick acting toggle valves. The output side of the valves was then connected to a manifold. The manifold in turn was connected through toggle valves to two precision Bourdon gages (Heise Gages) one covering the range -15 to + 45 psi and the other 0 to 600 psi. Thus by suitable selection of valves all pressures in the system could be read. Figures 18 and 19 show the manifold installed at the mercury tunnel facility. The low pressure gage and valves are visible on the cabinet, as is the line which connects the manifold to the high pressure gage which is installed and used in the regular loop control system also.

The procedure used to determine the pressure profiles was as follows. The pump speed, cooling rates, and gas contents were adjusted to provide the desired conditions i.e., flow, temperature and gas content, in the loop. Then the static pressure on the low pressure tank (in water loop) was set (or the throttling valve in the case of the mercury

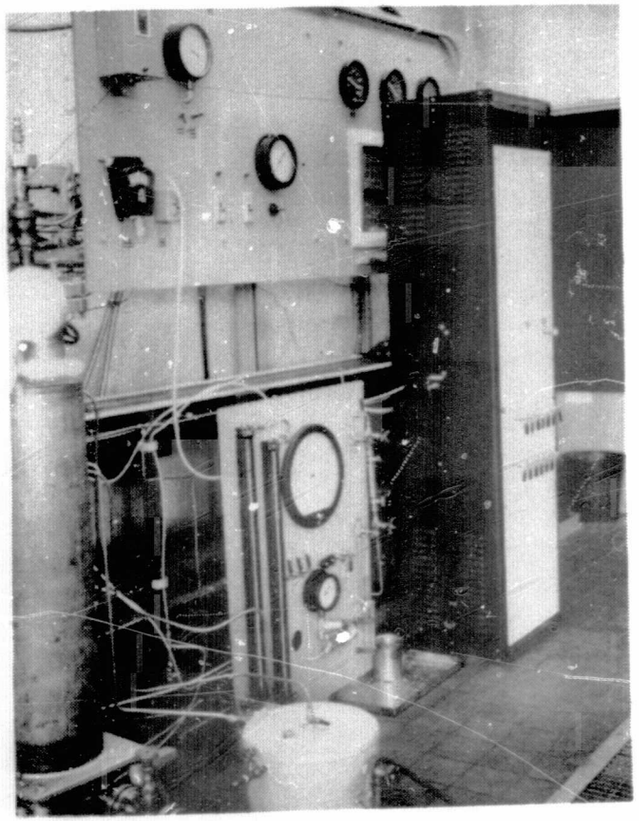

Figure 18. Pressure Tap Manifold and Mercury Loop Control Panel.

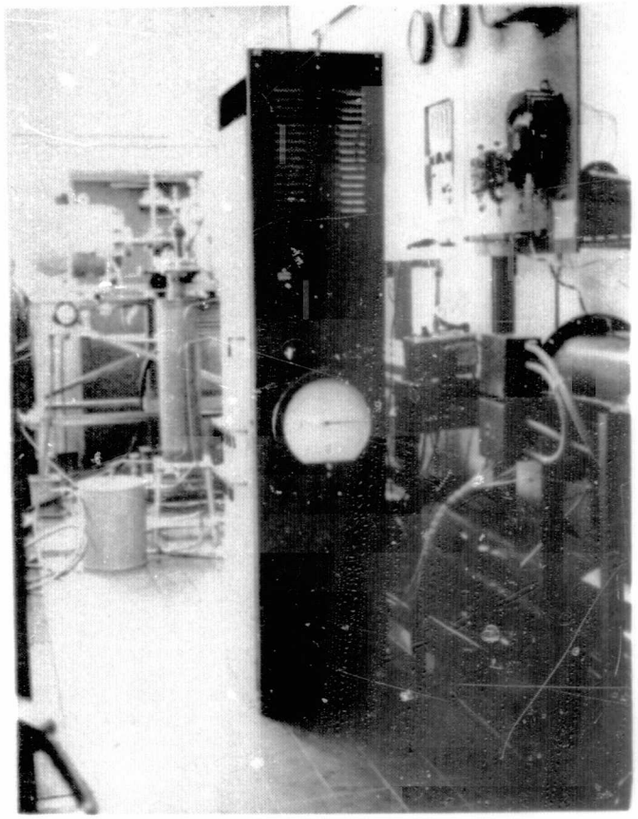

Figure 19. Pressure Gage and Presure Tap Lines.

loop) to establish the degree of cavitation for a particular run. At this point the various parameters (flow, temperature, system pressure, etc.) were recorded and the pressure profile taken by reading the various taps sequentially. During the pressure-profile readings, suitable samples were taken to determine gas contents. At the completion of the profile, the loop conditions would be "upset" and then the process repeated several times. This procedure enables one to then establish some confidence limits for the cavitation numbers calculated from the data for some initial set of conditions.

C. Gas Injection Apparatus and Gas Content Determination

For those tests conducted in the water facility, gas injection or addition was relatively simple. For all but the very highest concentrations, simply charging the system with fresh tap water was sufficient to increase the gas content which could then be reduced using the deaerator to the desired condition. The gas content of fresh tap water was approximately 2.5% by volume measured at STP. Also, since the water facility has parallel loops, only one of which was being used for scale-effects tests, simply opening a tap in the low pressure area of the throat of a venturi not in use would admit air to the system. The average transit time is short enough and turbulence levels are high enough in the system so that satisfactory homogenization occurs in just a few minutes. Figure 20 shows the appearance of the air bubbles in water near saturation as viewed under a high speed strobe light.

In the case of the mercury loop, the problem is somewhat more complex for several reasons. First, the scale-effects venturi

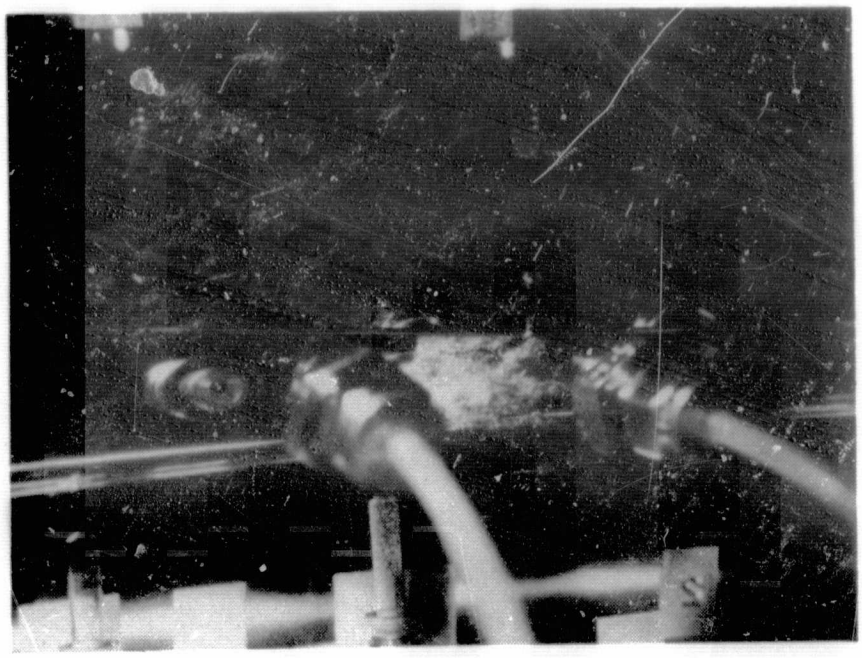

Figure 20. Typical Example of Air Bubbles in 1/2 inch Plastic Venturi with Water.

is the only one installed, so there is no convenient low-pressure point that can be bled to admit air. Second, air in contact with mercury tends to produce a surface scum, which can interfere with pressure measurements. Finally, the pump in this loop is a simple over-hung centrifugal pump running in a mercury sump with a free surface. Therefore, because gases are essentially insoluble in mercury, there is a disentrainment action taking place in the sump because of separation in the strong centrifugal field that exits there so that to maintain a fixed gas content requires continuous addition of gas to the loop.

The development of a system for gas injection and sampling in the mercury loop has been reported in detail[47], however, some pertinent points are discussed here. The schematic diagram of Figure 4 also shows these sample by-pass lines. Two 1/4 inch stainless steel sampling lines were used, one at the pump discharge (i.e., upstream of the test section) and the other downstream of the test section throttling value. Each line runs to a location on the facility control board where sampling capsules can be inserted between a pair of isolation values. The lines are joined downstream of the sampling point. A differential manometer is used to determine the ΔP across a straight section of the tubing to provide bypass flow rates. The manometer ΔP had been previously calibrated against a known volumetric flow rate. The sampling capsules and lines are visible in Figure 18.

Plates containing radial holes for the gas injection tube and the sampling tube were inserted between flanges at the locations cited

above. Figure 21 shows the upstream plate with both the injection and sampling tubes in place. For these tests only a sampling tube was inserted in the downstream plate. The sampling tubes were pointed upstream parallel to and on the pipe centerline. The tube end was suitably tapered (reduced in area) so that the flow velocity at tube inlet would be approximately that in the mainstream, even though the velocity generally existing in the bypass line was much less, and thus the flow pattern about the sampler would not deflect gas bubbles away from the tube (i.e., isokinetic sampling was used).

The injector used was made from 1/8 inch diameter stainless steel tubing. A section of tube was squeezed shut at one end, then ground off with a hand stone until a fine slit was visible. The center of the tube was then driven shut so that two separate openings were available which, as test in water indicated, provided good atomization. The injector needle is visible in Figure 21. The sampling tube and the injection tube each entered at an angle of 73° from the pipe axis, pointed upstream and downstream respectively, which increases the separation and minimizes flow interference between them. Thus gas was injected into the flow downstream of the upstream sampler. The injection apparatus is shown schematically in Figure 22. The bubbler was used to eliminate the possibility of a blocked injection orifice remaining unnoticed. Although the bubbler contained water, the level was unchanged after several hundred hours of gas flow, so it is quite certain that no measurable water vapor was carried into the loop. A typical view of entrained gas in mercury is shown in Figure 23.

One of the most frequently used methods for measurement of

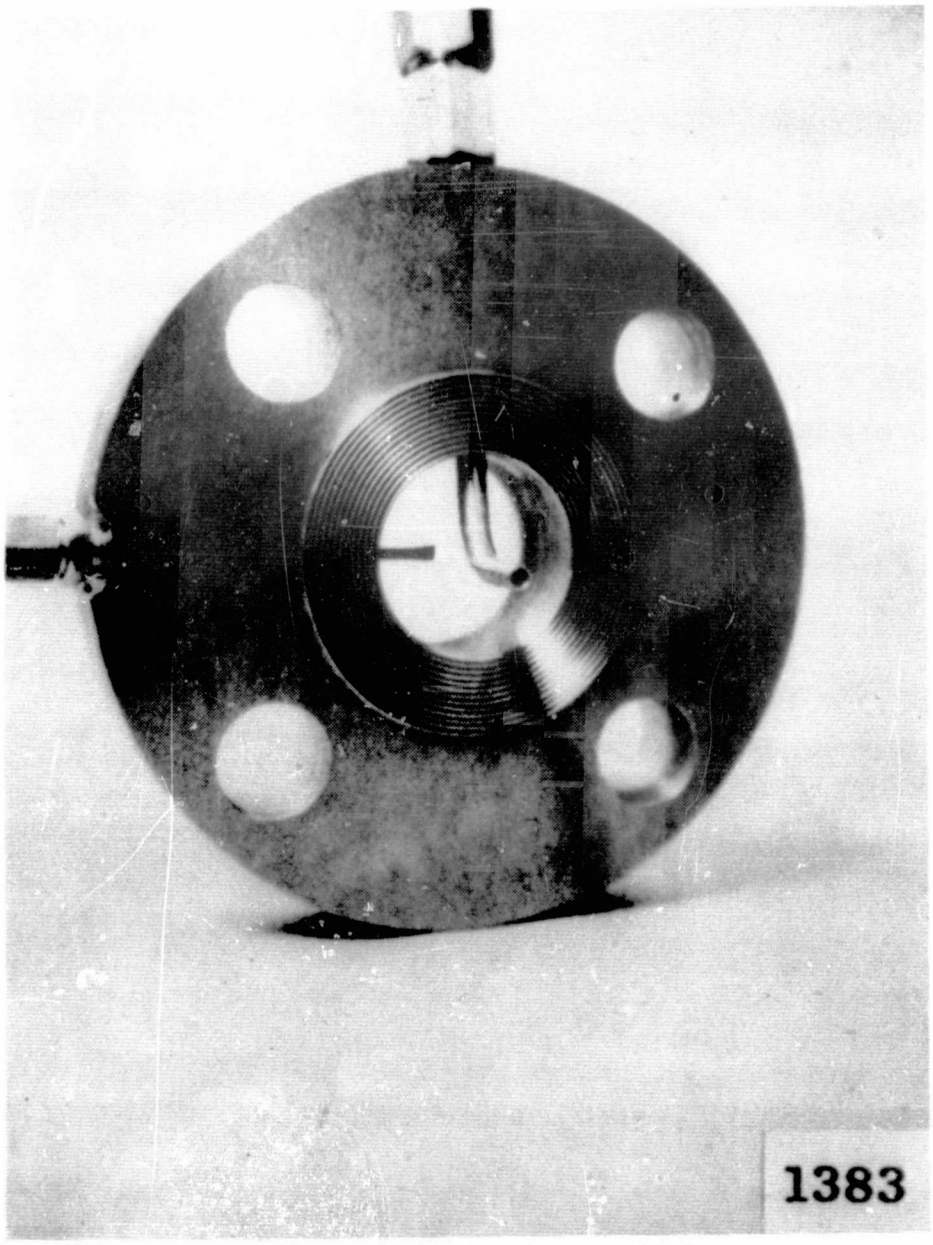

Figure 21. Plate for Insertion Between Flanges, Showing the Tapered Mercury Bypass Sampling Tube with the Gas Injection Tube in the Background.

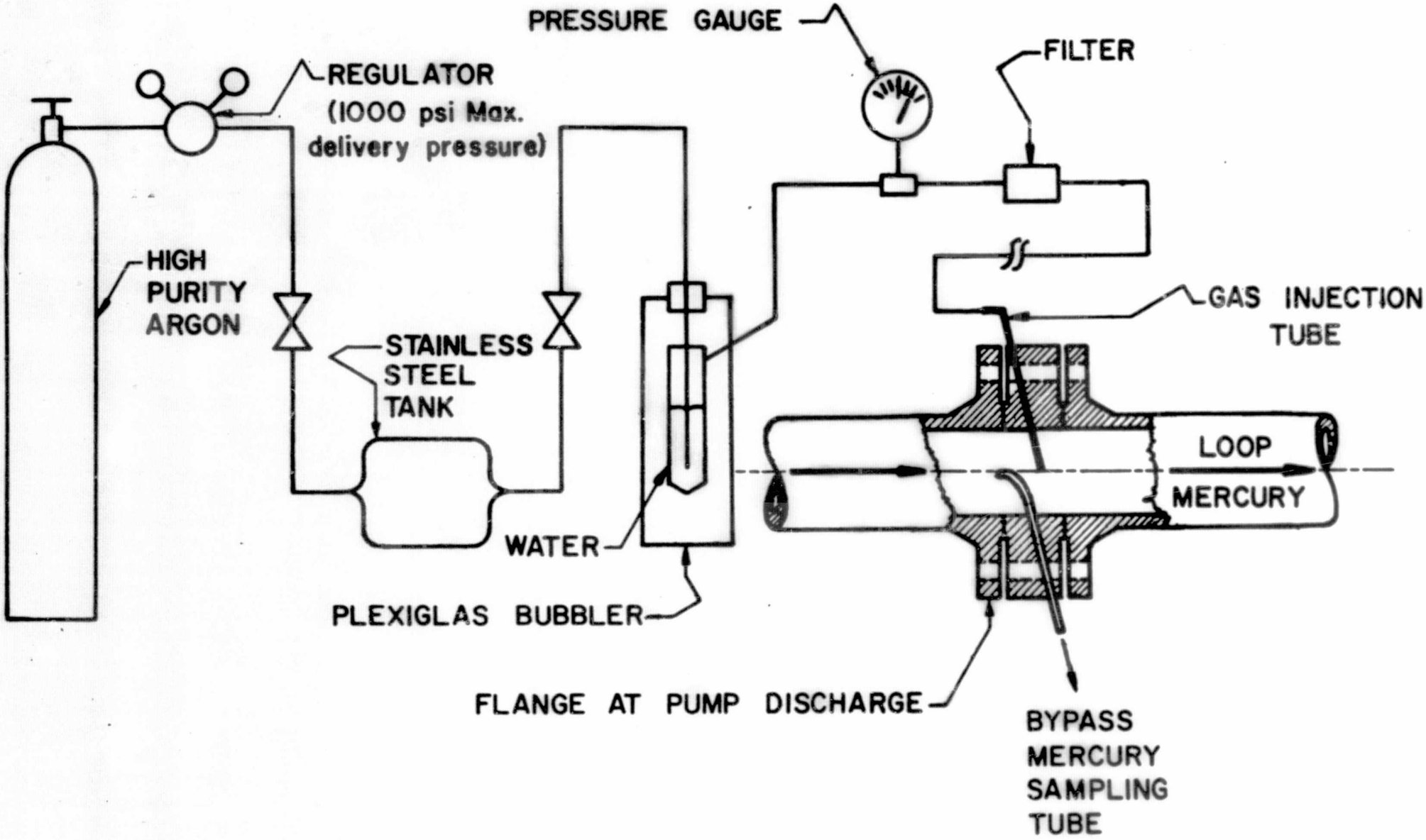

Figure 22. Gas Injection on Mercury Loop

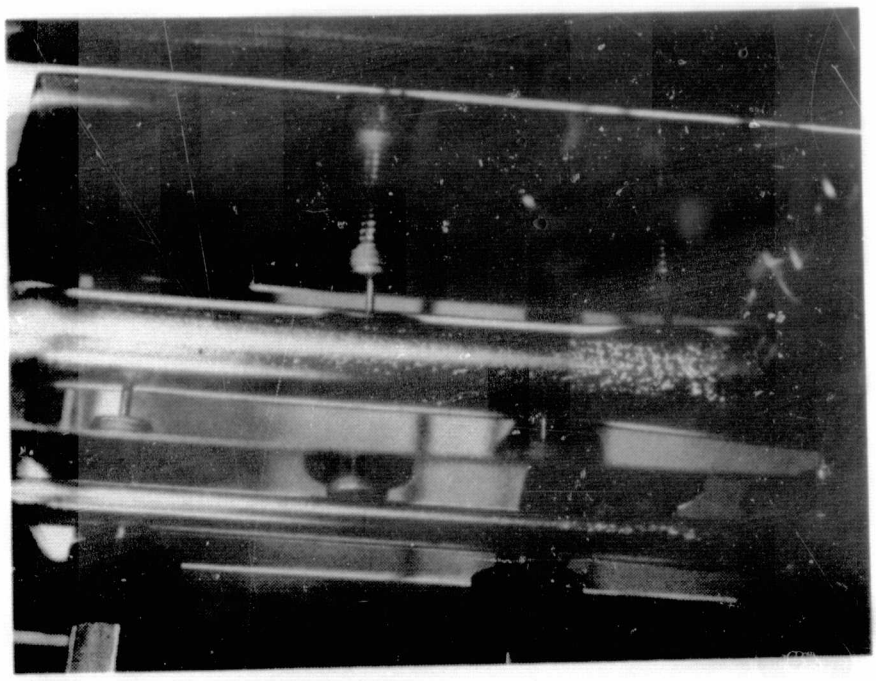

Figure 23. Typical Example of Gas Bubbles in 1/2 inch Venturi with Mercury.

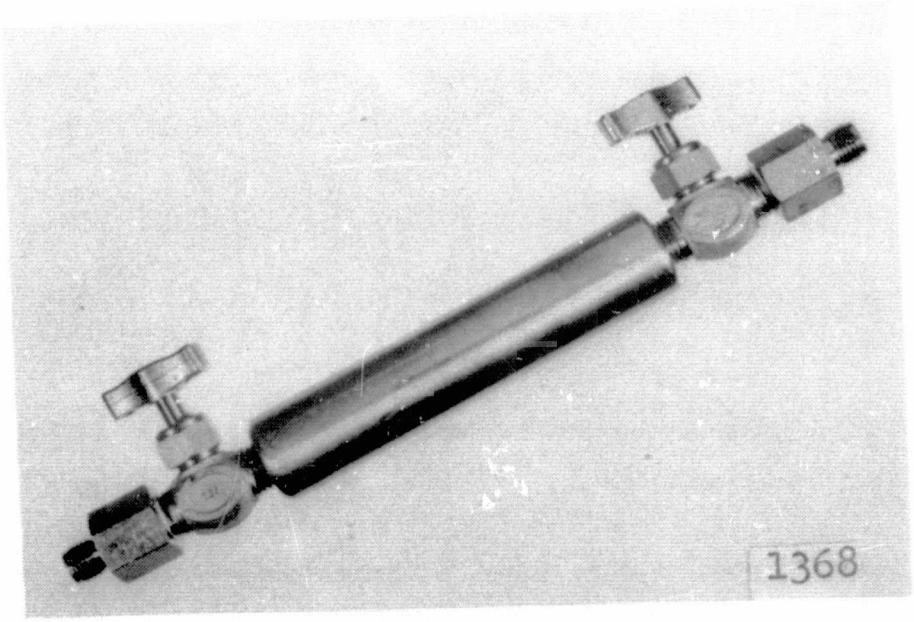

Figure 24. Stainless-Steel Sampling Capsule

gas content in water in cavitation laboratories is a Van Slyke apparatus. The water sample extracted from the test facility is usually transferred by pouring into a graduated cylinder on the Van Slyke instrument. Because most of the gas is dissolved rather than entrained in this case, and at less than the saturation concentration, there is negligible error introduced by the small amount of pouring in the presence of air. Thus for the water loop work standard Van Slyke techniques were used[48]. With mercury however, gas solubility is essentially zero, so the gas to be measured is entrained in small bubbles. Obviously then, if a pouring technique were used considerable error might be introduced because some of the buoyant bubbles would be lost. To preclude this error, closed stainless steel capsules shown in Figure 24 were used to transfer the mercury samples from the mercury loop to a modified Van Slyke. The modified Van Slyke arrangement to accommodate the capsules is shown schematically on Figure 25. The use of a Van Slyke for the measurement of gas in mercury is unique to this study so far as we know, but apparently was successful. In fact the procedures used are to be patented by the AEC, which supported this portion of the work. Because this technique differs from the usual Van Slyke procedures it is presented in some detail in Appendix B.

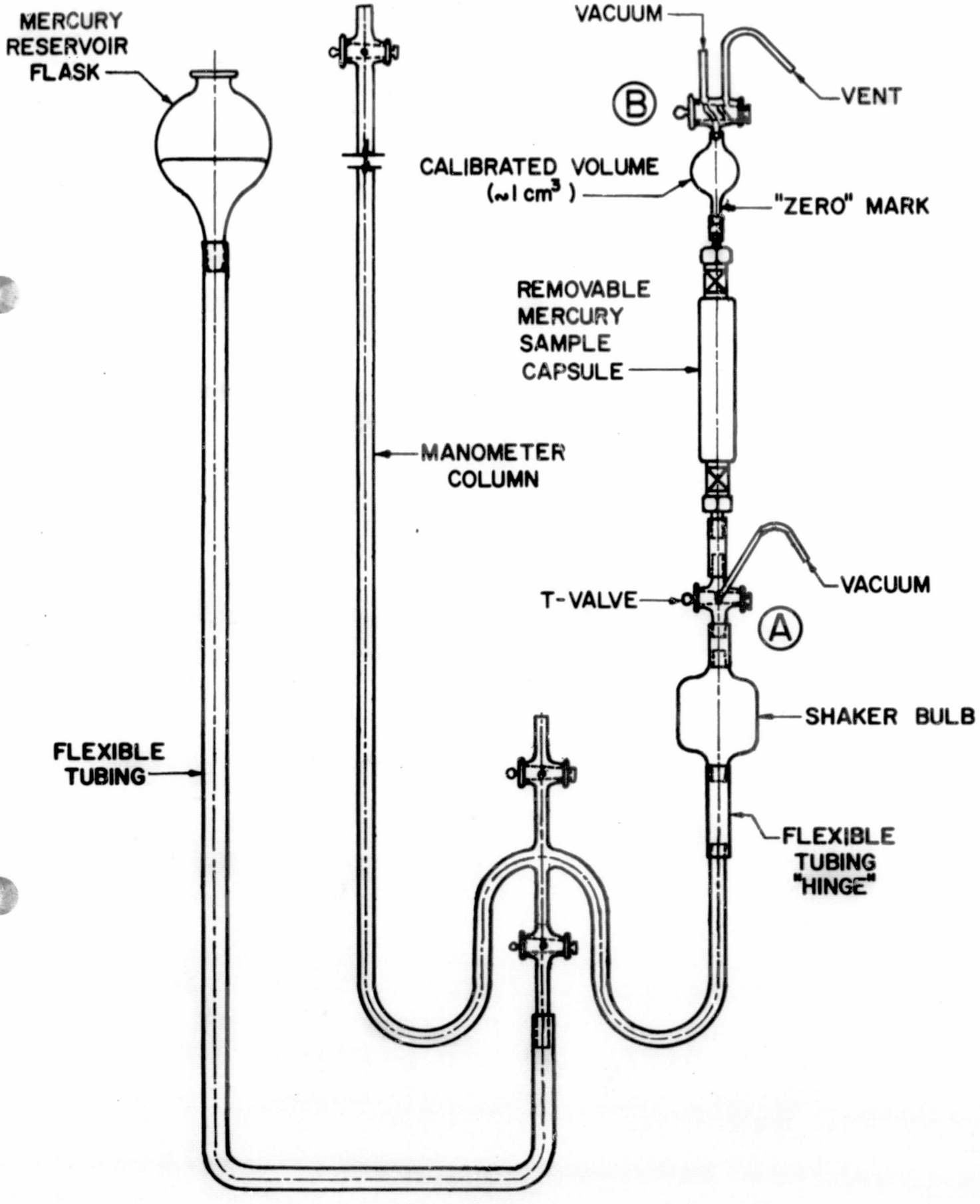

Figure 25. Modified Van Slyke Layout

CHAPTER IV

EXPERIMENTAL OBSERVATIONS

The data gathered in the course of this work can be represented either in graphical or tabular form. It is presented here graphically for two reasons; first, the ease with which large amounts of data can be handled in graphical form; second, it facilitates the comparison with the results of other workers who have in some instances only examined the effects of a single variable. The results and implications outlined here are the basis for the broader correlations discussed in Part V. A machine tabulation of the reduced data is included as Appendix G.

To analyze experimental data where one is primarily interested in the effect upon the dependent variable induced by variations in several independent variables, the ideal first step is to examine the dependency for each of the variables singly, i.e., vary one with the others held constant. Unfortunately, this is generally not possible in real cases because so many physical variables are interrelated; for example, in this study the variations induced by temperature changes will also include, but not be limited to, effects from density, viscosity, and vapor pressure variations, which are themselves temperature dependent. Furthermore, in the fluid systems used in this study it is impossible to adjust the experimental conditions to preselected values for the independent variables, especially in the case of temperature and gas content. Thus, it is occasionally necessary to consider

a range of values for one variable. Generally this range is believed to be narrow enough that the trends observable in cavitation number as function of one variable with the others "fixed" are valid. Likewise, it is believed that the correlation techniques employed later are sufficiently broad in scope in order to account for these minor variations. It is with these limitations in mind that the following discussions are presented. Unless otherwise stated, the cavitation condition under consideration is visible initiation or condition B as it is described in the definition of cavitation conditions in Appendix A. With this particular system it is possible to determine pressure before and after the venturi so that theoretically at least, one could relate the extent of cavitation to the total pressure drop across the venturi. However, because it was not clear at the start of the study that all three gases used (air, argon, and hydrogen) would behave the same way, the data is based upon a visual, or in the case of the stainless steel venturis, an acoustic, observation of the degree or extent of the cavitation. It turned out that a given volume percent of hydrogen has a much greater effect upon cavitation number than the same volume percent of air and this is discussed later.

Prior to presentation of the cavitation data it is perhaps wise to examine the range of variables available to the study. In Table 2 the maximum and minimum values of the variables and their ratio are presented. For water, with the possible exception of surface tension, the ratios are acceptable. In mercury, neither the viscosity and surface tension varied as much as might be desired.

TABLE 2

RANGE OF THE EXPERIMENTAL VALUES

A. Water

	V (ft/sec)	D (in)	μ (#/ft sec)	σ_{st} (#/ft)	ρ_v (#/ft^3)	T (°F)	Vol %
Minimum	64	.125	3.18×10^{-4}	4.46×10^{-3}	112×10^{-4}	50	.5
Maximum	220	.75	9.25×10^{-4}	4.99×10^{-3}	6.5×10^{-4}	135	2.3
Ratio	3.4	6.2	2.9	1.2	17.3	2.7	4.6

B. Mercury

Minimum	22	.125	.000672	.02996	$.0345 \times 10^{-5}$	55	0.01
Maximum	47	.50	.00104	.0319	136.8×10^{-5}	415	3.2
Ratio	2.14	4	1.55	1.06	39700	7.55	320

A. Gas Contents Effects in Water

1. One-half-inch Throat-Diameter Plastic Venturi

Because the 1/2 inch diameter throat venturis have been used for some time for various cavitation studies in this laboratory this throat diameter was adopted as the "base line" for the present investigations and therefore is presented first.

In Figure 26, the cavitation number σ_c is plotted as a function of gas content with the velocity in the venturi throat the parameter. For these points the water temperature ranges from 50 to 55°F at 64 ft/sec and approximately 70 to 80°F at 220 ft/sec. These represent the lowest temperatures that can be attained in the system, because even with full cooling water flow, the pump work input establishes these steady state conditions. The highest gas contents reported here are approximately equal to saturation conditions at STP. The several trends are readily apparent.

The cavitation number σ_c increases with air content, and indeed, one intuitively expects this sort of behavior assuming that the more air present the greater will be the percentage not dissolved but simply entrained, and thus the greater the number of nucleation sites that will be made available. In fact, one difficulty with treating gas content effects in water is that although this sort of qualitative statement is valid, there is no exact and convenient way in which the division of the gas between entrained and dissolved states can be determined. The Van Slyke method for gas determination used here (See Chapter III) gives only total gas content. Techniques involving sonic probes have been used in which the signal attenuation

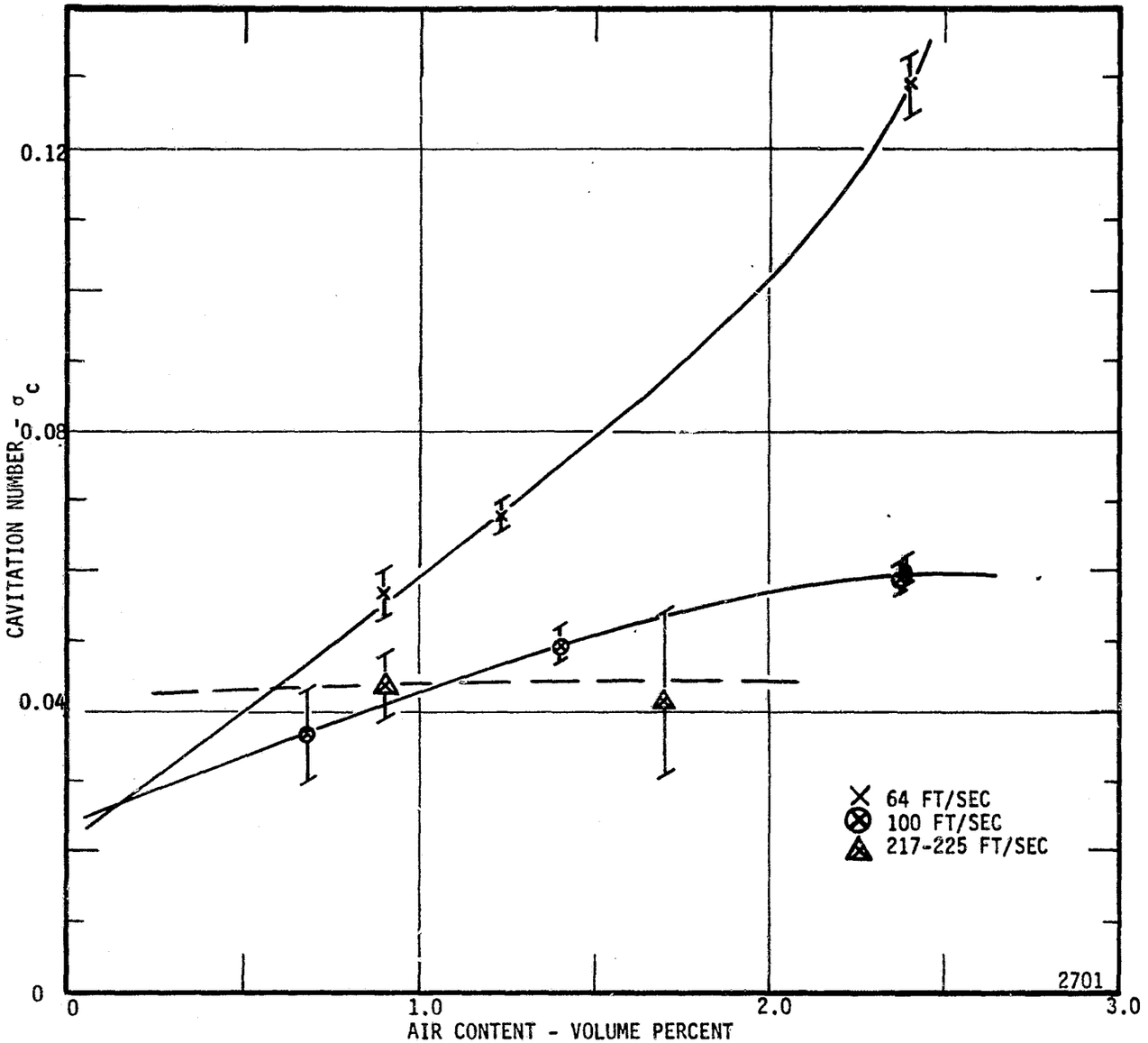

Figure 26. Cavitation Number versus Air Content, Venturi 412, Cold Water.

is used to establish entrained gas content making some assumption as to homogeniety and form of gas distribution. However, the apparatus is highly complex and the interpretation of the results somewhat uncertain at present so that development of such an instrument was not attempted in this study. Only a limited number of cases are treated here in which the gas content exceeds the saturation value at STP, and most of the gas can be assumed to be in solution, therefore only the total gas content as determined by the Van Slyke techniques is reported.

Similar cavitation number trends with increasing gas content have been reported by Ruggeri and Gelder[19] for "audible" initiation although that work did not cover as wide a range in air content or velocity as reported here. They report no gas content effect for their "visible" initiation, but "visible" in their tests is roughly equivalent to "Condition C" in this work, that is, a well established cavitation state and one for which the present study also revealed no major effect from gas-content changes. The results here also agree with the conclusions of Narayanon[35] who observed that in a pumping system σ_c increases as air is added. Straub and his co-workers[33,34] have reported similar trends, and the air-content work by Holl[14] can also be interpreted in this manner. Lehman and Young[20] report no effect on cavitation with variations in the gas content over the range of saturation to 25% of saturation at STP. However, there was no separation of the flow from the walls in their venturi such as occurs in the present instance. Holl[16], while investigating the effects of surface roughness, also found no influence of gas content

over the range of 5 to 15 ppm (moles of air per million moles of water, or about 0.6 to 1.8 volume percent at STP) unless the roughness was such that flow separation was induced. The mechanisms involved in this effect of separation are not completly understood. The severe pressure discontinuities associated with the separation may trigger growth of gas bubbles that are too small to grow otherwise, or the void adjacent to the wall may serve as a trap for gas that is subsequently entrained by vortex action in the region of separation.

It is also readily apparent from these data that the influence of the gas content decreases as the flow velocity increases and this has also been observed by other investigators[14,19]. The reason for the diminishing influence of gas content is not clear as yet. The argument has been made[14,37] that there is a constant gas pressure in the bubble regardless of fluid velocity. Because this pressure is added to p_v its effect upon σ_c is less for larger values of $V_T^2/2g$. Another possibility is that at the higher velocities the residence time in the area of low pressure is insufficient for nuclei to grow to an observable size. An alternate explanation is that in recirculating flow facilities such as the University of Mighigan water loops, as one increases the velocity, the system total pressure must also be increased in order to establish and maintain a given cavitation condition. Thus, gas may be forced into solution in the remainder of the system. For example, for "Condition B" cavitation in our system, the pressure on the sump tank, i.e., pump inlet, increases from 8 to 10 psig at 64 ft/sec to 280 to 290 psig at 200 ft/sec.

The problem with this argument is, of course, the cross-over in the 100 ft/sec and 215 ft/sec curves at lower gas content (Figure 26). Additional comment on this point is presented below.

Data taken at temperatures from 95 to 110°F over considerably fewer values of gas content reflect no significant variation in with gas content. These data are shown in Figure 27, although obviously any conclusions drawn from such a limited amount of data must be viewed as extremely tentative, and preliminary. The gross trend at 220 ft/sec is discounted because of severe problems in operating the loop at constant temperature and gas content at this flow rate. The thermodynamic effects and other temperature dependent factors (which are discussed below) may be masking and perturbing the gas content effects. As has been pointed out earlier, this inability to completely isolate single effects is one of the more severe experimental difficulties encountered in cavitation research.

A question that has not been answered in the above, but which is pertinent, is the effect of increasing the gas content above STP saturation values, that is, increasing the likelihood that the system contains substantial "entrained" and not just dissolved air. Standard conditions still provide a convenient reference for discussing gas content. When the experiments were run at these higher gas contents it was found that in every case the observed σ_c was lower than that for the saturation condition, an observation which was inconsistent with known arguments. At this point, it was noted that the operational procedure on the water loop had involved maintaining the pump inlet pressure considerably above that for cavitation initiation (especially

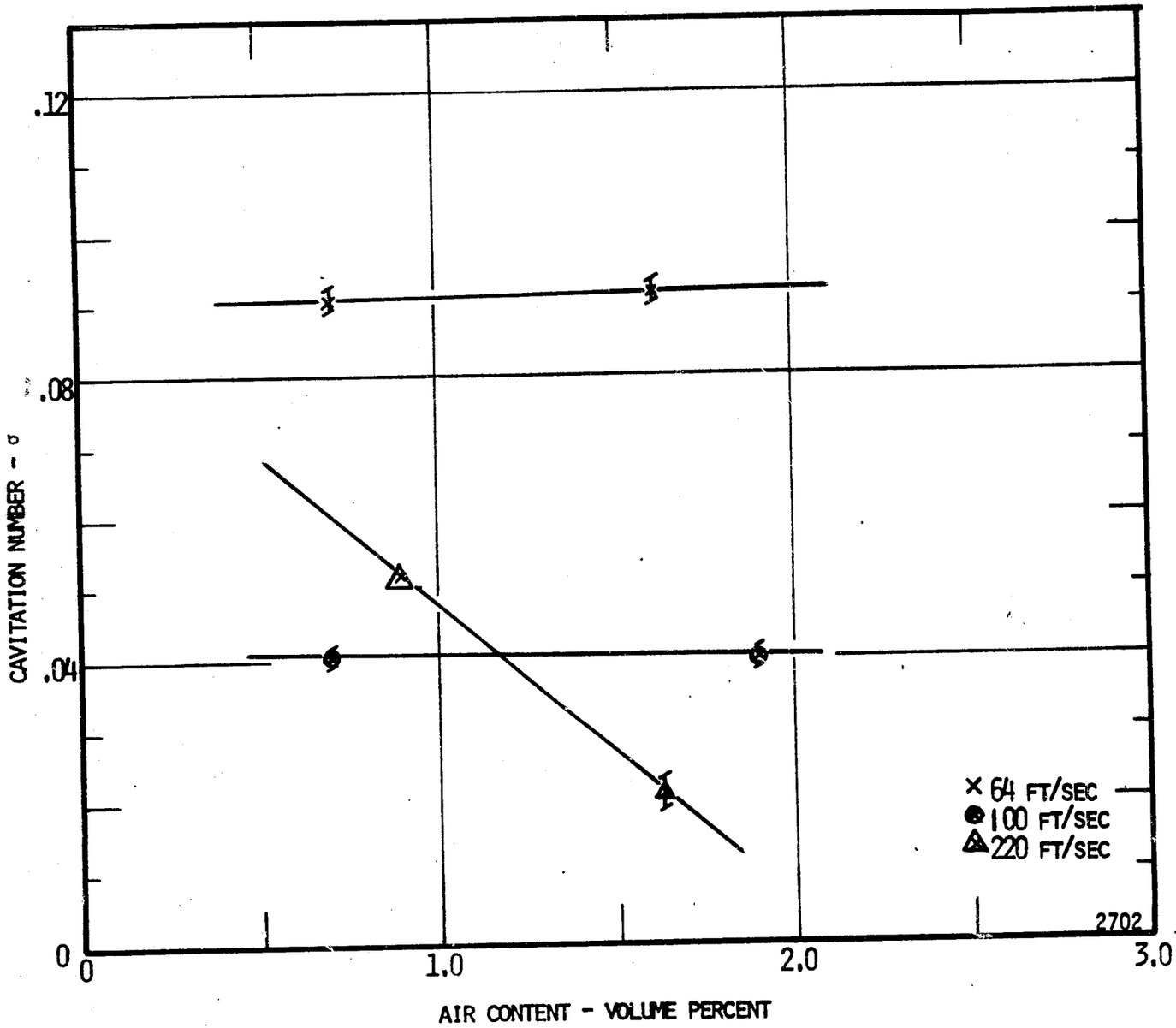

Figure 27. Cavitation Number versus Air Content, Venturi 412, Warm Water.

at the lower velocities) while air was being admitted and the air content evaluated simply because the system operates more stably this way. Arguments and data have been reported[20,50] indicating that pre-pressurization leads to increased tension capabilities (i.e., lower cavitation numbers) in water, therefore, several supplemental experiments were conducted. The system was set up with 2.25% air by volume and the pump intake pressure increased to approximately 400 psig (near maximum for this system) for about one hour. Cavitation was then initiated and pressure profiles recorded over several hours. The results are shown on Figure 28, Curve I. Subsequently, prior test data were examined for similar trends, which may have been masked by the averaging process in the computerized program for data reduction, and Curves II and III resulted. This short test appears to confirm the pre-pressurization theory. However, to adequately explore this phenomena would require a system capable of much higher static pressures, i.e., several thousands pounds per square inch. It is completely obvious though that the effects of variation in gas content depend significantly on the previous history of the fluid and thus, presumably on the gas disposition, that is, whether dissolved or entrained, bubble size spectrum, etc.

2. Three-quarter-inch Throat-Diameter Plastic Venturi

The data available from tests in the 3/4 inch venturi (shown in Figure 29) is not nearly as conclusive as that from the 1/2 inch venturi. Experimental difficulties forced us to accept data from a wider range of temperatures than really desirable for a given velocity.

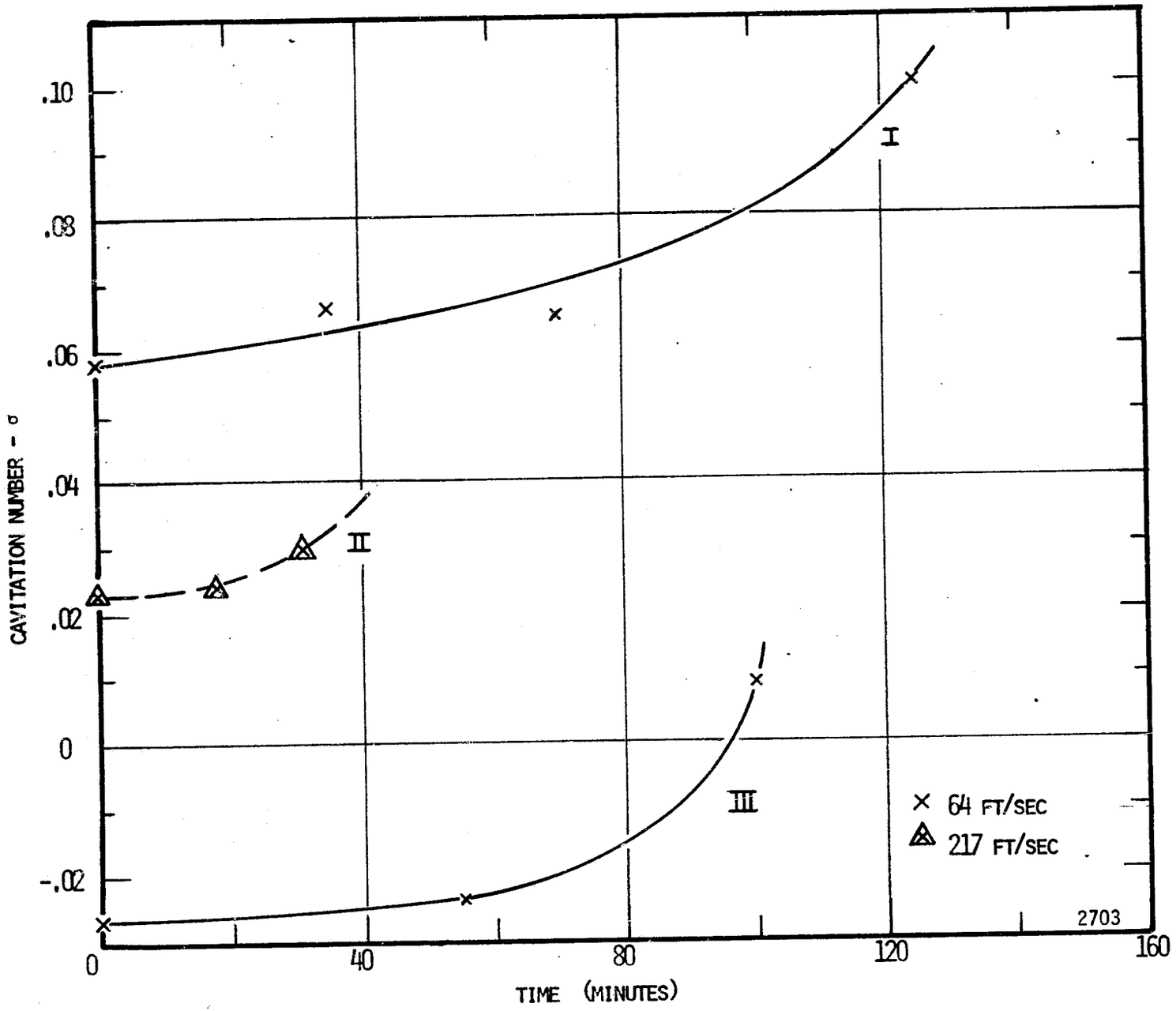

Figure 28. Cavitation Number versus Time After Initiation, Prepressurized Water, Venturi 412.

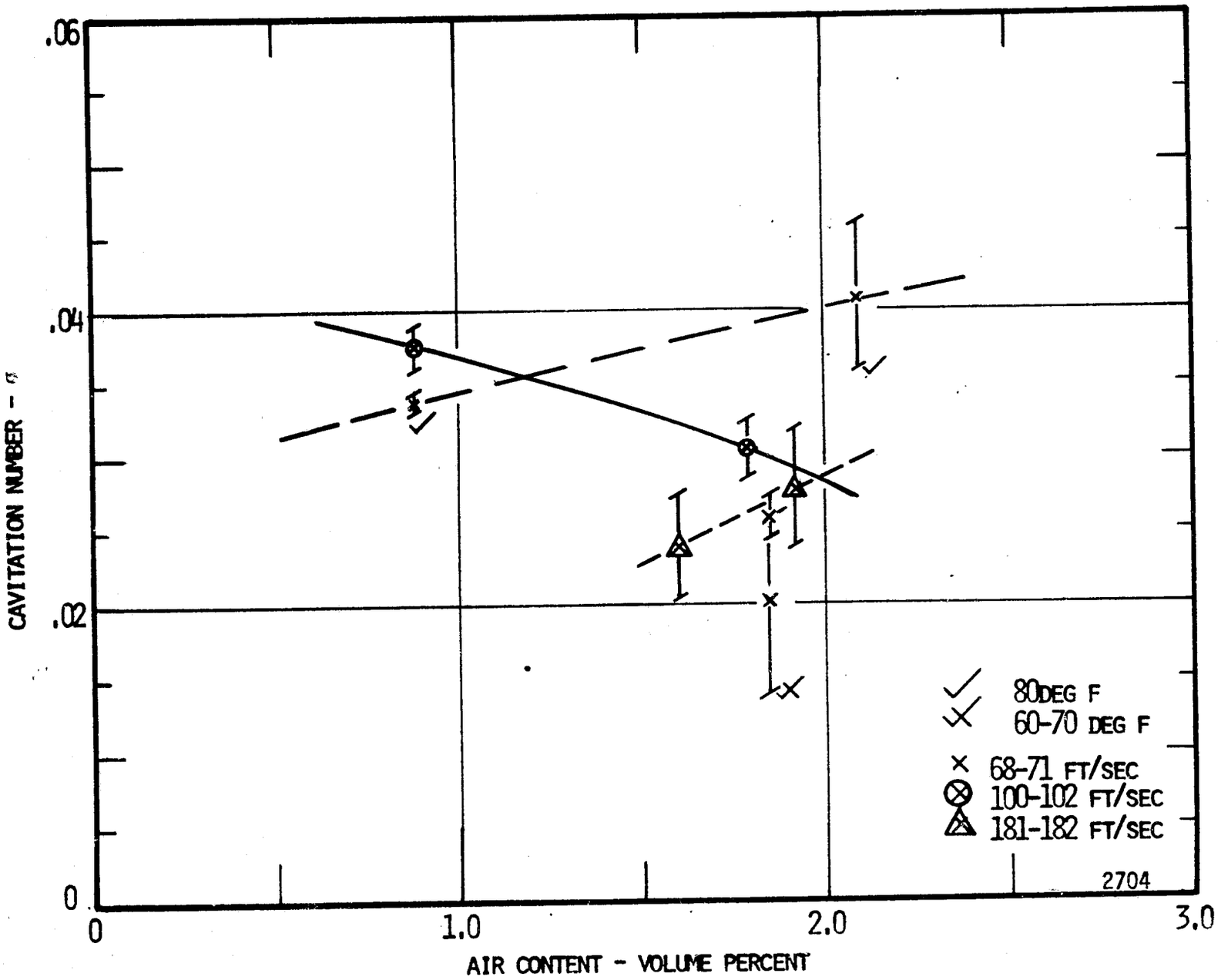

Figure 29. Cavitation Number versus Air Content, Venturi 534, Water.

For the low and high velocity cases, however, enough data are available to indicate agreement with the earlier trends. At 100 ft/sec, the decrease in σ_c with increasing air content is in all probability caused by thermal effects discussed below. It is observed that in this range the variations were to a first approximation

$\Delta\sigma_c / \Delta T \simeq .0005 \rightarrow .001.$

3. One-quarter-inch Throat-Diameter Plastic Venturi

The experimental data from the 1/2 inch venturi shown on Figure 30 agrees quite well with that from the 1/2 inch venturi. The cavitation number increases with increasing air content although this effect is lessened as velocity increases. One difference in the qualitative nature of the data between the two venturis is observable in that there is no crossover of the velocity curves as velocity increases, at least in the range where data were actually taken. Again the presence of and the interaction with, other effects can be observed since for the same air content and velocity the 1/2 inch σ_c values are considerably lower than those for the 1/2 inch case.

4. One-eight-inch Throat-Diameter Plastic Venturi

No unusual results or deviations from the results obtained with the 1/2 inch venturi are indicated by the 1/8 inch data shown in Figure 31. The remarks made above relative to comparison between 1/2 and 1/4 inch data on trend and levels are pertinent to this situation also.

5. Summary of Experimental Observations of Gas Content Effects in Water

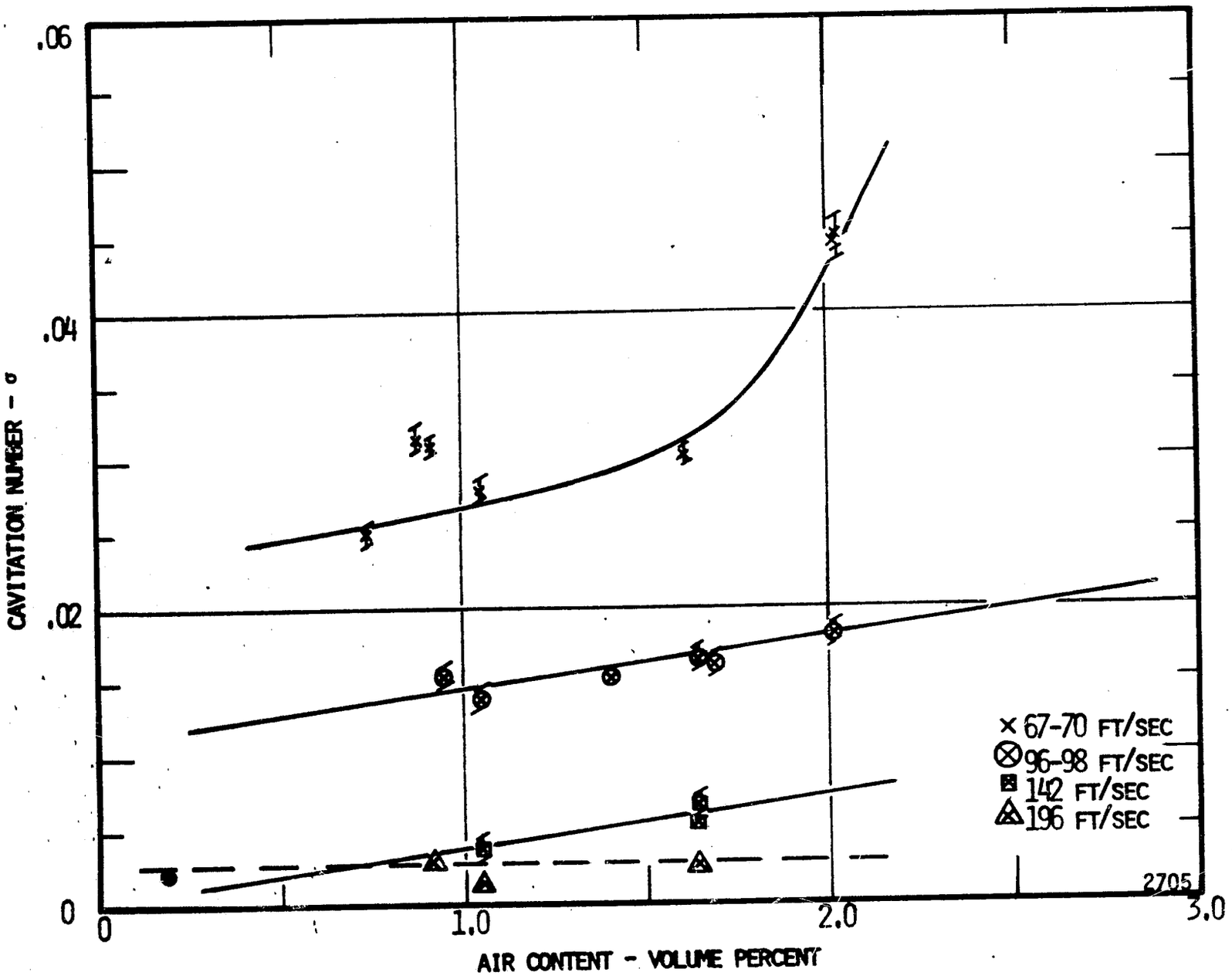

Figure 30. Cavitation Number versus Air Content, Venturi 614, Water.

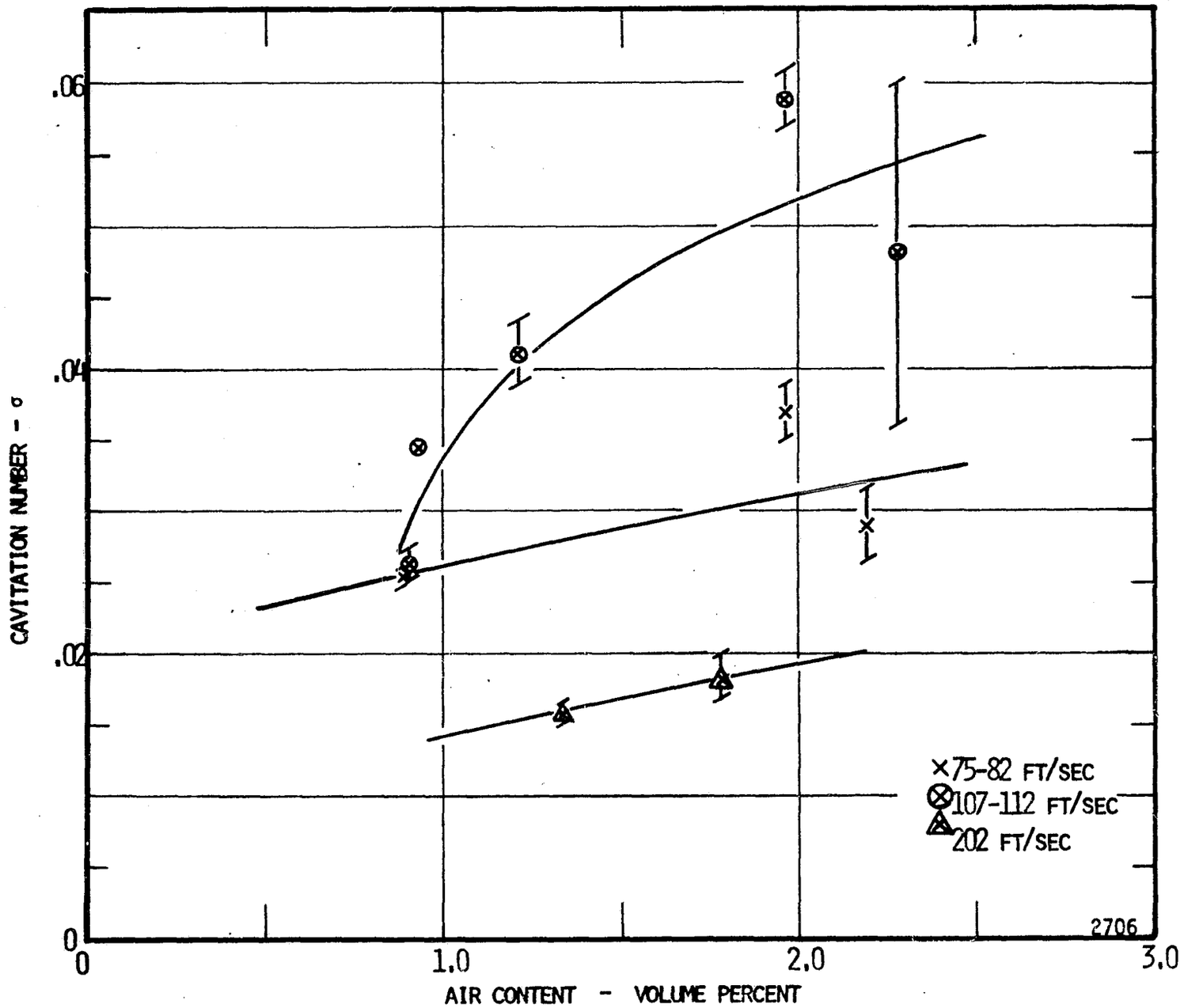

Figure 31. Cavitation Number versus Air Content, Venturi 818, Water.

Based upon the results presented above, the following conclusions may be drawn relative to gas content effects.

a. For all cases, the lower the flow velocity, the more pronounced are the effects of increasing gas content. This supports the argument that the longer the exposure time the more likely a fluid is to cavitate and that for lower values of $V^2/2g$, the greater is the effect of the gas pressure in the bubbles on σ_c. In this particular system, as the velocity is increased the pump suction pressure is increased, i.e., the system total pressure is increased. Therefore, the mean pressure the fluid sees is increased and the entrained gas portion of the total gas content is reduced which in turn tends to suppress cavitation, that is produced lower cavitation numbers at the higher velocity. Our limited pre-pressurization study seems to support this argument.

b. Because theretical studies indicate that fluids possess a definite tensile strength in the absence of entrained nuclei (i.e., zero gas content) with a resultant sharp decrease in the cavitation number, the results here where the air content could not be reduced below about 0.5 volume percent at STP, favor the conclusion that there is a "plateau" on the σ_c versus gas content curve along which gas content has little effect. Extending this argument, it may be postulated that the length of this plateau increases with velocity. Idealized this would lead to a family of curves such as that shown in Figure 32.

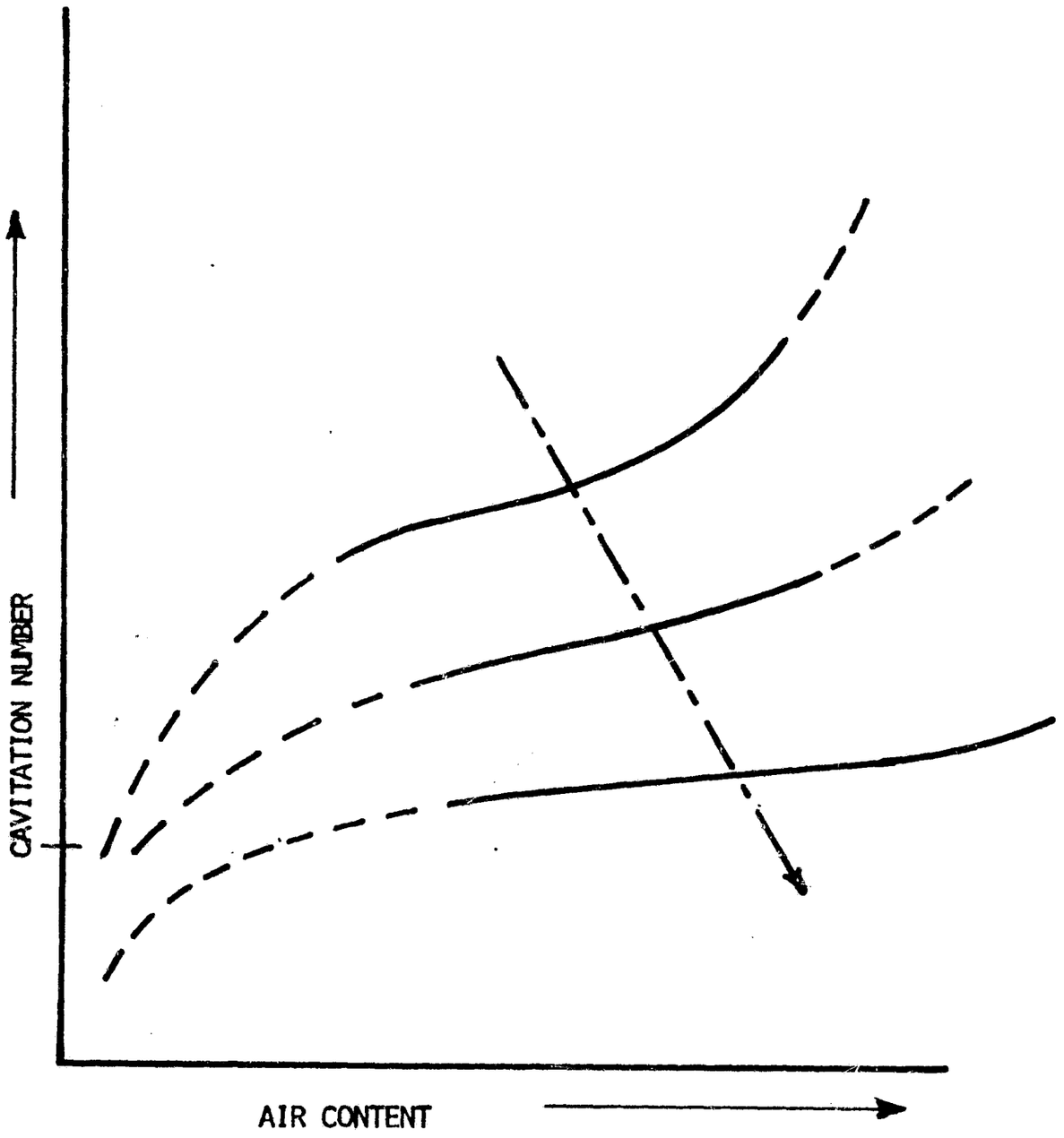

Figure 32. Idealized Cavitation Number Vs Gas Content Plot

c. Quite clearly, assuming all other factors constant, the prior history of the fluid as well as actual gas content has a significant influence upon the observed cavitation characteristics.

B. Velocity Effects in Water

1. One-half-inch-Throat-Diameter Plastic Venturi

The effects of velocity on cavitation number are illustrated on Figure 33. Here again, because of the problems with exact control of temperature and gas content discussed earlier the curves have been arbitrarily identified as cold, warm, hot and deaerated or saturated noting that some small range of values is included. For all cases the data exhibits a minimum value for σ_c at some intermediate velocity, although the relative change from the lowest to highest velocity is considerably less for the cases of reduced gas content. The effects of velocity are most pronounced at the lower velocities, a condition also noted by Holl and Wislicenus[9] in their paper on tip vortex cavitation, although those data were at even lower free stream velocities. Lehman and Young[20] report a minimum in the σ_c versus velocity plots in the aqueous systems they have investigated. This minimum in the σ_c versus velocity curve was not observed in earlier tests at the University of Michigan, however the maximum velocity achieved then was only 90 ft/sec. In a separate study using the University of Michigan water loop as a tool for studying cavitation damage on materials, Robinson[7] has observed the same sort of minimum in the σ_c versus velocity plot. The comment made earlier regarding the masking effects of other variables must continually be considered. Nevertheless the trends observed are present in a sufficient number of cases as to leave little question of their validity.

2. Three-quarter-inch-Throat-Diameter Plastic Venturi

Although the available experimental data includes a much narrower

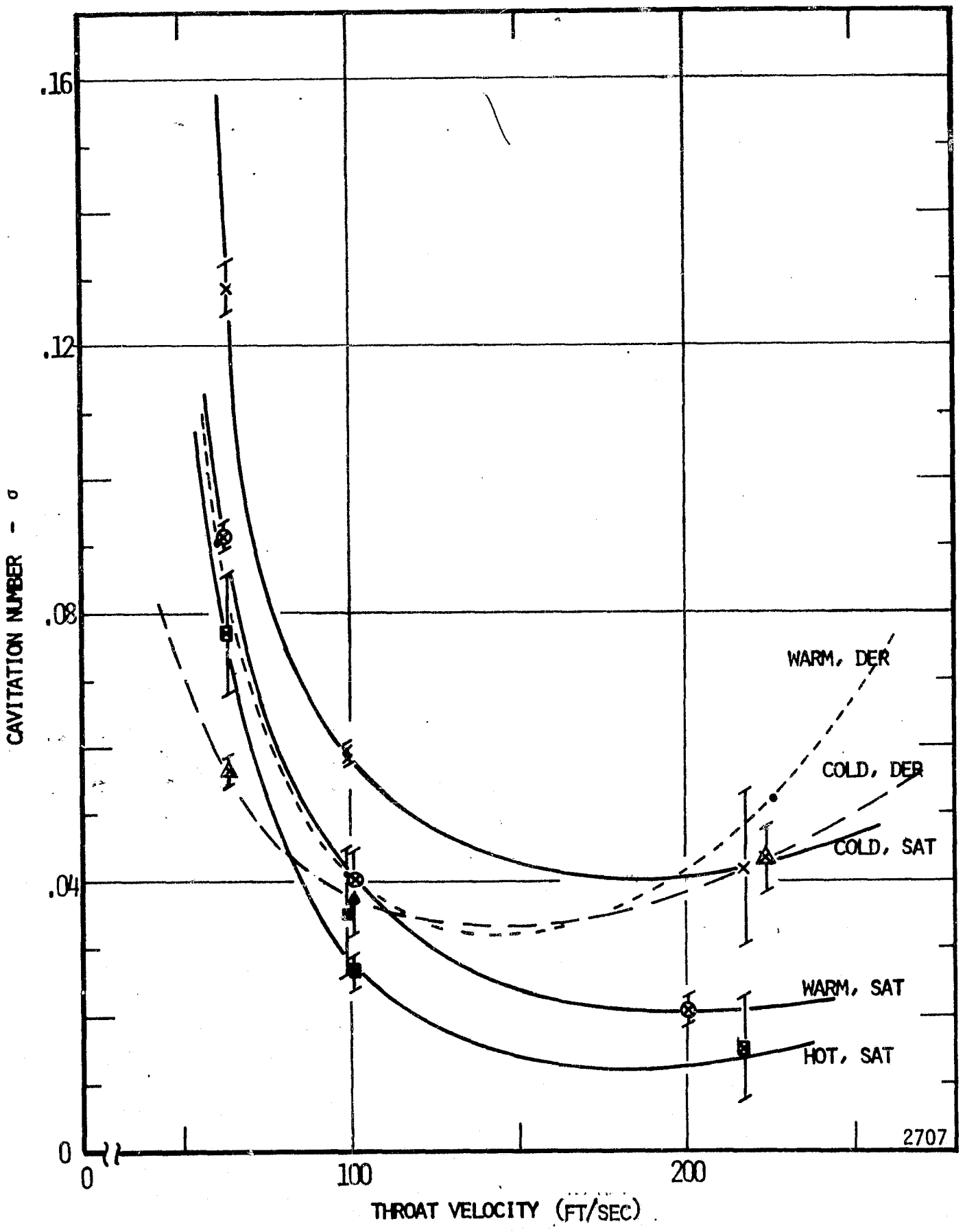

Figure 33. Cavitation Number versus Throat Velocity, Venturi 412, Visible Initiation, Water.

range of variables than the 1/2 inch case, the same trends are observable in Figure 34. The significant additional point that must be made here is that the generally lower values of cavitation numbers evidenced here for otherwise similar test conditions are strong evidence that other effects, e.g., size, roughness, perhaps other minor geometric non-similarities such as burrs also have a strong influence on the cavitation characteristics of these systems.

3. One-quarter-inch-Throat-Diameter Plastic Venturi

The data trends in Figure 35 agree extremely well with the 1/2 inch data plotted in Figure 33, and in fact the availability of the results from another velocity point provide concrete verification of the fact that the cavitation number versus velocity relationship exhibits a definite minimum. The influence of other factors is still observable; the values of cavitation number are generally lower than those for the 1/2-inch case, but perhaps more importantly, the difference in cavitation number for deaerated and saturated conditions is much smaller than that previously observed. There is no concise, unequivocal explanation for this difference presentable here, although the general correlations presented in Chapter V help to alleviate this problem somewhat.

4. One-eight-inch-Throat-Diameter Plastic Venturi

The data shown in Figure 36 are perhaps the strongest indication within this set of experiments in water for the existence of other effects. The increasing then decreasing nature of the curve as the velocity increases for the cold, saturated case is in direct contrast to the trends previously exhibited (Figure 33 for example). Conversely, if attention is directed

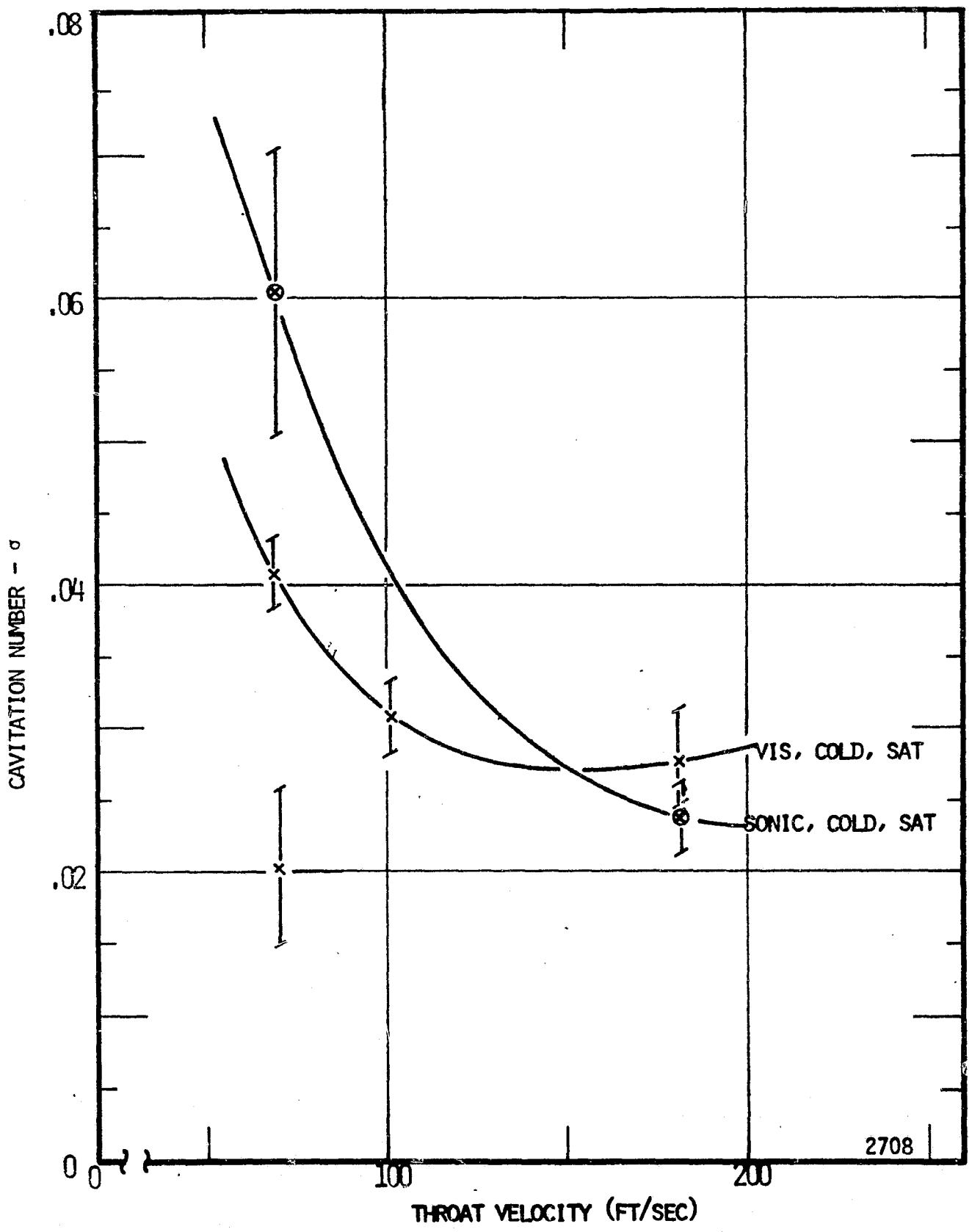

Figure 34. Cavitation Number versus Throat Velocity, Venturi 534, Visible Initiation, Water.

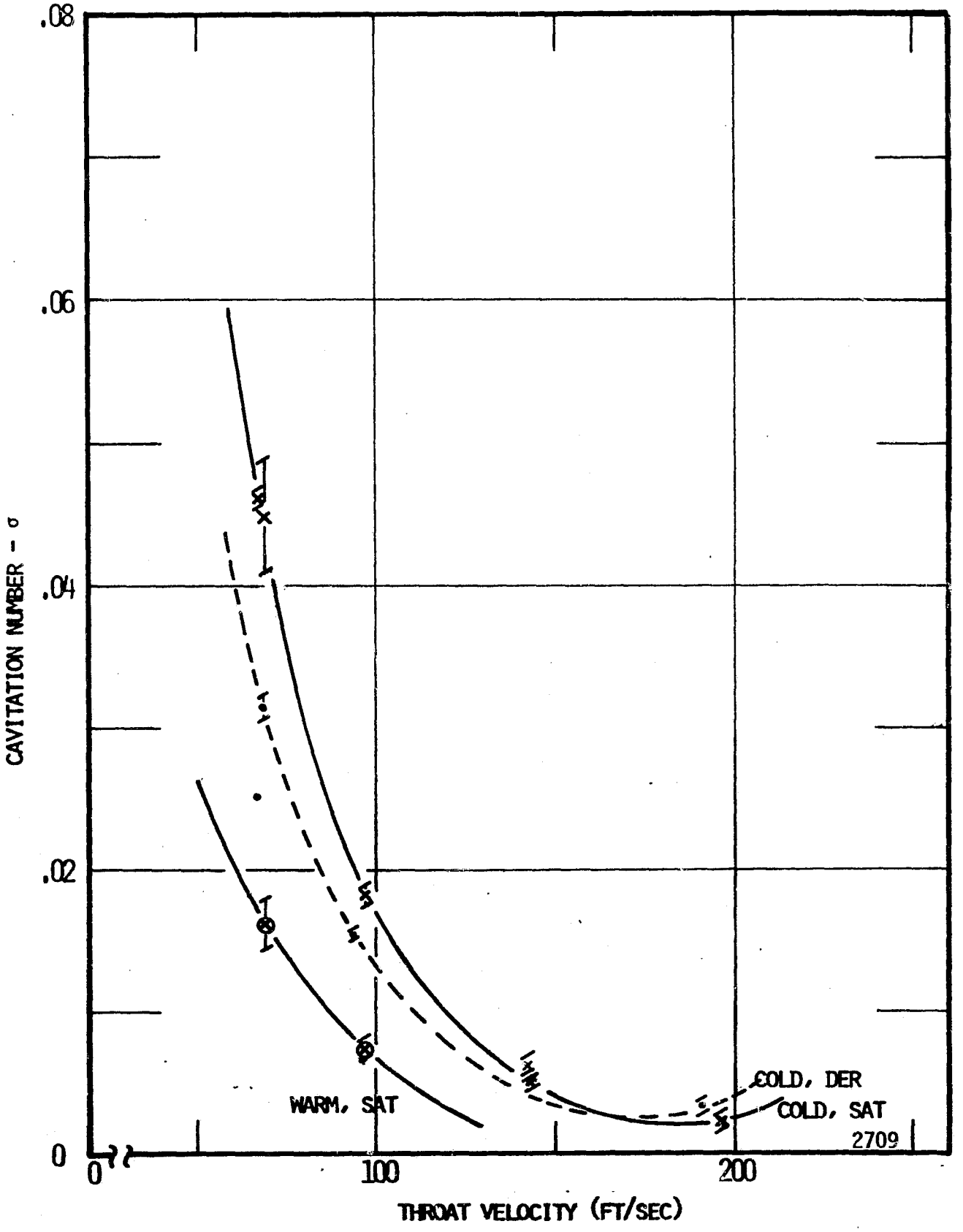

Figure 35. Cavitation Number versus Throat Velocity, Venturi 614, Visible Initiation, Water.

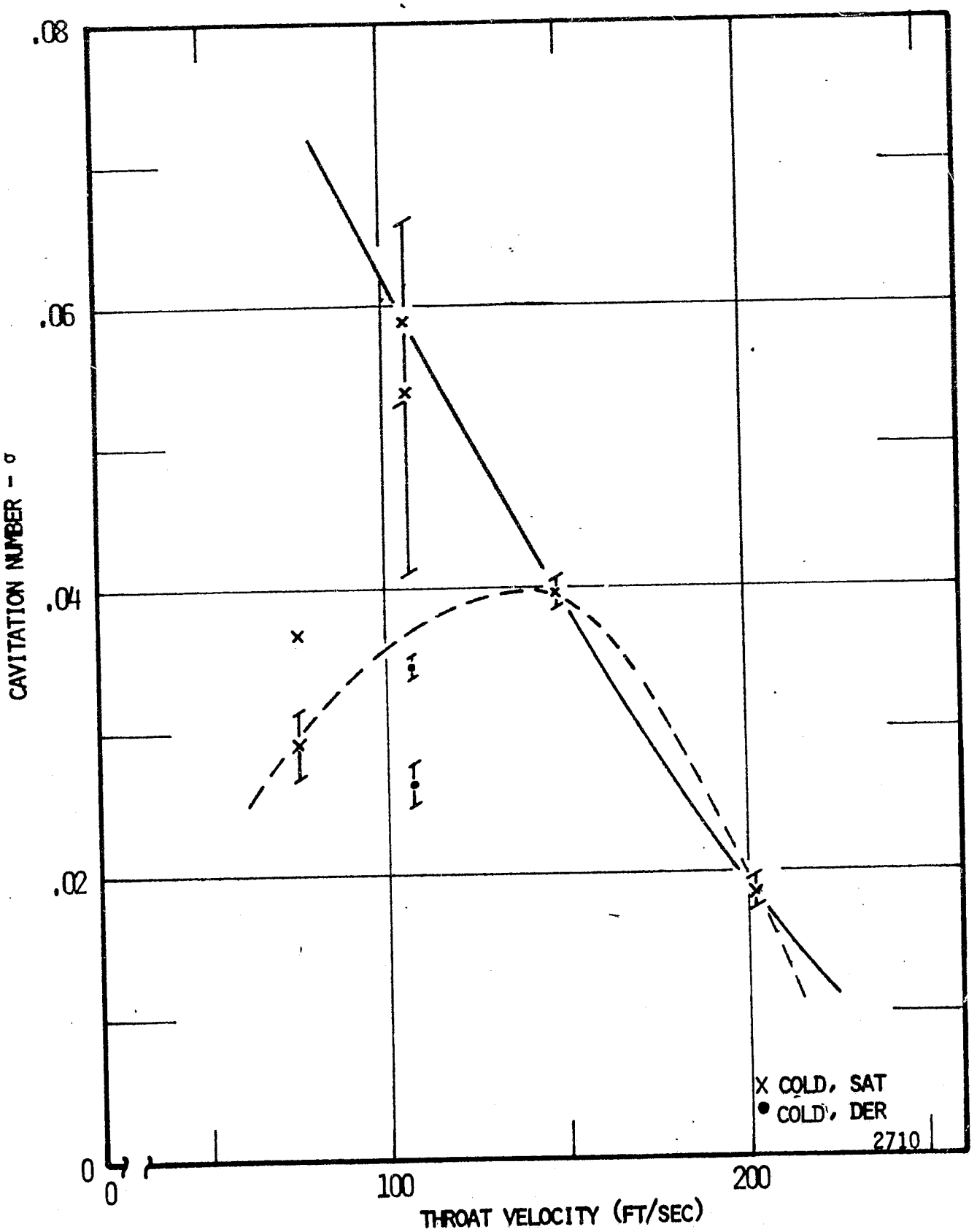

Figure 36. Cavitation Number versus Throat Velocity, Venturi 818, Visible Initiation, Water.

toward only those data points that support or exhibit a decreasing σ_c with velocity trend in the nature of the curve, the minimum between 100 to 200 feet/second throat velocity is not present as it is in Figure 33. It is quite obvious that for small flow passages, even minor surface imperfections, can and may have significant effects on the cavitation conditions prevailing in the system since they may account for severe local pressure depressions. As with the 1/4 inch venturi the broader correlations given later account for, if not full explain, these anomalies.

C. Temperature Effects in Water

The effect of variations in bulk water temperature on the cavitation number is shown on Figure 37 for two gas content conditions. The gas saturated tests exhibit decreasing values of cavitation number for increasing temperature. This same trend has been observed previously[51,52,53], and can be explained by the "thermodynamic effects" discussed earlier. This assumes that a given cavitation condition represents a fixed vapor volume regardless of the fluid velocity or temperature. Thus as the bulk temperature increases, vapor density in the bubbles must increase, which can only occur by mass addition from the cavity walls. As heat is transferred to evaporate the fluid, local temperature falls (and with it local vapor pressure) below bulk values and therefore the driving force for bubble growth is reduced, cavitation is more difficult to produce, so that the required cavitation number is lower. The very limited data available for the deaerated case exhibits a reverse trend, i.e., the cavitation number is increasing (cavitation is easier to produce) with increasing temperature.

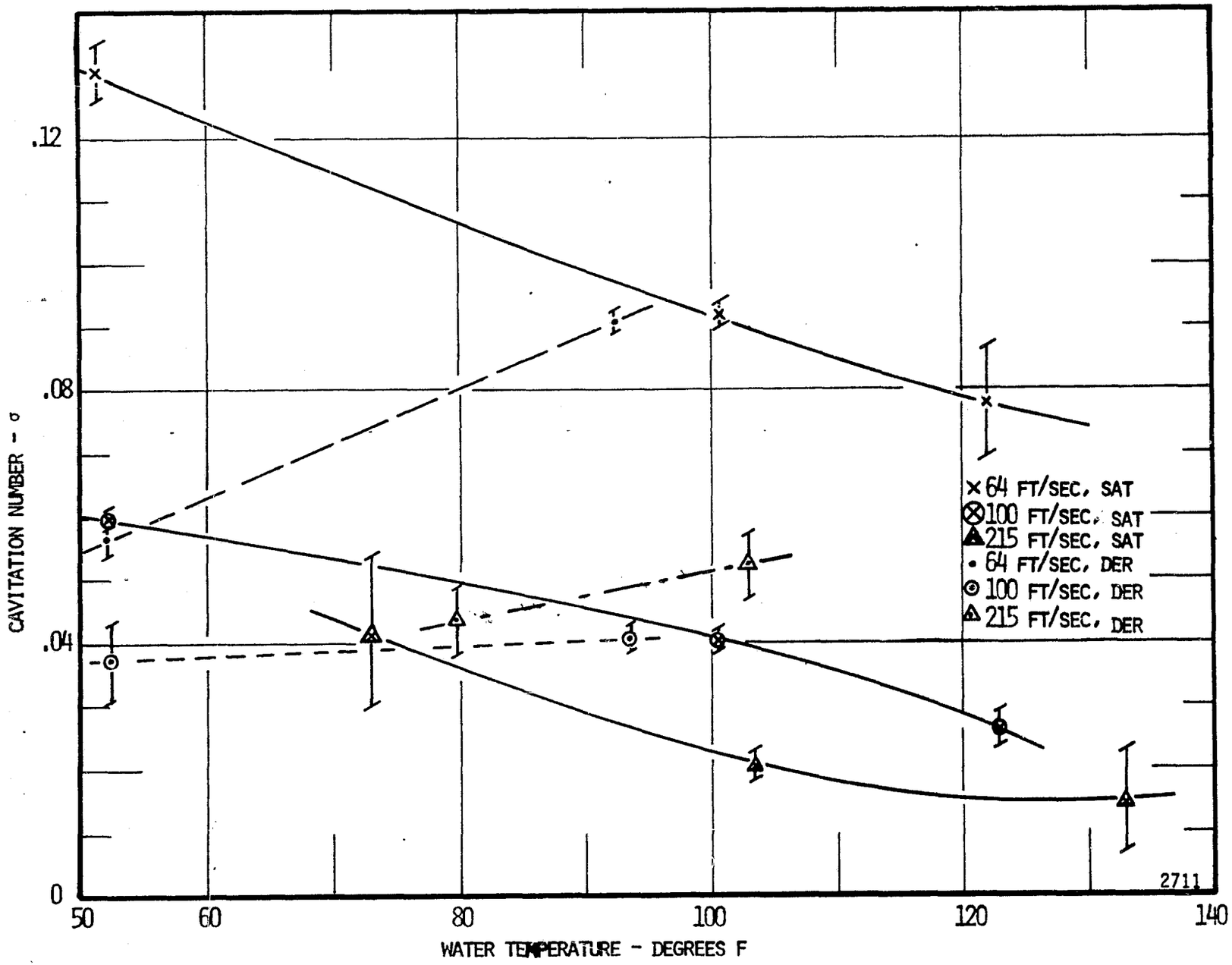

Figure 37. Cavitation Number versus Water Temperature, Venturi 412.

Although caution must be exercised in drawing conclusions it may well be that for lower total air content, percentage-wise more is in solution, then for higher bulk temperature increases dissolved air is reduced, increasing the amount of entrained gas and thus likelihood of cavity formation, i.e., raising σ_c , faster than the thermodynamic effects reduce it.

D. Observations for Highly Developed Cavitation

Because the principle area of concern for application of cavitation analyses is the prediction of the onset of cavitation, the majority of the present tests were conducted with incipient, or just visible, cavitation. To complete the study, a limited number of experiments were conducted at more fully developed cavitation conditions. On Figure 38, the cavitation number is plotted versus the throat velocity for the 1/8-inch, 1/4-inch and 1/2-inch venturis at the saturated air content condition, and "standard cavitation" or Condition D as characterized elsewhere in Appendix A. The observable trends duplicate those reported above for incipient cavitation, except that the variation in cavitation number between the low and the high velocity is not nearly as great. Similar data for "Condition E" or "Cavitation to First Mark" are shown on Figure 39. The available data on temperature effects and gas content effects for the more developed cavitation though not sufficient for plotting, do support the earlier conclusions (See Appendix G for the data).

E. Observations of Venturi Flow Patterns for Water

For all the velocities incorporated in the water portion of this work a pressure profile was obtained for each venturi under zero or no

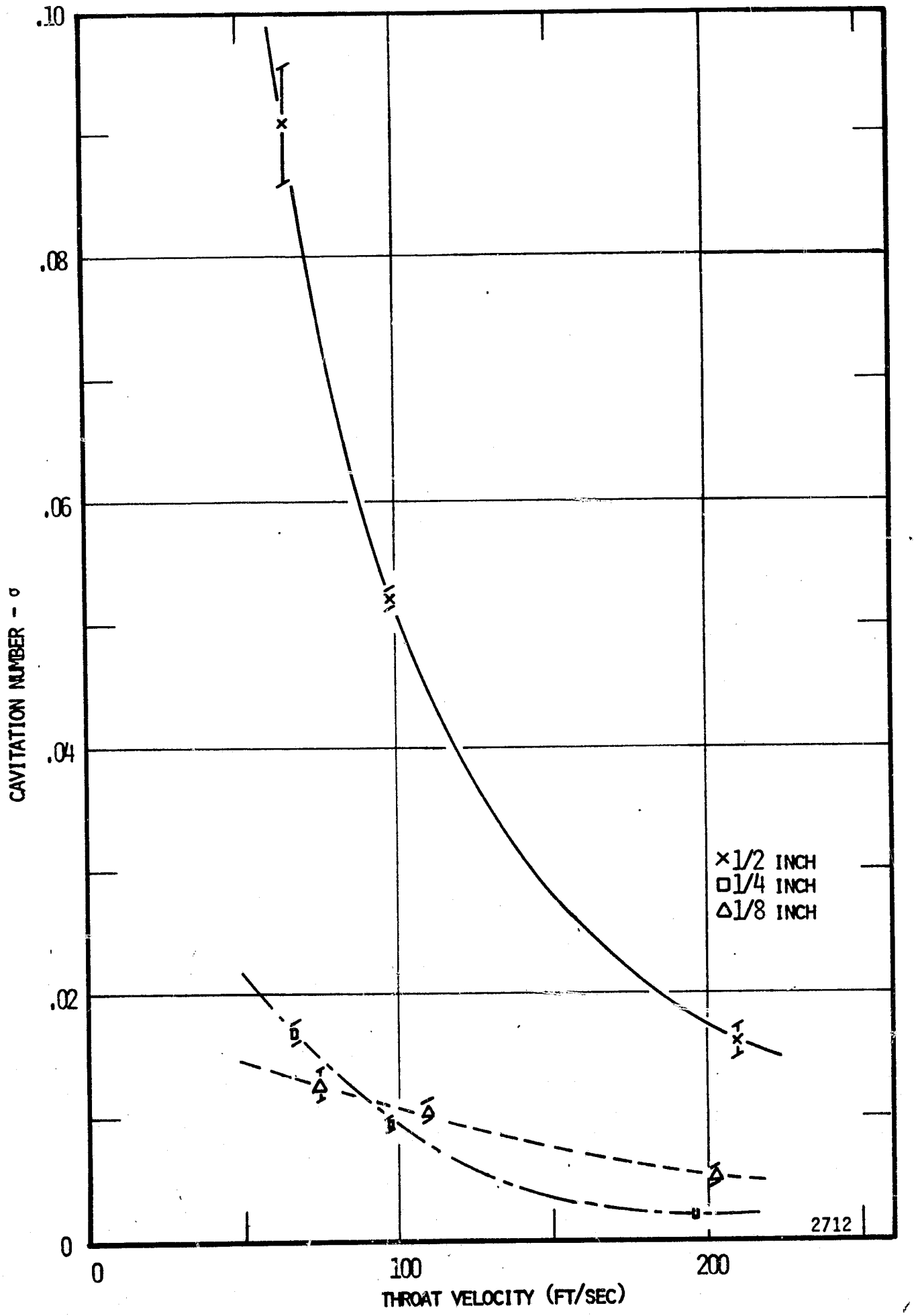

Figure 38. Cavitation Number versus Throat Velocity, 3 Venturis, Standard Cavitation, Water.

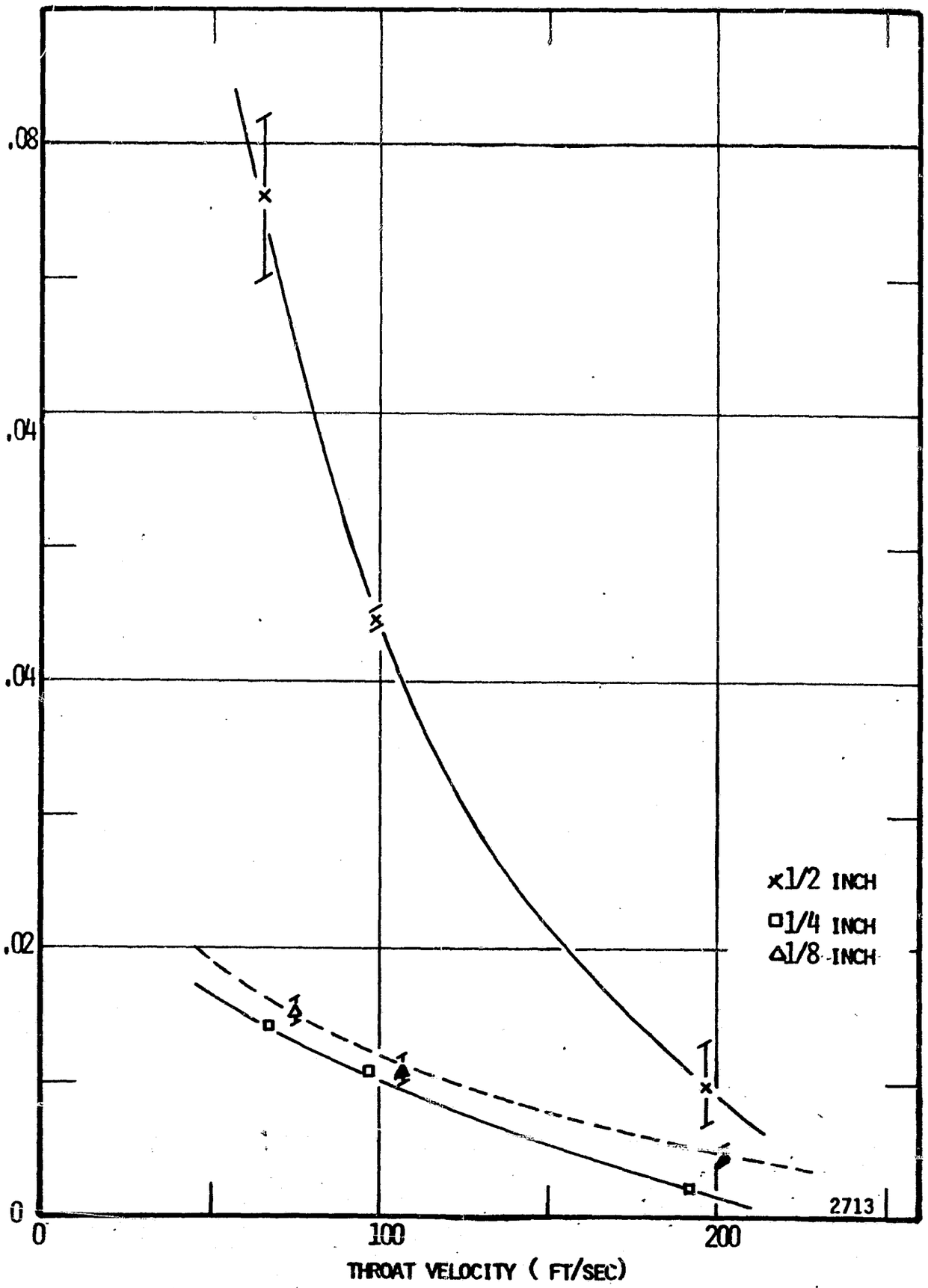

Figure 39. Cavitation Number versus Throat Velocity, 3 Venturis, Cavitation to First Mark, Water.

cavitation conditions as a control or check profile. When these data are subjected to the data reduction program RAWDAT (See Appendix E) and the outputs compared, it is quite clear that the axial location of the minimum pressure point thus computed, varies from one venturi to the next even though nominal geometric similarity was maintained in the design of these systems. A more graphic visualization of this trend is gained by an additional "normalization" of the data as follows. The value of the normalized pressure at the observed minimum is subtracted from each of the other values such that:

$$\Delta\sigma_c\,(\text{normalized}) = \sigma_c\,(\text{obs}) - \sigma_c\,(\text{obs,min})$$

where as before:

$$\sigma_c = (p_{obs} - p_v) \Big/ \frac{\rho V_T^2}{2g}$$

A normalized location is established by dividing the throat diameter into the distance from the throat inlet to the pressure point of interest, i.e.,

$$L_N = L_{\text{ENTR. TO TAP}} \Big/ D_T$$

Now plotting σ_c versus L_N for each velocity on a single plot illustrates the behavior of the minimum pressure point and thereby the point of cavitation. If complete similarity between the venturis had been obtained then the data points would all be at the same location on such a plot. As was mentioned earlier, certain fabrication problems precluded an exact correspondence of pressure tap location; nevertheless, the pressure minimum should be located at the same point because of the

similarity of the flow pattern. Examination of Figures 40 through 42 reveals at once that such is not the case for any of the velocities used here. In every instance as the venturi diameter decreases the minimum pressure point migrates upstream toward the throat inlet. Also it may be noted that the axial pressure drop in the throat of the 1/2-inch venturi more nearly approaches the linear decrease expected for flow in a cylindrical channel than for any of the other venturis. The most probable source for this phenomena seems to be that the 1/2-inch geometry (inlet and diffuser) were designed specifically for application in this flow system. Therefore, since the available length for the venturi installation is the same for all four sizes, the perturbations caused by either more or less rapid variations in flow to the point where the venturi geometry becomes similar may be responsible for the migration of the minimum point. The constancy of the minimum pressure point location and the noncavitating pressure profile for a given venturi are clearly demonstrated by Figure 43 where the normalized profile is plotted for three velocities in the 1/2-inch venturi.

F. Gas Content Effects in Mercury

The increasing emphasis placed upon liquid metals, and mercury in particular, as coolants and heat transfer agents in small nuclear power systems (SNAP-8,2, etc.) as well as the relative ease of handling mercury in the laboratory were responsible for our decision to use it as the companion fluid to water in this study. There are published water-cavitation results that deal at least in part with the points considered here. On the other hand, there are almost no data even for partial comparisons in the case of mercury. Gas content effects

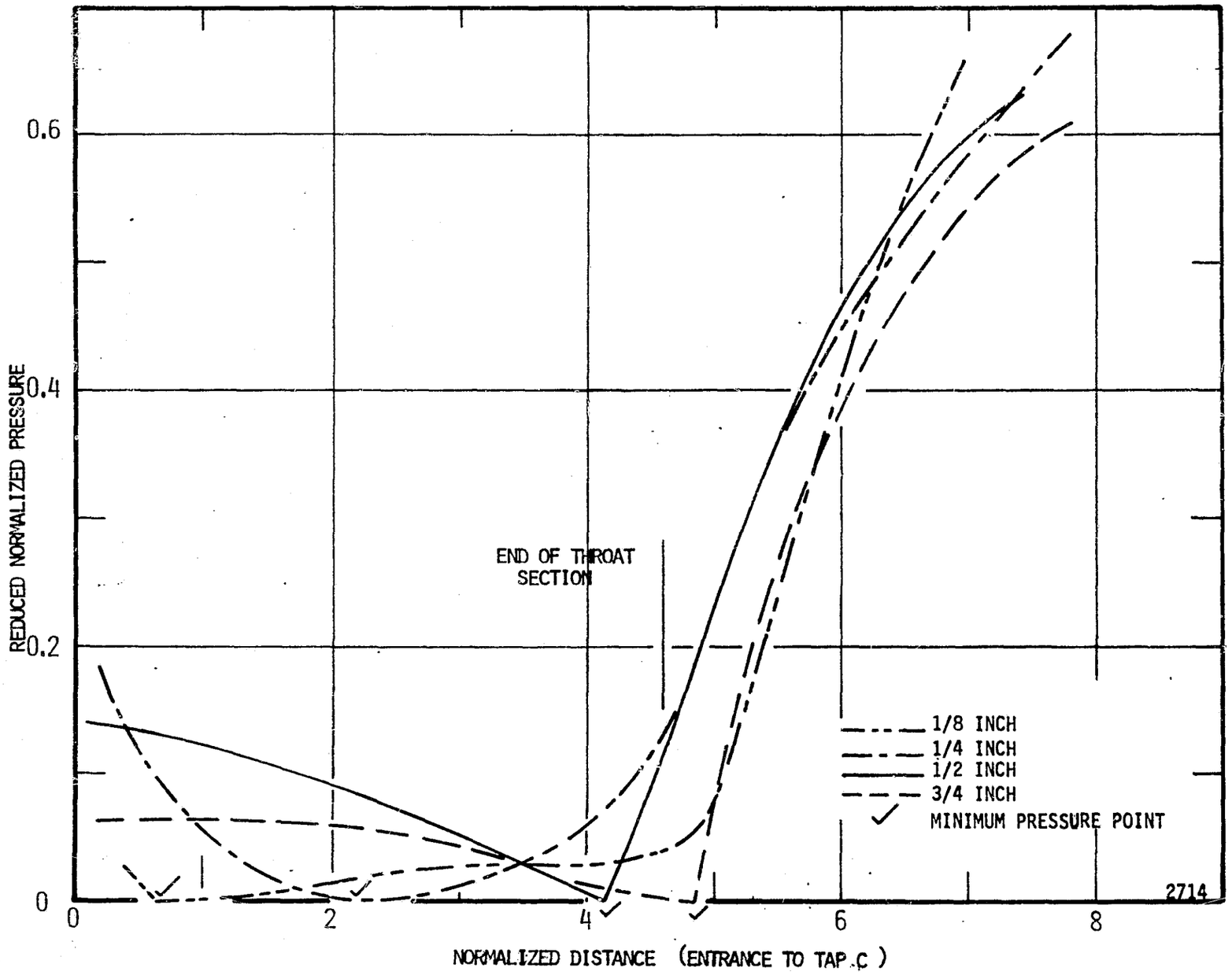

Figure 40. Reduced Normalized Pressure versus Normalized Distance, Water, 65 Feet per Second, All Venturis.

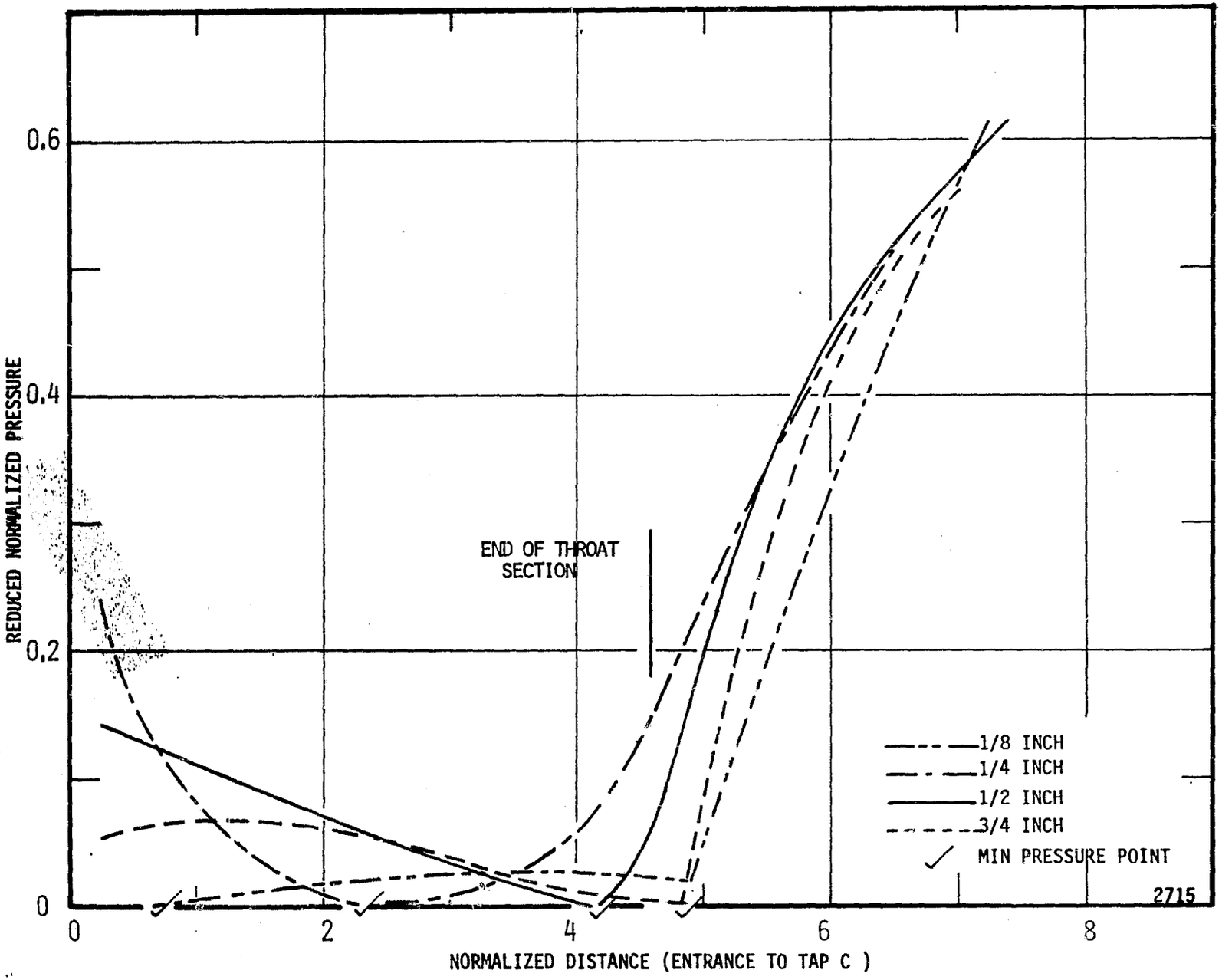

Figure 41. Reduced Normalized Pressure versus Normalized Distance, Water 100 Feet per Second, All Venturis

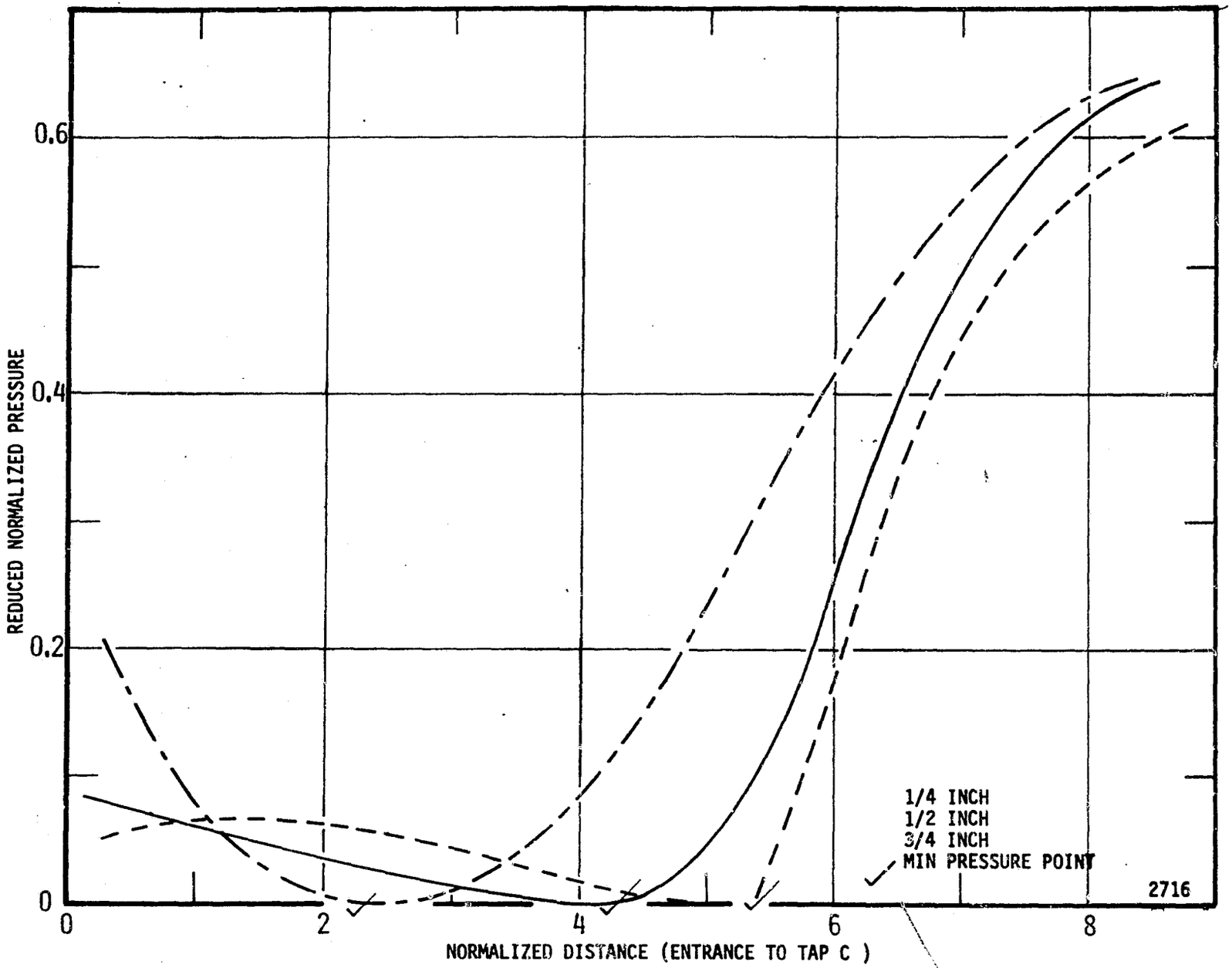

Figure 42. Reduced Normalized Pressure versus Normalized Distance, Water, 220 Feet per Second, All Venturis.

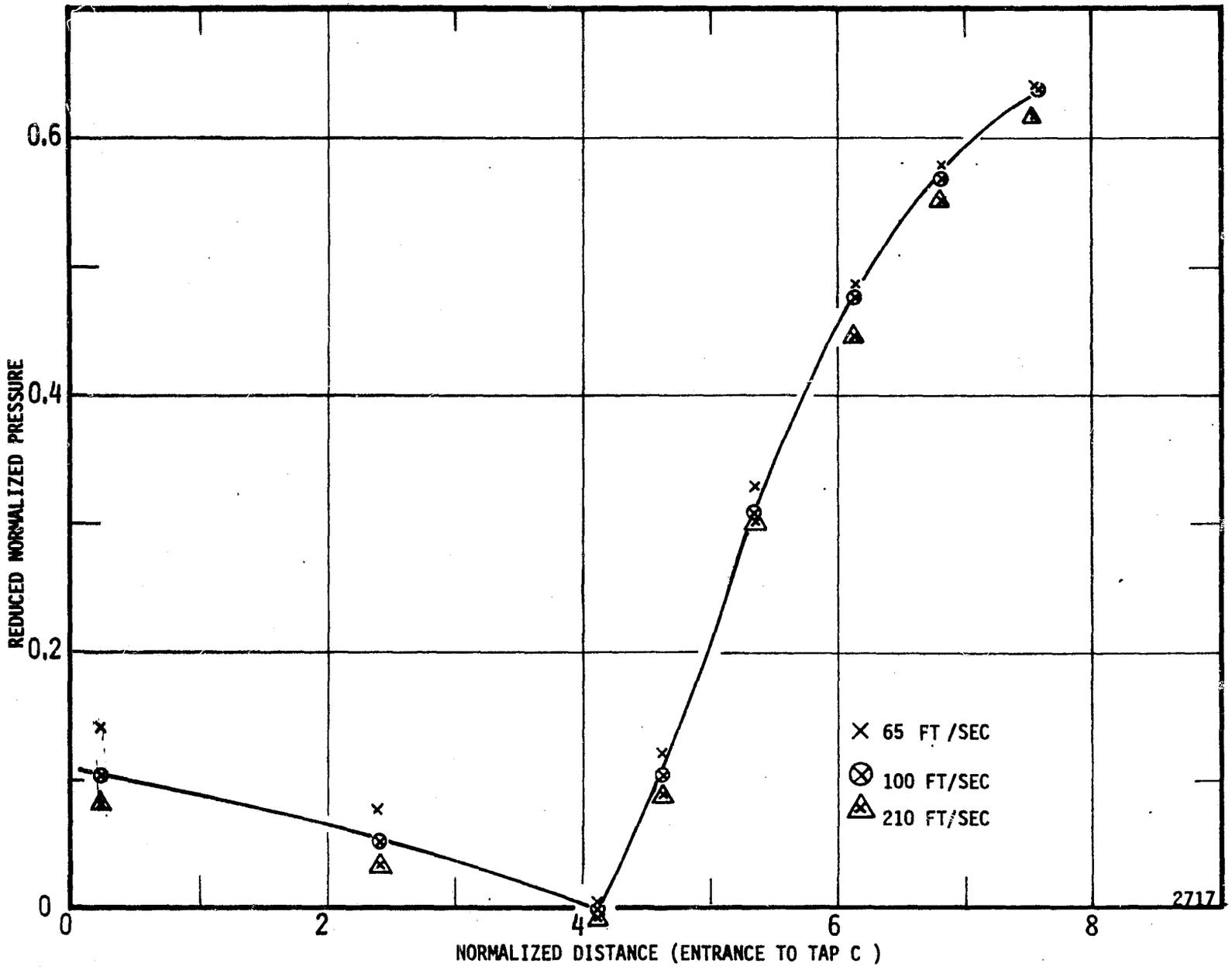

Figure 43. Reduced Normalized Pressure versus Normalized Distance, Water, All Velocities, Venturi 412.

are an excellent case in point. The available literature on water and some refrigerants deals nearly exclusively with situations in which the gas is largely present in the dissolved state, whereas in mercury the gas exists only in the entrained state. Thus we have no "a priori" reason to expect the effects of gas content in mercury to behave in any certain way, although theory gives some basis for assuming trends similar to those found for water. As a result, in the following discussion the only direct comparisons will be those with water data collected during this study.

1. One-half-inch-Throat-Diameter Plastic Venturi

In Figure 44 the cavitation number is plotted versus gas content with throat velocity as the parameter. These data were taken a temperatures form 75 to 125°F depending to some extent upon the flow rate and available coolant capacity. However, the pertinent properties for mercury are not significantly sensitive to temperature variations of this magnitude. For purposes of presentation and analysis those runs made where residual air was present in the mercury and those where argon was injected have been considered together. Again, as with water, the cavitation number increases with gas content and quite significantly so in the 33 ft/sec case. It should be noted that below about 0.6 volume percent at STP it is extremely difficult to arrive at any meaningful separation of the data by velocity groups. The major difference here, as compared to water, is that the lowest velocity did not produce the highest cavitation numbers, as has been the previous experience. There is no obvious explanation for this change from the earlier trends. It is noted again that there is an intermediate gas content range over which

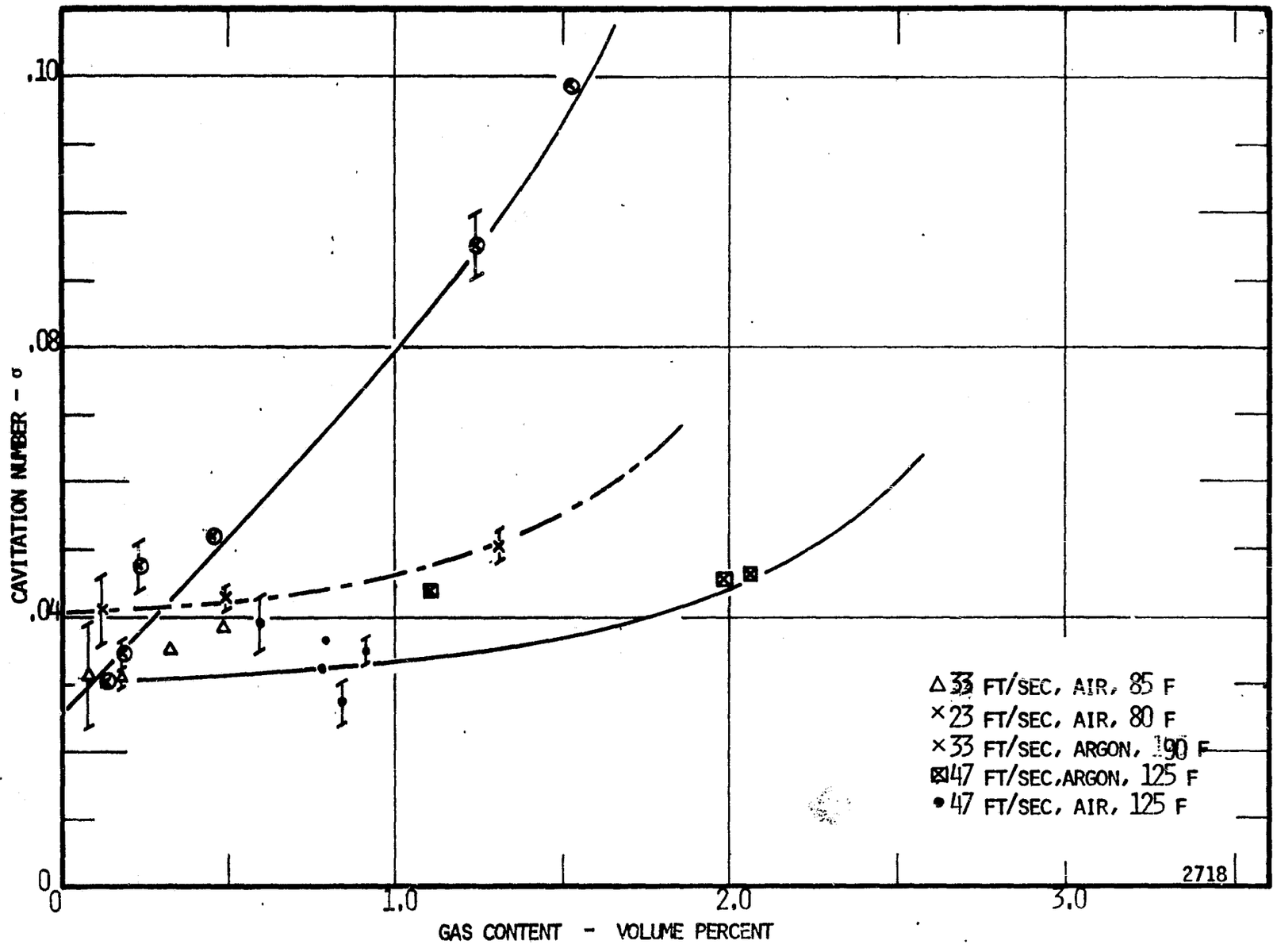

Figure 44. Cavitation Number versus Gas Content, Venturi 412, Mercury, Air and Argon.

there is little effect of changes in gas content but then a point is reached at which significant changes do occur.

2. One-half-inch-Throat-Diameter Stainless-Steel Venturi

On Figures 45 through 48 the cavitation number is plotted as a function of temperature for various velocities and throat temperatures. Unfortunately the range of available contents with air (Figure 45) is insufficient to allow complete curves to be established, nevertheless some specific points can be noted. The lower velocity (22 ft/sec) does yield cavitation numbers that are significantly higher than those of the middle velocity (33 ft/sec) similar to the observations in water. In Figure 47 the cavitation number is plotted versus gas content for argon injection. Here it is clearly evident that there is a region of little influence from the presence of the gas and then a drastic increase in cavitation number as the content rises above approximately 2%. In Figure 48, a similar plot with hydrogen as the injected gas, we see approximately the same trends although the data scatter is severe and thus obscures some of the data trends. In all cases the curves are "eye-ball" fitted and no analysis has been done. Some of this scatter is readily attributable to the difficulties in accurately evaluating gas contents for hydrogen.

3. One-eighth-inch-Throat-Diameter Plastic and Stainless-Steel Venturis

In Figure 48 the cavitation number is plotted versus gas content for both argon and air. The obvious indication is that a pronounced difference exists between the two cases since there is a factor of two difference in σ_c for approximately the same gas contents. Because

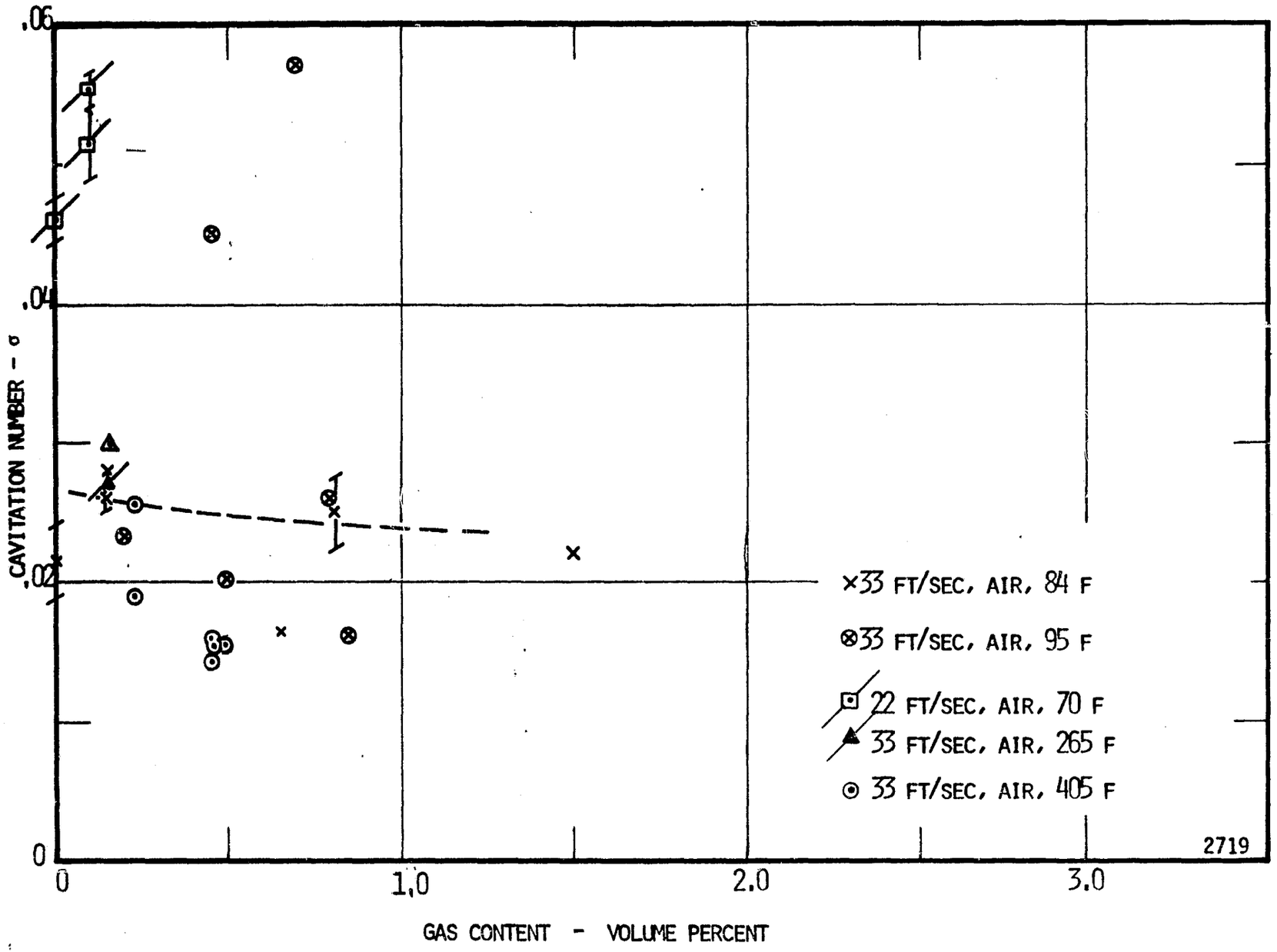

Figure 45. Cavitation Number versus Gas Content, Venturi 712. Mercury, Air.

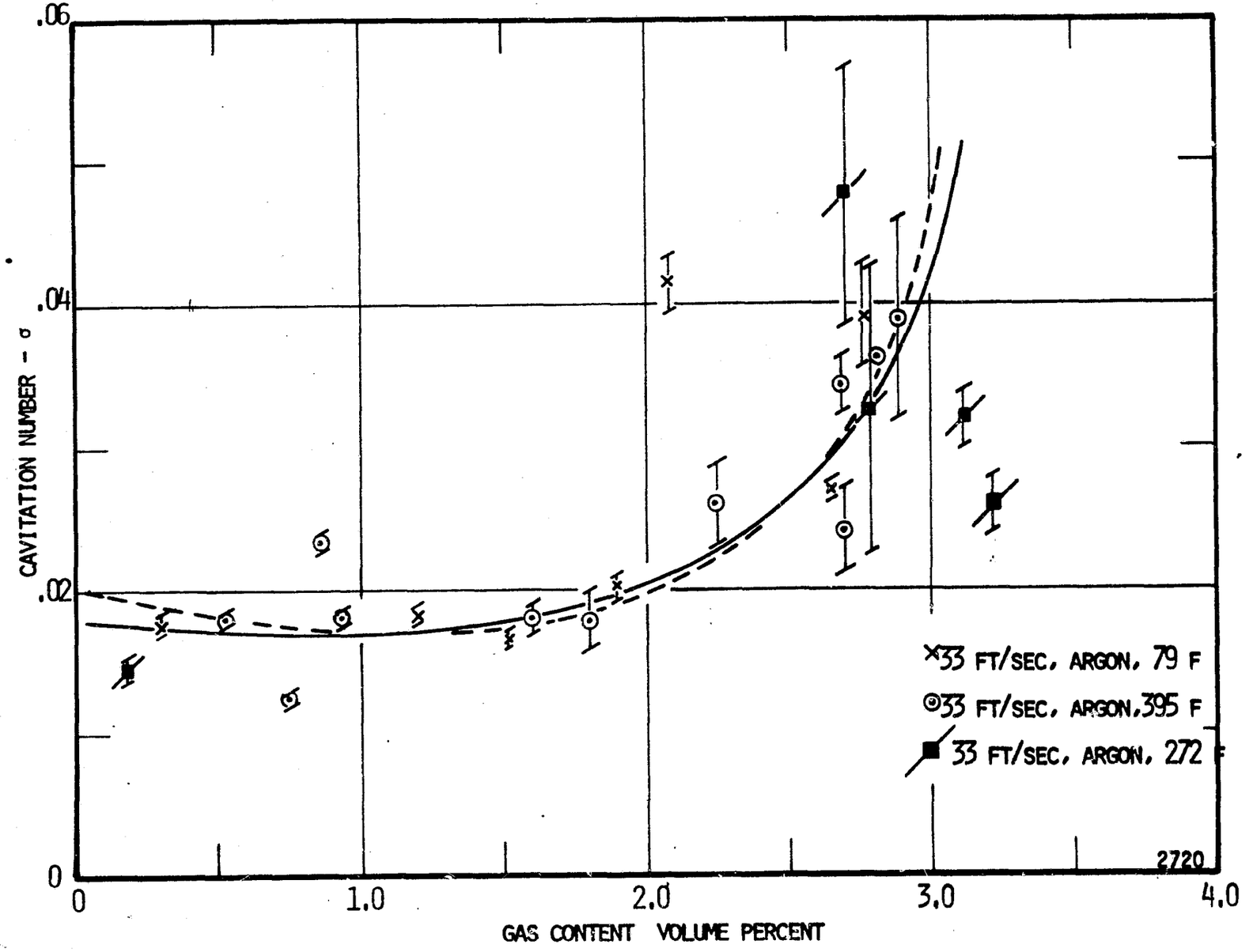

Figure 46. Cavitation Number versus Gas Content, Venturi 712, Mercury, Argon.

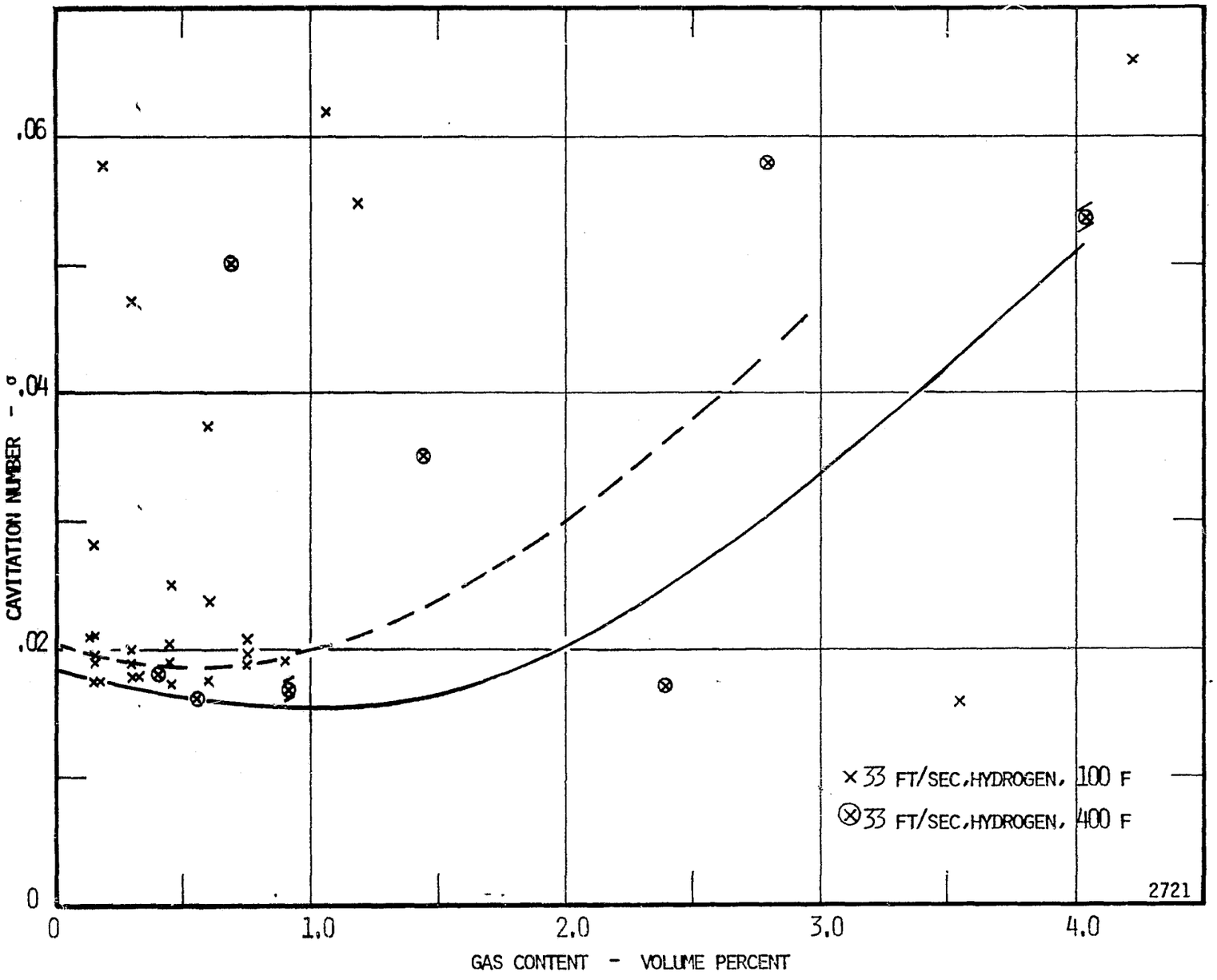

Figure 47. Cavitation Number versus Gas Content, Venturi 712, Mercury, Hydrogen.

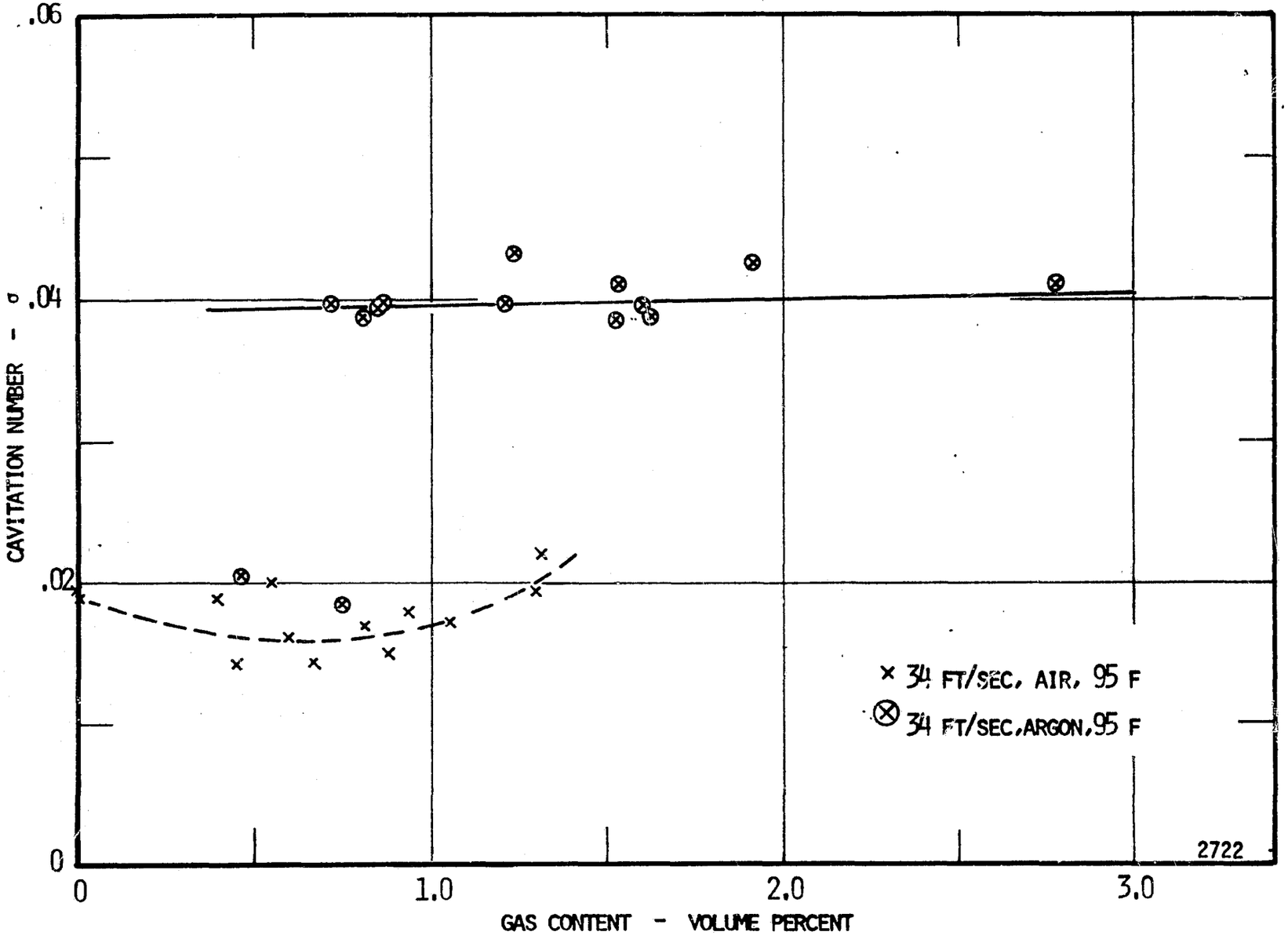

Figure 48. Cavitation Number versus Gas Content, Venturi 818, Mercury, Air and Argon.

there is no clear cut reason for such a difference, there is some justification in the argument that the data reflects a scatter in the means of determining gas content. There will be further analysis in Chapter V where the data is curve-fitted with a regression analysis that ascertains the goodness of fit to a particular curve. The argument for treating all the air-argon data together is reinforced by considering the results shown in Figure 49. Here in the stainless-steel venturi, the argon data include essentially the same region as do the air and argon in a plastic venturi. Also, dramatic increases in cavitation number with increasing gas content may be noted in the hydrogen case. As in several other instances there is no readily available explanation for such behavior. There may well be hydrogen and mercury interactions that produce gross changes in interfacial tensions, thus affecting the size of entrained nuclei. However, no indication of such has been found in the open literature. This difference is most noticable in the smaller venturis indicating that bubble size does not scale with throat size and that for hydrogen the bubbles may be of significant size compared to the throat diameter in the low-pressure region. The same data is plotted on Figure 50 with the 400°F results added. Again the data scatter is large, however the trend for increasing cavitation number with increasing gas content is evident.

G. Temperature Effects in Mercury

Although the use of mercury and the steel venturi provides a much wider latitude of temperature conditions that can be studied, the results here are not nearly as clear cut as those for water. In the 1/2-inch stainless-steel venturi where the gas is air (Figure 45),

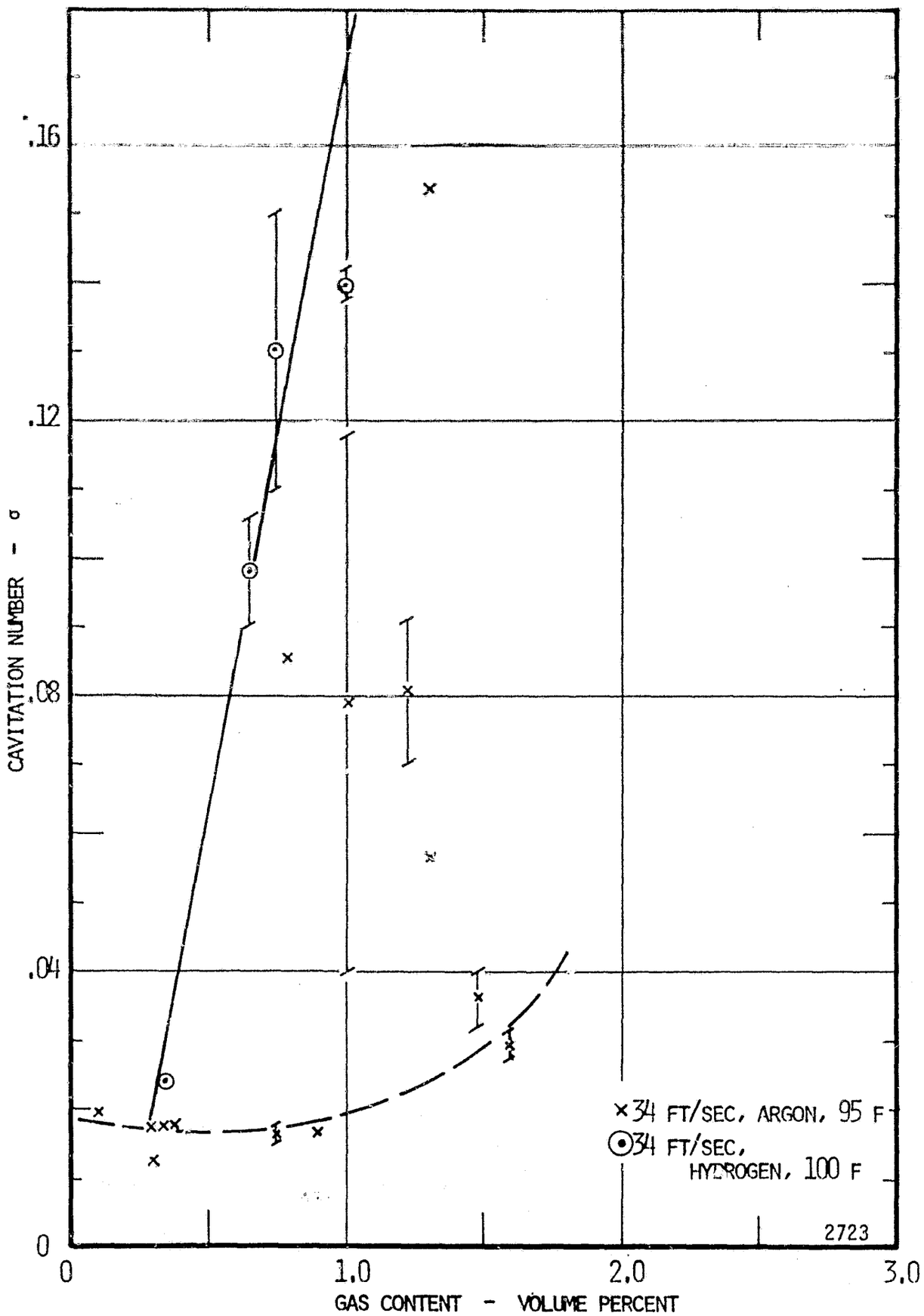

Figure 49. Cavitation Number versus Gas Content, Venturi 818, Mercury, Argon and Hydrogen.

as the mercury temperature is increased from room temperature to about 265°F there is no significant change, but as it further increases to 400°F we find the cavitation number decreasing as would be predicted by the "thermodynamic effect" discussed earlier. On the other hand, when argon is the gas (Figure 46) there is no discernible trend. That is, within the scatter of the data, results from cavitation tests at 80°, 270° and 395° define a single curve. The same holds true for the hydrogen case (Figure 47) except that in this instance, it is quite difficult to define a curve at all because of the data scatter. For the 1/8-inch diameter venturi (Figure 50) the situation is the reverse of that predicted by the "thermodynamic effect". For hydrogen, as the temperature increases the cavitation number also increases, although such an observation is based upon "eye-ball average" curves because the scatter is considerable. A similar situation exists for the argon cases though not nearly as pronounced.

H. Effects of High Vapor Pressure Additives

The initial technique for gas sealing and pressurizing the sump of the overhung pump used in these studies involved water cooling the shaft sealing gland. It was observed during a series of runs that water was entrained in the mercury, therefore, a few runs were made to investigate the effects of this entrained water on the cavitation number. It was hypothesized that additives with a vapor pressure significantly higher than mercury should exhibit characteristics similar to gas addition. The results of these tests are shown on Figure 51. As volume percent of water increases, the cavitation number increases,

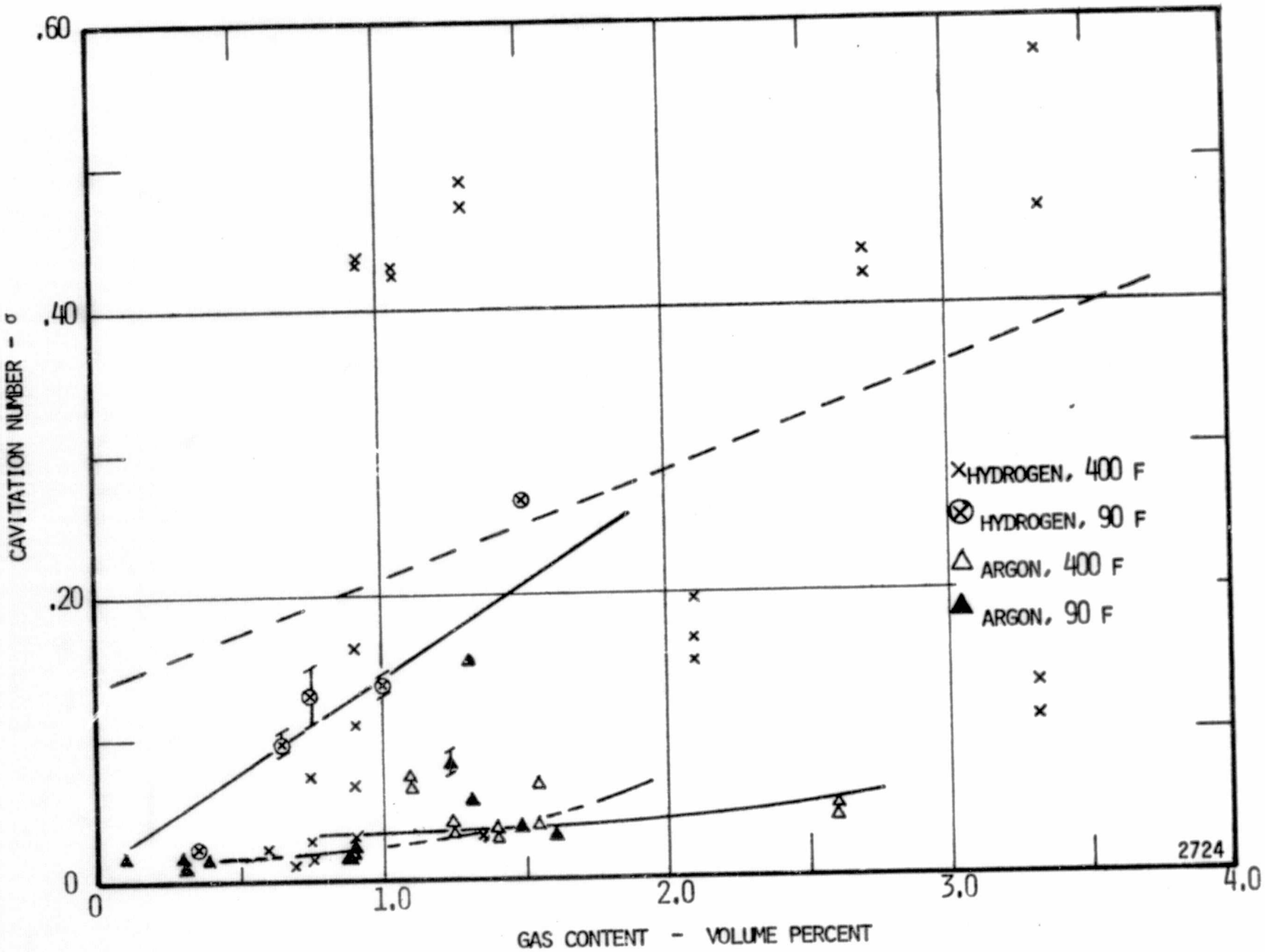

Figure 50. Cavitation Number versus Gas Content, Venturi 918, Argon and Hydorgen.

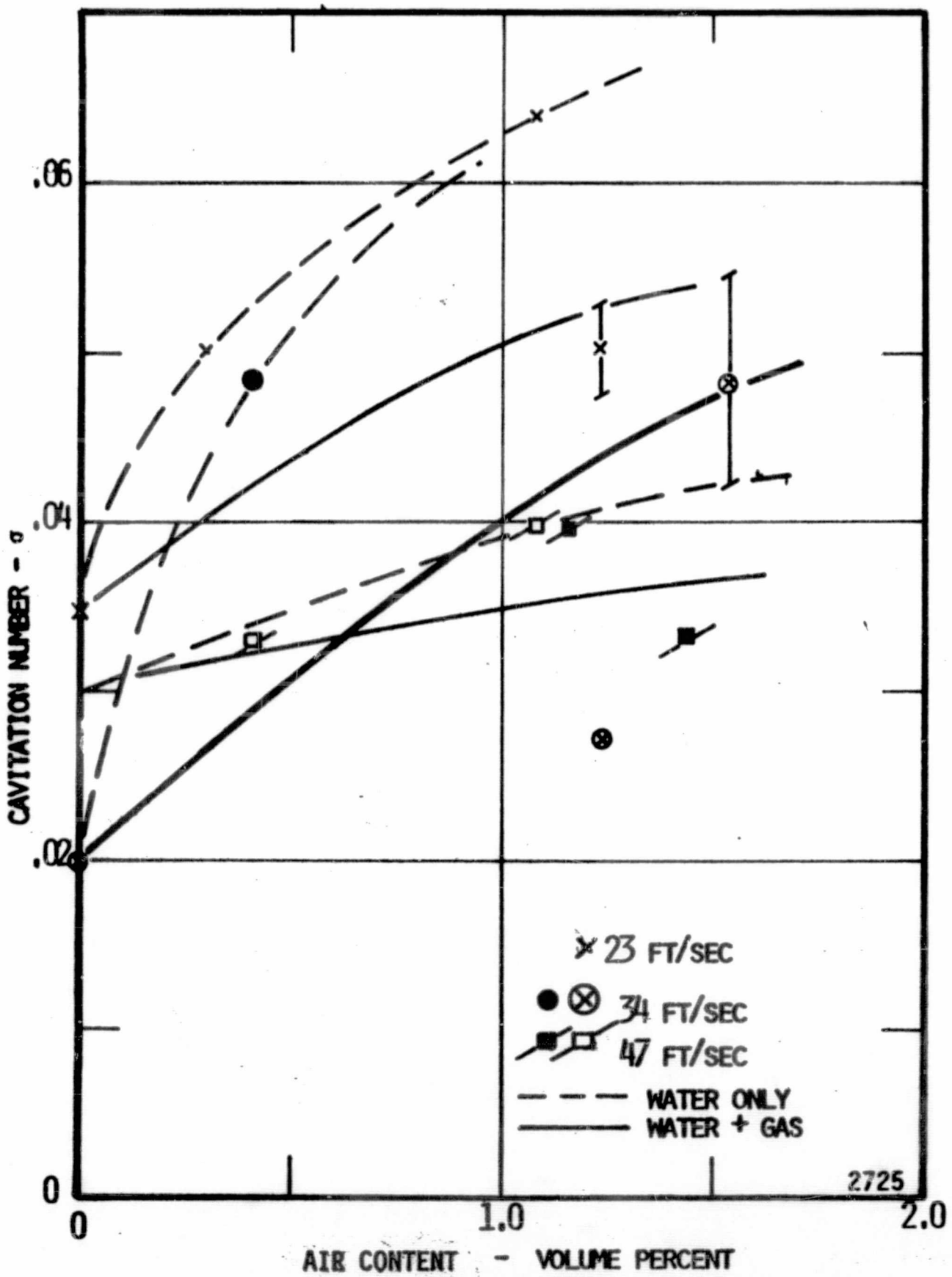

Figure 51. Cavitation Number versus "Total" Volume Percent of "Volatiles".

regardless of whether one plots σ_c versus water content or versus "total volatile" content. All subsequent runs were made such that the water content was less than 0.02% to insure a negligible contribution to the cavitation from this source. (See Appendix C for technique of measurement.) At the present time, in light of the various differences noted between hydrogen and argon as the entrained gas, it is unlikely that volume percent of all "volatiles" will be a suitable correlating parameter.

I. Observations of Venturi Flow Patterns

Because the analysis of the pressure profiles taken with water had indicated a substantial shift in the location of the minimum pressure point as venturi size varied, a similar check was made with the mercury data. The results, normalized in the manner described in paragraph E above, are shown on Figures 52 through 54. For the 1/2-inch and 1/4-inch plastic venturis (Figure 52) and 22 ft/sec velocity. However, when the data at 34 ft/sec in all the venturis are examined, it is found that with the exception of the 1/4-inch case, all the venturis show the minimum point to be located at or near the end of the throat section, so that this is partially contrary to the water findings discussed earlier. In Figure 54 the zero cavitation profile for all three velocities is plotted, and as with water, the location of the minimum point is independent of the velocity in a given venturi.

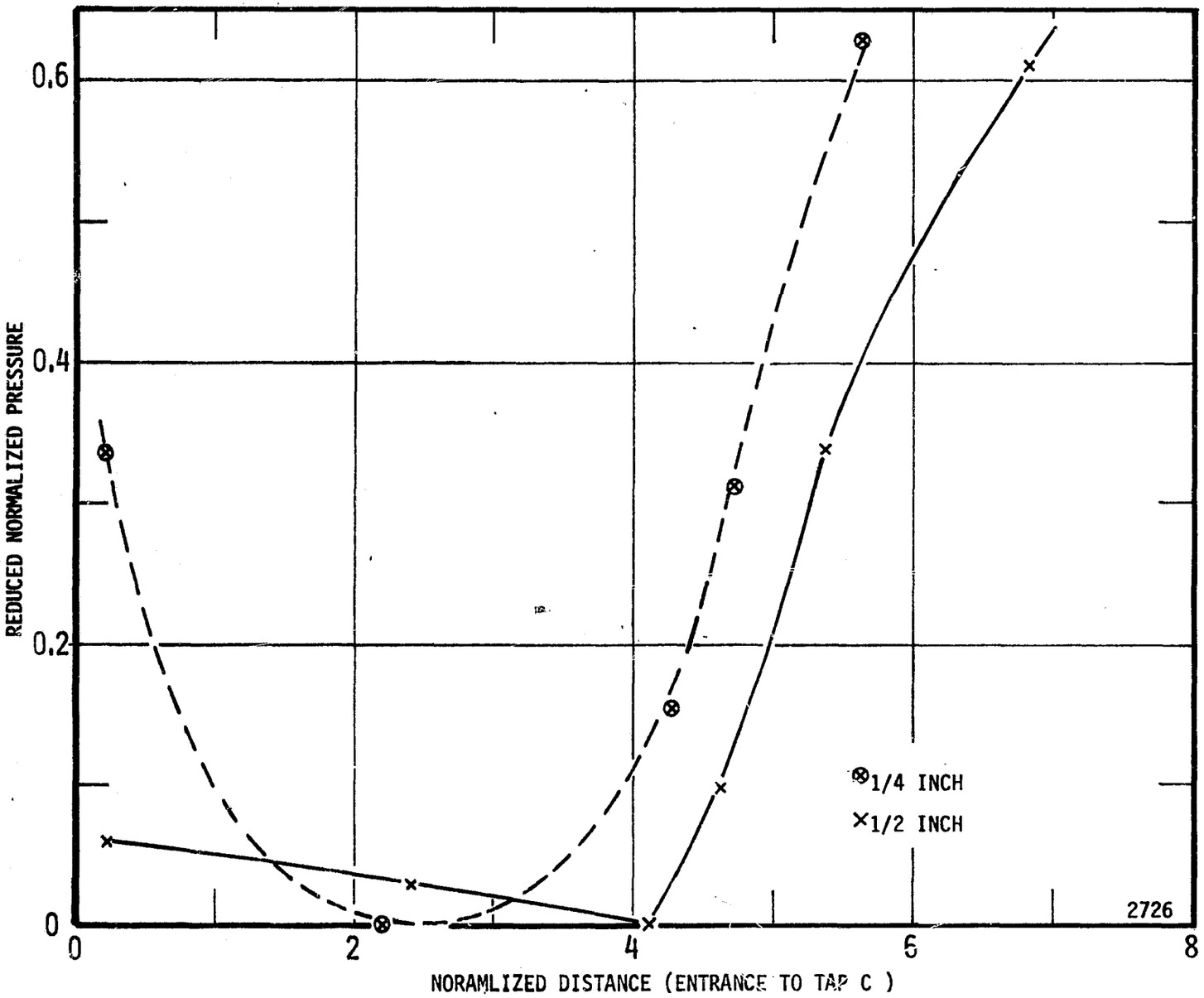

Figure 52. Reduced Normalized Pressure versus Normalized Distance, Mercury, 22 Feet per Second, Venturis 412 and 614.

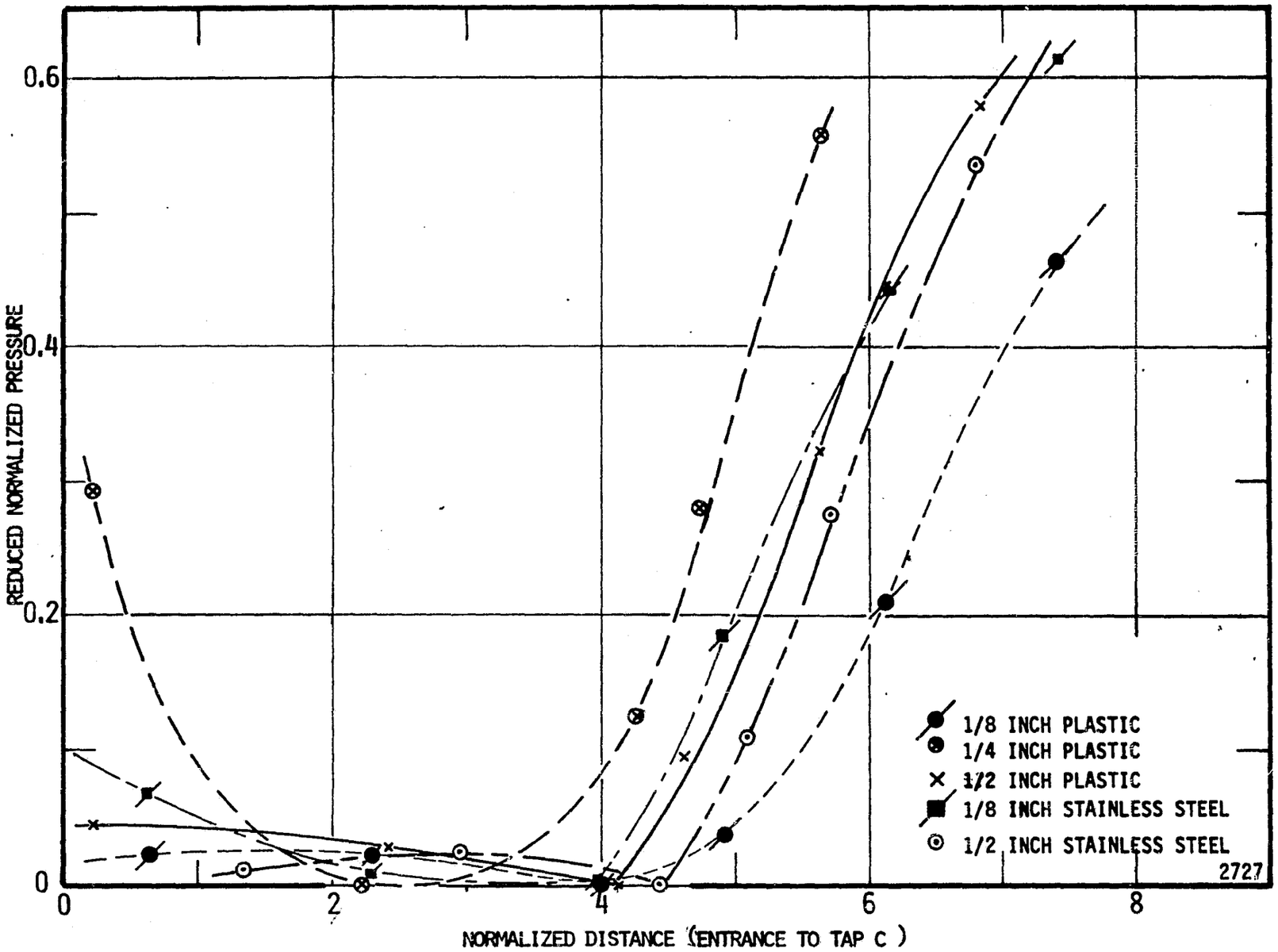

Figure 53. Reduced Normalized Pressure versus Normalized Distance, Mercury, 34 Feet per Second, All Venturis.

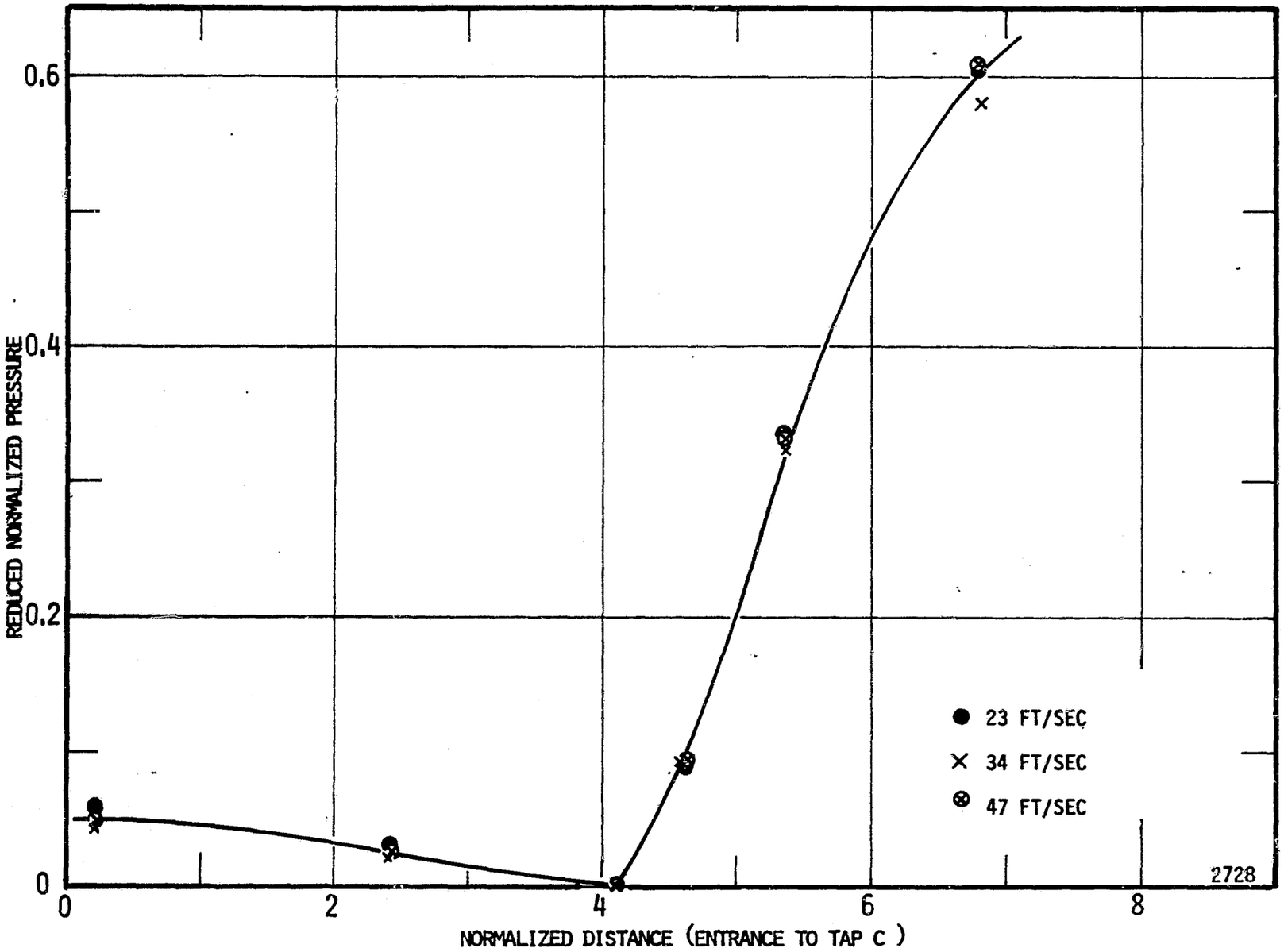

Figure 54. Reduced Normalized Pressure versus Normalized Distance, Mercury, All Velocities, Venturi 412.

J. General Comments on the Experimental Data

It is emphasized that the data that has been reported in this chapter is "raw" data in the sense that only the cavitation number has been computed, all other values are as experimentally determined. At the beginning of this chapter it was asserted that it is nearly impossible in fluid flow systems such as these venturis represent to vary just one parameter and thus to investigate only its effects. A review of the data just presented bears strong witness to this fact. Similarly, the data indicates that flow conditions are much easier to reproduce in the water system than in the mercury system. At first this seems to be somewhat of a paradox because the mercury loop, as described in Chapter III, has more means of control, i.e., pump speed, sump pressure, and throttle valves before and after the test section. Counteracting this is the fact that the gas content variations are more difficult to control and evaluate in the mercury system. Because a substantial portion of the gas in water is dissolved, the Van Slyke technique is an excellent means for evaluating the gas content. However, with the gas fully entrained as in mercury, the problem is much more difficult, as witnessed by the elaborate sampling techniques required. Furthermore, with these fully entrained gases, one is much more likely to obtain nonrepresentative samples because of the large influence local flow irregularities can have on the distribution and trajectory of the gas bubbles. The regression analyses which follow provide a technique for at least partial evaluation of these variations in terms of their statistical significance.

CHAPTER V

DATA ANALYSES

The objective of this study is to develop a correlation of the cavitation number with a set of independently determined, but broadly applicable (in fluid flow problems) dimensionless parameters; the goal of course being to predict cavitation or cavitation susceptibility by measurement of simple physical parameters of the system. The experimental data were reduced, the dimensionless parameters calculated, and the results tabulated as was previously indicated (see Appendix G). The data were then subjected to a computerized regression analysis developed at the University of Michigan[54,55] the essential features of which are discussed in Appendix H. Unfortunately, this approach was not as successful as had been anticipated and an alternate less sophisticated approach to analysis of the data was subsequently pursued. A brief summary of the correlation with the dimensionless parameters is presented below followed by the alternate analysis. A more complete description of the work with the dimensionless parameters may be found in Appendix I.

A. Dimensionless Parameter Correlations

As was indicated the 1/2 inch system has been the "standard" test system for cavitation damage studies at the University of Michigan; consequently it was selected as the baseline for these studies. In Table 3 a portion of the results from correlation attempts with the data are shown. In reviewing these results the following definition

TABLE 3

REGRESSION ANALYSIS RESULTS - MULTIPLE PARAMETERS
VENTURI 412 WATER CAVITATION

Standard Error of Data - 0.0619

	Standard Error of Estimate	Coefficient of Determination	Remarks
Part I Additive Terms			
1. $\sigma_c = .0375-.00299B_n^{-1.0}+.0471We_n^{-2.0}+.149\beta^2$	.0123	.964	(1)(2)(3)
2. $\sigma_c = .0347+0631We_n^{-2.0}+.0690\beta^2$	.0157	.939	(2)(3)
3. $\sigma_c = .0376-.0029B_n^{-1.0}+1.21We_n^{-2.0}+.149\beta^2$	0.124	.963	(1)(2)(4)(7)
4. $\sigma_c = .00580+.0359Re_n^{-1/4}+.0100We_n^{-2.0}-5.85X10^{-5}B_n^{-10.0}+.0734\beta$	.0149	.947	(2)(3)(5)(6)
5. $\sigma_c = .0296+.0574We_n^{-2.0}+.0526\beta$	.0158	.939	(2)(3)(6)
6. $\sigma_c = .00677+.0469Re_n^{-1/4}+.0729We_n^{-2.0}$	.0169	.929	(2)(3)(5)
7. $\sigma_c =0.0432+0.0167Gas/We_n^{2.0}-3.S2X10^{-6}Re_n^{3.0}$	.0143	.947	(2)(3)(5)(6)
8. $\sigma_c =0.0387+.0184Gas/We_n^{2.0}$	.0156	.939	(2)(3)
9. $\sigma_c = .00939+.0148Gas/We_n^{2.0}+.0756Re_n^{-1/4}$	.0137	.954	(2)(3)(5)(6)
10. $\sigma_c = .0515+0.0155Gas/We_n^{2.0}-.00159Re_n$	.0141	.951	(2)(3)(5)(6)

TABLE 3 (Con't)

	Standard Error of Estimate	Coefficient of Determination	Remarks
11. $\sigma_c = .0135+.0858\beta^2+.0557Re^{-1/2}+.0312We_n^{-2.0}$	.0147	.948	(2)(3)(5)
12. $\sigma_c = .0538+.189\,\beta/We_n^{2.0}-.0425B_n^{-.10}+0377Re_n^{-.25}$	.0128	.961	(1)(2)(3)(5)
Part II Multiplication Terms			
1. $\sigma_c = .0599-.000375Re_nWe_nB_n\beta$	.0264	.825	(1)(2)(3)(5)
2. $\sigma_c = .0489+\frac{.00926}{Re_nWe_nB_n\beta}$	.0264	.825	(1)(2)(3)(5)
3. $\sigma_c = .0536+2.56X10^{-14}Re_n^{-.25}We_n^{-2.0}B_n^{-10.}\beta$	.0275	.810	(1)(2)(3)(5)
4. $\sigma_c = .0429+1.097\,\frac{\beta}{Re_n^{-2.0}}$	.0157	.938	(1)(2)(3)(5)

REMARKS: (1) $B_n = B \times 10^{-5}$

(2) $We_n = B \times 10^{-2}$

(3) Weber used assumes 1 mil characteristic length

(4) Weber number used assumes D_t as characteristic length

(5) $Re_n = Re \times 10^{-5}$

(6) Terms inserted without regard to statistics

(7) $We_n = We \times 10^{-5}$

must be kept in mind. The data is perfectly correlated when the coefficient of determination is unity and no correlation exists when the value of the coefficient is zero. At first examination the results in Table 3 are quite encouraging as the coefficients are all greater than 0.9. However, this can be misleading as illustrated by examining Figures 55 and 56. In these figures we have plotted a calculated value for σ_c (using the experimental values for the independent variables) against the experimental σ_c . A perfect correlation would provide a single straight line with a slope of unity, therefore, the scatter of points about this line is a measure of the degree of correlation or the goodness of fit. In Figure 55 only the gas content, Weber number and Reynolds number are included. Here we note that there is a "skewing" of the distribution, or apparently some systematic omission. In Figure 56 the thermodynamic parameter has been included. The importance of this additional factor is obvious. Although the correlation is still imperfect, the points are better distributed about the line, implying that the gas content, Reynolds number, Weber number and the thermodynamic parameter are all important to the process. It is emphasized that no size effects are included. These results also point up to the fact that an exceptionally good correlation will be hard to establish since a number of combinations of parameters give nearly equivalent results in terms of coefficients of determination.

With the results from the 1/2 inch venturi in mind, similar correlations were attempted with all of the water data and a portion of the results are shown in Table 4. Clearly these results are not as satisfactory as those for the 1/2 inch case alone. On Figure 57,

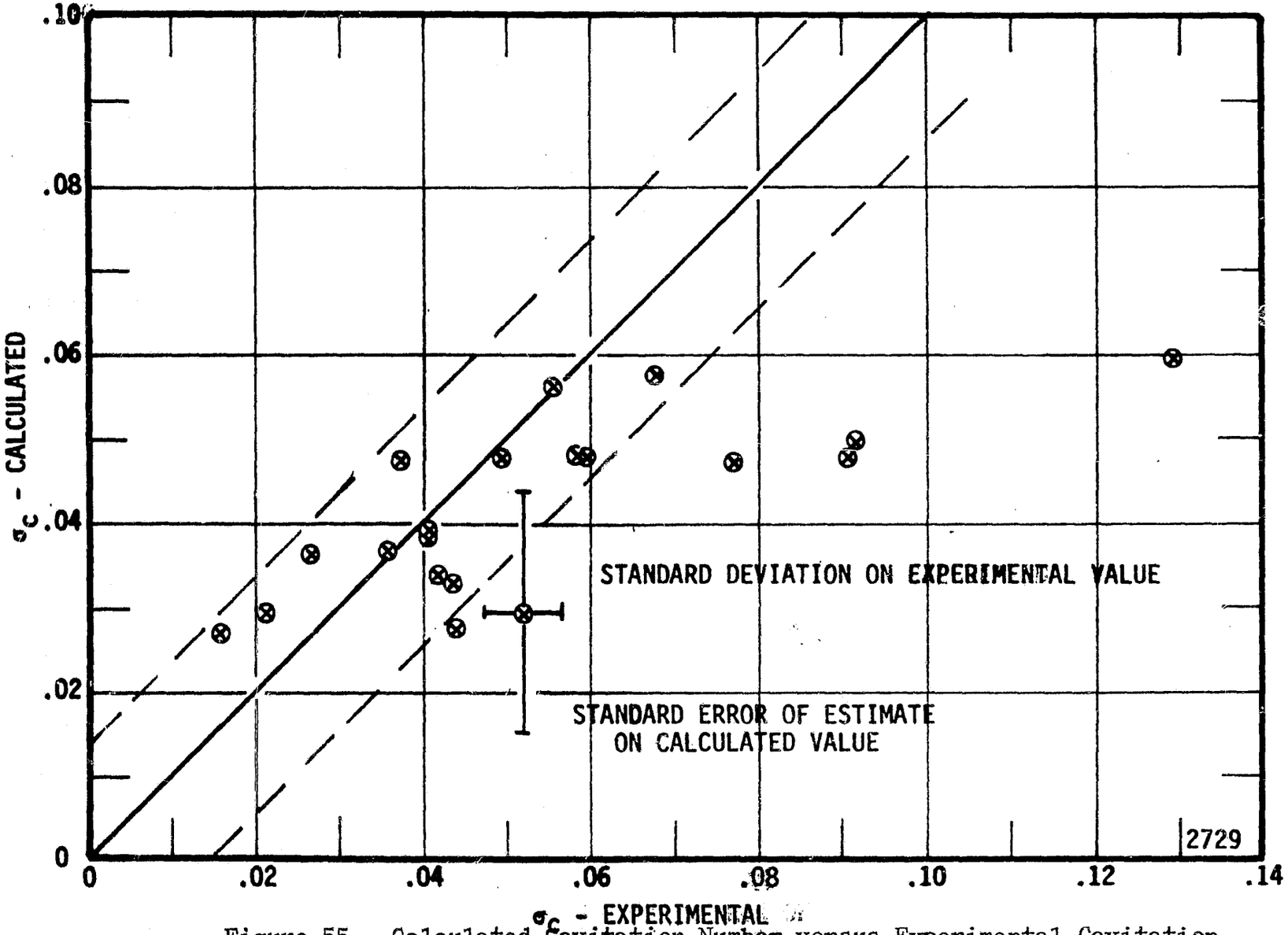

Figure 55. Calculated Cavitation Number versus Experimental Cavitation Number, Venturi 412, Water Cavitation, Equation 8, Part I, Table 3.

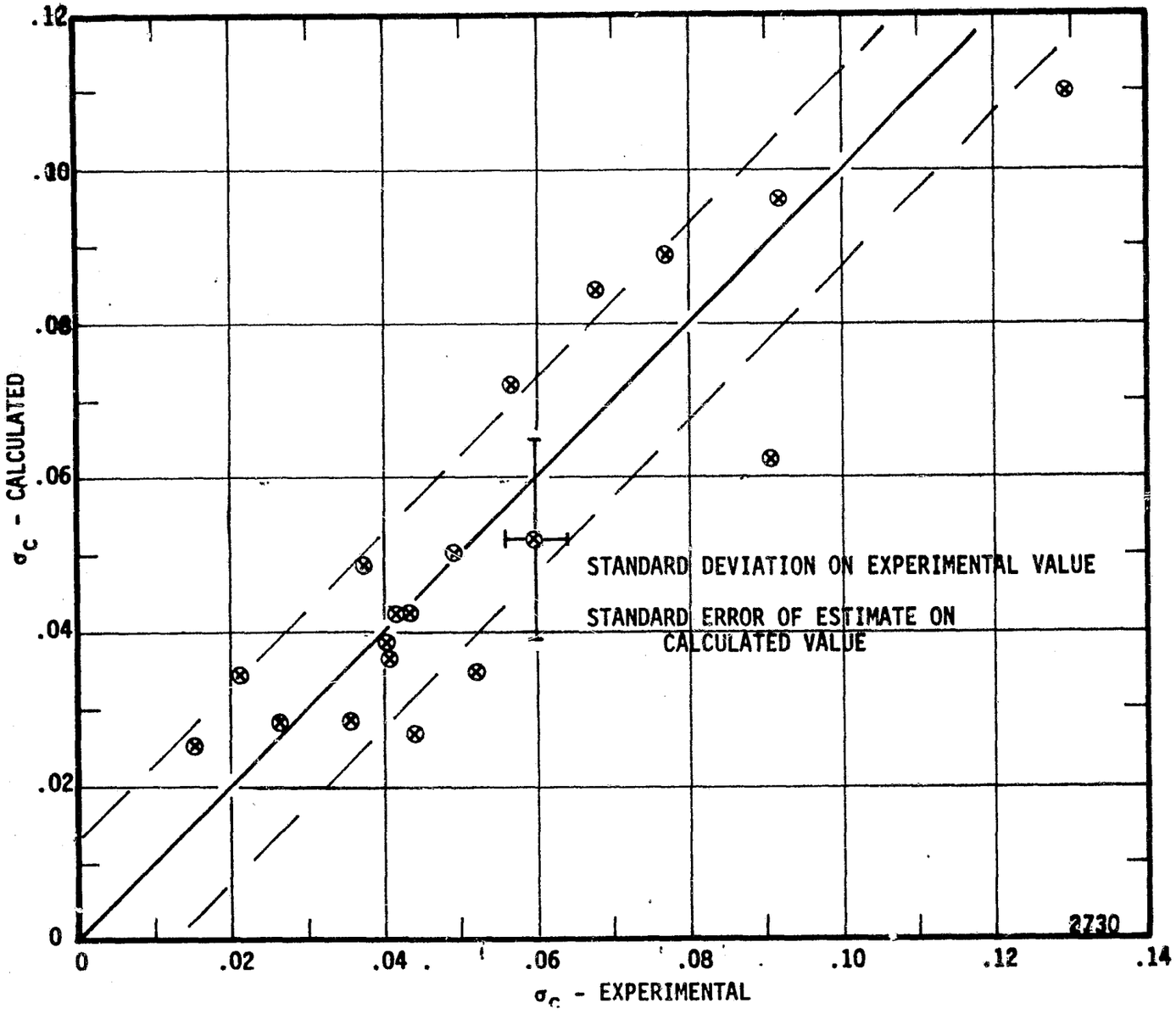

Figure 56. Calculated Cavitation Number versus Experimental Cavitation Number, Venturi 412, Water Cavitation, Equation 12, Part I, Table 3.

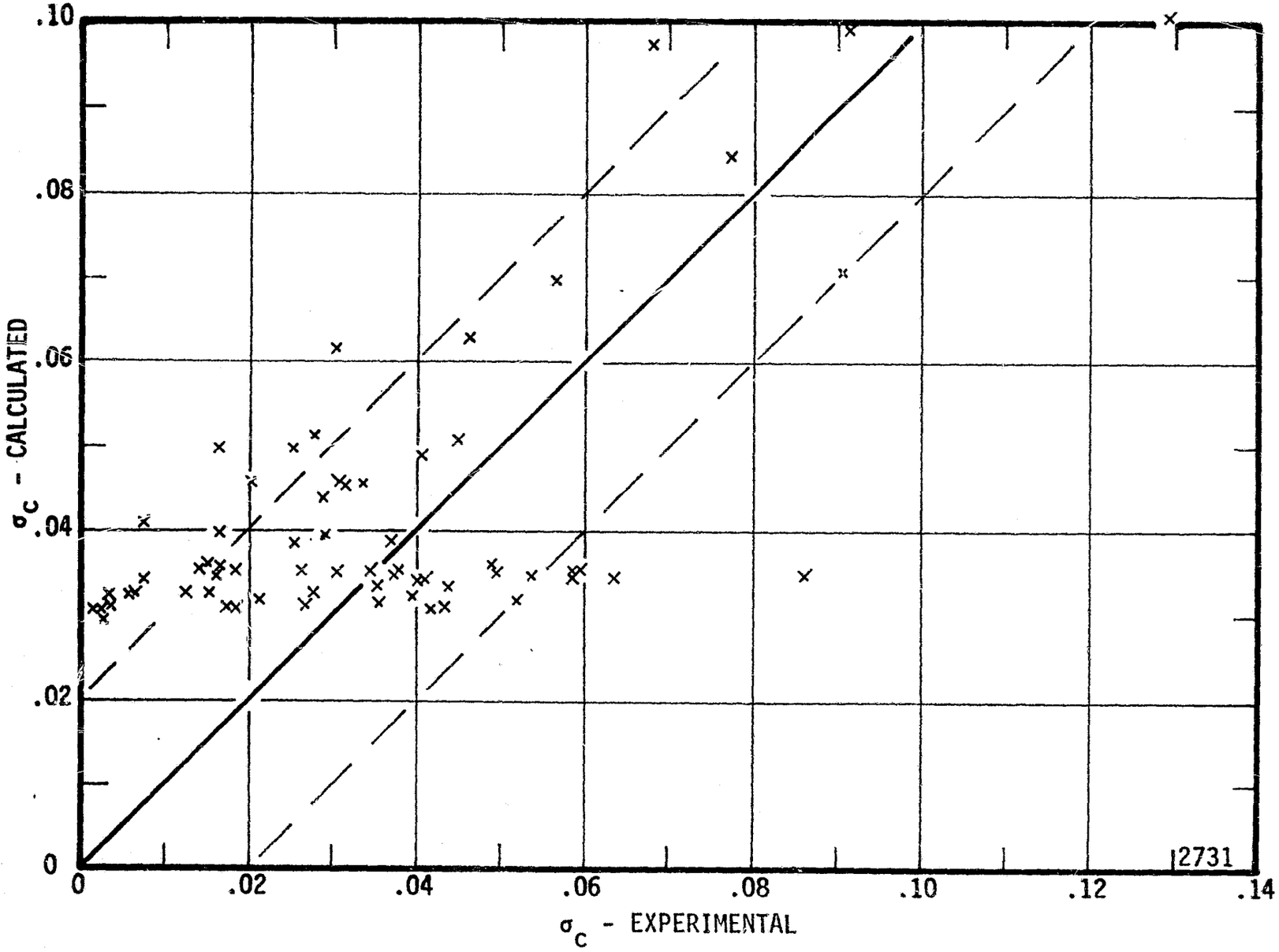

Figure 57. Calculated Cavitation Number versus Experimental Cavitation Number, All Plastic Venturis, Water Cavitation, Equation 13, Part I, Table 4.

TABLE 4

REGRESSION ANALYSIS - MULTIPLE PARAMETERS
ALL PLASTIC VENTURI - WATER CAVITATION

Standard Error of Data = .0447

	Standard Error of Estimate	Coefficient of Determination	Remarks
Part I Additive Terms			
1. $\sigma_c = .0258+.0612We_n^{-2.0}$	.0236	.742	(2)(3)
2. $\sigma_c = .0278+.0839We_n^{-3.0}$	.0233	.748	(2)(3)
3. $\sigma_c = .0286-.00470We_n^{1/2}+.000147We_n^{3}+.0147We_n^{-1}-0.00125We_n^{-2}$	.0189	.832	(2)(7)
4. $\sigma_c = .0214+1.35X10^{-6}-7.23X10^{-9}We_n^{-10}-.00269B_n^{-1/2}+.0791\beta$	.0237	.744	(1)(2)(3)(5)
5. $\sigma_c = .0566+3.19X10^{-6}Re_n^{3.0}+.0935We_n^{-10}-.00199B_n^{-1/2}+.0508\beta$	.0235	.748	(1)(2)(3)(5)
6. $\sigma_c = .0254+.152\beta/We_n^{2.}+9.15X10^{-3}Re_n^{3}$	.0211	.783	(2)(3)(5)
7. $\sigma_c = .0260+.150\beta/We_n^{2}$	.0210	.782	(2)(3)
8. $\sigma_c = .0265+6.95X10^{-7}Re_n^{3.0}+.315\beta/We_n^{4}$	.0199	.805	(2)(3)(5)
9. $\sigma_c = .0269+.312\beta/We_n^{4.0}$	.0202	.805	(2)(3)
10. $\sigma_c = .0276+2.19\beta/We_n^{10}+4.69X10^{-4}Re_n^{3}$	.0178	.844	(2)(3)(5)

TABLE 4 (Con't)

	Standard Error of Estimate	Coefficient of Determination	Remarks
11. $\sigma_c = .0278+2.17\varrho/We_n^{10}$	.0178	.844	(2)(3)
12. $\sigma_c = .324+2.13\frac{\varrho}{We_n}10-.00112B_n^{-.5}$	.0199	.817	(1)(2)(3)
13. $\sigma_c = .0234+2.023\frac{\varrho}{We_n^{10}}-.00164B_n^{-.5}+7.84X10^{-7}Re_n^{3.0}+.0109We_n^{-.333}$	.0220	.817	

Part II Multiplicative Terms

1. $\sigma_c = .0377-.000154Re_nWe_nB_n\varrho$	.0270	.649	(1)(2)(3)(5)
2. $\sigma_c = .0358+.00530Re_n^{3.0}We_n^{-10.0}B_n^{-.5}\varrho$	.0252	.704	(1)(2)(3)(5)
3. $\sigma_c = .035+.0940Re_nWe_n^{-3.0}B_n\varrho$	.0232	.741	(1)(2)(3)(5)
4. $\sigma_c = .036+.00115Re_nWe_n^{-1.0}B_n^{-10}\varrho$	.0257	.693	(1)(2)(3)(5)
5. $\sigma_c = .0305+.227\varrho^2/We_n^2$	.0241	.720	(1)(2)(3)(5)

TABLE 4 (Con't)

REMARKS: (1) $B_n = BX10^{-5}$

(2) $We_n = WeX10^{-2}$

(3) Weber number used assumes 1 mil characteristic length

(4) Weber number used assumes D_t as characteristic length

(5) $Re_n = ReX10^{-5}$

(6) Terms inserted without regard to statistics

(7) $We_n = WeX10^{-4}$

equation 13 from Table 4 is plotted. Again we see a considerable "skewing" of the data, and in fact, the bulk of the calculated values for σ_c lie between 0.03 and 0.04 regardless of the experimental value which seems to imply that again some systematic omission has occurred. This provides further convincing proof that one must be extremely careful in the application of a statistical analysis. That is, the numerical statistics may appear quite acceptable but the distribution of the data may leave much to be desired.

In general the results with mercury are less satisfactory than those with water. Partial results from correlation attempts using all the venturis with mercury are in Table 5. The coefficients of determination are low enough that the scatter diagrams are not included in the summary.

B. Summary Comments on Initial Correlations

Based upon the results to this point and the previously presented experimental data the following preliminary conclusions may be drawn.

1. The cavitation observed here in water is heavily influenced by the permanent gas present. This obscures the details of any vaporous cavitation that occurs, although the cavitation number is dependent upon both. This is based upon the fact that the air content could not be reduced below about 0.5 volume percent at STP and that the dominant term in these initial correlations is a gas content parameter modified by some surface tension considerations.

2. Size effects are not controlling over the range of venturis tested. This is evidenced by the fact that the goodness of the correlation as indicated by the coefficient of determination is not changed

TABLE 5

REGRESSION ANALYSIS RESULTS - MULTIPLE PARAMETER
MERCURY CAVITATION

I. 1/2" Plastic Venturi Standard Error Data = .0613

	Standard Error of Estimate	Coefficient of Determination	Remarks
1. $\sigma_c = .0400+1.02X10^{6}\beta^{2}-78.7\beta$	.026	.808	
2. $\sigma_c = .0259+6.42X10^{10}Re^{-2.0}-121We^{2.0}-.00161B_n+9.08X10^{5}\beta^{2}$	.0271	.822	
3. $\sigma_c = .0518-7.63X10^{9}Re^{-2.0}+1.00X10^{9}\beta^{2}/We^{2}-.00103B_n$	.0294	.787	

II. All Venturis Standard Error of Data = .0956

1. $\sigma_c = .662+5.92X10^{5}Re^{-1.}+2.43X10^{-7}Re-2.46X10^{-4}B_n^{2}-3.74X10^{-5}B_n^{-1/2}+3.24X10^{5}\beta^{2}-1220X10^{11}Re^{-2.0}$	.0640	.562	
2. $\sigma_c = .0530-4.86X10Re^{-8}+1.69X10^{-6}We^{2.0}-1.16X10^{-5}B_n^{-1/2}+4.05\beta^{1/2}$	.0729	.428	
3. $\sigma_c = .278-3.71X10^{-4}B+4.45X10^{9}Re^{-2.0}+3.51X10^{5}X\beta^{2}$	.0761	.376	
4. $\sigma_c = .0849-5.61X10^{-8}Re-9.39X10^{-6}B^{-1/2}+4.42X10^{5}\beta^{2}+2.04X10^{-6}We^{2}$	.0725	.434	

TABLE 5 (Con't)

	Standard Error of Estimate	Coefficient of Determination	Remarks
5. $\sigma_c = .0102-1.85X10^{3}\beta/We^{2.0}-4.42X10^{-6}B^{-1/2}-4.67X10^{-8}Re$	.0758	.379	
6. $\sigma_c = .0102-4.66X10^{-8}Re-1.11X10^{7}\beta^{2}/We^{2}-4.35X10^{-6}B_n^{-1/2}$	.0759	.378	

dramatically by inclusion or deletion of the Reynolds number. However, it is clear from the improvement in the distribution of the "scatter diagrams" when the Reynolds number is included that there are significant Reynolds number influences.

3. Thermodynamic effects, although present and important, are, like size effects, not dominant. Again this is evidenced by the fact that inclusion or deletion of the thermodynamic parameter does not produce much change in the correlation statistics although the distribution is improved. Nevertheless, it is still anticipated that in the absence of permanent gas, thermodynamic considerations will be important. However, the overwhelming importance of gas effects here, obscures the vaporous cavitation and any attendant thermodynamic effects.

4. Not included in analyses here are other effects that do seriously affect the cavitation. This is evidenced by our failure to achieve a complete correlation. Because the cavitation was frequently observed to occur in relatively isolated spots, it is concluded that most likely the key factors not included in the analysis are surface roughness or discontinuities, or localized turbulence leading to severe, unmeasurable, and very localized pressure reductions that can initiate cavitation. Unfortunately, it is extremely difficult to quantify this effect and essentially impossible to scale it geometrically across a range of venturi sizes.

5. In mercury as was the case with water, the gas content is the variable or parameter of predominant importance, and therefore some effects, such as the temperature related thermodynamic effects are masked.

6. Since the water data from several different venturis did correlate reasonably well as compared with the mercury data, it must be assumed that the cavitation in the stainless steel and plastic venturis is different, even though the designs have the same geometry. For instance, this could be the result of necessarily different detection methods leading to different degrees of cavitation being compared due to the different methods of detection (i.e., sonic versus visible initiation) or from variations in surface roughness.

As stated, a more complete discussion of this regression analysis approach is contained in Appendix I.

C. Alternate Analysis of Water Cavitation

The presentation of data in Chapter IV, coupled with the foregoing analysis, gives some guidance for an alternate avenue of investigation.

It is reasonable to postulate (based upon our knowledge of the physics involved) that:

$$\sigma_c \propto f(vp, V, D, T)$$

where vp is the volume percent of gas present, and V,D, and T are the velocity, diameter and temperature as previously defined. Because temperature alone is inadequate to account for the change in cavitation number with temperature, we will rely on already substantiated knowledge in this regard[23,43,44] and substitute for the temperature the thermodynamic parameter as defined by equation 6, Chapter II, i.e., the unnormalized parameter. Doing so, we may say:

$$\sigma_c \propto f(v_p, D, V, B)$$

Expressing the relationship in this manner further implies that although it may not yet be possible to predict the cavitation number from measured variables in a given system, it may still be possible to predict σ_c for a new system, having previously determined σ_c in some similar reference system. That is, assume:

$$\frac{\sigma}{\sigma_o} = \frac{f(v_p, D, V, B)}{f(v_{p_o}, D_o, V_o, B_o)}$$

and it may be possible to determine the effective ratio of the two cavitation numbers without establishing the exact functional relation between the cavitation number and the independent variables. Such a line of reasoning is pursued in the following manner.

For the 1/2 inch venturi, for which the most data exist, Figure 26 and 33 indicate definite gas content and velocity effects. This is especially clear when the curves from Figure 26 are cross-plotted as in Figure 58. A continuously increasing cavitation number with velocity is exhibited for low gas content while higher gas contents exhibit the trends already shown in Figure 33. This agrees with the arguments presented in Chapter II relative to the influence of gas pressure within a cavitation bubble. That is, for higher gas contents σ_c is proportional to the amount of gas present and these effects overshadow any surface tension effects. However, at very low or zero

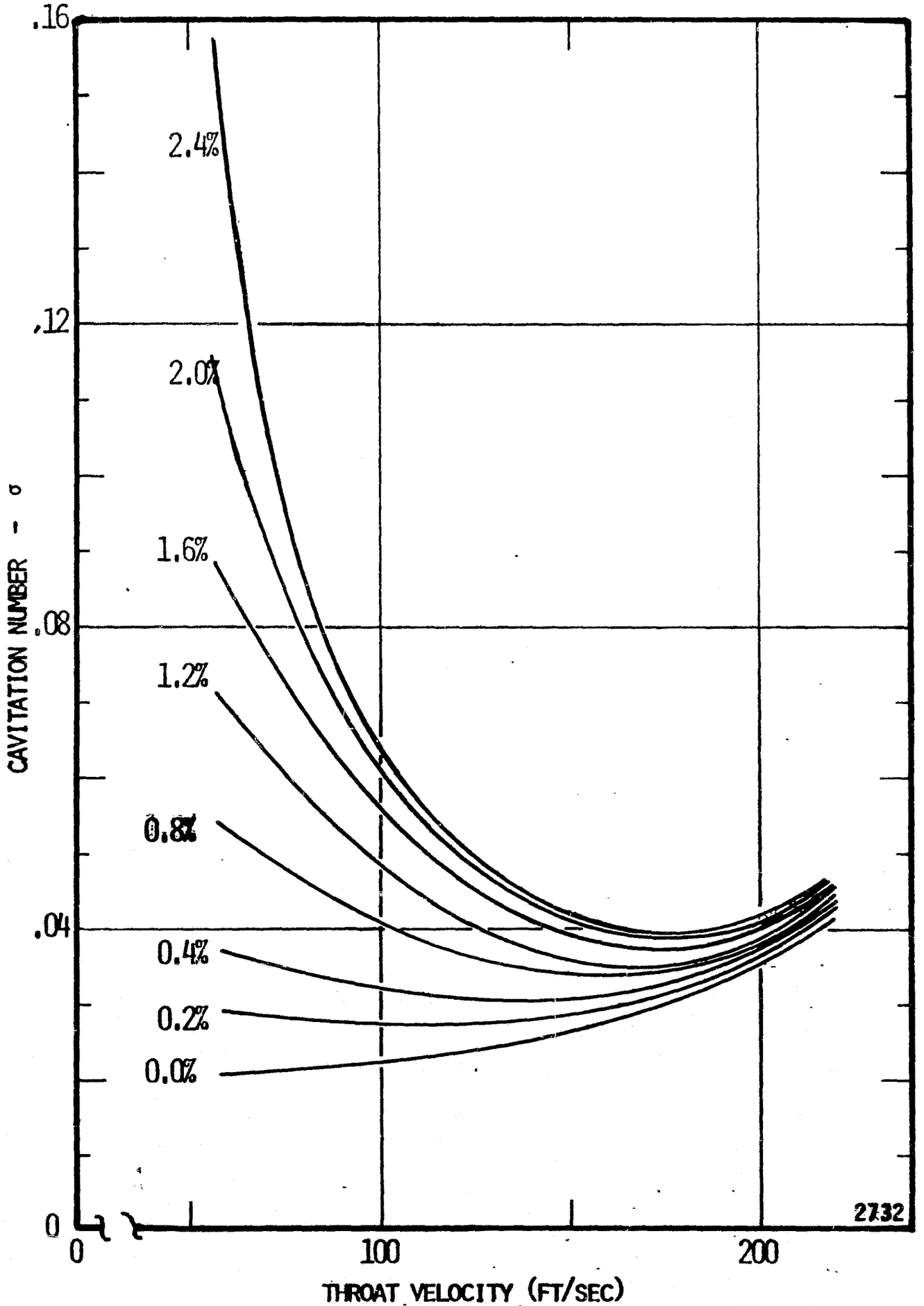

Figure 58. Cavitation Number versus Throat Velocity, Gas Content as Parameter, Venturi 412, Water.

contents surface tension effects become significant and serve to inhibit cavitation. The trends presented here for gas content values below approximately 0.7 percent by volume are extrapolations from the existing test data. The trends in Figure 58 are essentially consistent with those reported by Ruggeri and Gelder[19]. In Figure 59 the cavitation numbers obtained in the 1/4 inch venturi are plotted in a similar manner against throat velocity with gas content as the parameter, cross-plotting from Figure 30. Although the 1/4 inch curve does not provide an exact duplicate of the 1/2 inch curve there is sufficient similarity to postulate a relationship between the two which is some function only of size, for a given velocity, gas content, and temperature. On Figure 60 the cavitation number is plotted as a function of velocity for the 1/2 and 1/4 inch venturis for two gas conents. Examining Figures 59 and 60 it may be observed that for the higher gas contents, and velocities below 100 ft/sec, the cavitation number scales approximately as the ratio of the diameters. Above 100 ft/sec this ratio increases. For our model, we will assume that the ratio of the diameters (D/Do) provides the size scaling required. The shape of the curves, certainly below 170 ft/sec suggests an inverse relationship with velocity, such as that presented by Holl[14]. We may say that $\sigma_c \propto \frac{1}{V^n}$, where a simple numerical check indicates that below 170 ft/sec $n \cong 1$ for the 1/2 inch case, and $n \cong$ 2-2.5 for the 1/4 inch case. Therefore, since our purpose is to generate an expression which will relate the two cases, we will choose $n = 2$ for the velocity exponent. This selection of $n = 2$ rather than $n = 1.5$ stems from a desire to generate a "simple" expression and further reflects the

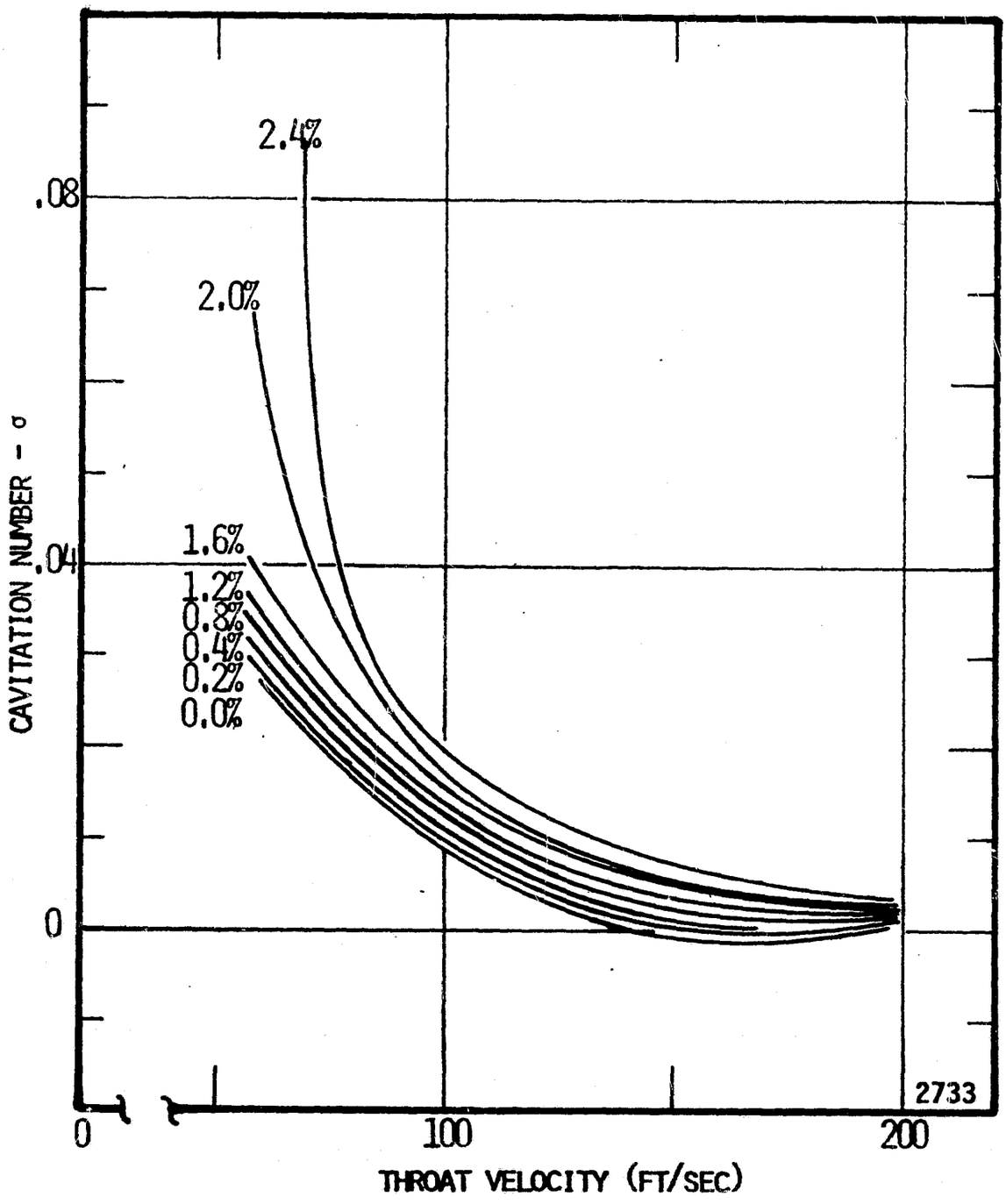

Figure 59. Cavitation Number versus Throat Velocity, Gas Content as Parameter, Venturi 614, Water.

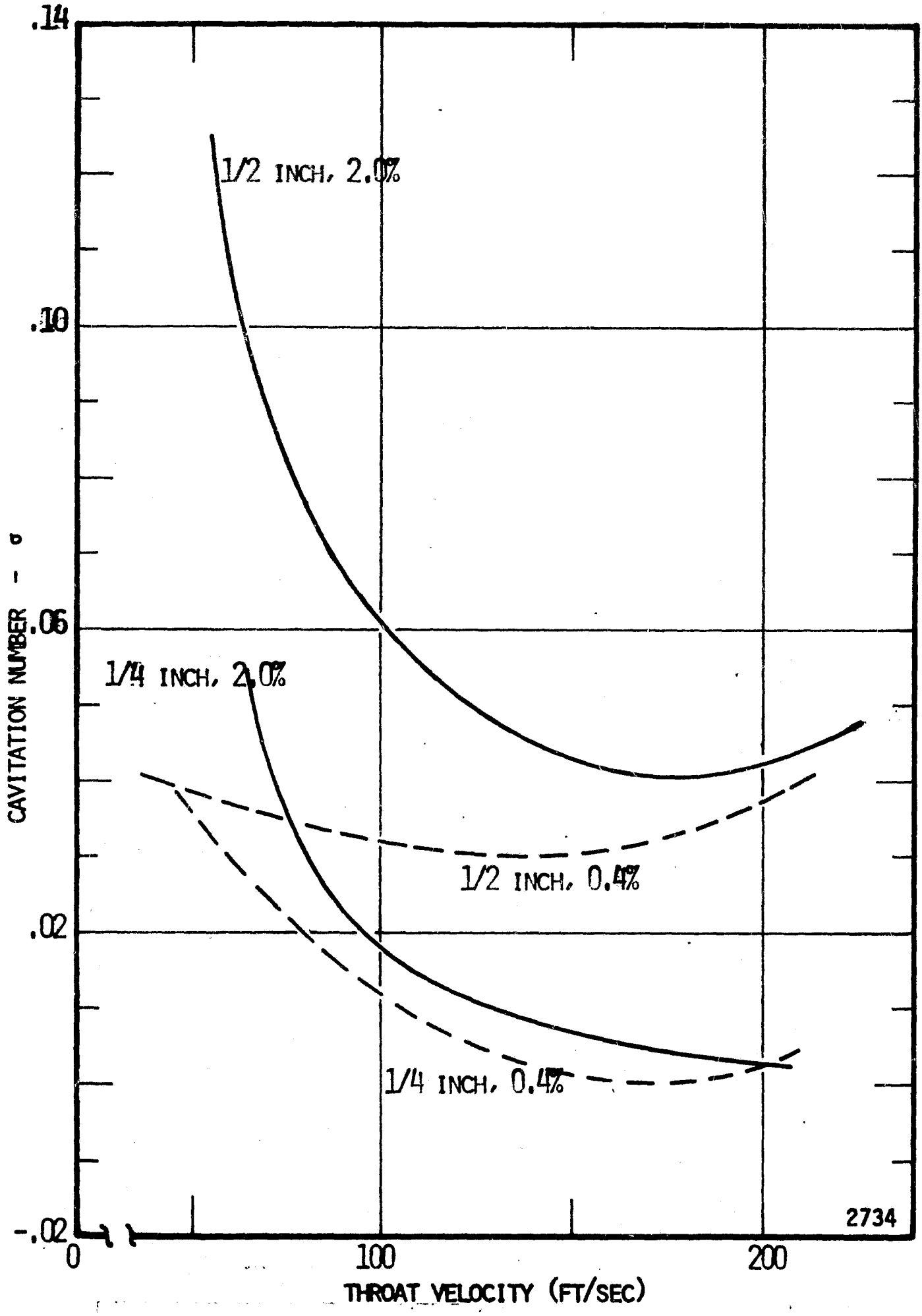

Figure 60. Cavitation Number versus Throat Velocity, Selected Gas Contents as Parameter, Venturis 412 and 614, Water.

success Holl[14] had using $n = 2$. If we reexamine Figures 26 and 30 at this point, we observe that in the 1/2 inch venturi (Figure 26) for a fixed velocity σ_c is approximately linearly proportional to the volume percent of gas present (vp). This also applies for the 1/4 inch venturi (Figure 30) except for the lowest velocity case. Therefore, we will assume that $\sigma_c \propto$ vp in establishing our ratios. The only effects not considered to this point are those due to temperature or thermodynamics. Figure 38 provides a means for examining these effects. A numerical check indicates that the cavitation number is roughly proportional to the thermodynamic parameter, B, raised to the 0.25 power. Therefore, the tentative relationship is established.

$$\frac{\sigma}{\sigma_o} = \left(\frac{v\rho}{v\rho_o}\right)\left(\frac{D}{D_o}\right)\left(\frac{V_o}{V}\right)^{2.0}\left(\frac{B}{B_o}\right)^{0.25}$$

Using this proposed relationship and a single set of data from the 1/2 inch experiments as the reference point, σ_c was calculated for visible initiation in the balance of the 1/2 and 1/4 inch case. The results of these calculations are shown on Figure 61, where the observed σ_c is plotted against the calculated σ_c . Obviously, if the postulated equation was exact, and there were no experimental errors, all of the points would fall on a straight line. The prediction of the 1/4 inch data is reasonable but the 1/2 inch data exhibit much more scatter. Further examination shows that the high velocity (V_T greater than 200 ft/sec) is consistently underpredicted (flagged points).

Reexamination of Figure 58 reveals that such a behavior should not be unexpected since the 1/2 inch data clearly do not follow an inverse square relationship for higher velocities, i.e., the cavitation number increases with velocity above 100 ft/sec. If one neglects this higher velocity data and does a least squares analysis of σ_c (obs) versus σ_c (calc), curve A on Figure 61 results. The closeness of Curve A to the 45° perfect prediction line implies that the prediction is reasonably good, recognizing that our data are confined to gas contents between approximately 0.5 and 2.0 percent. The next obvious step is to extend this analysis to the data from the other two venturis. In light of the minimal amount of data for the 3/4 and 1/8 inch cases no prior cross-plotting was attempted and a clear cut result may not be forthcoming. Nevertheless, the postulated equation was used,to generate σ_c (calc) for both the 3/4 and 1/8 inch venturis. A plot of σ_c (obs) versus σ_c (calc) is shown on Figure 62 for all venturis. Curve A represents a least squares fit of σ_c (obs) versus σ_c (calc) for the 1/2, 1/4 and 3/4 inch venturis (neglecting the 1/2 inch venturi high velocity points). The slope of this curve and its tolerance indicate that our postulated equation is predicting the cavitation number with less precision the wider the range we attempt to include. Curve B represents a similar least squares fit for all the data. Clearly our equation is not predicting the 1/8 inch data nearly as well as it does just the 1/2 and 1/4 inch.

Further examination of the results shown in Chapter IV provides some insight into the problem encountered with the 1/8 inch data. From Figure 31 it may be noted that the behavior of the cavitation

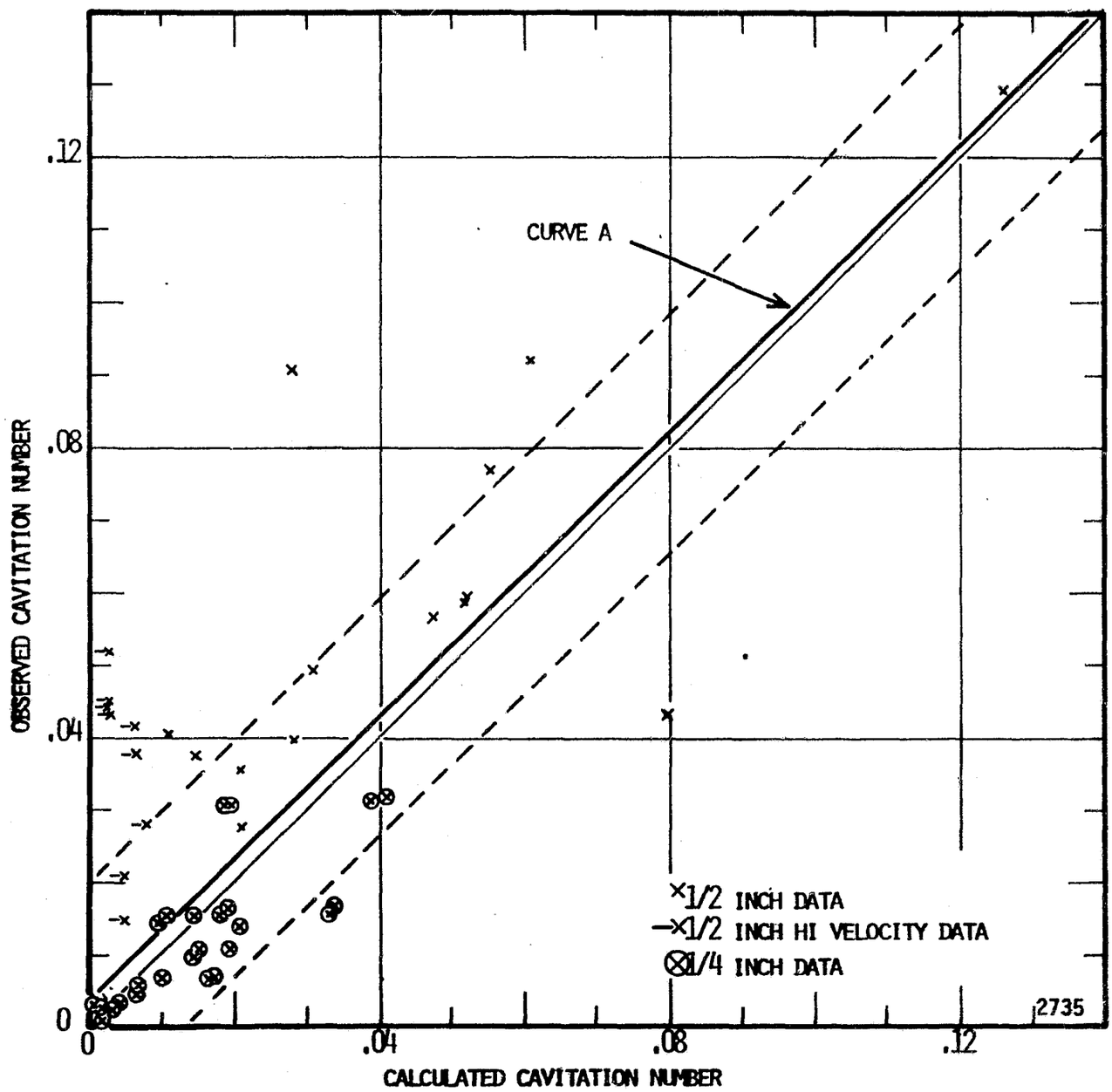

Figure 61. Experimental Cavitation Number versus Calculated Cavitation Number, Venturis 412 and 614, Water.

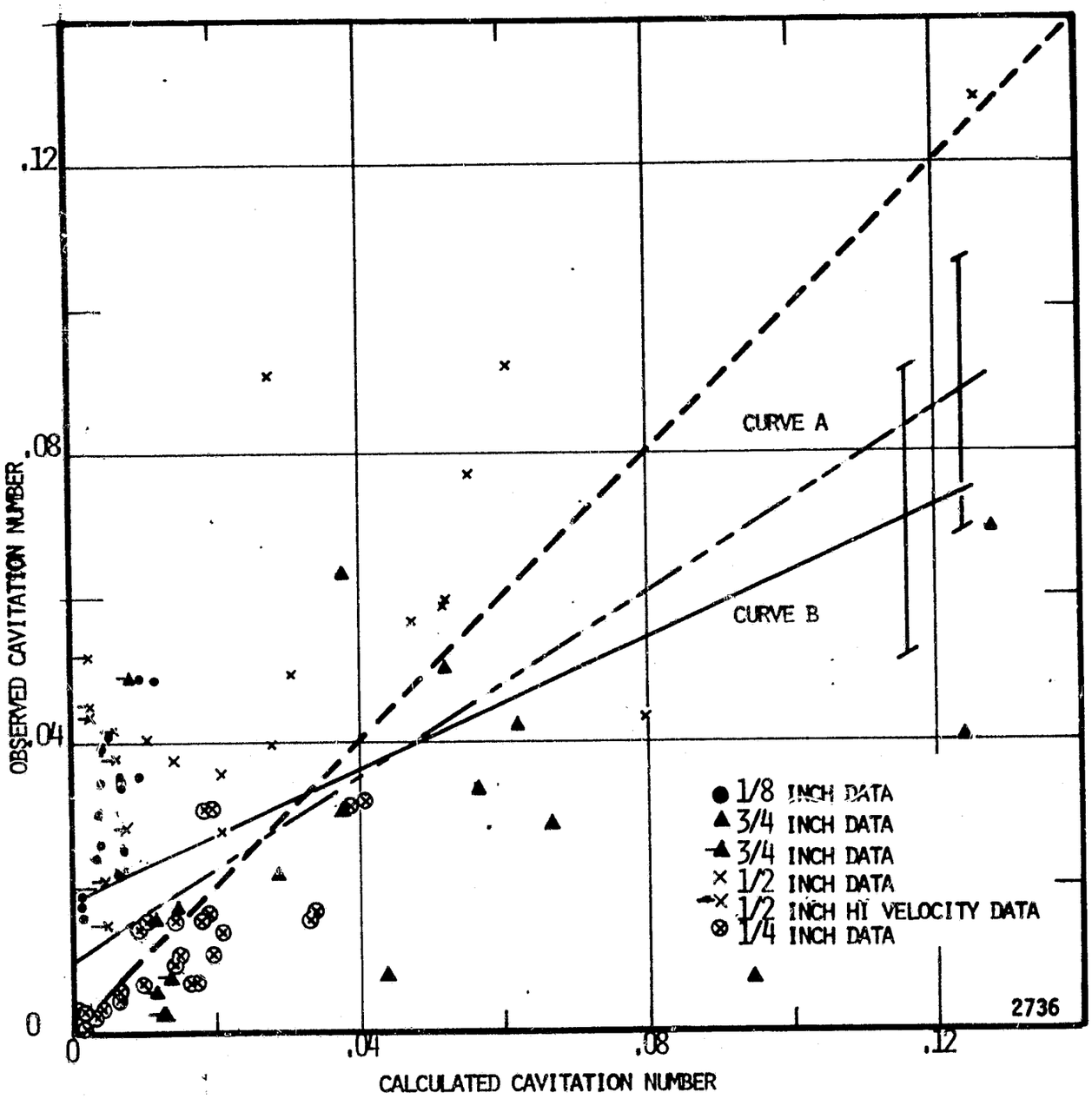

Figure 62. Experimental Cavitation Number versus Calculated Cavitation Number, All Plastic Venturis, Water.

number as a function of velocity in the 1/8 inch case is different in that σ_c decreases with decreasing velocity. Likewise, from Figure 41 we observe that the cavitation inception occurs at a different location in the 1/8 inch venturi, i.e., at the throat inlet rather than exit. Likewise, the limited photographic data (not included here) reveals that for the high velocity runs in the 1/2 inch venturi and the runs in the 1/8 inch venturi the cavitation occurred at very isolated points. In the other cases it was more evenly distributed around the venturi. This leads to the conclusion that unless the cavitation is uniformly distributed the postulated similarity conditions will not apply. At this point one is tempted to explain this behavior in terms of some critical Reynolds number. However, this is not really sufficient. We observe the deviation (or non-prediction) at high velocities in the 1/2 inch venturi (i.e., higher Reynolds numbers) and at lower velocities and size in the 1/8 venturi (therefore, lower Reynolds number). The actual behavior of σ_c with Reynolds number is shown in Figure 63, where σ_c is plotted against the Reynolds number ($\ell_n R_e$) for two gas contents and a nearly constant temperature. This indicates that Reynolds number alone is insufficient to correlate the data. The 1/8 and 1/4 inch data appear to define a single curve, but the 1/2 and 3/4 inch are clearly distinct and separate. Therefore we can only state here that the scaling relation should be used with caution at high velocities or in small diameter venturis.

In summary, for water cavitation in cylindrical throat venturis we may say to a reasonable approximation that:

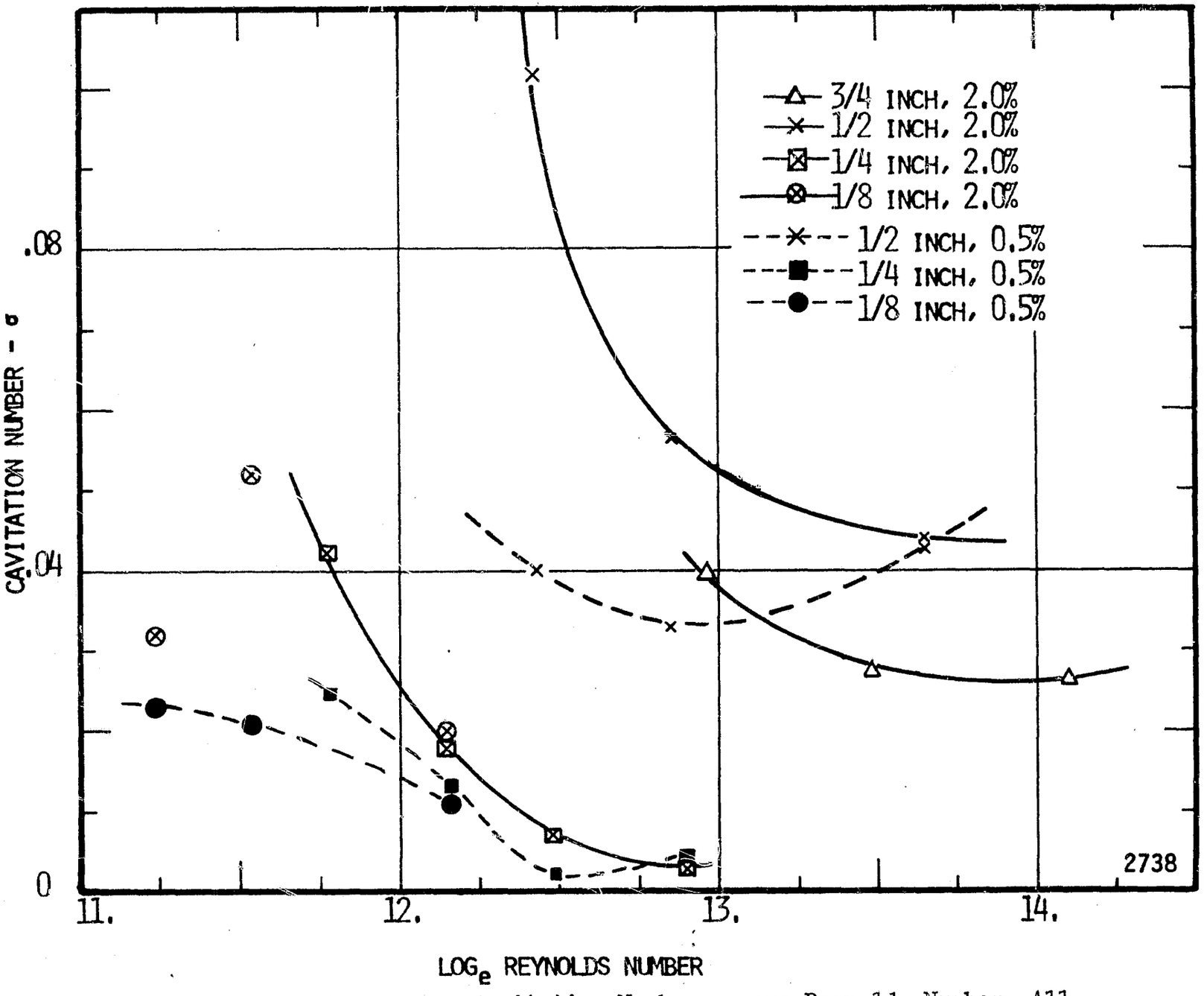

Figure 63. Cavitation Number versus Reynolds Number, All Plastic Venturis, Water.

$$\frac{\sigma}{\sigma_o} = \left(\frac{v_p}{v_{p_o}}\right)\left(\frac{D}{D_o}\right)\left(\frac{V_o}{V}\right)^{2.0}\left(\frac{B}{B_o}\right)^{0.25}$$

Further, several trial calculations indicate that best results accrue when the reference system is near the middle of the available range of variables. Likewise, it must be noted that the relationship has yet to be tested outside the range of gas content, velocities and sizes of the present study.

D. Alternate Analysis of Mercury Cavitation

The results of plotting the cavitation number versus throat velocity with gas content as the parameter appear on Figure 64 which is cross-plotted from Figure 44 . Here we see a departure from the trends noted in water but similar results with mercury were reported by Robinson[7] in a venturi designed for damage studies. An interesting comparison can be made with the water data from the 1/8 inch venturi (Figure 36). In the case of water in the 1/8 inch venturi, a maximum occurs in the σ_c versus velocity plot near 100 ft/sec (Re No $\cong$ 1×10^5), but for mercury in a 1/2 inch venturi the peak appears near 30 ft/sec (Re No $\cong 2 \times 10^6$). This is still further evidence that we are dealing with something more subtle than simple Reynolds number effects.

Therefore, accepting the postulate that under certain conditions the qualitative nature of the cavitation does change, and recognizing that with mercury (at least as visually observed in the plastic venturis) it was relatively easy to trigger very localized cavitation, then

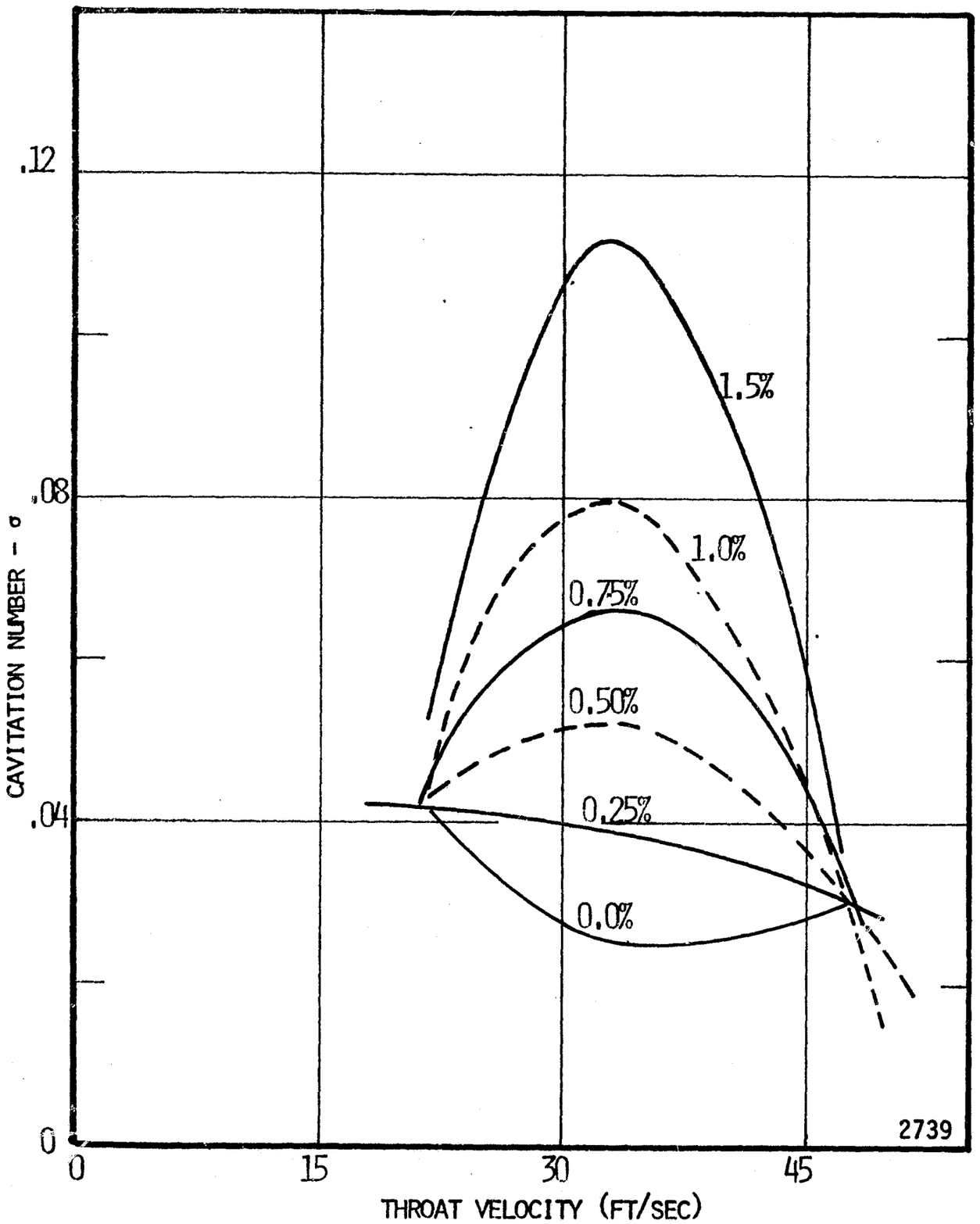

Figure 64. Cavitation Number versus Throat Velocity, Gas Content as Parameter, Venturi 412, Mercury.

difficulty achieving a significant prediction of the mercury data may be expected.

Nevertheless, as a first step, several cavitation numbers at the same gas content, velocity and size were compared at different temperatures to establish the thermodynamic effects. The thermodynamic parameter for mercury varies from 10^{12} to 10^{5} over the temperature range from 50 to 500°F. Because there is not a great difference in the observed cavitation numbers the apparent thermodynamic effects are unexpectedly relatively minor. This may well be related to the presence of the entrained gases or other cavitation triggering mechanisms and also to the fact that the large variation in B occurs in a range where the cavitation behavior is not sensitive to thermodynamic restraints. This was also noted in a cavitation damage study[40] performed earlier with mercury in this laboratory. For the present data it was established that $\sigma/\sigma_o \propto (B/B_0)^{0.005}$, which does in fact indicate a very small influence from temperature effects.

Because Figure 64 definitely indicates a cavitation number-velocity relationship which is not an inverse square relation, a simple triangular function was assumed. That is, σ_c is proportional to V for velocities less than 33 ft/sec and proportional to 1/V for velocities greater than 33 ft/sec. On this basis the following equation was selected, using the same vp and D variation as with water in order to keep the relations as similar as possible.

$$\frac{\sigma}{\sigma_o} = \left(\frac{vp}{vp_o}\right)\left(\frac{D}{D_o}\right)\left(f(v)\right)\left(\frac{B}{B_o}\right)^{.005}$$

where $f(V) = (V/V_o)^{1.0}$ for $V < 33$ ft/sec and $f(V) = (V_o/V)^{1.0}$ for $V > 33$ ft/sec.

The result of using this relationship with the mercury cavitation data from the plastic venturis (1/2, 1/4 and 1/8 inch) is shown on Figure 65. Again as with water, the 1/8 inch data exhibits a consistent underprediction. It is also noted that the data for the 1/8 and 1/4 inch venturis fall into two rather distinct groups. For the 1/8 inch venturi where the velocity and temperature were approximately constant, this separation appears to occur as some function of gas content. With few exceptions, the lower grouping of the observed cavitation numbers occurs at gas contents below about 1 percent, and the higher values occur when the gas content is greater than 1 percent. This may be attributed in part to the selection of a linear relation between gas contents and cavitation number. However, from Figures 44 and 49 such a linear relationship is valid especially when the velocity is about 30 ft/sec. The grouping of the 1/4 inch data appears more related to velocity. In any case the 1/8 inch data is grossly underpredicted. On Figure 65, Curve A represents a least squares fit of σ_c (obs) as a function of σ_c (calc) for all the data. The slope of this line ($\simeq .6$) indicates that we are not predicting nearly as successfully for the mercury as we did for water in the same systems. Attempts to handle the balance of the mercury data (stainless steel venturis and high temperatures) with the same equation and reference point were even less satisfactory and are not reported. It appears that cavitation numbers observed for mercury are not strongly dependent upon any of the measurable effects, with the possible

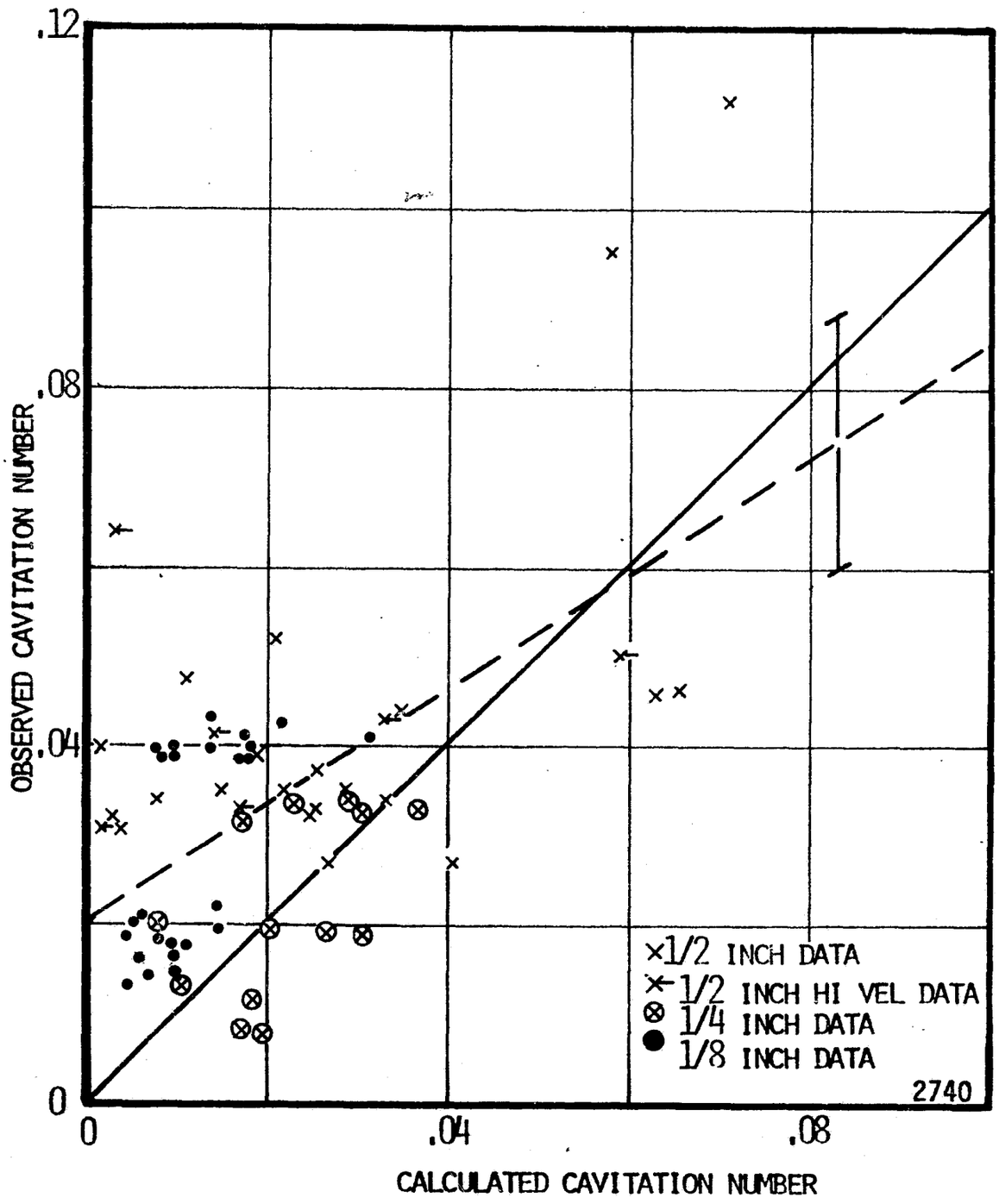

Figure 65. Experimental Cavitation Number versus Calculated Cavitation Number, Plastic Venturis, Mercury.

exception of gas content (Figures 44 - 50). It is postulated that the cavitation in mercury (particularly in the small venturi) is occurring in very isolated spots. This is assumed to occur from surface irregularities inducing very strong local turbulence with the accompanying underpressures sufficient to cause cavitation. These irregularities may be the result of either the machining operations, particularly in the case of the stainless steel venturis, or wall damage caused by the cavitation itself. The "erosion" of the walls is plainly evident in the plastic venturis. The analysis considered all available data without respect to the entrained gas and it may well be that the interaction between the various gases (air, argon, hydrogen) and mercury is in fact different, possibly through differences in interfacial tension which would influence bubble size and thereby exert an influence on the cavitation characteristics, although how this occurs is completely unclear at the present time.

In summary, the mercury cavitation results from this study do not follow the prediction approach established for water, even with the modification of the velocity treatment. And, in fact, there appear to be other influences on the cavitation which cannot be accounted for in this analysis.

E. Summary of the Alternate Analyses

Although the cavitation number cannot be closely predicted based only on the various physical properties of the system, we have established that for water a first approximation to the cavitation

number in a prototype system can be established based upon the results from a reference system. The study here was for cylindrical throat venturis but there is no apparent "a priori" reason why such an approach should not be applicable to other geometries such as centrifugal pumps inlet passages, etc.

For water we have shown that:

$$\frac{\sigma}{\sigma_o} = \left(\frac{\nu_\ell}{\nu_{\ell_o}}\right)\left(\frac{D}{D_o}\right)\left(\frac{V_o}{V}\right)^{2.0}\left(\frac{B}{B_o}\right)^{0.25}$$

to a reasonable approximation so long as:

a. Gas content is in the range 0.5 to 2.0 percent.

b. Cavitation is uniformily distributed.

For the existing mercury data we have established that the reference system prediction established above is insufficient. Further, the "bunching" of the data points, more or less independently of the measured variables, gas content, size, velocity and temperature implies a triggering mechanism for cavitation inception undetermined in this study. It is postulated that wall roughness, whether due to fabrication techniques or cavitation damage is a major contributor to this situation. On the other hand, the success achieved with the water data, and the very limited results from mercury in the plastic venturis, suggest that this is an area worthy of further investigation.

F. Supplemental Analysis of Gas Content Effects

The dominant role gas content plays in the cavitation observed during the course of this study prompts a further consideration of approaches to systematizing the results. Also, during this study a "correction" to the gas content data plotted in Figure 26 was investigated. It was argued that the presence of the cavitation could be affecting the pressure readings from those taps in or near the bubble cloud. Therefore, it was assumed that the nearly linear pressure drop ($\Delta P/\Delta L$) observed in the throat section in the absence of cavitation could be applied to the cavitating case, using the throat inlet tap as the common or normalizing point. Such a procedure may provide a useful correction or modification to the data, although it cannot be verified experimentally or theoretically, unless friction effects alone are important. Hence, it was not used in general, but it is reported here for the insights it may offer. The effect of applying this linear extrapolation to a portion of the 1/2 inch data are shown in Figure 66, which is similar to Figure 26. A cross plot of this extrapolated versus velocity is shown in Figure 67.

Now if we examine again the σ_c versus velocity plots (Figures 58, 59 and 67) we can see a pattern to the data similar to that reported by Ripken and Killen[15] and to that of Ruggeri and Gelder[19]. The velocity dependence for high gas content is also quite similar to that reported by Holl[14]. It must be remembered here however, that the 0% line is the result of a considerable extrapolation of the gas content data (Figures 26, 30 and 66) and therefore certainly does not represent a true experimental value, but only an approximation thereto.

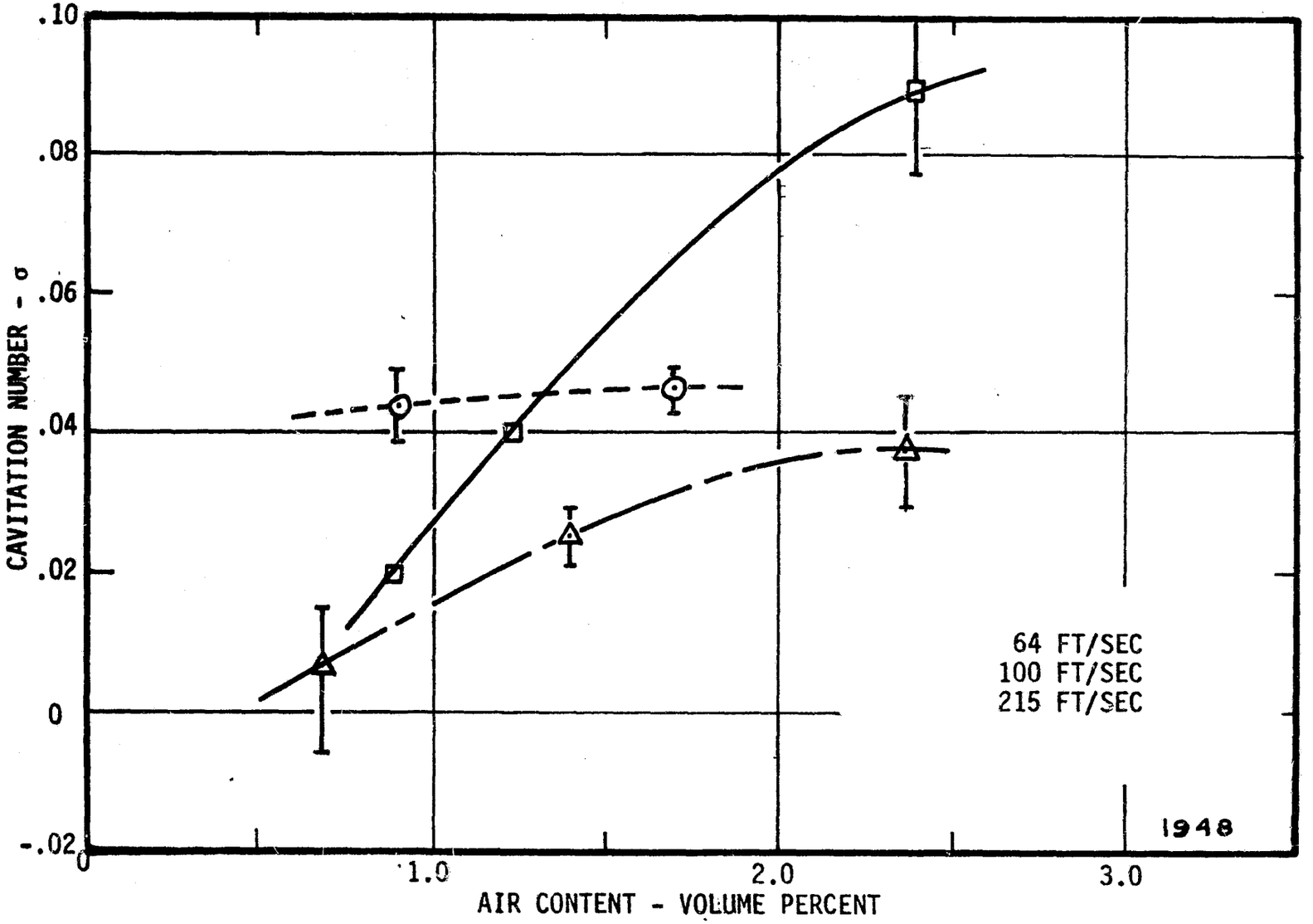

Figure 66. "Corrected" Cavitation Number versus Air Content, Venturi 412, Cold Water.

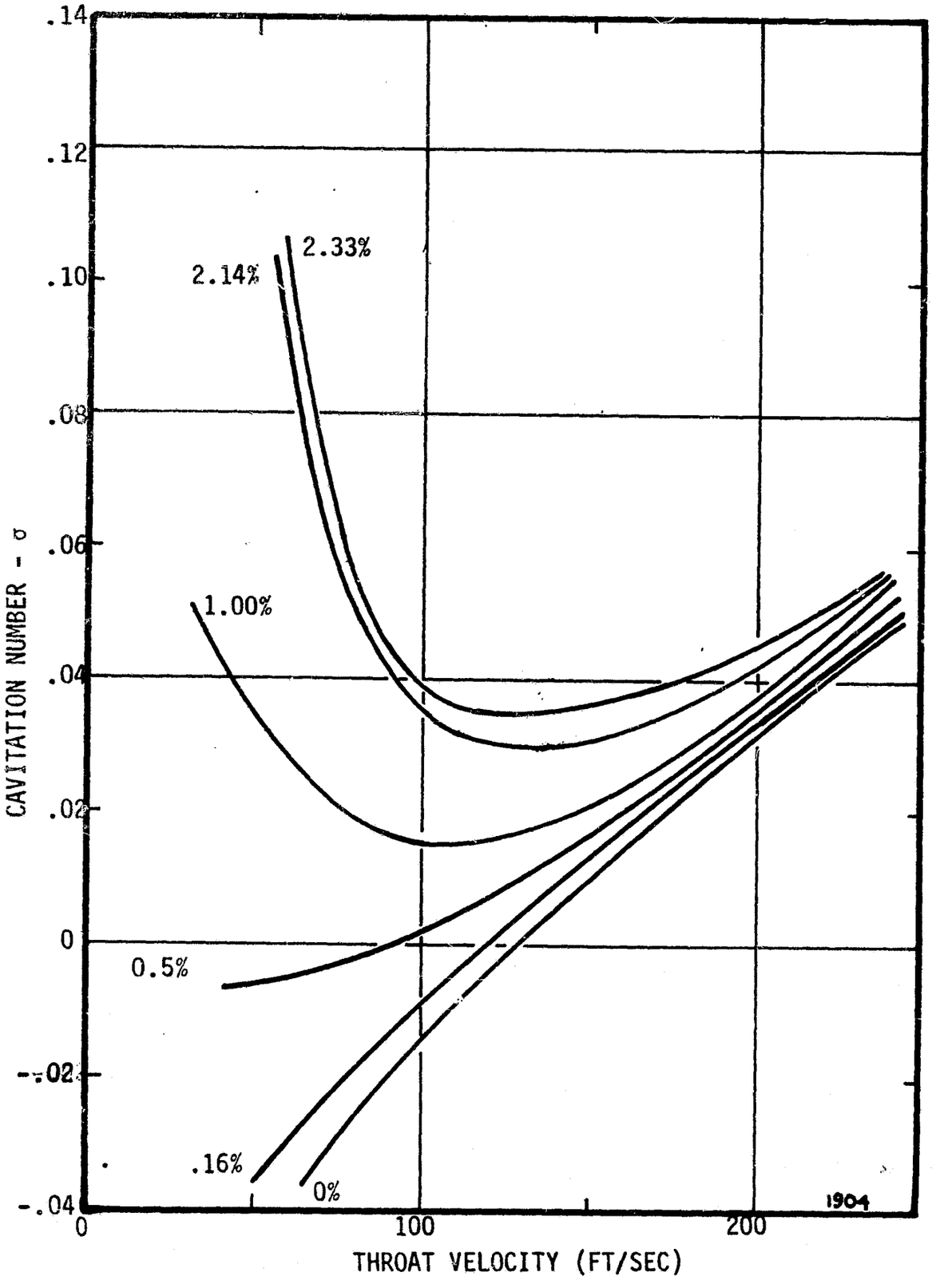

Figure 67. "Corrected" Cavitation Number versus Throat Velocity, Gas Content as Parameter, Venturi 412, Water.

Now the results of the water investigations may be partially explained if it is assumed that those bubbles which serve as cavitation nuclei contain some partial gas pressure that is in all cases proportional to the entrained, and therefore, the total gas content. Recall that the total gas content is all that can be determined with the Van Slyke technique, and that we have assumed consistently that the entrained gas content is proportional to the total gas content. Using the approach suggested by Holl[14], essentially that outlined in Chapter II, we may define a partial cavitation number based upon gas pressure alone. This partial value must then be added to that for zero gas content to obtain the experimentally measured cavitation number. That is,

$$\sigma_c = \sigma_a + \sigma_{No}$$

where:

$$\sigma_a = \frac{p_a}{\frac{1}{2}\rho V_T^2} = \frac{k\alpha}{\frac{1}{2}\rho V_T^2}$$

From the data in Figures 58, 59 and 67 we can solve for σ_a, and subsequently the proportionality constant, k. This was done using the maximum gas contents and 100 ft/sec and 200 ft/sec as the "bench marks" with the results as shown below.

Venturi Diameter Inches	k psi/vol% gas
1/2 Inch (Figure 66)	1.50
1/2 Inch (Figure 58)	0.96
1/4 Inch (Figure 59)	0.34

In Figure 68 a comparison between measured and computed gas cavitation numbers is shown for the "corrected" 1/2 inch data. For this plot the measured and computed values have been forced to coincide at a throat velocity of 200 ft/sec. As reported above, from Figure 67 it can be established that the gas pressure for all test conditions in the cavitating region is approximately 1.5 psi per volume percent of total gas at STP, that is, the gas pressure computed from this data is also proportional to total gas content. It may also be noted by comparing the data at 100 ft/sec and 200 ft/sec that the gas cavitation number is nearly inversely proportional to velocity squared as it would be if the gas pressure is constant as assumed. Figure 69 and 70 show similar plots for the "uncorrected" 1/2 inch and the 1/4 inch data. Here we note that the inverse square velocity relationship is nearly satisfied at the higher gas content, but the relationship changes as the gas content decreases. This would be expected from the nature of Figures 58 and 59.

Unfortunately, the hypothesized model is clearly not consistent with the mercury data (Figure 64) since the cavitation number first increases and then decreases with velocity. If one considers only the case of maximum gas effect (V_T = 33 ft/sec), it is found that the proportionality constant, k, is much greater than that for water. That is, k $\simeq$ 5.8 psi/volume % in mercury compared to k $\leq$ 1.5 psi/volume % in water. Such a behavior of k is not unreasonable however, since relatively very little of the gas can be in solution in mercury. The wide variation in k

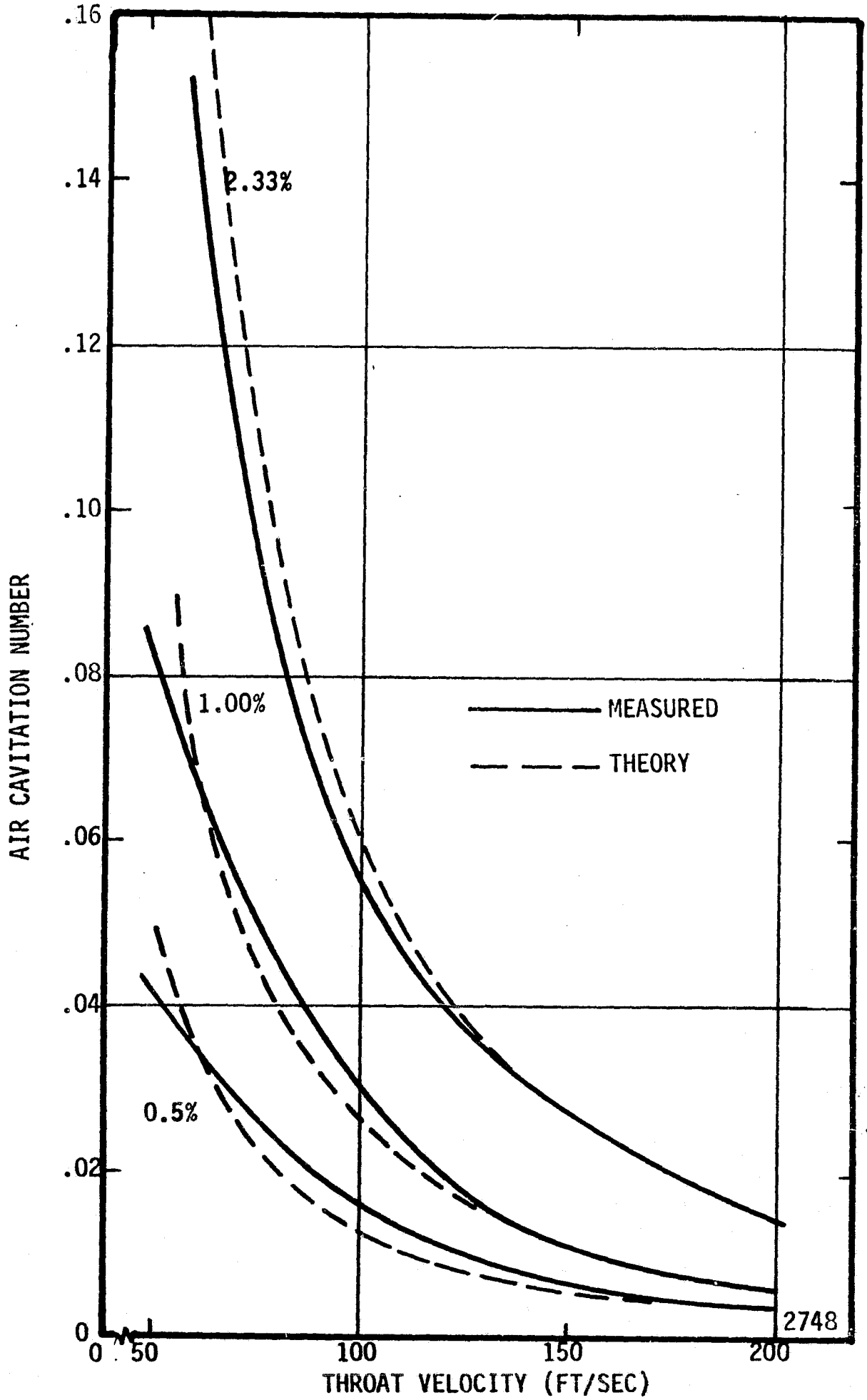

Figure 68. Air Cavitation Number versus Throat Velocity, Gas Content as Parameter, Venturi 412, "Corrected" Data.

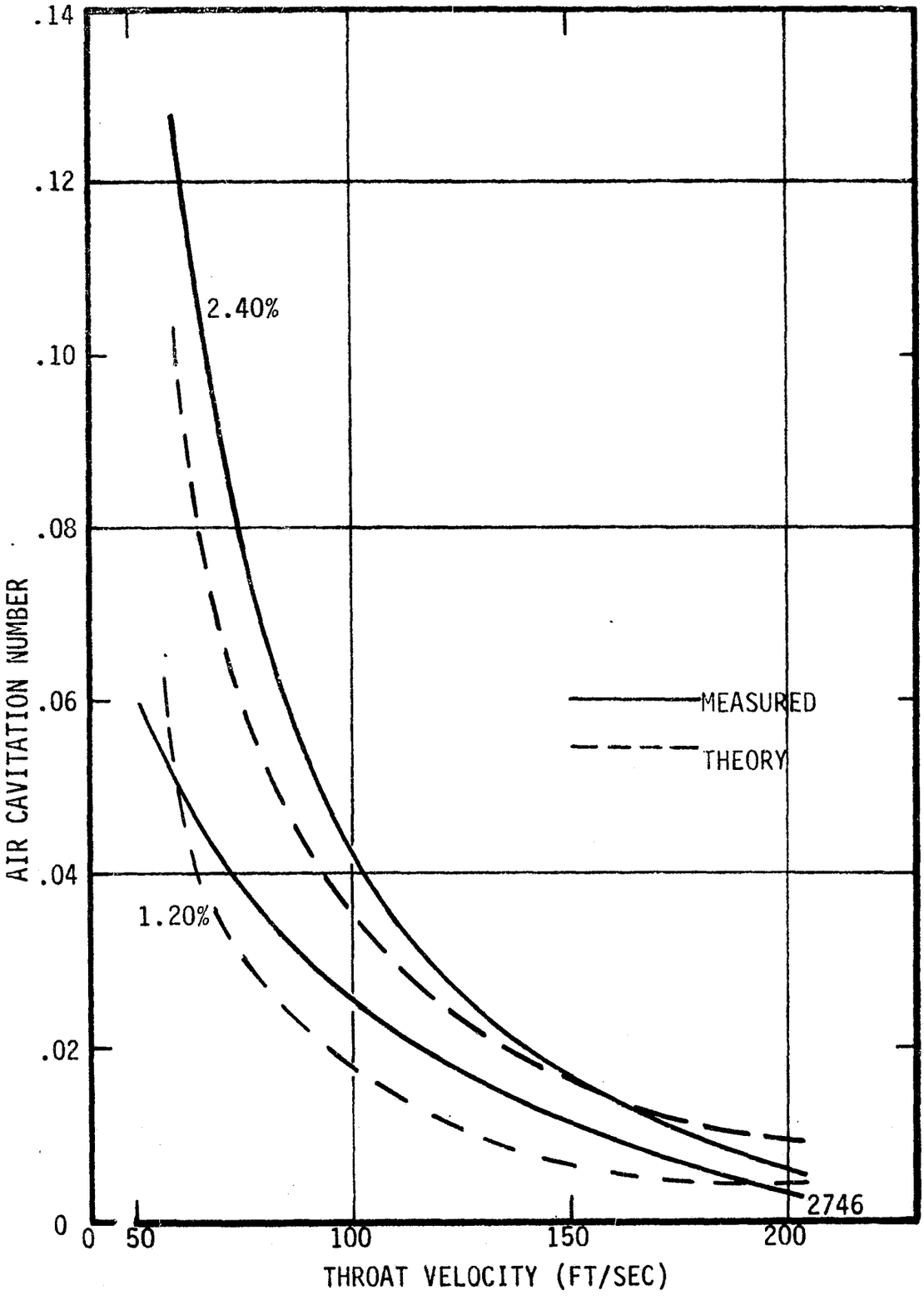

Figure 69. Air Cavitation Number versus Throat Velocity, Gas Content as Parameter, Venturi 412.

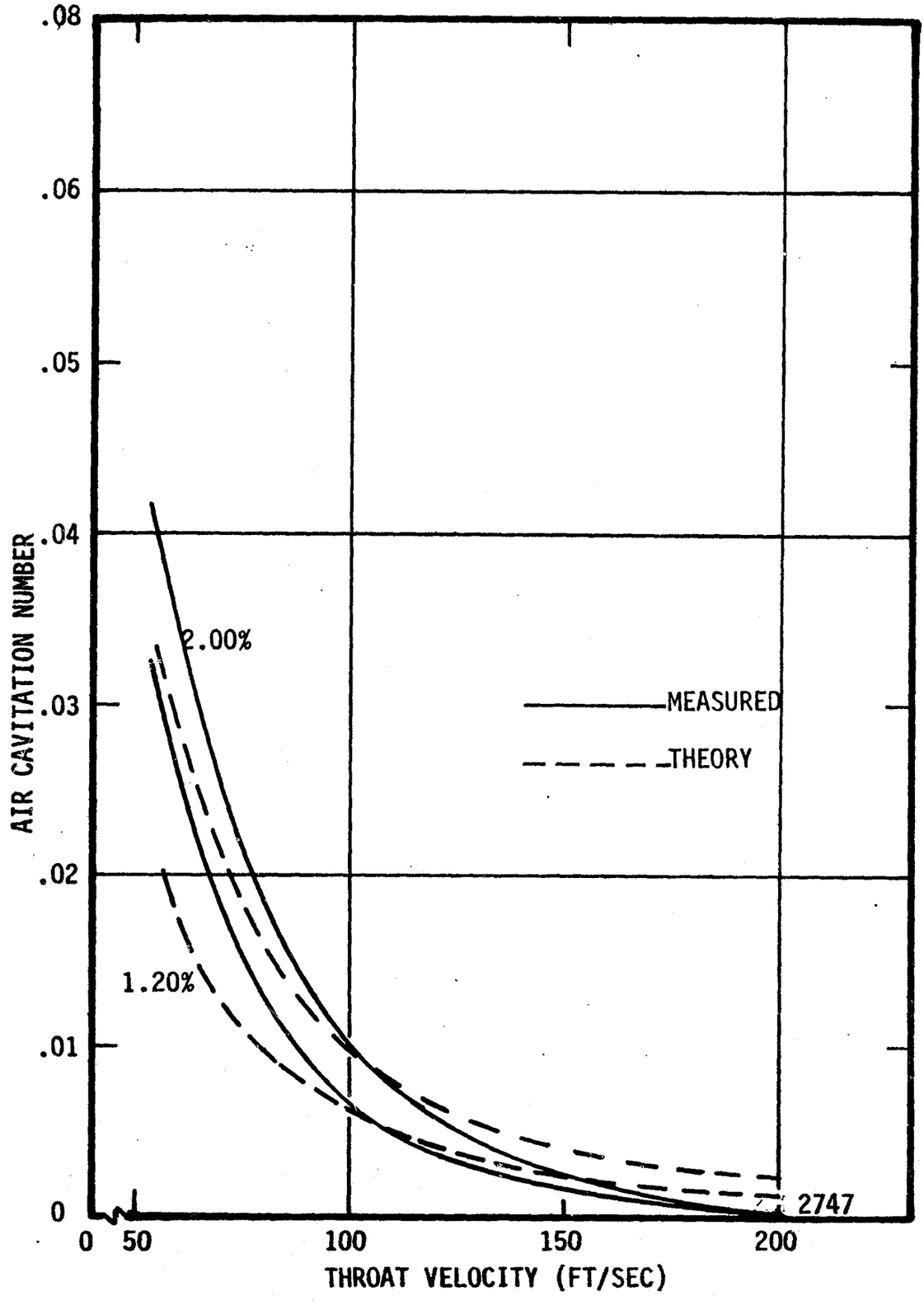

Figure 70. Air Cavitation Number versus Throat Velocity, Gas Content as Parameter, Venturi 614.

across the water tests is certainly caused in part by the alternate approaches used to calculate the cavitation number and also because of inadvertently different pretreatment (prepressurization, settling, etc.) during the water tests. We may also be witnessing scale effects between the 1/2 and 1/4 inch venturis since the time for exposure to low pressure varies between the two cases.

The arguments and discussion above indicate that at least for water the division of the overall venturi cavitation number into two additive portions is a reasonably realistic model. The proportionality constant, k, between pressure and the total volumetric gas content depends upon the previous history of the water and also perhaps temperature and other variables. It also appears that k must be measured for a given test setup. Of course, what remains now is to delineate those scale effects which relate to the near zero gas content for any given test arrangement, in order to obtain an estimate of the complete cavitation number variation for the venturi. We expect that this will be a function of the various parameter groupings (Reynolds number, Weber number, etc.) discussed earlier. The difficulty experienced in establishing a correlation with these parameters was discussed previously.

Combining this present analysis with earlier arguments, we may propose an approximate predicting equation for cavitation scale effects in a venturi. That is,

$$\sigma_c = \sigma_a + \sigma_{No} \cong \frac{k\alpha}{\frac{1}{2}\rho V_T^2} + f(D_T, B, V_T)$$

or similarly to the earlier analysis (Section C, Chapter V),

$$\frac{(\sigma_{No})_2}{(\sigma_{No})_1} \cong \left(\frac{D_{T_2}}{D_{T_1}}\right)\left(\frac{B_2}{B_1}\right)^{1/4} f(V)$$

the velocity relationship f(v) varies widely between tests and therefore it will have to measured in each instance.

In summary, the effect of gas content in a cavitating venturi is found to be predictable, assuming a gas pressure within the cavitation bubble that is proportional to the total volumetric gas content. This still leaves uncertain the influence of the other parameters on the cavitation number at near zero gas content. It is assumed, although not experimentally verified, that results from a reference system could be scaled to another system.

CHAPTER VI

CONCLUSIONS

Based upon the available experimental data and the subsequent analyses the following general conclusions have been drawn.

1. The observation of other experimenters that cavitation does not scale classically is substantiated. That is, $\sigma_c = (p-p_v)/\frac{\rho V^2}{2}$ being constant (i.e., the same for two systems) is not sufficient to insure that the observed cavitation is the same in extent, intensity or character.

2. The effect of gas content in a cavitating venturi has been found to be predictable, assuming a gas pressure within the bubble that is proportional to the total volumetric gas content. That is,

$$\sigma_c = \sigma_{gas} + \sigma_{no\,gas}$$

which may be written as:

$$\sigma_c \cong \frac{k\alpha}{\frac{1}{2}\rho V^2} + f(D, V, B)$$

3. Limited success was achieved in the water systems predicting the cavitation number in one system based upon results from a "reference" system. A relationship of the form:

$$\frac{\sigma}{\sigma_o} = \left(\frac{v_p}{v_{p_o}}\right)\left(\frac{D}{D_o}\right)\left(\frac{V_o}{V}\right)^{2.}\left(\frac{B}{B_o}\right)^{0.25}$$

gave acceptable results for these cylindrical throat venturis under certain constraints. Namely, the cavitation must be uniformly distributed, the gas content is in the range 0.5 to 2.0 volume percent and

the size to mass flow ratio remains greater than some critical value. The mercury data did not follow a similar relation even when modified to handle the velocity characteristic for mercury cavitation.

4. The idea of using "standard" fluid dynamic parameters such as Reynolds number, Weber number, thermodynamic parameter and a gas content parameter is sound, but it is incomplete in that the data available to the present study could not be completely correlated using only these parameters. There are definitely other effects not considered here. Most important perhaps are very localized flow turbulences induced by surface roughness or irregularity. These can play a major role in the cavitation inception process. This effect seems particularly influential in the mercury flows where important wall surface damage, and consequently flow perturbation near the wall, occurs in the short time span of the tests.

5. In these venturi systems, over the range of variables tested, the permanent gas content is the most influential parameter examined and essentially controls the nature of the cavitation. This is probably true for other systems as well.

6. In these venturi systems there was no observable difference between "desinent" and "incipient" cavitation number. The present work corroborates prior experimental evidence that the prior pressure history of the fluid does have an influence on the observed cavitation. This is attributable to the importance of the permanent gas and the effect pressure has on nuclei size.

7. The inherent problems with scaling surface effects and other localized phenomena tend to preclude and exact correlation of cavitation with other flow parameters. Also, inthis regard, the normal manufac-

turing tolerances and variations may simply mean that cavitation performance connot be precisely predicted under ordinary circumstances.

8. A considerable amount of study must still be done to understand the basic mechanisms of single bubble growth and collapse in turbulent flowing streams. For example, determination of the nature and size distribution of potential cavity nuclei should provide needed insight into the triggering mechanisms and the growth processes.

APPENDIX A

DEFINITION OF CAVITATION CONDITIONS

Three degrees of cavitation in the venturis are discussed in this work. At the onset five conditions were established but two of these were not actually subject to experimental observation. The five conditions are:

1. Condition A - A cavitation condition sometimes characterized as "sonic initiation". No visible bubbles in the stream but a definite increase in sound level in the venturi which can be described as a "hiss".

2. Condition B - Generally referred to as "visible initiation". Cavitation that is characterized by the definite appearance of observable bubbles. For the base line 1/2 inch throat-diameter venturi, this was usually a bubble cloud approximately 1/16 to 1/8 inch wide by 1/4 to 3/8 inch long on the throat wall in the vicinity of Tap No. 3.

3. Condition C - A complete ring of visible bubbles around the exit of the throat. This was only seen in a limited number of cases in the 3/4 inch venturis.

4. Condition D - An advanced state of cavitation, sometimes labeled "standard cavitation" in past University of Michigan tests and characterized by a visible cloud of bubbles extending a distance of about 1.5 x D_t from the throat exit. In the 1/2 inch venturi, this is then about 3/4 inch from throat exit.

5. Condition E - A very advanced state of cavitation, sometimes referred to as "cavitation to first mark" in past University of Michigan tests and characterized by a visible cloud extending to a point 3 to 3.5 x D_t from the throat exit. This is 1-1/2 inch to 1-3/4 inch in the 1/2 inch venturi.

In order to have a common measuring point each of the plastic venturis had scribe marks placed in the interior wall to indicate the downstream location of Conditions D and E. It was only the most advanced cavitation condition that the bubble cloud uniformly filled the passage. In the visible initiation case in particular the cavitation was very localized. Typical patterns are shown in Figure 71.

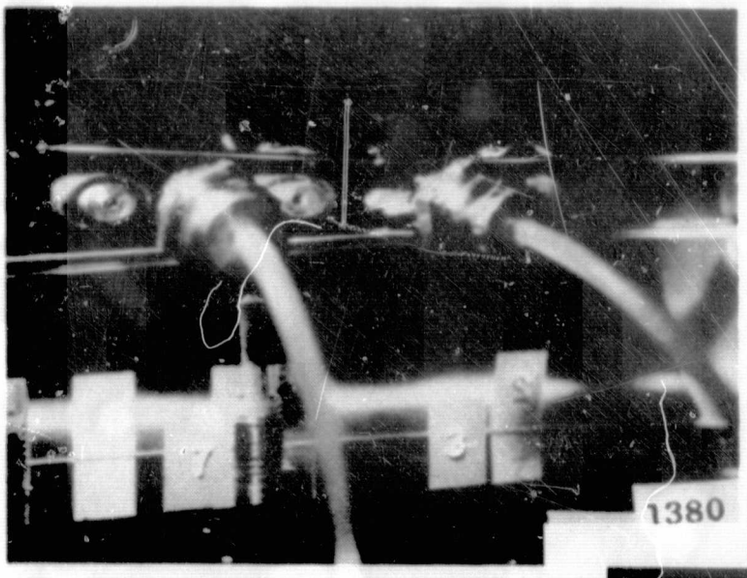

Visible Initiation
215 Ft/Sec
2% Air

Standard
100 Ft/Sec
2.2% Air

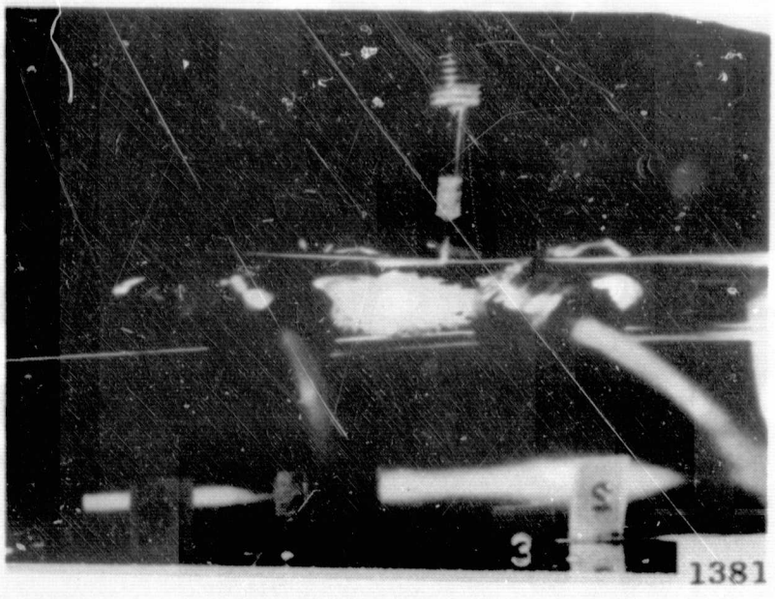

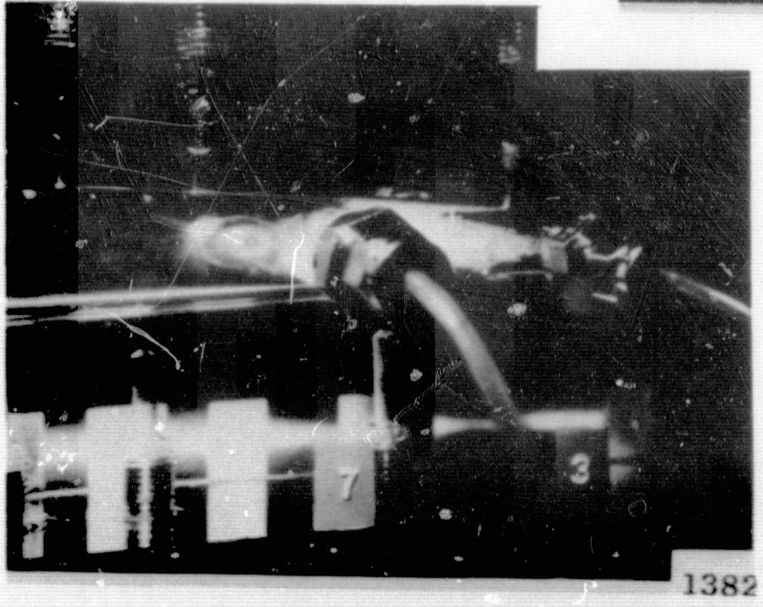

First Mark
100 Ft/Sec
2.2 % Air

Figure 71. Cavitation in Water, Three Conditions.

APPENDIX B

MODIFIED VAN SLYKE PROCEDURES FOR MERCURY

The sample capsule was connected to the Van Slyke with standard stainless steel tubing fittings. With the capsule in place, all the glass tubing on the Van Slyke, Figure 72, was filled with mercury to the bottom of the T valve, (A). Valve A) is turned to open the vacuum pump to the capsule connection, and valve (B) is turned to open the vacuum to the connection and calibrated volume on the other end of the capsule. The system is held under this vacuum for 10 minutes. Valve (B) is then closed and valve (A) turned to permit mercury from the capsule to flow into the shaker bulb when the capsule valves are opened. The free mercury surface with the sample is lowered into the shaker bulb, and agitated for 5 minutes under the vacuum resulting from lowering of the mercury level when the mercury reservoir flask is lowered. The level of mercury is then raised to the zero mark on the calibrated volume and thus the height of mercury in the manometer above the zero mark represents the pressure on the known volume of gas.

The gas is then pushed out the vent on valve (B), the valve is closed, and the mercury level lowered again into the shaker bulb, agitated, raised to the zero mark, and the manometer reading taken. This procedure is repeated for a total of four manometer readings. Generally, the last two readings will be within several millimeters of one another. This mercury flushing procedure ensures that all the gas initially in the capsule is removed and measured. The sum

of the differences between each reading and the last reading is the total sample gas pressure. Because the volume, pressure, temperature, and molecular weight of the gas are known, the ideal gas law may be used to calculate the gas mass.

At this point in the procedure, the manometer column and the vent at valve (A) are opened to the atmosphere and the manometer level corresponding to the zero mark observed. This level will usually be below the last reading taken with a closed system, but should always be less than the vapor pressure of water at room temperature. This latter point is significant only for the experiments run here, because water was used for pressurization in the pump sump in the mercury system originally, as well as for cooling purposes on the seal between pump shaft and sump. Therefore, any appreciable increase in this difference, i.e., should it begin to approach vapor pressure of water, would indicate the presence of unwanted water in the mercury stream (see Appendix C).

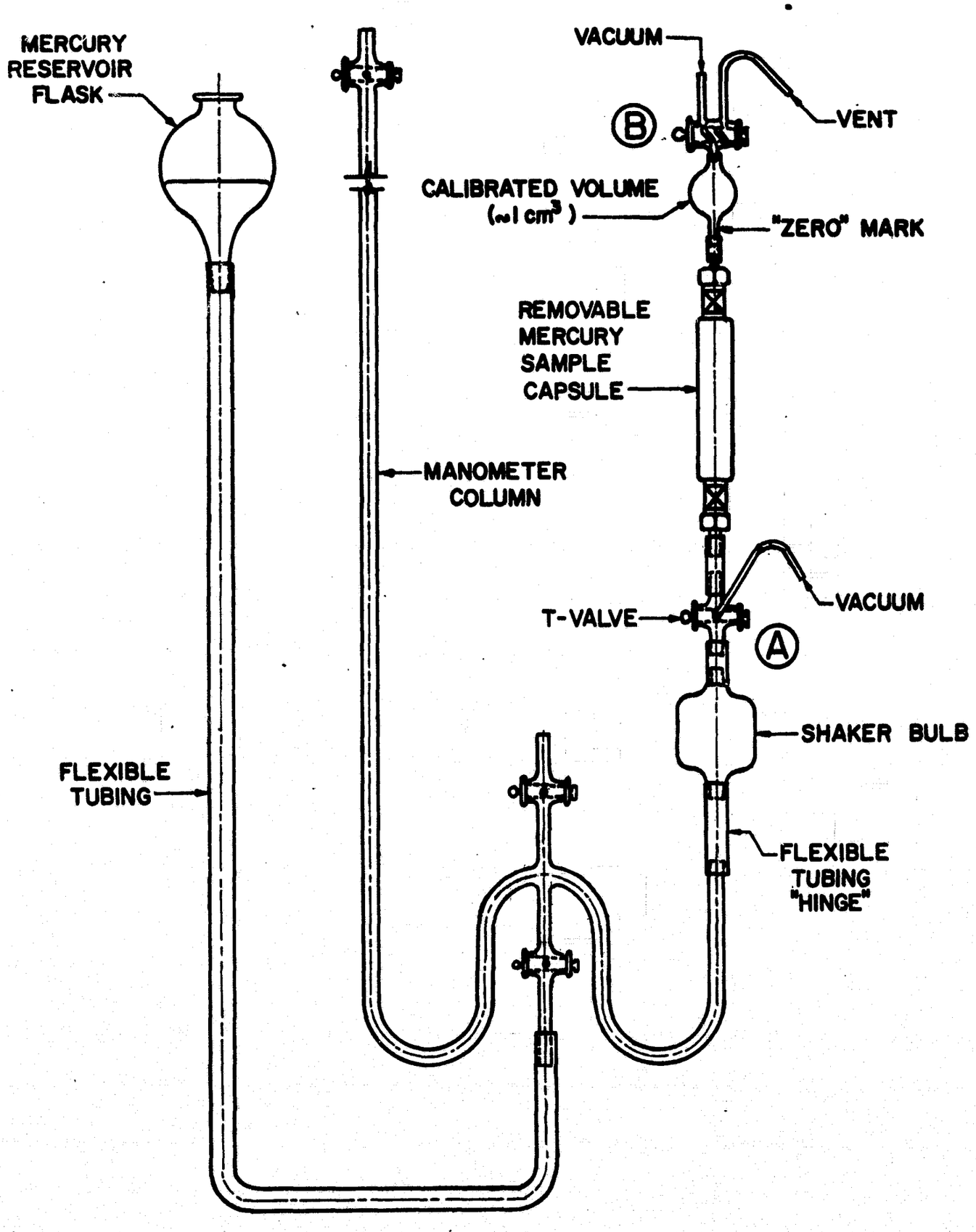

Figure 72. Modified VanSlyke Layout.

APPENDIX C

DETERMINATION OF HIGH VAPOR PRESSURE COMPONENT IN MERCURY

The pumping system used in the portions of this study devoted to mercury consists of an overhung, centrifugal sump pump. Originally, this sump was pressurized with gas over water. During the process of this and related studies the question of the effect of the entrainment of water in the mercury was raised. The following is a description of a technique developed by Hammitt, Robinson, and Ivany[57] to determine the mass of water present in a given sample of mercury.

The apparatus for determining the mass of water present in mercury is shown in Figure 73. The sample to be analyzed for the high vapor pressure component is initially contained in a closed sample capsule with appropriate connectors and valves to permit the capsule to be emptied into the apparatus. The procedure is as follows:

1. SAMPLE CAPSULE is attached above valve C.
2. All valves are closed and mercury is added to RESERVOIR.
3. Valve E is opened to position ⊤.
4. Valve C is opened to position ⊢.
5. Pull VACUUM 1 for 10 minutes.
6. Rotate Valve E to position ⊣ and fill U-TUBE to CALIBRATED VOLUME LINE.
7. Rotate Valve to position ⊤ and pull VACUUM 1 for five minutes.
8. Rotate Valve E to closed position ⊗.

9. Open Valve A and pull VACUUM 2 for five minutes and then close Valve A.
10. Rotate Valve C to position ⊖.
11. Open Valve B to drain sample into FLASK.
12. Rotate Valve C to position ⊖.
13. Rotate Valve E to position ⊖ and add mercury to MANOMETER until level in U-TUBE is again at CALIBRATED VOLUME LINE.
14. Rotate Valve E to closed position ⊘, and record level of mercury in MANOMETER at room temperature.
15. Place both into HIGH TEMPERATURE BATH in GLASS CONTAINER.
16. Use Valve E to adjust mercury level to CALIBRATED VOLUME LINE every 5 minutes and note temperature on THERMOMETER. Continue until temperature and pressure equilibrium is reached.
17. Record final MANOMETER and THERMOMETER readings.

The vapor is now contained in a known volume at a known pressure and temperature. The volume is sufficient so that the vapor is in a superheated condition, therefore the mass can be determined by reference to appropriate steam tables. This technique is particularly effective with water or mercury since there is such a large disparity between the vapor pressures.

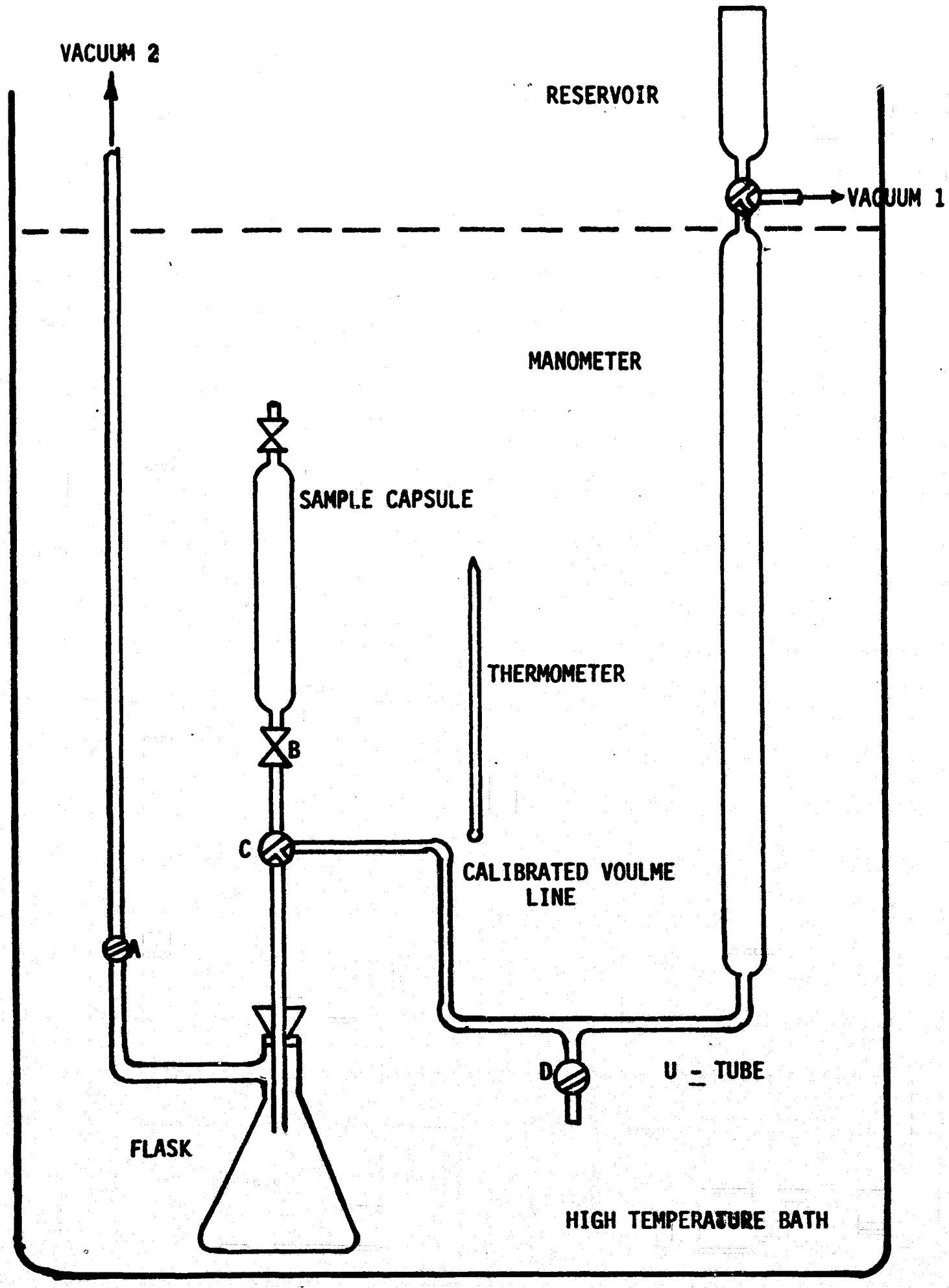

Figure 73. High Vapor Pressure Component Measuring Apparatus.

APPENDIX D

VENTURI NOMENCLATURE

Because of facilities employed in this study are used in a variety of cavitation studies and because a simplified identification scheme was required for the data reduction programs, the following code was established to identify the venturis used.

534 - the 3/4 inch throat-diameter plastic venturi (see Figure 8).

412 - the 1/2 inch throat-diameter plastic venturi (see Figure 9).

614 - the 1/4 inch throat-diameter plastic venturi (see Figure 10).

818 - the 1/8 inch throat-diameter plastic venturi (see Figure 11).

712 - the 1/2 inch throat-diameter stainless steel venturi.

918 - the 1/8 inch throat-diameter stainless steel venturi.

APPENDIX E

RAWDAT

I. INTRODUCTION

The computer program RAWDAT is designed to take raw static pressure data from an instrumented venturi and reduce it via appropriate mathematics to a set of normalized pressures from which the cavitation number can be determined. For this purpose the cavitation number is defined as the minimum observed value of the normalized pressure. In addition, the program performs an analysis on the data to provide confidence limits for the calculations and observations. The program as it stands can handle from 8 to 16 taps with a maximum of 10 readings for each tap at a single combination of flow rate, temperature, barometric pressure and cavitation condition.

II. DESCRIPTION OF THE PROGRAM

A. General. From the input data the program first computed the density and vapor pressure for the test fluid, basing the calculation on the temperature and a number of empirical relationships developed from the several handbook tabulations of physical properties. Next a pressure correction term is determined based upon the barometric pressure and any height differential between the Heise gage and the venturi which cannot be biased out mechanically in the gage. The throat velocity (VT) is calculated from the volumetric flow rate (measured by calibrated orifice plates) and the throat diameter, after which the kinetic head is obtained from the usual relationship.

$$KE = (VT)^2/2g$$

(Note: Here and in subsequent relationships the expressions are written in essentially the same way as they appear in the MAD write-up for the computer.) The net positive suction head (NPSH) is calculated from

$$NPSH = (PTD + PC - VAP)/DEN$$

where: PTD = measured static pressure

PC = pressure correction term

VAP = vapor pressure of test fluid

DEN = density of the test fluid

with appropriate numerical conversion factors so that NPSH and KE are in terms of feet of fluid. The normalized pressure (NRMPR) is then given by

$$NRMPR = NPSH/KE$$

The program computes the average of the normalized pressures for each of the taps (AVGNP); then the deviations (DEVNP), the variance (VAR), the standard deviation (STDDEV) and the coefficient of variation (COVAR) are computed in turn. These may be expressed as follows:

$$AVGNP = 1/NRD \sum_{i=1}^{NRD} NRMPR_i$$

$$DEVNP_i = NRMPR_i - AVGNP$$

$$VAR = 1/NRD \sum_{i=1}^{NRD} (DEVNP_i)^2$$

$$STDDEV = (VAR)^{\frac{1}{2}}$$

$$COVAR = STDDEV \times 100/AVGNP$$

where NRD is the number of runs at the same temperature, barometric pressure, flow rate and cavitation condition. In calculating COVAR the absolute value of the standard deviation and AVGNP are used since on some runs the latter of these may be a negative number. In the machine program the various terms are actually doubly subscripted to account for multiple runs with multiple taps, but in the above notation we have assumed only one location. The program will also compute the loss coefficient (LOSC) if desired. LOSC is simply the normalized pressure upstream of the venturi minus that downstream of the venturi and is a measure of how well the venturi diffuser recovers the static pressure. The program then selects the minimum AVGNP and reports it as the cavitation number.

Up to this point the program has handled data obtained at a single combination of temperature, barometric pressure, flow rate, and cavitation condition. Quite frequently, however, data at a given flow rate and cavitation condition may be available at several slightly different temperatures and barometric pressures. The program is so written that when the input is properly prepared the values calculated above (AVGNP, VAR, STDDEV, and COVAR) may be stored in memory for up to five different temperatures and pressures. Then the program computes the mean average normalized pressure (MEAVG), the deviations of the several AVGNP from this mean (DEVME), the variance (VARM), the standard deviation of the AVGNP about MEAVG (STDEM) and a coefficient of variance (COVRM). These may be expressed as:

$$\text{MEAVG} = 1/\text{NRS} \sum_{j=1}^{\text{NRS}} \text{AVGNP}_j$$

$$\text{DEVME}_j = \text{AVGNP}_j - \text{MEAVG}$$

$$\text{VARM} = 1/\text{NRS} \sum_{j=1}^{\text{NRS}} (\text{DEVME}_j)^2$$

$$\text{STDEM} = (\text{VARM})^{\frac{1}{2}}$$

$$\text{CORM} = \text{STDEM} \times 100/\text{MEAVG}$$

where NRS is the number of sets at the same flow rate and cavitation condition. Again we have not always indicated the double subscript where the machine uses it. Finally the minimum value of MEAVG is determined and reported as an overall cavitation number

The program is so written that at this point the values for MEAVG are plotted against the distance from the venturi throat entrance. The grid for this plot is prepared by the machine based upon the venturi used.

III. DESCRIPTION OF PROGRAM INPUT

The input necessary to run the program can be described in general as follows:

A. First Data Card. This card, written in simplified MAD I/O statement form, tells the computer how many flow rate-cavitation condition combinations are being submitted.

B. Second Data Card. This card contains a combination of floating point and integer Hollerith fields that provide the computer with the following information.

1. Cavitation condition
2. Barometric pressure
3. Height correction
4. Number runs at same temperature and pressure at given flow rate and cavitation condition.
5. Number pressure taps used
6. Number runs at same flow rate and cavitation condition.
7. Test fluid temperature
8. Flow rate in "inches" of test fluid
9. Flow rate in GPM
10. Pump Speed RPM
11. Venturi used
12. Gas entrained in fluid
13. Test fluid
14. Venturi throat diameter
15. Page number in original data book.

C. Third Data Card. Contains in simplified MAD I/O form the volumetric concentration of the gas in the fluid.

D. Fourth and Fifth Data Cards. Contains the observed static pressures in floating point Hollerith format with one-half the total readings for a single profile on a card. Cards 4 and 5 are repeated until the number of pairs is equal to the number of profiles at the same temperature and barometric pressure for a given flow rate and cavitation condition.

IV. PROGRAM OUTPUT

The output from the program is essentially self-explanatory as can be seen from the example in the appendices. It consists of a recap of the input data and the calculated output with the appropriate dimensions included plus a plot of the results. The only item not self-evident perhaps is the venturi identification. Each of the venturis used for scale effects has been coded with a three-digit number to facilitate data identification. This code is explained in Appendix D.

Definitions of Program Variables

The following list of program variables defines only those terms which are used as input or for major operations. Loop titles and field specifications are not included as they are usually quite self-explanatory. The variables are defined in order of their appearance in the program.

DEX	Loop index compared with NRS to determine extent of calculations.
COND	Integer index, values 1 to 10 which specify the cavitation condition.
HB	Barometric pressure in inches of mercury
HC	Height correction is inches of fluid to account for gages and venturi centerline being at different elevations.
NRD	Integer numbers, values 1 to 10, specifying number of runs at same temperature and barometric pressure.
NPT	Integer number indicating number of pressure taps being used.
NRS	Integer index, values 1 to 5, specifying the number of sets at the same cavitation condition and flow rate.
TEMP	Fluid temperature in °F.
FR	Flow rate in inches of fluid.
FLORAT	Volumetric flow rate in gallons per minute.
RPM	Pump speed in revolutions per minute.
VENT	Integer index indicating the venturi used.

GAS	Integer code, values 1 to 3, indicating the gas entrained in the fluid.
FL	Integer code, values 1 to 2, indicating the fluid under test.
DT	Venturi throat diameter in inches.
REC	Page number in the original data books.
CONC	Volume % concentration of the gas in the fluid.
PTD	The observed pressure tap data ($\#/in^2$)
AT	Area of the throat (in^2)
B	Conversion factor in the program (min. ft./gal. sec.).
DEN	Density of the test fluid.
LNVP	Natural log of the vapor pressure.
VAP	Vapor Pressure of the fluid.
PC	Pressure correction term ($\#/in^2$).
VT	Throat velocity (ft/sec).
KE	Kinetic head (ft).
NPSH	Net positive suction head (ft).
NRMPR	Normalized pressure (dimensionless).
SUM	Sum of normalized pressures for given run and taps.
AVGNP	Average normalized pressure for a given tap.
LOSC	Loss coefficient.
DEVNP	Deviations of normalized pressures for given run and tap.
SQDEV	Square of the deviation for given run and tap.
SUMSQ	Sum of the squares of the deviations for a given tap.
VAR	Variance of normalized pressure for a given tap.

STDDEV	Standard deviation of normalized pressure for a given tap.
COVAR	Coefficient of variation of normalized pressure for a given tap.
CAVN	Cavitation number.
SUMAVG	Sum of average normalized pressures at given tap.
MEAVG	Mean of average normalized pressures at given tap.
DEVME	Deviations of average normalized pressures in given set and tap.
SQDME	Square of the deviations.
SQSUME	Sum of the square of deviations.
VARM	Variance of the average normalized pressures at a given tap.
STDEM	Standard deviation in average normalized pressure at a given tap.
COVRM	Coefficient of variation in average normalized pressure at a given tap.
MECAV	Mean average cavitation number

```
      COMTUTER PROGRAM  RAWDAT5

          INTEGER COND,NRD,NPT,NRS,RPM,VENT,GAS,FL,I,J,PP, L,M,N,
         1DEX,CORR,TPC1,TPC2,K,TOTAL,REPEAT,REC,YES
          REPEAT = 1
BEGIN     READ DATA TOTAL
BEGIN1    DEX = 1
START     READ FORMAT IN1, COND,HB,HC,NRD,NPT,NRS,TEMP,FR,FLORAT,RPM,
         1VENT,GAS,FL,DT,REC
          VECTOR VALUES IN1 = $I3,2F8.4,3I3,3F7.3,I5,3I3,F7.4,I8*$
          PRINT FORMAT HEAD
          VECTOR VALUES HEAD = $1H1,S10,40HPRESSURE PROFILE CALCULATION
         1S DME THE_IS,S15,28HRESULTS FROM RAWDAT  PROGRAM*$
          TRANSFER TO SPA(FL)
SPA(1)    PRINT FORMAT LIQ1
          VECTOR VALUES LIQ1 = $1HO,S10,19HTEST FLUID IS WATER*$
          TRANSFER TO SPB(COND)
SPA(2)    PRINT FORMAT LIQ2
          VECTOR VALUES LIQ2 = $1HO,S10,21HTEST FLUID IS MERCURY*$
          TRANSFER TO SPB(COND)
SPB(1)    PRINT FORMAT WOS1
          VECTOR VALUES WOS1=$1HO,S10,39HNO TEST SPECIMEN RUNS, SONIC I
         1NITIATION*$
          TRANSFER TO ALPHA
SPB(2)    PRINT FORMAT WOS2
          VECTOR VALUES WOS2=$1HO,S10,41HNO TEST SPECIMEN RUNS, VISIBLE
         1 INITIATION*$
          TRANSFER TO ALPHA
SPB(3)    PRINT FORMAT WOS3
          VECTOR VALUES WOS3=$1HO,S10,42HNO TEST SPECIMEN RUNS, STANDAR
         1D CAVITATION*$
          TRANSFER TO ALPHA
SPB(4)    PRINT FORMAT WOS4
          VECTOR VALUES WOS4=$1HO,S10,47HNO TEST SPECIMEN RUNS, CAVITAT
         1ION TO FIRST MARK*$
          TRANSFER TO ALPHA
SPB(5)    PRINT FORMAT WOS5
          VECTOR VALUES WOS5=$1HO,S10,36HNO TEST SPECIMEN RUNS, NO CAVI
         1TATION*$
          TRANSFER TO ALPHA
SPB(6)    PRINT FORMAT WIS1
          VECTOR VALUES WIS1=$1HO,S10,41HRUNS WITH TEST SPECIMEN, SONIC
         1 INITIATION*$
          TRANSFER TO ALPHA
SPB(7)    PRINT FORMAT WIS2
          VECTOR VALUES WIS2=$1HO,S10,43HRUNS WITH TEST SPECIMEN, VISIB
         1LE INITIATION*$
          TRANSFER TO ALPHA
SPB(8)    PRINT FORMAT WIS3
          VECTOR VALUES WIS3=$1HO,S10,44HRUNS WITH TEST SPECIMEN, STAND
         1ARD CAVITATION*$
          TRANSFER TO ALPHA
SPB(9)    PRINT FORMAT WIS4
          VECTOR VALUES WIS4=$1HO,S10,49HRUNS WITH TEST SPECIMEN, CAVIT
         1ATION TO FIRST MARK*$
          TRANSFER TO ALPHA
```

```
SPB(10)     PRINT FORMAT WIS5
            VECTOR VALUES WIS5=$1HO,S10,38HRUNS WITH TEST SPECIMEN, NO CA
           1VITATION*$
            TRANSFER TO ALPHA
ALPHA       READ DATA CONC
            TRANSFER TO SPC(GAS)
SPC(1)      PRINT FORMAT GCON1, CONC
            VECTOR VALUES GCON1=$1HO,S10,18HTHE GAS IS AIR AT F6.2,18H PE
           1RCENT BY VOLUME*$
            TRANSFER TO BETA
SPC(2)      PRINT FORMAT GCON2, CONC
            VECTOR VALUES GCON2=$1HO,S10,23HTHE GAS IS ARGON    AT F6.2,1
           18H PERCENT BY VOLUME*$
            TRANSFER TO BETA
SPC(3)      PRINT FORMAT GCON3, CONC
            VECTOR VALUES GCON3=$1HO,S10,23HTHE GAS IS HYDROGEN AT F6.2,1
           18H PERCENT BY VOLUME*$
            TRANSFER TO BETA
BETA        PRINT FORMAT INFO,TEMP,HB,HC,FR,FLORAT,RPM,VENT,REC
            VECTOR VALUES INFO=$1HO,S10,14HTEMPERATURE = F7.3,2H F/
           11H ,S10,22HBAROMETRIC PRESSURE = F8.4,8H IN. HG./
           21H ,S10,20HHEIGHT CORRECTION = F8.4,10H IN. FLUID/
           31H ,S10,12HFLOW RATE = F7.3,14H IN. FLUID OR F7.3,4H GPM/
           41H ,S10,12HPUMP SPEED = I5,4H RPM/
           51H ,S10,17HVENTURI USED WAS I3/1H ,S10,27HORIGINAL DATA ON SH
           6EET NO. I8*$
            FORMAT VARIABLE QQ
            QQ = NPT/2
            V1(2) = NPT
            V2(2) = NPT
            TRANSFER TO SP(NPT)
SP(8)       PRINT FORMAT TAPS8
            VECTOR VALUES TAPS8=$1HO,S10,3HF-1,S4,3HP-1,S4,3HP-2,S4,3HP-3
           1,S4,3HP-4,S4,3HP-5,S4,3HP-6,S4,3HF-2*$
            TRANSFER TO BETA1
SP(10)      PRINT FORMAT TAPS10
            VECTOR VALUES TAPS10=$1HO,S10,3HF-1,S3,4HP-00,S4,3HP-0,S4,3HP
           1-1,S4,3HP-2,S4,3HP-3,S4,3HP-4,S4,3HP-5,S4,3HP-6,S4,3HF-2*$
            TRANSFER TO BETA1
SP(12)      PRINT FORMAT TAPS12
            VECTOR VALUES TAPS12=$1HO,S10,3HF-I,S4,3HT-1,S4,3HT-2,S4,3HT-
           13,S4,3HT-4,S4,3HT-5,S4,3HT-6,S4,3HT-7,S4,3HT-8,S4,3HT-9,S3,4H
           2T-10,S4,3HF-0*$
            TRANSFER TO BETA1
SP(14)      PRINT FORMAT TAPS14
            VECTOR VALUES TAPS14=$1HO,S10,3HF-I,S4,3HT-1,S4,3HT-2,S4,3HT-
           13,S4,3HT-4,S4,3HT-5,S4,3HT-6,S4,3HT-7,S4,3HT-8,S4,3HT-9,S3,4H
           2T-10,S3,4HT-11,S3,4HT-12,S4,3HF-0*$
            TRANSFER TO BETA1
SP(16)      PRINT FORMAT TAPS16
            VECTOR VALUES TAPS16=$1HO,S10,3HF-I,S4,3HT-1,S4,3HT-2,S4,3HT-
           13,S4,3HT-4,S4,3HT-5,S4,3HT-6,S4,3HT-7,S4,3HT-8,S4,3HT-9,S3,4H
           2T-10,S3,4HT-11,S3,4HT-12,S3,4HT-13,S3,4HT-14,S4,3HF-0*$
            TRANSFER TO BETA1
BETA1       READ FORMAT IN2, PTD(1,1)...PTD(NRD,NPT)
            VECTOR VALUES IN2=$('QQ'F7.2/'QQ'F7.2)*$
            FORMAT VARIABLE PP
```

```
            PP = NPT
            PRINT FORMAT INFO1
            VECTOR VALUES INFO1=$1HO,S10,26HORIGINAL PRESSURE TAP DATA*$
            PRINT FORMAT OUT1, PTD(1,1)...PTD(NRD,NPT)
            VECTOR VALUES OUT1=$1HO,S8,'PP'F7.2/(S9,'PP'F7.2)*$
            AT = 3.1416*(DT.P.2.0)/576.
            B = 0.002228/AT
            WHENEVER FL .E. 1
              TRANSFER TO BETA1A
              OR WHENEVER FL .E. 2
              TRANSFER TO BETA2
            END OF CONDITIONAL
BETA1A      DEN = 1.0409*(1/TEMP.P.0.01089)*62.3689
            WHENEVER TEMP .LE. 113.
              LNVP = 2.303 + 0.03175*(TEMP - 50.)
              OR WHENEVER TEMP .G. 113.
            LNVP = 4.290 + 0.0261*(TEMP - 113.)
            END OF CONDITIONAL
            VAP = EXP.(LNVP)*(14.7/760.)
            TRANSFER TO GAMMA
BETA2       DEN = (13.5708-0.001448*(TEMP-50.))*62.3689
            WHENEVER TEMP .LE. 190.0
              VAP = 0.0
              TRANSFER TO GAMMA
            O'R TEMP .G. 190.0 .AND. TEMP .LE. 225.0
              VAP = 0.12 + 0.00686*(T - 190.0)*0.0193
              TRANSFER TO GAMMA
            O'R TEMP .G. 225.0 .AND. TEMP .LE. 267.0
              VAP = 0.35 + 0.01857*(T - 225.)*0.0193
              TRANSFER TO GAMMA
            O'R TEMP .G. 267.0 .AND. TEMP .LE. 301.0
              VAP = 1.12 + 0.0497*(T - 267.)*0.0193
              TRANSFER TO GAMMA
            O'R TEMP .G. 301.0
              TRANSFER TO ERROR 1
            END OF CONDITIONAL
GAMMA       PC = HB*(14.7/29.92) + HC*DEN/1728.
            VT = FLORAT*B
            KE = (VT.P.2.)/64.4
            THROUGH DELTA, FOR I=1,1,I.G.NRD
            THROUGH DELTA, FOR J=1,1,J.G.NPT
            NPSH(I,J) = (PTD(I,J) + PC - VAP)*144.*1./DEN
DELTA       NRMPR(I,J) = NPSH(I,J)/KE
            PRINT FORMAT INFO2
            VECTOR VALUES INFO2=$1HO,S10,36HTHE UNCORRECTED NORMALIZED PR
           1ESSURES*$
            PRINT FORMAT OUT2, NRMPR(1,1)...NRMPR(NRD,NPT)
            VECTOR VALUES OUT2=$1HO,S8,'PP'F7.4/(S9,'PP'F7.4)*$
            PRINT FORMAT OUT3, VT
            VECTOR VALUES OUT3=$1HO,S10,18HTHROAT VELOCITY = F7.2,7H FT/S
           1EC*$
            READ FORMAT IN3, CORR, TPC1, TPC2, LTH1, LTH2, MULT, YES
            VECTOR VALUES IN3=$(3I5,3F7.4,I3)*$
            WHENEVER CORR .E. 2
              TRANSFER TO ZETA
              OTHERWISE
              PRINT FORMAT INFO2A
```

```
            TRANSFER TO THETA
          END OF CONDITIONAL
          VECTOR VALUES INFO2A=$1H0,S10,43HNO CORRECTIONS MADE TO NORMA
         1LIZED PRESSURES*$
ZETA      THROUGH ZETA1, FOR N=1,1,N.G.NRD
          DELP(N) = (NRMPR(N,2) - NRMPR(N,3))/LTH1
          CALNPR(N) = NRMPR(N,3) - (DELP(N)*LTH2*MULT)
ZETA1     FACTOR(N) = NRMPR(N,4) - CALNPR(N)
          THROUGH ZETA2, FOR J=1,1,J.G.NRD
          THROUGH ZETA2, FOR I=TPC1,1,I.G.TPC2
ZETA2     NRMPR(J,I) = NRMPR(J,I) - FACTOR(J)
ETA       PRINT FORMAT INFO3
          VECTOR VALUES INFO3=$1H0,S10,34HTHE CORRECTED NORMALIZED PRES
         1SURES*$
          PRINT FORMAT OUT2, NRMPR(1,1)...NRMPR(NRD,NPT)
THETA     THROUGH THETA2, FOR I=1,1,I.G.NPT
          SUM(DEX,I) = 0.0
          THROUGH THETA1, FOR J=1,1,J.G.NRD
THETA1    SUM(DEX,I) = SUM(DEX,I) + NRMPR(J,I)
THETA2    AVGNP(DEX,I) = SUM(DEX,I)/NRD
THETA3    WHENEVER YES .E. 1
            LOSC(DEX) = AVGNP(DEX,1) - AVGNP(DEX,NPT)
            OTHERWISE
            TRANSFER TO IOTA
          END OF CONDITIONAL
IOTA      THROUGH IOTA1, FOR M=1,1,M.G.NRD
          THROUGH IOTA1, FOR L=1,1,L.G.NPT
          DEVNP(M,L) = NRMPR(M,L) - AVGNP(DEX,L)
IOTA1     SQDEV(M,L) = DEVNP(M,L).P.2.
          THROUGH IOTA3, FOR I=1,1,I.G.NPT
          SUMSQ(DEX,I) = 0.0
          THROUGH IOTA2, FOR J=1,1,J.G.NRD
IOTA2     SUMSQ(DEX,I) = SUMSQ(DEX,I) + SQDEV(J,I)
          VAR(DEX,I) = SUMSQ(DEX,I)/NRD
          STDDEV(DEX,I) = VAR(DEX,I).P.0.50
IOTA3     COVAR(DEX,I) = (.ABS.STDDEV(DEX,I)*100.)/(.ABS.AVGNP(DEX,I))
KAPPA     PRINT FORMAT INFO4
          VECTOR VALUES INFO4=$1H0,S10,32HTHE AVERAGE NORMALIZED PRESSU
         1RES*$
          PRINT FORMAT OUT4, AVGNP(DEX,1)...AVGNP(DEX,NPT)
          VECTOR VALUES OUT4=$1H0,(S8,'PP'F7.4)*$
          WHENEVER YES .E. 1
            PRINT FORMAT OUT4A, LOSC(DEX)
            OTHERWISE
            TRANSFER TO KAPPA1
          END OF CONDITIONAL
          VECTOR VALUES OUT4A=$1H0,S10,23HTHE LOSS COEFFICIENT = F8.4*$
KAPPA1    PRINT FORMAT INFO5
          VECTOR VALUES INFO5=$1H0,S10,37HTHE VARIANCES IN NORMALIZED P
         1RESSURES*$
          PRINT FORMAT OUT5, VAR(DEX,1)...VAR(DEX,NPT)
          VECTOR VALUES OUT5=$1H0,(S8,'PP'F7.4)*$
          PRINT FORMAT INFO6
          VECTOR VALUES INFO6=$1H0,S10,23HTHE STANDARD DEVIATIONS*$
          PRINT FORMAT OUT6, STDDEV(DEX,1)...STDDEV(DEX,NPT)
          VECTOR VALUES OUT6=$1H0,(S8,'PP'F7.4)*$
          PRINT FORMAT INFO7
```

```
          VECTOR VALUES INFO7=$1HO,S10,29HTHE COEFFICIENTS OF VARIATION
         1*$
          PRINT FORMAT OUT7, COVAR(DEX,1)...COVAR(DEX,NPT)
          VECTOR VALUES OUT7=$1HO,(S8,'PP'F7.2)*$
LAMBDA    CAVN(DEX) = AVGNP(DEX,1)
          THROUGH LDA1, FOR K=2,1,K.G.NPT
          WHENEVER AVGNP(DEX,K) .LE. CAVN(DEX)
          CAVN(DEX) = AVGNP(DEX,K)
LDA1      END OF CONDITIONAL
MU        PRINT FORMAT OUT8, CAVN(DEX)
          VECTOR VALUES OUT8=$1HO,S10,24HTHE CAVITATION NUMBER = F8.4*$
NU        WHENEVER DEX .L. NRS
            DEX = DEX + 1
            TRANSFER TO START
            OR WHENEVER DEX .E. 1 .AND. TOTAL .E. 1
            TRANSFER TO BEGIN
            OTHERWISE
            TRANSFER TO PI
          END OF CONDITIONAL
PI        THROUGH PI2, FOR I=1,1,I.G.NPT
          SUMAVG(I) = 0.0
          THROUGH PI1, FOR J=1,1,J.G.NRS
PI1       SUMAVG(I) = SUMAVG(I) + AVGNP(J,I)
          MEAVG(I) = SUMAVG(I)/NRS
PI2       Y(I) = MEAVG(I)
          THROUGH PI3, FOR L=1,1,L.G.NRS
          THROUGH PI3, FOR M=1,1,M.G.NPT
          DEVME(L,M) = AVGNP(L,M) - MEAVG(M)
PI3       SQDME(L,M) = DEVME(L,M).P.2.
          THROUGH PI5, FOR J=1,1,J.G.NPT
          SQSUME(J) = 0.0
          THROUGH PI4, FOR I=1,1,I.G.NRS
PI4       SQSUME(J) = SQSUME(J) + SQDME(I,J)
          VARM(J) = SQSUME(J)/NRS
          STDEM(J) = VARM(J).P.0.5
PI5       COVRM(J) = (.ABS.STDEM(J)*100.)/(.ABS.MEAVG(J))
          PRINT FORMAT HEAD
RHO       PRINT FORMAT INFO8, NRS
          VECTOR VALUES INFO8=$1HO,S10,16HMEAN VALUES FOR I3,49H SETS A
         1T SAME FLOW, RPM, AND CAVITATION CONDITION*$
          PRINT FORMAT INFO9, FLORAT, VT, RPM, VENT
          VECTOR VALUES INFO9=$1HO,S10,12HFLOW RATE = F7.3,4H GPM/1H ,S
         110,18HTHROAT VELOCITY = F7.2,7H FT/SEC/1H ,S10,13HPUMP SPEED
         2= I5,4H RPM/1H ,S10,17HVENTURI USED WAS I3*$
          TRANSFER TO RHO(COND)
RHO(1)    PRINT FORMAT WOS1
          TRANSFER TO RH(NPT)
RHO(2)    PRINT FORMAT WOS2
          TRANSFER TO RH(NPT)
RHO(3)    PRINT FORMAT WOS3
          TRANSFER TO RH(NPT)
RHO(4)    PRINT FORMAT WOS4
          TRANSFER TO RH(NPT)
RHO(5)    PRINT FORMAT WOS5
          TRANSFER TO RH(NPT)
RH(8)     PRINT FORMAT TAPS8
          TRANSFER TO SIGMA
```

```
RH(10)      PRINT FORMAT TAPS10
            TRANSFER TO SIGMA
RH(12)      PRINT FORMAT TAPS12
            TRANSFER TO SIGMA
RH(14)      PRINT FORMAT TAPS14
            TRANSFER TO SIGMA
RH(16)      PRINT FORMAT TAPS16
            TRANSFER TO SIGMA
SIGMA       PRINT FORMAT INFO4
            PRINT FORMAT OUT9, MEAVG(1)...MEAVG(NPT)
            VECTOR VALUES OUT9=$1HO,(S8,'PP'F7.4)*$
            PRINT FORMAT INFO5
            PRINT FORMAT OUT10, VARM(1)...VARM(NPT)
            VECTOR VALUES OUT10=$1HO,(S8,'PP'F7.4)*$
            PRINT FORMAT INFO6
            PRINT FORMAT OUT11, STDEM(1)...STDEM(NPT)
            VECTOR VALUES OUT11=$1HO,(S8,'PP'F7.4)*$
            PRINT FORMAT INFO7
            PRINT FORMAT OUT12, COVRM(1)...COVRM(NPT)
            VECTOR VALUES OUT12=$1HO,(S8,'PP'F7.2)*$
TAU         MECAV = MEAVG(1)
            THROUGH TAU1, FOR J=2,1,J.G.NPT
            WHENEVER MEAVG(J) .LE. MECAV
              MECAV = MEAVG(J)
TAU1        END OF CONDITIONAL
            PRINT FORMAT OUT13, MECAV
            VECTOR VALUES OUT13=$1HO,S10,29HTHE MEAN CAVITATION NUMBER =
           1F8.4*$
            PRINT FORMAT TITLE
            VECTOR VALUES TITLE = $1H1,S50,33HPRESSURE PROFILE PLOTS DME
           1THESIS*$
            WHENEVER VENT .E. 412
            EXECUTE PLOT1.(NSCALE,5,10,5,20)
            EXECUTE PLOT2.(IMAGE,7.000,-1.000,1.900,-0.100)
            EXECUTE PLOT3.($*$,X(1),Y(1),NPT)
            EXECUTE PLOT4.(49,ORD)
            PRINT FORMAT BOTTOM
            OR WHENEVER VENT .E. 534
            EXECUTE PLOT1.(NSCALE,5,10,5,20)
            EXECUTE PLOT2.(IMAGE,11.000,-1.000,1.900,-0.100)
            EXECUTE PLOT3.($*$,Z(1),Y(1),NPT)
            EXECUTE PLOT4.(49,ORD)
            PRINT FORMAT BOTTOM
            OR WHENEVER VENT .E. 614
            EXECUTE PLOT1.(NSCALE,5,10,5,20)
            EXECUTE PLOT2.(IMAGE,7.500,-0.500,1.900,-0.100)
            EXECUTE PLOT3.($*$,U(1),Y(1),NPT)
            EXECUTE PLOT4.(49,ORD)
            PRINT FORMAT BOTTOM
            OR WHENEVER VENT .E. 712
            EXECUTE PLOT1.(NSCALE,5,10,5,20)
            EXECUTE PLOT2.(IMAGE,7.000,-1.000,1.900,-0.100)
            EXECUTE PLOT3.($*$,W(1),Y(1),NPT)
            EXECUTE PLOT4.(49,ORD)
            PRINT FORMAT BOTTOM
            OR WHENEVER VENT .E. 818
            EXECUTE PLOT1.(NSCALE,5,10,5,20)
```

```
      EXECUTE PLOT2.(IMAGE,3.000,-1.000,1.900,-0.100)
      EXECUTE PLOT3.($*$,Q(1),Y(1),NPT)
      EXECUTE PLOT4.(49,ORD)
      PRINT FORMAT BOTTOM
      END OF CONDITIONAL
      VECTOR VALUES NSCALE = 1,0,3,0,3
      VECTOR VALUES Q(1) = -1.000,0.080,0.290,0.500,0.615,0.766,
     10.925,3.000
      VECTOR VALUES U(1) = -0.500,0.056,0.554,1.069,1.186,1.412,
     11.915,2.197,2.754,2.993,7.132,7.500
      VECTOR VALUES X(1) = -1.000,0.115,1.233,2.104,2.362,2.735,
     13.138,3.478,3.853,4.266,4.524,5.008,5.412,5.766,6.167,7.000
      VECTOR VALUES Z(1) = -1.000,0.172,1.940,3.155,3.631,4.029,
     14.755,5.346,5.704,6.399,6.779,7.430,7.939,11.000
      VECTOR VALUES W(1) = -1.000,0.675,1.475,2.225,2.519,2.858,
     13.427,3.606,4.375,4.384,4.713,5.132,5.531,7.000
      VECTOR VALUES ORD = $              AVERAGE NORMALIZED PRESSURES
     1          *$
      VECTOR VALUES BOTTOM = $1H ,S31,58H DISTANCE FROM THROAT ENTR
     1ANCE TO TAP     ---     (INCHES)  *$
      DIMENSION Q(8),U(12),W(14),X(16),Y(16),Z(14),IMAGE(1000)
OMEGA  WHENEVER REPEAT .L. TOTAL
        REPEAT = REPEAT + 1
        TRANSFER TO BEGIN1
        OTHERWISE
        TRANSFER TO BEGIN
      END OF CONDITIONAL
      TRANSFER TO START
ERROR1 PRINT FORMAT ERR1
      VECTOR VALUES ERR1=$1HO,S10,25HTEMPERATURE LIMIT EXCEEDED*$
      TRANSFER TO BEGIN
      DIMENSION PTD(160,V1),NPSH(160,V1),NRMPR(160,V1),DELP(10),
     1CALNPR(10),FACTOR(10),SUM(80,V2),AVGNP(80,V2),DEVNP(160,V1),
     2SUMSQ(96,V2),VAR(80,V2),STDDEV(80,V2),COVAR(80,V2),CAVN(5),
     3SUMAVG(16),MEAVG(16),DEVME(80,V2),SQDME(80,V2),SQSUME(16),
     4VARM(16),STDEM(16),COVRM(16),SQDEV(160,V1),LOSC(10)
      VECTOR VALUES V1 = 2,1,16
      VECTOR VALUES V2 = 2,1,16
      END OF PROGRAM
```

PRESSURE PROFILE CALCULATIONS DME THESIS RESULTS FROM RAWDAT5 PROGRAM

TEST FLUID IS WATER

NO TEST SPECIM N RUNS, VISIBLE INITIATION

THE GAS IS AIR AT 1.39 PERCENT BY VOLUME

TEMPERATURE = 53.300 F
BAROMETRIC PRESSURE = 29.3450 IN. HG.
HEIGHT CORRECTION = .0000 IN. FLUID
FLOW RATE = 79.400 IN. FLUID OR 40.200 GPM
PUMP SPEED = 1165 RPM
VENTURI USED WAS 412
ORIGINAL DATA ON SHEET NO. 197772

F-I	T-1	T-2	T-3	T-4	T-5	T-6	T-7	T-8	T-9	T-10	T-11	T-12	T-13	T-14	F-O
ORIGINAL PRESSURE TAP DATA															
17.90	-11.35	-12.15	-12.40	-11.25	-5.90	-1.90	.30	1.95	3.35	4.15	5.05	5.75	6.30	7.00	10.50
THE UNCORRECTED NORMALIZED PRESSURES															
.2014	.1068	.0768	.0675	.1105	.3107	.4604	.5427	.6045	.6569	.6868	.7205	.7467	.7673	.7935	.9244

THROAT VELOCITY = 63.14 FT/SEC

THE CORRECTED NORMALIZED PRESSURES															
.2014	.1068	.0768	.0401	.1105	.3107	.4604	.5427	.6045	.6569	.6868	.7205	.7467	.7673	.7935	.9244
THE AVERAGE NORMALIZED PRESSURES															
.2014	.1068	.0768	.0401	.1105	.3107	.4604	.5427	.6045	.6569	.6868	.7205	.7467	.7673	.7935	.9244

THE LOSS COEFFICIENT = .2769

THE VARIANCES IN NORMALIZED PRESSURES															
.0000	.0000	.0000	.0000	.0000	.0000	.0000	.0000	.0000	.0000	.0000	.0000	.0000	.0000	.0000	.0000
THE STANDARD DEVIATIONS															
.0000	.0000	.0000	.0000	.0000	.0000	.0000	.0000	.0000	.0000	.0000	.0000	.0000	.0000	.0000	.0000
THE COEFFICIENTS OF VARIATION															
.00	.00	.00	.00	.00	.00	.00	.00	.00	.00	.00	.00	.00	.00	.00	.00

THE CAVITATION NUMBER = .0401 —

PRESSURE PROFILE CALCULATIONS DME THESIS RESULTS FROM RAWDAT5 PROGRAM

TEST FLUID IS WATER

NO TEST SPECIMEN RUNS, VISIBLE INITIATION

THE GAS IS AIR AT 1.15 PERCENT BY VOLUME

TEMPERATURE = 53.300 F
BAROMETRIC PRESSURE = 29.3450 IN. HG.
HEIGHT CORRECTION = .0000 IN. FLUID
FLOW RATE = 79.400 IN. FLUID OR 40.200 GPM
PUMP SPEED = 1160 RPM
VENTURI USED WAS 412
ORIGINAL DATA ON SHEET NO. 197772

F-I	T-1	T-2	T-3	T-4	T-5	T-6	T-7	T-8	T-9	T-10	T-11	T-12	T-13	T-14	F-O
ORIGINAL PRESSURE TAP DATA															
17.75	-11.35	-12.15	-12.45	-11.55	-6.15	-2.45	-.20	1.50	3.05	3.95	4.90	5.60	6.25	6.80	10.20
17.90	-11.25	-12.10	-12.30	-11.50	-6.25	-2.25	.20	1.80	3.15	3.90	4.85	5.50	6.20	6.70	10.45
THE UNCORRECTED NORMALIZED PRESSURES															
1.1957	.1068	.0768	.0656	.0993	.3013	.4398	.5240	.5876	.6456	.6793	.7149	.7411	.7654	.7860	.9132
1.2014	.1105	.0787	.0712	.1011	.2976	.4473	.5390	.5989	.6494	.6774	.7130	.7373	.7635	.7822	.9226
THROAT VELOCITY = 63.14 FT/SEC															
THE CORRECTED NORMALIZED PRESSURES															
1.1957	.1068	.0768	.0401	.0993	.3013	.4398	.5240	.5876	.6456	.6793	.7149	.7411	.7654	.7860	.9132
1.2014	.1105	.0787	.0396	.1011	.2976	.4473	.5390	.5989	.6494	.6774	.7130	.7373	.7635	.7822	.9226
THE AVERAGE NORMALIZED PRESSURES															
1.1985	.1086	.0777	.0398	.1002	.2995	.4436	.5315	.5932	.6475	.6784	.7139	.7392	.7644	.7841	.9179
THE LOSS COEFFICIENT = .2807															
THE VARIANCES IN NORMALIZED PRESSURES															
.0000	.0000	.0000	.0000	.0000	.0000	.0000	.0001	.0000	.0000	.0000	.0000	.0000	.0000	.0000	.0000
THE STANDARD DEVIATIONS															
.0028	.0019	.0009	.0002	.0009	.0019	.0037	.0075	.0056	.0019	.0009	.0009	.0019	.0009	.0019	.0047
THE COEFFICIENTS OF VARIATION															
.23	1.72	1.20	.53	.93	.62	.84	1.41	.95	.29	.14	.13	.25	.12	.24	.51

THE CAVITATION NUMBER = .0398 -

PRESSURE PROFILE CALCULATIONS DME THESIS RESULTS FROM RAWDAT5 PROGRAM

MEAN VALUES FOR 2 SETS AT SAME FLOW, RPM, AND CAVITATION CONDITION

FLOW RATE = 40.200 GPM
THROAT VELOCITY = 63.14 FT/SEC
PUMP SPEED = 1160 RPM
VENTURI USED WAS 412

NO TEST SPECIMEN RUNS, VISIBLE INITIATION

F-I	T-1	T-2	T-3	T-4	T-5	T-6	T-7	T-8	T-9	T-10	T-11	T-12	T-13	T-14	F-O
THE AVERAGE NORMALIZED PRESSURES															
1.2000	.1077	.0773	.0400	.1053	.3051	.4520	.5371	.5989	.6522	.6826	.7172	.7429	.7659	.7888	.9212
THE VARIANCES IN NORMALIZED PRESSURES															
.0000	.0000	.0000	.0000	.0000	.0000	.0001	.0000	.0000	.0000	.0000	.0000	.0000	.0000	.0000	.0000
THE STANDARD DEVIATIONS															
.0014	.0009	.0005	.0001	.0051	.0056	.0084	.0056	.0056	.0047	.0042	.0033	.0037	.0014	.0047	.0033
THE COEFFICIENTS OF VARIATION															
.12	.87	.61	.27	4.88	1.84	1.86	1.05	.94	.72	.62	.46	.50	.18	.59	.36

THE MEAN CAVITATION NUMBER = .0400 ✓

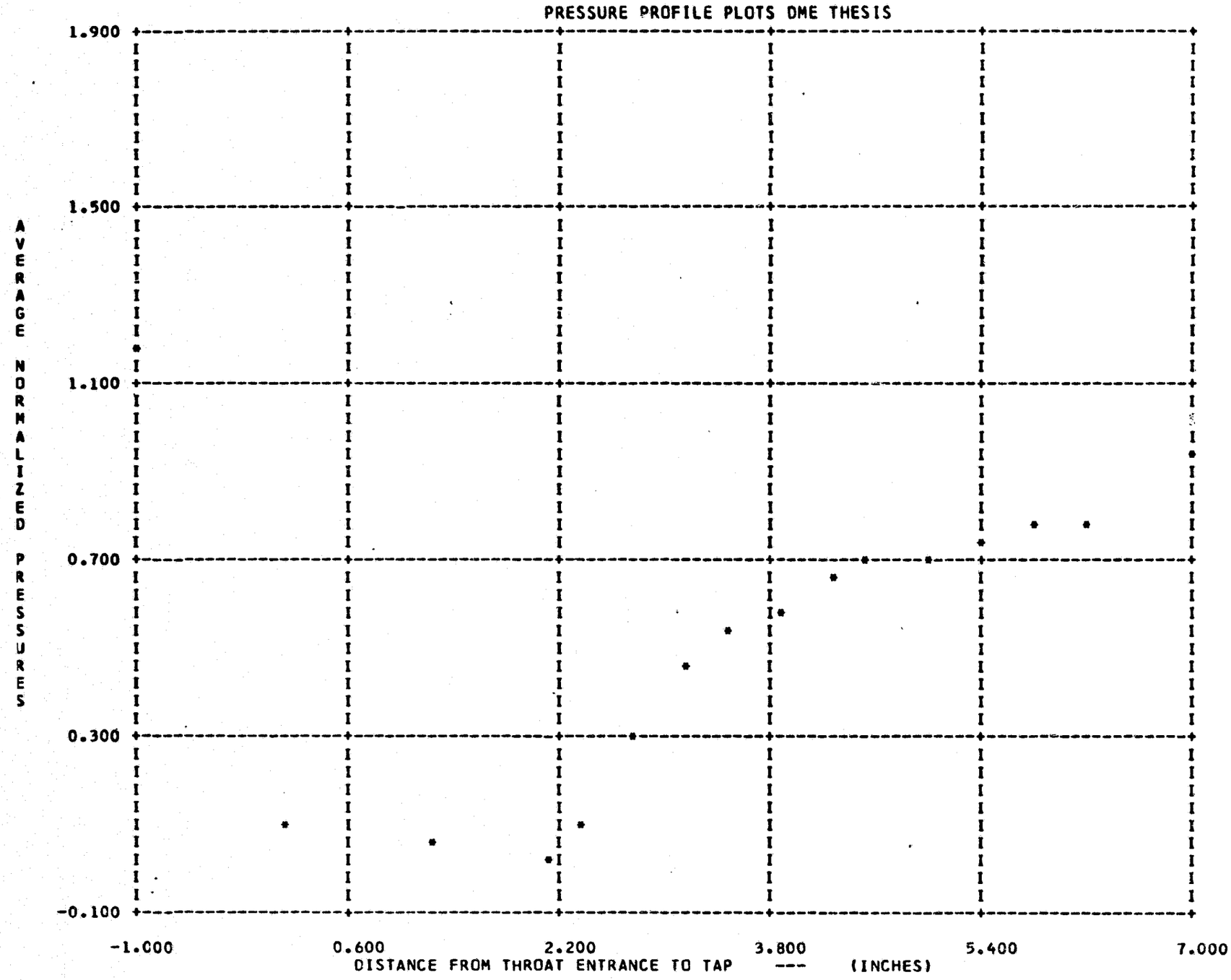
PRESSURE PROFILE PLOTS DME THESIS
1.900
1.500
1.100
0.700
0.300
-0.100
AVERAGE NORMALIZED PRESSURES
-1.000
0.600
2.200
3.800
5.400
7.000
DISTANCE FROM THROAT ENTRANCE TO TAP --- (INCHES)

APPENDIX F

THE COMPUTER PROGRAM CALPRM

I. INTRODUCTION

The computer program CALPRM is designed to take raw data in the form of velocity, temperature, etc., from the pressure profile measurements in water and mercury and compute a series of dimensionless parameters for use in the correlation analysis. As presently formulated it contains subroutines for computing Reynolds number, Weber number, Prandtl number, a thermodynamic parameter, a gas content parameter, exposure time parameter, and the Net Positive Suction Head. This program is written in FORTRAN IV and contains no specialized functions not normally available in a machine library. Standard handbooks were used in compiling the physical properties data.

II. DESCRIPTION OF THE PROGRAM

The main program provides bookkeeping and control functions and thus does no direct computations. The data are read in and reprinted on the output with appropriate identification.

A. REYNO. This subroutine computes the flow Reynolds number based upon throat velocity and diameter from the relation:

$$\text{REYNO} = \text{DEN} * \frac{DT}{12} * \frac{VT}{VIS}$$

where: REY NO - Reynolds number

DEN - Density of fluid at test temperature ($\#/ft^3$)

DT - Throat diameter (in)

VT - Throat velocity (ft/sec)

VIS - Fluid viscosity ($/ft-sec)

The density is computed on the basis of a curve fit to the literature data of density versus temperature. The viscosity is determined from a series of linear piecewise curve fits from the viscosity logarithm versus temperature plots. The computed values agree with the handbook values to less than 1% over the temperature range of consideration here (32° to 176°F for water, 32° to 600°F for mercury)[58,59,60,61].

B. WEBNO. This subroutine computes the Weber number based upon the throat velocity and one of three options for a diameter. The first two options compute a Weber number based upon the gas bubble characteristics in the fluid, while the third uses the system characteristics. Option (1) is based upon a diameter with linear relation (arbitrary) to the gas concentration; option (2) assumes a constant diameter of 0.001 inch for the gas bubbles regardless of gas content, temperature or flow rate. The Weber number is computed from the relation:

$$WNUMR = \frac{DEN}{SURTEN} * \frac{D}{12.} * \frac{VT^2}{32.}$$

where:

WNUMR - Weber number

DEN - Density of fluid at test temperature (#/ft^3)

D - Diameter from option 1, 2, or 3. (in)

SURTEN - Fluid surface tension (#/ft)

VT - Throat velocity (ft/sec)

The density is determined in the same fashion as for the REYNO, while the surface tension is computed from a linear piecewise curve fit of surface tension versus temperature. The values of surface tension agree with handbook data to better than 3% with ranges used here.[58,59,60,61]

C. THERM. This subroutine computes the thermodynamic parameter discussed in Chapter II. The only inputs required are the fluid temperature and velocity and the parameter is computed from the relation:

$$BPRIME = \frac{DENL * CP * DELT}{DENV * HFG} * EKIN$$

where:
- BRIME - Thermodynamic parameter
- DENL - Fluid density at test temperature (#/ft^3)
- CP - Heat capacity of fluid (BTU/°F)
- DELT - Change of temperature with pressure along the saturation vapor pressure line (°F/ft)
- DENV - Vapor density at bulk fluid temperature (#/ft^3)
- HFG - Latent heat of vaporization at test temperature (BTU/#)
- EKIN - Kinetic head (ft) - $V_t^2/2g$

In all cases, the values were calculated from a linear piecewise curve fits to available data, which in most cases were ploted of the variable versus temperature. This procedure was used since the regression analysis for curve fitting was not available at the time this data was required. Again the values computed are within 3 to 5% of handbook values for any given point.[58,59,60,61]

D. PRDTL. This subroutine computes the fluid Prandtl number based solely on the temperature as an input using the relation:

$$PRDTL = \frac{VIS * CP}{CK}$$

where: PRDTL - Prandtl number

VIS - Fluid viscosity (#/ft-sec)

CP - Fluid heat capacity (BTU/#)

CK - Thermal conductivity (BTU/ft-hr-°F)

The values are computed from curve fits to handbook data as indicated about and agree with the published data.

E. TIME. This subroutine computes the dimensionless exposure parameter based upon the venturi throat diameter (converted to length with the L/D ratio) and the fluid velocity in the throat. The relationship used is:

$$TAU = \frac{DT * CONSTANT}{12. * VT * OTAU}$$

where: TAU - Exposure time parameter

VT - Throat velocity (ft/sec)

DT - Throat diameter (in)

OTAU - Molecular relaxation time for liquids

CONSTANT - L/D ratio for these venturis

F. GASFAC. This subroutine computes the dimensionless gas concentration factor based on gas content and throat velocity from the relation:

$$AIR = \frac{ALPHA * BETA * CONSTANT}{DEN * EKIN}$$

where: AIR - Gas concentration factor

ALPHA - Gas concentration (ppm)

BETA - Henry's Law constant ($\#/in^2$)

DEN - Fluid density ($\#/ft^3$)

EKIN - Kinetic head (ft) - $VT^2/2g$

G. POSHD. This subroutine computes the net positive suction head from the relation:

$$SHNP = CAVN * ENKIN$$

where: SHNP - Net positive suction head

CAVN - Cavitation number as computed by RAWDAT

ENKIN - Kinetic head (ft) - $VT^2/2g$

III. PROGRAM INPUT

The CALPRM input is in the form of two cards. The first card is an integer number which indicates the number of data sets to be considered, the second contains the physical data in a combination of integer and floating point fields. The data is provided in the following order:

a. Cavitation condition

b. Number of runs in the set

c. Test fluid temperature

d. Flow rate in inches of test fluid

e. Flow rate in GPM

f. Pump speed in RPM

g. Venturi used

h. Gas entrained in fluid

i. Test fluid

j. Venturi throat diameter in inches

k. Cavitation number

1. Standard deviation on cavitation number

m. Throat velocity in feet per second

n. Gas content in volume percent

o. Page number in the original data book

IV. PROGRAM OUTPUT

The output of the program is essential self-explanatory as can be seen from the example following the program listing. It includes a recap of the input data and the calculated output with the appropriate dimensions. The output also includes any physical constants which have been calculated from curve fits.

V. DEFINITION OF PROGRAM VARIABLES

The following list defines only those terms which are used for input/output or major operations. The variables are defined in order of their appearance in the program.

IPEAT - Loop index compared with ITOT

ITOT - Number of cases to be run

ICON - Integer index, value 1-5, specifies cavitation condition

NRD - Integer specifying number of runs at same test conditions

TEMP - Fluid temperature in degrees Fahrenheit

FR - Flowrate in inches of test fluid

FLORAT - Flowrate in GPM

NRPM - Pump speed in RPM

IVENT - Integer index indicating venturi used

NGAS - Integer index indicating which gas is present

IFL - Integer index indicating test fluid

DT - Venturi throat diameter in inches

CAVN - Cavitation number

STD - Standard deviation of cavitation number

VT - Throat velocity in feet per second

CONC - Gas concentration in volume percent

IREC - Page number in original data book

VISLN - Logarithm of the fluid viscosity

VIS - Fluid viscosity at test temperature

DEN - Fluid density at test temperature

VALUE - Subroutine code for Reynolds number

SURTEN - Fluid surface tension at test temperature

WNUMR - Weber number

CP - Heat capacity

DPDT - Change in pressure with temperature along saturation vapor pressure line

DELT - Reciprocal of DPDT

DENL - Fluid density

DENV - Vapor density

HFG - Latent heat of vaporization

B - Thermodynamic parameter

BPRIME - Normalized Thermodynamic Parameter

```
      PROGRAM CALPRM (INPUT,OUTPUT)
      IPEAT = 1
100   READ 1001, ITOT
101   READ 1011, ICON,NRD,TEMP,FR,FLORAT,NRPM,IVENT,NGAS,IFL,DT,CAVN,STD
     1,VT,CONC,IREC
      PRINT 1012
      GO TO (102,103),IFL
102   PRINT 1021
      GO TO 104
103   PRINT 1031
      GO TO 104
104   GO TO (105,106,107,108,109),ICON
105   PRINT 1051
      GO TO 110
106   PRINT 1061
      GO TO 110
107   PRINT 1071
      GO TO 110
108   PRINT 1081
      GO TO 110
109   PRINT 1091
      GO TO 110
110   GO TO (111,112,113),NGAS
111   PRINT 1111, CONC
      GO TO 114
112   PRINT 1121, CONC
      GO TO 114
113   PRINT 1131, CONC
      GO TO 114
114   PRINT 1141, TEMP,NRD,FR,FLORAT,NRPM,IVENT,IREC,DT,VT,CAVN,STD
115   CALL REYNO (TEMP,DT,VT,IFL)
116   CALL WEBNO (TEMP,DT,VT,IFL,CONC)
117   CALL PRDTL (TEMP,IFL)
118   CALL THERM (TEMP,VT,IFL)
      CALL TIME (VT,DT)
      CALL GASFAC (TEMP,CONC,VT,IFL,NGAS)
119   CALL POSHD (CAVN,STD,VT)
      IF (IPEAT .LT. ITOT) GO TO 120
      IF (IPEAT .GE. ITOT) GO TO 100
120   IPEAT = IPEAT + 1
      GO TO 101
1001  FORMAT (I3)
1011  FORMAT (2I2,3F7.3,I5,I3,2I2,3F7.4,F6.2,F5.2,I7)
1012  FORMAT (1H1,10X,33HPARAMETER CALCULATIONS DME THESIS,15X,28HRESULT
     1S FROM CALPRM PROGRAM )
1021  FORMAT (1H0,10X,19HTEST FLUID IS WATER)
1031  FORMAT (1H0,10X,21HTEST FLUID IS MERCURY)
1051  FORMAT (1H0,10X,39HNO TEST SPECIMEN RUNS, SONIC INITIATION)
1061  FORMAT (1H0,10X,41HNO TEST SPECIMEN RUNS, VISIBLE INITIATION)
1071  FORMAT (1H0,10X,42HNO TEST SPECIMEN RUNS, STANDARD CAVITATION)
1081  FORMAT (1H0,10X,47HNO TEST SPECIMEN RUNS, CAVITATION TO FIRST MARK
     1)
1091  FORMAT (1H0,10X,36HNO TEST SPECIMEN RUNS, NO CAVITATION)
1111  FORMAT (1H0,10X,18HTHE GAS IS AIR AT F6.2,18H PERCENT BY VOLUME)
1121  FORMAT (1H0,10X,23HTHE GAS IS ARGON    AT F6.2,18H PERCENT BY VOLU
     1ME)
1131  FORMAT (1H0,10X,23HTHE GAS IS HYDROGEN AT F6.2,18H PERCENT BY VOLU
```

```
     1ME)
1141  FORMAT (1H0,10X,14HTEMPERATURE = F7.3,2H F/
     11H ,10X,17HNUMBER OF RUNS = I3/
     21H ,10X,12HFLOW RATE = F7.3,12H IN. HG. OR F7.3,4H GPM/
     31H ,10X,13HPUMP SPEED = I5,4H RPM/
     41H ,10X,17HVENTURI USED WAS I3/
     51H ,10X,27HORIGINAL DATA ON SHEET NO. I8/
     61H0,10X,18HTHROAT DIAMETER = F7.4,4H IN./
     71H0,10X,18HTHROAT VELOCITY = F6.2,7H FT/SEC/
     81H0,10X,20HCAVITATION NUMBER = F7.4,11H STD. DEV. F7.4)
      END



      SUBROUTINE REYNO(TEMP,DT,VT,IFL)
      GO TO (10,20), IFL
10    IF (TEMP .GT. 32. .AND. TEMP .LT. 95.) VISLN = 2.485 - 0.0145*(TEM
     1P - 32.)
      IF (TEMP .GE. 95. .AND. TEMP .LT. 176.) VISLN = 1.549 - 0.00960*(T
     1EMP - 95.)
      IF (TEMP .GT. 176.) GO TO 40
      DEN = 1.0409*(1./TEMP**0.01089)*62.3689
      VIS = EXP(VISLN)*(.0001)
      GO TO 30
20    IF (TEMP .GT. 32. .AND. TEMP .LT. 86.) VIS = (11.320 - 0.02296*(TE
     1MP - 32.))*(.0001)
      IF (TEMP .GE. 86. .AND. TEMP .LT. 156.) VIS = (10.08 - 0.01614*(TE
     1MP - 86.))*(.0001)
      IF (TEMP .GT. 156. .AND. TEMP .LT. 300.) VIS = (8.95 - 0.01198*(TE
     1MP - 156.))*(.0001)
      IF (TEMP .GE. 300. .AND. TEMP .LT. 400.) VIS = (2.76 - 0.0024*(TEM
     1P - 300.))/3600.
      IF (TEMP .GE. 400. .AND. TEMP .LT. 500.) VIS = (2.52 - 0.0020*(TEM
     1P - 400.))/3600.
      IF (TEMP .GE. 500. .AND. TEMP .LT. 600.) VIS = (2.32 - 0.0014*(TEM
     1P - 500.))/3600.
      IF (TEMP .GT. 600.) GO TO 40
      DEN = (13.5708 - 0.001448*(TEMP - 50.))*62.3689
      GO TO 30
30    VALUE = DEN*(DT/12.0)*VT/VIS
      PRINT 301
      PRINT 302, VIS,DEN,VALUE
      GO TO 50
40    PRINT 401
      GO TO 50
50    RETURN
301   FORMAT (1H //,11X,19HRESULTS FROM REYNO.)
302   FORMAT (1H0,10X,12HVISCOSITY = E11.4,10H LB/FT-SEC/
     11H ,10X,10HDENSITY = F7.3,9H LB/CU FT/
     21H ,10X,18HREYNOLDS NUMBER = E11.4)
401   FORMAT (1H0,10X,26HTEMPERATURE LIMIT EXCEEDED)
      END
```

```
      SUBROUTINE WEBNO (TEMP,DT,VT,IFL,CONC)
      GO TO (10,20), IFL
10    IF (TEMP .GT. 40. .AND. TEMP .LE. 122.) SURTEN = (508.55 - 0.6004*
     1(TEMP - 50.))*(0.00001)
      IF (TEMP .GT. 122. .AND. TEMP .LT. 180.) SURTEN = (465.32 - 0.6967
     1*(TEMP - 122.))*(0.00001)
      IF (TEMP .GT. 180.) GO TO 50
      DEN = 1.0409*(1./TEMP**0.01089)*62.3689
      GO TO 30
20    IF (TEMP .GT. 600.) GO TO 50
      IF (TEMP .GT. 32. .AND. TEMP .LT. 300.) SURTEN = 0.0319 - (4.21*(0
     1.000001)*(TEMP - 65.))
      IF (TEMP .GE. 300. .AND. TEMP .LT. 400.) SURTEN = 0.03085 - (8.9*(
     10.000001)*(TEMP - 300.))
      IF (TEMP .GE. 400. .AND. TEMP .LT. 600.) SURTEN = 0.02996 - (1.23*
     1(0.000001)*(TEMP - 400.))
      DEN = (13.5708 - 0.001448*(TEMP - 50.))*62.3689
      GO TO 30
30    IF (CONC .GT. 0. .AND. CONC .LT. 0.5) D1 = 0.0003
      IF (CONC .GE. 0.5 .AND. CONC .LT. 1.) D1 = 0.0006
      IF (CONC .GE. 1. .AND. CONC .LT. 1.5) D1 = 0.0012
      IF (CONC .GE. 1.5 .AND. CONC .LT. 2.) D1 = 0.0015
      IF (CONC .GE. 2.) D1 = 0.0018
      D2 = 0.001
40    WNUMR1 = (DEN/SURTEN)*(D1/12.)*(VT**2.)*1./32.
      WNUMR2 = (DEN/SURTEN)*(D2/12.)*(VT**2.)*1./32.20
      WNUMR3 = (DEN/SURTEN)*(DT/12.)*(VT**2.)*1./32.2
      PRINT 401
      PRINT 402, SURTEN,WNUMR1,WNUMR2,WNUMR3
      GO TO 60
50    PRINT 501
60    RETURN
401   FORMAT (1H //,11X,19HRESULTS FORM WEBNO.)
402   FORMAT (1H0,10X,18HSURFACE TENSION = E11.4,6H LB/FT/
     11H ,10X,35HWEBER NO. BASED ON CONCENTRATION = E11.4/
     21H ,10X,27HWEBER NO. 1 MIL DIAMETER = E11.4/
     31H ,10X,38HWEBER NO. BASED ON VENTURI DIAMETER = E11.4)
501   FORMAT (1H0,10X,26HTEMPERATURE LIMIT EXCEEDED)
      END



      SUBROUTINE TIME (VT,DT)
      OTAU = 10.**-13.
      TRANS = (DT*4.55)/(12.*VT)
      TAU = TRANS/OTAU
      PRINT 10, TRANS,TAU
      RETURN
   10 FORMAT (1H0,11X,18HRESULTS FROM TIME./
     11H0,10X,16HEXPOSURE TIME = E11.4,4H SEC/
     11H ,10X,6HTAU = E11.4)
      END
```

```
      SUBROUTINE THERM (TEMP,VT,IFL)
      GO TO (10,20), IFL
10    IF (TEMP .GT. 40. .AND. TEMP .LT. 68.) CP = 1.002625 - 1.357*(0.00
     101)*(TEMP - 40.)
      IF (TEMP .GE. 68. .AND. TEMP .LT. 86.) CP = 0.99883 - 0.3682*(0.00
     101)*(TEMP - 68.)
      IF (TEMP .GE. 86. .AND. TEMP .LT. 106.) CP = 0.9980
      IF (TEMP .GE. 106. .AND. TEMP .LT. 140.) CP = 0.99800 + 4.206*(0.0
     1001)*(TEMP - 106.)
      IF (TEMP .GE. 140. .AND. TEMP .LT. 176.) CP = 0.99943 + 7.526*(0.0
     10001)*(TEMP - 140.)
      IF (TEMP .GE. 176.) GO TO 40
      IF (TEMP .GT. 35. .AND. TEMP .LE. 65.) DPDT = (2.937*.0001)*(TEMP*
     1*0.806)
      IF (TEMP .GT. 65. .AND. TEMP .LE. 87.) DPDT = (1.696*.00001)*(TEMP
     1**1.517)
      IF (TEMP .GT. 87. .AND. TEMP .LE. 115.) DPDT = (1.072*.000001)*(TE
     1MP**2.141)
      IF (TEMP .GT. 115. .AND. TEMP .LE. 150.) DPDT = (3.263*10.**-7.)*(
     1TEMP**2.492)
      IF (TEMP .GT. 150.) GO TO 40
      DELT = 0.433/DPDT
      DENL = (1.0409/(TEMP**0.01089))*62.3689
      IF (TEMP .GT. 35. .AND. TEMP .LE. 150.) HFG = 1075.8 - 0.586*(TEMP
     1 - 35.)
      IF (TEMP .GT. 150.) GO TO 40
      IF (TEMP .GT. 53. .AND. TEMP .LT. 66.5) VOL = 1533.3 - 42.658*(TEM
     1P - 53.)
      IF (TEMP .GT. 66.5 .AND. TEMP .LT. 90.) VOL = 957.4 - 20.146*(TEMP
     1 - 66.5)
      IF (TEMP .GT. 90. .AND. TEMP .LT. 118.) VOL = 484. - 10.3*(TEMP -
     190.)
      IF (TEMP .GT. 118. .AND. TEMP .LT. 150.) VOL = 195.6 - 3.275*(TEMP
     1 - 118.)
      IF (TEMP .GT. 150.) GO TO 40
      DENV = 1./VOL
      GO TO 30
20    IF (TEMP .GT. 600.) GO TO 50
      IF (TEMP .GE. 32. .AND. TEMP .LT. 176.) CP = 0.033382 - 3.366*(10.
     1**-6.)*(TEMP - 32.)
      IF (TEMP .GE. 176. .AND. TEMP .LT. 298.) CP = 0.032877 - 2.4*(10.*
     1*-6.)*(TEMP - 176.)
      IF (TEMP .GE. 298. .AND. TEMP .LT. 430.) CP = 0.03255 - 1.4*(10.**
     1-6.)*(TEMP - 298.)
      IF (TEMP .GE. 430. .AND. TEMP .LT. 514.) CP = 0.03238 - 0.6756*(10
     1.**-6.)*(TEMP - 430.)
      IF (TEMP .GE. 514. .AND. TEMP .LT. 600.) CP = 0.03233
      S1 = 0.000063
      S2 = 0.000183
      S3 = 0.000366
      S4 = 0.000698
      S5 = 0.00128
      S6 = 0.00224
      S7 = 0.00385
      S8 = 0.00636
      S9 = 0.01024
      S10= 0.0160
```

```
      S11= 0.0244
      S12= 0.0366
      S13= 0.0651
      S14= 0.1277
      S15= 0.23583
      S16= 0.4123
      S17= 0.6866
      S18= 1.0956
      S19= 1.710
C     FOR TEMP RANGE 50 TO 900 DEG F
      IF (TEMP .GT. 600.) GO TO 40
      HFG = 128.55 - 0.004464*(TEMP - 40.)
      DENL = (13.5708 - 0.001445*(TEMP -50.))*62.368
      IF (TEMP .GT. 540.) GO TO 401
      IF (TEMP .GT. 50. .AND. TEMP .LE. 86.) GO TO 201
      IF (TEMP .GT. 86. .AND. TEMP .LE. 104.) GO TO 202
      IF (TEMP .GT. 104. .AND. TEMP .LE. 122.) GO TO 203
      IF (TEMP .GT. 122. .AND. TEMP .LE. 140.) GO TO 204
      IF (TEMP .GT. 140. .AND. TEMP .LE. 158.) GO TO 205
      IF (TEMP .GT. 158. .AND. TEMP .LE. 176.) GO TO 206
      IF (TEMP .GT. 176. .AND. TEMP .LE. 194.) GO TO 207
      IF (TEMP .GT. 194. .AND. TEMP .LE. 212.) GO TO 208
      IF (TEMP .GT. 212. .AND. TEMP .LE. 230.) GO TO 209
      IF (TEMP .GT. 230. .AND. TEMP .LE. 248.) GO TO 210
      IF (TEMP .GT. 248. .AND. TEMP .LE. 266.) GO TO 211
      IF (TEMP .GT. 266. .AND. TEMP .LE. 284.) GO TO 212
      IF (TEMP .GT. 284. .AND. TEMP .LE. 320.) GO TO 213
      IF (TEMP .GT. 320. .AND. TEMP .LE. 356.) GO TO 214
      IF (TEMP .GT. 356. .AND. TEMP .LE. 392.) GO TO 215
      IF (TEMP .GT. 392. .AND. TEMP .LE. 428.) GO TO 216
      IF (TEMP .GT. 428. .AND. TEMP .LE. 464.) GO TO 217
      IF (TEMP .GT. 464. .AND. TEMP .LE. 500.) GO TO 218
      IF (TEMP .GT. 500. .AND. TEMP .LE. 536.) GO TO 219
201   PRESS = 0.00049 + S1*(TEMP - 50.)
      DELT = 304.7/S1
      GO TO 220
202   PRESS = 0.002777 + S2*(TEMP -86.)
      DELT = 304.7/S2
      GO TO 220
203   PRESS = 0.006079 + S3*(TEMP -104.)
      DELT = 304.7/S3
      GO TO 220
204   PRESS = 0.01267 + S4*(TEMP - 122.)
      DELT = 304.7/S4
      GO TO 220
205   PRESS = 0.02524 + S5*(TEMP - 140.)
      DELT = 304.7/S5
      GO TO 220
206   PRESS = 0.04825 + S6*(TEMP - 158.)
      DELT = 304.7/S6
      GO TO 220
207   PRESS = 0.08880 + S7*(TEMP - 176.)
      DELT = 304.7/S7
      GO TO 220
208   PRESS = 0.1582 + S8*(TEMP - 194.)
      DELT = 304.7/S8
      GO TO 220
```

```
209   PRESS = 0.2729 + S9*(TEMP - 212.)
      DELT = 304.7/S9
      GO TO 220
210   PRESS = 0.4572 + S10*(TEMP - 230.)
      DELT = 304.7/S10
      GO TO 220
211   PRESS = 0.7457 + S11*(TEMP - 248.)
      DELT = 304.7/S11
      GO TO 220
212   PRESS = 1.186 + S12*(TEMP - 266.)
      DELT = 304.7/S12
      GO TO 220
213   PRESS = 1.845 + S13*(TEMP - 284.)
      DELT = 304.7/S13
      GO TO 220
214   PRESS = 4.189 + S14*(TEMP - 320.)
      DELT = 304.7/S14
      GO TO 220
215   PRESS = 8.796 + S15*(TEMP - 356.)
      DELT = 304.7/S15
      GO TO 220
216   PRESS = 17.287 + S16*(TEMP - 392.)
      DELT = 304.7/S16
      GO TO 220
217   PRESS = 32.133 + S17*(TEMP - 428.)
      DELT = 304.7/S17
      GO TO 220
218   PRESS = 56.855 + S18*(TEMP - 464.)
      DELT = 304.7/S18
      GO TO 220
219   PRESS = 96.296 + S19*(TEMP - 500.)
      DELT = 304.7/S19
      GO TO 220
220   DENV = (PRESS*2.78)/(7.73*(TEMP + 460.))
      GO TO 30
30    EKIN = VT**2./64.4
      B = (DENL*CP*DELT)/(DENV*HFG)
      BPRIME = B*EKIN
      PRINT 301
      PRINT 302, DELT,HFG,DENV,B,BPRIME
      GO TO 50
40    PRINT 401
      GO TO 50
50    RETURN
301   FORMAT (1H1,11X,19HRESULTS FROM THERM.)
302   FORMAT (1H0,10X,30HDELTA T PER UNIT DELTA HEAD = E11.4,9H DEG F/FT
     1/
     21H ,10X,23HHEAT OF VAPORIZATION = F7.2,7H BTU/LB/
     31H ,10X,16HVAPOR DENSITY = E11.4,9H LB/CU FT/
     41H ,10X,19HTHERMO PARAMETER = E11.4,7H PER FT/
     51H ,10X,23HTHERMODYNAMIC NUMBER = E11.4)
401   FORMAT (1H0,10X,26HTEMPERATURE LIMIT EXCEEDED)
      END
```

```
      SUBROUTINE PRDTL (TEMP,IFL)
      GO TO (10,20), IFL
10    IF (TEMP .GT. 32. .AND. TEMP .LT. 130.) CK = 0.3263 + 5.02*(10.**-
     14.)*(TEMP - 32.)
      IF (TEMP .GE. 130. .AND. TEMP .LT. 212.) CK = 0.3755 + 1.987*(10.*
     1*-4.)*(TEMP - 130.)
      IF (TEMP .GE. 212.) GO TO 50
      IF (TEMP .GT. 32. .AND. TEMP .LT. 95.) VISLN = 2.485 - 0.01485*(TE
     1MP - 32.)
      IF (TEMP .GE. 95. .AND. TEMP .LT. 176.) VISLN = 1.549 - 0.00960*(T
     1EMP - 95.)
      IF (TEMP .GT. 176.) GO TO 50
      VIS = EXP(VISLN)*(0.36)
      IF (TEMP .GT. 40. .AND. TEMP .LT. 68.) CP = 1.002625 - 1.357*(0.00
     101)*(TEMP - 40.)
      IF (TEMP .GE. 68. .AND. TEMP .LT. 86.) CP = 0.99883 - 0.3682*(0.00
     101)*(TEMP - 68.)
      IF (TEMP .GE. 86. .AND. TEMP .LT. 106.) CP = 0.9980
      IF (TEMP .GE. 106. .AND. TEMP .LT. 140.) CP = 0.99800 + 4.206*(0.0
     1001)*(TEMP - 106.)
      IF (TEMP .GE. 140. .AND. TEMP .LT. 176.) CP = 0.99943 + 7.526*(0.0
     10001)*(TEMP - 140.)
      IF (TEMP .GE. 176.) GO TO 50
      GO TO 30
20    IF (TEMP .GT. 600.) GO TO 50
      IF (TEMP .GE. 32. .AND. TEMP .LT. 176.) CP = 0.033382 - 3.366*(10.
     1**-6.)*(TEMP - 32.)
      IF (TEMP .GE. 176. .AND. TEMP .LT. 298.) CP = 0.032877 - 2.4*(10.*
     1*-6.)*(TEMP - 176.)
      IF (TEMP .GE. 298. .AND. TEMP .LT. 430.) CP = 0.03255 - 1.4*(10.**
     1-6.)*(TEMP - 298.)
      IF (TEMP .GE. 430. .AND. TEMP .LT. 514.) CP = 0.03238 - 0.6756*(10
     1.**-6.)*(TEMP - 430.)
      IF (TEMP .GE. 514. .AND. TEMP .LT. 600.) CP = 0.03233
      IF (TEMP .GE. 30. .AND. TEMP .LT. 600.) CK = 4.875 + 0.00357*(TEMP
     1 - 30.)
210   IF (TEMP .GT. 32. .AND. TEMP .LT. 86.) VIS = (11.320 - 0.02296*(TE
     1MP - 32.))*(0.36)
      IF (TEMP .GE. 86. .AND. TEMP .LT. 156.) VIS = (10.08 - 0.01614*(TE
     1MP - 86.))*(0.36)
      IF (TEMP .GE. 156. .AND. TEMP .LT. 300.) VIS = (8.95 - 0.01198*(TE
     1MP - 156.))*(0.36)
      IF (TEMP .GE. 300. .AND. TEMP .LT. 400.) VIS = 2.76 - 0.0024*(TEMP
     1 - 300.)
      IF (TEMP .GE. 400. .AND. TEMP .LT. 500.) VIS = 2.52 - 0.0020*(TEMP
     1 - 400.)
      IF (TEMP .GE. 500. .AND. TEMP .LT. 600.) VIS = 2.32 - 0.0014*(TEMP
     1 - 500.)
      GO TO 30
30    SIG = (VIS*CP)/CK
      PRINT 301
      PRINT 302, CK,CP,SIG
      GO TO 60
50    PRINT 501
      GO TO 60
60    RETURN
301   FORMAT (1H //,11X,19HRESULTS FROM PRDTL.)
```

```
302   FORMAT (1H0,10X,23HTHERMAL CONDUCTIVITY = E11.4,16H BTU/FT/HR/DEG.
     1F/
     21H ,10X,16HHEAT CAPACITY = E11.4,13H BTU/LB/DEG.F/
     31H ,10X,17HPRANDTL NUMBER = E11.4)
501   FORMAT (1H0,10X,26HTEMPERATURE LIMIT EXCEEDED)
      END


      SUBROUTINE GASFAC (TEMP,CONC,VT,IFL,NGAS)
      GAS = CONC
      VEL = VT
      GO TO (118,119),IFL
118   IF(TEMP .GT. 50. .AND. TEMP .LE. 100.) BETA = 0.807 + 0.00895*(TEM
     1P - 50.)
      IF (TEMP .GT. 100. .AND. TEMP .LE. 142.) BETA = 1.254 + 0.00558*(T
     1EMP - 100.)
      DEN = 1.0409*(1./TEMP**0.01089)*62.3689
      ALPHA = GAS*8.076
      GO TO 120
 119  GO TO (1191,1192,1193),NGAS
 1191 ALPHA = GAS*6.618
      GO TO 1194
 1192 ALPHA = GAS*6.582
      GO TO 1194
 1193 ALPHA = GAS*6.680
      GO TO 1194
 1194 BETA = 0.001934
      DEN = (13.5708 - 0.001448*(TEMP - 50.))*62.3689
      GO TO 120
 120  EKIN = (VEL**2.)/64.4
      FAC = (ALPHA*BETA*144.)/DEN
      AIR = FAC/EKIN
      PRINT 121, AIR
      RETURN
121   FORMAT (1H //,11X,20HRESULTS FROM GASFAC./
     11H0,10X,31HTHE GAS CONCENTRATION FACTOR = E11.4)
      END


      SUBROUTINE POSHD (CAVN,STD,VT)
      ENKIN = (VT**2.)/64.4
      SHNP = CAVN*ENKIN
      STDNP = STD*ENKIN
      PRINT 10
      PRINT 11, ENKIN,SHNP,STDNP
      RETURN
10    FORMAT (1H //,11X,19HRESULTS FROM POSHD.)
11    FORMAT (1H0,10X,15HKINETIC HEAD = E11.4,3H FT/
     11H ,10X,7HNPSH = E11.4,15H FT WITH DEV = E11.4,3H FT)
      END
```

PARAMETER CALCULATIONS DME THESIS

TEST FLUID IS MERCURY

NO TEST SPECIMEN RUNS, VISIBLE INITIATION

THE GAS IS ARGON AT 1.52 PERCENT BY VOLUME

TEMPERATURE = 97,000 F
NUMBER OF RUNS = 1
FLOW RATE = 1,250 IN. HG. OR 14.600 GPM
PUMP SPEED = 1185 RPM
VENTURI USED WAS 412
ORIGINAL DATA ON SHEET NO. 198753

THROAT DIAMETER = .5100 IN.

THROAT VELOCITY = 22,93 FT/SEC

CAVITATION NUMBER = .2954 STD. DEV. .0295

RESULTS FROM REYNO.

VISCOSITY = 9,9025E-04 LB/FT-SEC
DENSITY = 842.151 LB/CU FT
REYNOLDS NUMBER = 8,2878E+05

RESULTS FORM WEBNO.

SURFACE TENSION = 3,1765E-02 LB/FT
WEBER NO. BASED ON CONCENTRATION = 5,4451E+01
WEBER NO. 1 MIL DIAMETER = 3,5075E+01
WEBER NO. BASED ON VENTURI DIAMETER = 1,8398E+04

RESULTS FROM PRDTL.

THERMAL CONDUCTIVITY = 5,1142E+00 BTU/FT/HR/DEG.F
HEAT CAPACITY = 3,3163E-02 BTU/LB/DEG.F
PRANDTL NUMBER = 2,3117E-02

```
 RESULTS FROM THERM,

DELTA T PER UNIT DELTA HEAD =  1.6650E+06 DEG F/FT
HEAT OF VAPORIZATION =  128.30 BTU/LB
VAPOR DENSITY =  3.0928E-06 LB/CU FT
THERMO PARAMETER =  1.1720E+11 PER FT
THERMODYNAMIC NUMBER =  9.5682E+11

 RESULTS FROM TIME,

EXPOSURE TIME =  8.4333E-03 SEC
TAU =  8.4333E+10

RESULTS FROM GASFAC,

THE GAS CONCENTRATION FACTOR =  4.0524E-04

RESULTS FROM POSHD,

KINETIC HEAD =  8.1644E+00 FT
NPSH =  2.4118E+00 FT WITH DEV =  2.4085E-01 FT
```

APPENDIX G

REDUCED SCALE EFFECTS DATA

This appendix contains the data used in this analysis. These data sets were used as inputs to the regression analysis. This reduced data results from the treatment of the experimental data by the programs RAWDAT and CALPRM which are discussed in Appendixes E and F.

The data is presented in tabular form with the water data listed first followed by the mercury data. Two lines are required to present each set. The format is listed on each page and the abbreviations are defined below.

SET - An arbitrary set number assigned for bookkeeping purposes in the regression analysis. The first number indicates the venturi used, i.e., 4 is venturi 412, 7 is venturi 712, etc.

VOL - The volume percent at STP of the gas present in the test.

REY NUM - The Reynolds number based upon the throat diameter and flow rate.

WEB NUM 1 - The Weber number calculated with an "arbitrary" value for bubble diameter, based upon an assumed linear relation between gas content and bubble size.

WEB NUM 2 - The Weber number calculated by assuming a constant 1 mil bubble diameter.

WEB NUM 3 - The Weber number calculated by using the throat diameter as the characteristic length.

PR NUM - The calculated value of the Prandtl number for the fluid under consideration.

THERMO - This is the calculated value for the normalized thermodynamic parameter based on bulk fluid properties.

TIME - A normalized exposure time based upon the measured fluid velocity in the throat.

GAS NUM - A normalized parameter for gas content.

VEL - The fluid velocity in the venturi throat. Values all between 20 and 230 feet per second, therefore numbers here for mercury should be read with decimal point two places to right, i.e., .2293 = 22.93.

TEMP - Bulk fluid temperature at time cavitation was being observed, reported in °F.

LOSS COEF - The loss coefficient obtained from the Δ P measured acrpss the venturi. For a given size venturi this number should be approximately the same for all runs with a given degree of cavitation.

CAV NUM - The cavitation number determined by examination of the normalized pressure profile data in RAWDAT.

STD DEV - The standard deviation in the cavitation number for those sets where more than several observations have been averaged together.

NUM RUNS - The actual number of raw data runs (pressure profiles) incorporated in a given data set.

DATA PG - The actual page number in the permanent project record books on which the observed pressure profile data may be found.

REDUCED SCALE EFFECTS DATA

SET	VOL GASNUM	REYNUM VEL	WEBNUM2 TEMP	WEBNUM2 LOSSCOEF	WEBNUM3 CAVNUM	PRNUM STD DEV	THERM NUM RUNS	TIME DATA PG
	NO CAVITATION		WATER					
527	1.85	4.64E5	2.45E2	1.62E2	12.17E4	5.90	0.962E5	4.04E10
	0.491	70.44	81.40	0.2658	0.1011	0.0020	3.	198760
528	1.79	6.75E5	5.03E2	3.34E2	25.02E4	5.80	1.88E5	2.82E10
	0.233	100.94	82.40	0.2746	0.0893	0.0115	3.	198761
529	1.60	12.4E5	15.08E2	9.99E2	74.90E4	5.40	4.47E5	1.63E10
	0.0725	174.00	86.60	0.1506	0.0569	0.0006	1.	198763
530	1.60	12.99E5	16.05E2	10.93E2	81.98E4	5.40	4.88E5	1.56E10
	0.0663	182.30	86.80	0.2257	0.0588	0.0006	1.	198764
531	1.62	12.61E5	16.34E2	10.82E2	81.16E4	5.56	5.33E5	1.57E10
	0.0790	181.55	85.00	0.2240	0.0674	0.	2.	198764
441	2.60	1.92E5	2.41E2	1.33E2	6.77E4	9.47	7.97E5	2.99E10
	0.0620	64.71	52.51	0.2850	1.1021	0.0021	7.	197752
442	2.60	0.01E5	5.71E2	3.15E2	16.06E4	9.25	7.97E5	1.94E10
	0.266	99.57	53.90	0.2694	0.0706	0.0071	16.	197751
443	1.70	1.22E5	20.41E2	13.52E2	68.90E4	6.67	11.49E5	0.947E10
	0.0503	204.17	73.88	0.2011	0.0903	0.0009	1.	197759
444	1.70	8.97E5	22.73E2	15.06E2	76.80E4	6.41	11.42E5	0.899E10
	0.0463	215.16	76.33	0.2111	0.0681	0.0029	2.	197760
635	2.02	1.09E5	2.81E2	1.55E2	3.88E4	7.11	1.57E5	1.37E10
	0.501	69.28	70.00	0.1559	0.6206	0.0620	1.	187766
636	2.02	1.26E5	2.65E2	1.46E2	3.66E4	7.11	1.48E5	1.41E10
	0.531	67.32	70.00	0.1882	0.5834	0.0268	2.	198766
637	2.02	1.86E5	5.49E2	3.03E2	7.57E4	6.89	2.82E5	0.979E10
	0.262	98.73	71.90	0.2599	0.2404	0.0240	2.	198767
638	1.64	2.96E5	9.98E2	6.61E2	16.50E4	6.30	4.76E5	0.665E10
	0.103	142.00	77.40	0.2305	0.1223	0.0065	2.	198768
639	1.64	4.52E5	19.05E2	12.62E2	31.50E4	5.59	6.32E5	0.483E10
	0.0557	196.08	84.70	0.2145	0.0574	0.0002	2.	198769
827	2.19	0.653E5	3.34E2	1.85E2	2.31E4	7.79	2.81E5	3.625E10
	0.430	75.82	64.40	0.3563	0.4483	0.0299	2.	198774
828	2.26	0.937E5	6.69E2	3.69E2	4.62E4	7.76	4.70E5	0.442E10
	0.226	107.19	65.45	0.2752	0.1905	0.0141	2.	198776
829	1.96	1.42E5	10.7E2	7.09E2	8.86E4	6.88	6.57E5	0.320E10
	0.109	147.97	72.00	0.3110	0.0768	0.0142	2.	198777
830	1.78	2.14E5	20.3E2	13.4E2	16.77E4	6.17	9.13E5	0.234E10
	0.0556	202.87	78.60	0.2739	0.0516	0.0015	2.	198778

REDUCED SCALE EFFECTS DATA

SET	VOL GASNUM	REYNUM VEL	WEBNUM2 TEMP	WEBNUM2 LOSSCOEF	WEBNUM3 CAVNUM	PRNUM STD DEV	THERM NUM RUNS	TIME DATA PG
	CONDITION B		WATER					
55	2.09	[illegible]6E5	2.78E2	1.58E2	11.51E4	7.33	1.69E5	4.12E10
	0.514	68.[illegible]9	68.10	0.2828	0.0408	0.0055	2.	198779
56	1.85	[illegible].63E5	2.45E2	1.62E2	12.16E4	5.91	0.971E5	4.04E10
	0.490	70.44	81.70	0.2668	0.0202	0.0057	3.	198760
57	0.88	3.33E5	0.909E2	1.51E2	11.30E4	8.37	2.87E5	4.14E10
	0.202	6[illegible].63	60.00	0.2854	0.0338	0.0000	2.	198782
58	1.73	6.[illegible]5E5	5.04E2	3.34E2	25.01E4	5.80	1.88E5	2.82E10
	0.225	10[illegible].94	82.40	0.2525	0.0307	0.0022	3.	198761
59	0.88	5.04E5	1.99E2	3.31E2	24.80E4	8.17	5.86E5	2.80E10
	0.0935	101.67	61.50	0.2565	0.0377	0.0014	2.	198782
510	1.74	8.[illegible]5E5	5.15E2	3.41E2	25.90E4	4.37	0.685E5	2.82E10
	0.263	10[illegible].94	102.00	0.2251	0.0635	0.0086	3.	198780
511	1.60	12.4E5	1.51E2	9.99E2	74.95E4	5.40	4.47E5	1.63E10
	0.0725	174.29	86.80	0.1481	0.0125	0.0013	1.	198763
512	1.92	12.6E5	16.34E2	10.82E2	81.20E4	5.56	5.33E5	1.57E10
	0.0790	181.55	85.00	0.2252	0.0278	0.0042	3.	198764
513	1.85	4.65E5	2.45E2	1.62E2	12.2E4	5.90	0.962E5	4.04E10
	0.191	7[illegible].44	81.40	0.2763	0.0075	0.0005	3.	198760
514	1.4[illegible]	6.16E5	1.97E2	1.63E2	12.2E4	4.33	0.311E5	4.08E10
	0.466	6[illegible].72	103.00	0.2380	0.0288	0.0008	2.	198780
41	2.4[illegible]	1.94E5	2.41E2	1.33E2	.678E5	9.34	3.45E5	2.98E10
	0.577	6.471	53.35	0.2898	0.1292	0.0038	3.	197754
42	1.23	1.89E5	1.53E2	1.27E2	.646E5	9.35	3.29E5	3.06E10
	0.311	6.314	53.30	0.2794	0.0679	0.0001	3.	197772
43	0.89	1.95E5	0.788E2	1.31E2	.666E5	9.17	3.22E5	3.02E10
	0.221	6.408	54.46	0.2701	0.0567	0.0026	3.	197762
44	1.61	3.77E5	2.03E2	1.35E2	.686E5	4.39	0.274E5	3.05E10
	0.614	6.314	101.77	0.2387	0.0917	0.0015	3.	197766
45	0.[illegible]0	3.53E5	0.799E2	1.32E2	.675E5	4.71	0.370E5	3.06E10
	0.258	6.314	95.23	0.2322	0.0908	0.0015	3.	197767
46	1.63	4.65E5	2.09E2	1.39E2	.709E5	3.49	0.0551E5	3.04E10
	0.675	6.361	123.39	0.2357	0.0773	0.0092	3.	197764
47	2.38	3.07E5	5.85E2	3.23E2	1.65E5	9.04	7.48E5	1.94E10
	0.247	9.957	55.35	0.2483	0.0597	0.0009	3.	197756
48	2.37	3.06E5	5.71E2	3.15E2	1.61E5	9.08	7.58E5	1.94E10
	0.2[illegible]5	9.9[illegible]7	55.06	0.2458	0.0588	0.0009	3.	197757

REDUCED SCALE EFFECTS DATA

SET	VOL GASNUM	REYNUM VEL	WEBNUM2 TEMP	WEBNUM2 LOSSCOEF	WEBNUM3 CAVNUM	PRNUM STD DEV	THERM NUM RUNS	TIME DATA PG
	CONDITION B		WATER					
55	2.09	[illegible]76E5	2.78E2	1.58E2	11.51E4	7.33	1.69E5	4.12E10
	0.514	68.[illegible]9	68.10	0.2828	0.0408	0.0055	2.	198779
56	1.85	[illegible].63E5	2.45E2	1.62E2	12.16E4	5.91	0.971E5	4.04E10
	0.490	70.44	81.70	0.2668	0.0202	0.0057	3.	198760
57	0.88	3.33E5	0.909E2	1.51E2	11.30E4	8.37	2.87E5	4.14E10
	0.202	60.63	60.00	0.2854	0.0338	0.0000	2.	198782
58	1.73	6.[illegible]5E5	5.04E2	3.34E2	25.01E4	5.80	1.88E5	2.82E10
	0.225	10[illegible].94	82.40	0.2525	0.0307	0.0022	3.	198761
59	0.88	5.04E5	1.99E2	3.31E2	24.80E4	8.17	5.86E5	2.80E10
	0.0935	101.67	61.50	0.2565	0.0377	0.0014	2.	198782
510	1.74	8.[illegible]5E5	5.15E2	3.41E2	25.90E4	4.37	0.685E5	2.82E10
	0.262	10[illegible].94	102.00	0.2251	0.0635	0.0086	3.	198780
511	1.60	12.4E5	1.51E2	9.99E2	74.95E4	5.40	4.47E5	1.63E10
	0.0725	174.29	86.80	0.1481	0.0125	0.0013	1.	198763
512	1.92	12.6E5	16.34E2	10.82E2	81.20E4	5.56	5.33E5	1.57E10
	0.0790	181.55	85.00	0.2252	0.0278	0.0042	3.	198764
513	1.85	4.65E5	2.45E2	1.62E2	12.2E4	5.90	0.962E5	4.04E10
	0.191	7[illegible].44	81.40	0.2763	0.0075	0.0005	3.	198760
514	1.4[illegible]	6.16E5	1.97E2	1.63E2	12.2E4	4.33	0.311E5	4.08E10
	0.466	6[illegible].72	103.00	0.2380	0.0288	0.0008	2.	198780
41	2.40	1.94E5	2.41E2	1.33E2	.678E5	9.34	3.45E5	2.98E10
	0.577	6.471	53.35	0.2898	0.1292	0.0038	3.	197754
42	1.23	1.89E5	1.53E2	1.27E2	.646E5	9.35	3.29E5	3.06E10
	0.311	6.314	53.30	0.2794	0.0679	0.0001	3.	197772
43	0.89	1.95E5	0.788E2	1.31E2	.666E5	9.17	3.22E5	3.02E10
	0.221	6.408	54.46	0.2701	0.0567	0.0026	3.	197762
44	1.61	3.77E5	2.03E2	1.35E2	.686E5	4.39	0.274E5	3.05E10
	0.614	6.314	101.77	0.2387	0.0917	0.0015	3.	197766
45	0.[illegible]5	3.53E5	0.799E2	1.32E2	.675E5	4.71	0.370E5	3.06E10
	0.258	6.314	95.23	0.2322	0.0908	0.0015	3.	197767
46	1.63	4.65E5	2.09E2	1.39E2	.709E5	3.49	0.0551E5	3.04E10
	0.678	6.361	123.39	0.2357	0.0773	0.0092	3.	197764
47	2.38	3.07E5	5.85E2	3.23E2	1.65E5	9.04	7.48E5	1.94E10
	0.247	9.957	55.35	0.2483	0.0597	0.0009	3.	197756
48	2.37	3.06E5	5.71E2	3.15E2	1.61E5	9.08	7.58E5	1.94E10
	0.2[illegible]5	9.957	55.06	0.2458	0.0588	0.0009	3.	197757

4S	1.40	1.04E5	3.81E2	3.15E2	1.61E5	9.04	7.72E5	1.94E10
	0.144	9.957	54.66	0.2643	0.0496	0.0015	3.	197758
410	0.68	3.08E5	1.92E2	3.22E2	1.64E5	9.09	7.75E5	1.92E10
	0.069	10.056	54.99	0.2572	0.0375	0.0065	3.	197761
411	1.90	5.05E5	5.11E2	3.39E2	1.73E5	4.42	0.716E5	1.92E10
	0.286	10.067	100.99	0.2248	0.0403	0.0009	3.	197766
412	0.70	5.72E5	2.04E2	3.37E2	1.72E5	4.62	0.866E5	1.92E10
	0.103	10.067	97.00	0.2173	0.0406	0.0013	3.	197767
413	1.58	7.09E5	5.25E2	3.48E2	1.77E5	3.41	0.127E5	1.92E10
	0.265	10.051	125.53	0.2136	0.0267	0.0025	3.	197762
414	1.51	7.33E5	5.08E2	3.37E2	1.72E5	3.43	0.126E5	1.95E10
	0.261	9.894	124.92	0.2384	0.0354	0.0111	1.	197777
415	1.70	9.04E5	23.2E2	15.4E2	7.84E5	6.43	11.8E5	0.889E10
	0.0452	21.752	76.13	0.2099	0.0418	0.0116	3.	197750
417	0.90	9.83E5	9.94E2	16.5E2	8.39E5	6.06	13.6E5	0.861E10
	0.0232	22.459	79.70	0.1937	0.0433	0.0049	3.	197775
419	1.63	13.8E5	24.7E2	16.4E2	8.36E5	4.15	2.57E5	0.876E10
	0.0525	22.066	106.75	0.1986	0.0212	0.0017	3.	197768
420	0.90	14.0E5	10.4E2	17.2E2	8.77E5	4.18	2.80E5	0.855E10
	0.0275	22.616	106.10	0.1759	0.0522	0.0052	1.	197776
421	1.73	17.9E5	24.9E2	16.5E2	8.43E5	3.06	0.393E5	0.889E10
	0.0647	21.752	136.00	0.2054	0.0151	0.0079	3.	197774
422	1.21	17.5E5	20.9E2	12.4E2	8.86E5	3.23	0.514E5	0.864E10
	0.0419	22.380	130.75	0.1862	0.0439	0.0043	2.	197777
64	2.02	1.29E5	2.81E2	1.55E2	3.88E4	7.11	1.57E5	1.37E10
	0.501	69.28	70.00	0.2026	0.0315	0.0032	1.	198766
65	2.02	1.25E5	2.65E2	1.46E2	3.66E4	7.11	1.48E5	1.41E10
	0.531	67.32	70.30	0.1890	0.0321	0.0001	3.	198766
66	1.61	1.25E5	2.17E2	1.44E2	3.59E4	7.08	1.44E5	1.42E10
	0.432	66.67	70.20	0.1885	0.0157	0.0000	2.	198771
67	1.05	1.26E5	1.77E2	1.46E2	3.66E4	7.12	1.49E5	1.41E10
	0.276	67.32	69.90	0.1832	0.0138	0.0008	2.	198772
68	0.92	1.12E5	0.909E2	1.51E2	3.77E4	8.28	2.78E5	1.38E10
	0.213	68.63	60.70	0.1681	0.0310	0.0031	1.	198784
69	0.80	1.12E5	0.909E2	1.51E2	3.77E4	8.32	2.82E5	1.38E10
	0.203	68.63	60.40	0.1729	0.0314	0.0008	2.	198784
610	0.74	1.24E5	2.67E2	1.43E2	3.59E4	7.08	1.44E5	1.42E10
	0.198	66.67	70.20	0.1919	0.0107	0.0011	1.	198771
611	2.11	1.93E5	2.89E2	1.59E2	3.99E4	4.61	0.406E5	1.37E10
	0.655	69.28	97.20	0.2362	0.0164	0.0016	2.	198783
612	2.02	1.86E5	5.49E2	3.03E2	7.57E4	6.89	2.82E5	0.979E10
	0.262	96.73	71.90	0.2634	0.0114	0.0004	3.	198767
613	1.69	1.54E5	0.675E2	2.83E2	7.08E4	8.28	5.22E5	0.979E10
	0.207	94.12	60.70	0.1889	0.0163	0.0004	2.	198783
614	1.64	2.25E5	4.69E2	3.11E2	7.78E4	5.59	1.56E5	1.01E10
	0.234	97.39	84.70	0.2561	0.0098	0.0010	1.	198770

615	1.40	1.60E5	3.67E2	3.04E2	7.59E4	8.22	5.49E5	0.973E10
	0.161	97.39	61.10	0.1827	0.0154	0.0015	1.	198783
616	1.05	1.86E5	3.66E2	3.03E2	7.57E4	6.88	2.81E5	0.979E10
	0.136	96.73	72.00	0.1048	0.0071	0.0004	2.	198772
617	0.95	1.56E5	1.71E2	2.84E2	7.09E4	8.14	4.97E5	1.00E10
	0.118	94.12	61.70	0.1931	0.0155	0.0000	2.	198783
618	2.15	2.76E5	5.66E2	3.12E2	7.81E4	4.50	0.710E5	0.979E10
	0.345	96.73	99.50	0.2448	0.0074	0.0000	2.	198783
619	1.64	2.96E5	9.97E2	6.61E2	16.50E4	6.30	4.76E5	0.665E10
	0.103	142.28	77.40	0.2312	0.0064	0.0002	3.	198768
620	1.64	2.96E5	9.98E2	6.61E2	16.50E4	6.30	4.76E5	0.665E10
	0.103	142.28	77.40	0.2324	0.0051	0.0004	2.	198768
621	1.05	2.87E5	7.96E2	6.59E2	16.50E4	6.51	5.22E5	0.665E10
	0.0647	142.28	75.40	0.2434	0.0035	0.0004	2.	198772
622	1.64	4.52E5	19.04E2	12.62E2	31.50E4	5.59	6.32E5	0.483E10
	0.0577	196.08	84.70	0.2171	0.0024	0.0001	3.	198769
623	1.64	4.52E5	19.04E2	12.62E2	31.50E4	5.59	6.32E5	0.483E10
	0.0577	196.08	84.70	0.2164	0.0024	0.0001	3.	198769
624	1.05	4.35E5	15.19E2	12.58E2	31.50E4	5.83	7.20E5	0.483E10
	0.0362	196.08	82.10	0.2202	0.0013	0.0001	1.	198772
625	0.91	3.76E5	7.18E2	11.89E2	29.70E4	6.71	10.30E5	0.495E10
	0.0305	191.50	73.50	0.2347	0.0033	0.0000	2.	198784
81	2.19	0.653E5	3.34E2	1.85E2	2.31E4	7.79	2.81E5	0.625E10
	0.430	75.82	64.40	0.3628	0.0166	0.0026	2.	198774
82	2.28	0.937E5	6.69E2	3.69E2	4.62E4	7.66	4.70E5	0.442E10
	0.226	107.19	65.45	0.2781	0.0862	0.0120	4.	198775
83	2.19	0.653E5	3.34E2	1.85E2	2.33E4	7.79	2.81E5	0.625E10
	0.430	75.82	64.40	0.3602	0.0179	0.0026	2.	198774
84	1.96	0.728E5	2.81E2	1.86E2	2.33E4	6.88	1.72E5	0.625E10
	0.414	75.82	72.00	0.3645	0.0369	0.0004	1.	198777
85	0.88	0.627E5	1.11E2	1.84E2	2.30E7	8.17	3.26E5	0.625E10
	0.168	75.82	61.50	0.3873	0.0254	0.0000	2.	198786
86	2.09	1.20E5	3.99E2	2.20E2	2.75E4	4.33	0.421E5	0.585E10
	0.491	81.05	103.00	0.4014	0.0493	0.0063	2.	198785
87	2.28	0.937E5	6.69E2	3.69E2	4.62E4	7.66	4.70E5	0.442E10
	0.226	107.19	65.90	0.2804	0.0483	0.0128	4.	198776
88	1.95	1.03E5	5.61E2	3.72E2	4.65E4	6.88	3.44E5	3.442E10
	0.207	107.19	72.00	0.2761	0.0588	0.0006	1.	198777
89	1.21	0.857E5	4.22E2	3.50E2	4.37E4	8.24	7.31E5	0.453E10
	0.121	104.57	61.10	0.2951	0.0411	0.0024	2.	198785
810	0.93	0.872E5	2.16E2	3.50E2	4.38E4	8.08	5.98E5	0.453E10
	0.0940	104.57	62.20	0.2957	0.0345	0.0003	1.	198785
811	0.90	0.873E5	2.16E2	3.05E2	4.38E4	8.08	5.98E5	0.453E10
	0.0909	104.57	62.20	0.3074	0.0263	0.0014	2.	198786
812	1.20	1.12E5	6.63E2	3.66E2	4.57E4	4.37	0.734E5	0.453E10
	0.309	104.57	102.00	0.3922	0.0355	0.0038	2.	198785

813	1.96	1.42E5	10.7E2	7.09E2	8.86E4	6.88	6.57E5	0.320E10
	0.102	147.97	72.00	0.3110	0.0396	0.0012	2.	198777
814	1.76	2.14E5	20.3E2	13.4E2	16.77E4	6.17	9.13E5	0.234E10
	0.0556	202.87	78.60	0.2666	0.0184	0.0014	2.	198778
815	1.33	1.87E5	14.3E2	11.8E2	14.80E4	6.71	10.2E5	0.248E10
	0.0449	190.85	73.50	0.3140	0.0176	0.0001	2.	198786

REDUCED SCALE EFFECTS DATA

SET	VOL GASNUM	RE NUM VEL	WEBNUM2 TEMP	WEBNUM2 LOSSCOEF	WEBNUM3 CAVNUM	PRNUM STD DEV	THERM NUM RUNS	TIME DATA PG
	CONDITION C		WATER					
515	1.79	6.75E5	5.04E2	3.34E2	25.0E4	5.80	1.88E5	2.82E10
	0.233	100.94	82.40	0.2550	0.0079	0.0018	3.	198761
516	1.74	8.85E5	5.15E2	3.41E2	25.6E4	4.37	0.433E5	2.82E10
	0.262	100.94	102.00	0.2293	0.0308	0.0031	2.	198780
517	1.60	12.4E5	15.08E2	9.99E2	74.95E4	5.40	4.46E5	1.63E10
	0.0725	174.29	86.80	0.1506	0.0034	0.0003	1.	198763
518	1.60	12.99E5	16.50E2	10.93E2	81.98E4	5.40	4.88E5	1.56E10
	0.0663	182.28	86.80	0.2279	0.0058	0.0006	1.	198763
519	1.92	12.61E5	16.34E2	10.82E2	81.16E4	5.56	5.33E5	1.57E10
	0.0790	181.55	85.00	0.2286	0.0083	0.0008	2.	198764
520	1.47	18.90E5	13.46E2	11.15E2	83.60E4	3.57	0.485E5	1.58E10
	0.0752	180.10	121.00	0.1949	0.0491	0.0050	1.	197781

REDUCED SCALE EFFECTS DATA

SET	VOL GASNUM	REYNUM VEL	WEBNUM2 TEMP	WEBNUM2 LOSSCOEF	WEBNUM3 CAVNUM	PRNUM STD DEV	THERM NUM RUNS	TIME DATA PG
	CONDITION D		WATER					
521	1.85	4.65E5	2.45E2	1.62E2	12.17E4	5.90	0.962E5	4.04E10
	0.491	70.44	81.40	0.3170	0.0060	0.0010	3.	197760
522	1.79	6.75E5	5.04E2	3.34E2	25.01E4	5.80	1.88E5	2.82E10
	0.233	100.94	82.40	0.3015	0.0069	0.0009	3.	198761
523	0.86	7.22E5	2.05E2	3.39E2	25.50E4	5.43	1.55E5	2.80E10
	0.117	101.67	61.50	0.3093	0.0132	0.0013	1.	198782
531	1.60	12.99E5	16.49E2	10.93E2	81.98E4	5.40	4.89E5	1.56E10
	0.0663	182.28	86.80	0.2708	0.0033	0.0003	1.	198763
423	2.60	1.94E5	2.41E2	1.33E2	6.78E4	9.32	3.43E5	2.99E10
	0.627	64.71	54.48	0.3158	0.0918	0.0098	3.	197755
424	1.63	4.21E5	2.07E2	1.37E2	6.99E4	3.89	0.151E5	3.04E10
	0.669	63.61	113.06	0.2788	0.0322	0.0018	3.	197764
425	2.37	3.07E5	5.72E2	3.16E2	16.1E4	9.04	7.48E5	1.94E10
	0.246	99.57	55.35	0.2878	0.0541	0.0013	3.	197756
426	2.37	3.06E5	5.71E2	3.15E2	16.1E4	9.08	7.58E5	1.94E10
	0.246	99.57	55.06	0.2910	0.0528	0.0009	3.	197757
427	0.68	2.11E5	1.94E2	3.22E2	16.4E4	9.04	7.63E5	1.92E10
	0.0693	100.56	55.36	0.2991	0.0319	0.0096	3.	197761
428	1.55	7.34E5	5.26E2	3.48E2	17.8E4	3.50	0.139E5	1.92E10
	0.257	100.75	123.10	0.2577	0.0144	0.0011	4.	197762
430	1.70	8.86E5	21.60E2	14.31E2	72.9E4	6.31	10.38E5	0.922E10
	0.0492	206.67	77.27	0.2760	0.0152	0.0025	3.	197760
431	1.73	18.20E5	23.86E2	15.81E2	80.6E4	2.90	0.307E5	0.912E10
	0.0693	212.02	140.30	0.2532	-0.0080	0.0008	1.	197774
626	2.02	1.27E5	2.65E2	1.47E2	3.66E4	7.11	1.43E5	1.41E10
	0.535	67.32	70.80	0.2311	0.0167	0.0008	2.	198765
627	0.83	1.12E5	0.909E2	1.51E2	3.77E4	8.32	2.81E5	1.38E10
	0.203	68.63	60.40	0.2220	0.0290	0.0029	1.	198784
628	2.02	1.85E5	5.47E2	3.03E2	7.57E4	6.89	2.82E5	0.979E10
	0.262	96.73	71.90	0.3095	0.0097	0.0004	2.	199767
629	0.90	1.61E5	1.83E2	3.03E2	7.59E4	8.17	5.38E5	0.973E10
	0.104	97.39	61.50	0.2048	0.0150	0.0015	1.	198784
630	2.15	2.82E5	5.87E2	3.25E2	8.12E4	4.49	0.739E5	0.961E10
	0.335	98.69	99.50	0.2714	0.0071	0.0000	2.	198783
631	1.64	4.52E5	19.05E2	12.62E2	31.50E4	5.59	6.32E5	0.483E10
	0.0577	196.08	84.70	0.2759	0.0022	0.0000	2.	198769

816	2.19	0.653E5	3.34E2	1.85E2	2.31E4	7.79	2.81E5	0.625E10
	0.430	75.82	64.40	0.4304	0.0127	0.0013	2.	198774
817	0.28	0.627E5	1.11E2	1.84E2	2.30E4	8.17	3.26E5	0.625E10
	0.168	75.82	61.50	0.3821	0.0241	0.0024	1.	198786
818	2.09	1.200E5	3.99E2	2.20E2	2.75E4	4.33	0.421E5	0.585E10
	0.491	81.05	103.00	0.4460	0.0144	0.0014	1.	198785
819	2.28	0.937E5	6.69E2	3.69E2	4.62E4	7.66	4.70E5	0.442E10
	0.226	107.19	65.45	0.2910	0.0106	0.0005	3.	198776
820	0.90	0.873E5	2.11E2	3.50E2	4.38E4	8.08	5.99E5	0.453E10
	0.090	104.57	62.20	0.3211	0.0119	0.0012	1.	198786
821	2.20	1.530E5	15.90E2	13.10E2	16.40E4	4.37	0.736E5	0.453E10
	0.309	104.57	102.00	0.4437	0.0105	0.0010	1.	198785
822	1.78	2.18E5	20.30E2	13.40E2	16.79E4	6.06	6.67E5	0.235E10
	0.0561	202.87	79.70	0.3012	0.0053	0.0003	2.	198788
823	1.33	1.878E5	14.30E2	11.80E2	14.80E4	6.71	10.2E5	0.248E10
	0.0449	190.85	73.50	0.3522	0.0064	0.0006	1.	198786

REDUCED SCALE EFFECTS DATA

SET	VOL GASNUM	REYNUM VEL	WEBNUM2 TEMP	WEBNUM2 LOSSCOEF	WEBNUM3 CAVNUM	PRNUM STD DEV	THERM NUM RUNS	TIME DATA PG
	CONDITION F		WATER					
524	1.85	4.50E5	2.30E2	1.52E2	11.43E4	5.89	0.914E5	4.17E10
	0.522	68.26	81.40	0.5467	0.0080	0.0011	2.	198760
525	1.79	6.75E5	5.03E2	3.34E2	25.02E4	5.80	1.88E5	2.82E10
	0.233	100.94	82.40	0.3971	0.0068	0.0011	2.	198761
526	1.60	12.99E5	16.49E2	10.93E2	81.98E4	5.40	4.88E5	1.56E10
	0.0663	182.28	86.80	0.3566	0.0031	0.0003	1.	198763
432	2.60	1.94E5	2.41E2	1.33E2	6.78E4	9.32	3.43E5	2.98E10
	0.627	64.71	53.48	0.3959	0.0762	0.0062	3.	197755
433	1.63	3.97E5	2.06E2	1.36E2	6.94E4	4.15	0.214E5	3.04E10
	0.632	63.61	106.73	0.4953	0.0207	0.0023	3.	197764
434	2.37	3.07E5	5.71E2	3.16E2	16.1E4	9.04	7.48E5	1.94E10
	0.246	99.57	55.35	0.3481	0.0449	0.0001	3.	197756
435	2.37	3.06E5	5.71E2	3.15E2	16.1E4	9.08	7.58E5	1.94E10
	0.246	99.57	55.06	0.3462	0.0451	0.0012	3.	197757
436	0.68	3.11E5	1.94E2	3.22E2	16.4E4	9.01	7.57E5	1.92E10
	0.0694	100.56	55.54	0.3748	0.0273	0.0081	3.	197761
437	1.54	7.03E5	5.24E2	3.47E2	17.7E4	3.67	0.166E5	1.92E10
	0.250	100.83	118.48	0.3478	0.0093	0.0002	3.	197763
439	1.70	8.31E5	09.09E2	12.64E2	64.5E4	6.33	9.25E5	0.981E10
	0.0555	197.10	77.08	0.3412	0.0099	0.0034	3.	197760
440	1.73	15.9E5	09.98E2	13.24E2	67.5E4	3.09	0.328E5	0.993E10
	0.0804	194.75	135.00	0.3437	0.0035	0.0004	1.	197774
632	2.02	1.27E5	2.65E2	1.47E2	3.66E4	7.01	1.43E5	1.41E10
	0.535	67.32	70.80	0.3467	0.0142	0.0014	1.	198765
633	2.02	1.85E5	5.47E2	3.02E2	7.57E4	6.89	2.82E5	0.979E10
	0.262	96.73	71.90	0.3919	0.0101	0.0010	1.	198767
634	1.64	4.52E5	19.05E2	12.62E2	31.50E4	5.59	6.32E5	0.483E10
	0.057	196.08	84.70	0.3627	0.0022	0.0002	1.	198769
824	2.19	0.653E5	3.34E2	1.85E2	2.31E4	7.79	2.81E5	0.625E10
	0.430	75.82	64.40	0.4889	0.0153	0.0013	2.	198774
825	2.28	0.937E5	6.69E2	3.69E2	4.62E4	7.66	4.70E5	0.442E10
	0.226	107.19	65.45	0.4008	0.0110	0.0014	3.	198776
826	1.78	1.27E5	20.30E2	13.50E2	16.85E4	5.78	7.52E5	0.234E10
	0.0575	202.87	72.90	0.3596	0.0048	0.0002	2.	198778

APPENDIX H

COMPUTER REGRESSION ANALYSIS PROGRAM

The regression analysis program used to analyze the data for this study was developed by Westervelt[54] and has been in continuous use at the University of Michigan for about 6 years[55]. This program was adapted to the CDC-1604/6600 facilities of the Air Force Weapons Laboratory by the author and Marie T. Smith, mathematician with the Laboratory. The program is long and complex so it is not reproduced here in its entirety. However, the following general characteristics and unique operational features are presented to clarify the predictions with respect to scale effects data which are discussed in Chapter V and Appendix I.

The regression program accepts as input experimental observations and based upon them determines a predicting equation for some dependent variable. The program can handle as many as 59 independent variables against one dependent variable, and it is structured so that terms consisting of both positive and negative integer powers (and their reciprocals) as well as cross products of the independent variables may be considered. Thus, fits of an independent variable Y are tried against terms of the form, $x(1)$; $x(2)^n$; $x(1)^n x(3)^n$, and so on. Because of the tremendous number of possible terms if the full capacity of the program is used, a process of "learning" has been incorporated into the statistical analysis. The program begins by selecting a subset of terms (maximum 59) out of the total set of terms that are possible.

Considering a problem with 4 variables, and 10 terms per variable, (i.e., $x(1)^1$, $x(1)^{-1}$, ..., $x(4)^{-1/3}$) then there are only 40 possible terms; however, if one allows second order interactions (i.e., x(1)x(3), etc.) the number of possible terms increases to 640. Thus, it is obvious that any very elaborate array would require an excessively long time to examine all the terms. The simple "learning" technique used in this program consists of weighting each of the untried terms in the matrix according to whether or not similar terms were successfully used in previous passes. Therefore, the randomness in selecting the second and subsequent sets of terms to be examined is biased in favor of types already successful. This scheme allows the analyses to converge much more rapidly on the "best fit" curve.

The completion of regression analysis is controlled by three principal criteria: (1) if the possibility of adding another term to the equation, or deleting a term from the equation, that is adding a bad term or removing a good term, exceeds some preset control value; (2) the total number of possible terms has been examined and there are no more possibilities; (3) the number of trial passes selected by the programmer have been completed.

The analysis proceeds as follows. The specified control information and the data are read into the program. The program computes the number of possible terms and sets up an appropriate bookkeeping system and then picks a subset of these at random. Individual correlation coefficients are computed for each term against the dependent variable and the term with the highest correlation coefficient is selected to be entered into an equation.

A least squares analyses is then used to generate an equation of the form:

$$Y = C_o + C_1 Z_1$$

and various statistical data regarding the fit of the data to this curve is computed. Next, an importance factor is determined for each term and this is used to decide which term not yet used best accounts for the difference between the predictions and the actual data. If the best term, in this respect, passes the insertion and deletion error test, it is put into the equation and the statistics recomputed. (If a term cannot be entered or deleted, the regression is terminated.) This process is continued until the best fit possible with the given set of terms has been selected. This constitutes a standard trial. At the operator's discretion the standard trial may be followed by one or more random trials. In this case the above procedure is followed through insertion of the first term, and then the second term is selected randomly, without regard for the importance factors. This is continued until the regression is terminated by one of the three factors cited earlier. There are cases where the random trial provides a better predicting equation than a standard trial due to the fact that two terms used together may give better results than a single term with a higher importance factor than either of the two alone.

At this point, prior to beginning a second pass the learning technique is used to bias the random selection of a second subset for consideration. The program is also constructed so that terms success-

fully included in a preceding standard pass are included in the next subset. Another pass such as that described above is then carried out and the process repeated until the possible terms have been exhausted or a specified number of passes completed. At the conclusion of the analysis the program prints out the best trial of the best pass and the statistics of the degree of fit. The version of the program available at the University of Michigan also can print out the predicting equation, the CDC-6600 version does not have this option at present, although the equation can readily be determined from the results of each pass.

A typical output from the regression analysis follows to help clarify the foregoing statements. The control parameters used in this pass were:

Prescribed Coefficient of Determination = 0.97

Prescribed Standard Error of Y = 0.00

Probability of Insertion Error = 0.01

Probability of Deletion Error = 0.01

Number of Independent Variables = 4

Number of Terms per Variable = 10

Interaction Order = 4

Number of Terms per Pass = 40

The total number of possible terms is 14640. For the term shown here the independent variables were as follows:

$x(1) = Re_n$

$x(2) = We_n$ (Based on 1 mil arbitrary diameter)

$x(3) = B_n$

$x(4) = B$ (Gas content parameter)

```
EDITOR PROGRAM                                    REXWEXTHERMXGAS VS CAVIT NO

PROBLEM NO.    9                                  POSSIBLE TERMS=      14640
SOLUTION PASS NO.    1                            STARTER PROGRAM
NO. OF INDEPENDENT VARIABLES =    4
NO. OF TRIAL TERMS =   40                         PROBLEM NO.    9

TRIAL TERM DEFINITIONS FOR PASS NO.    1

TERM( 1) = 1.0, CONSTANT TERM.

TERM( 2) = INTERACTION OF ORDER  2, WHERE THE COMPONENTS ARE DEFINED TO BE --
         COMPONENT( 1) = X( 2) .P.    -2.00000
         COMPONENT( 2) = X( 4) .P.     2.00000

TERM( 3) = INTERACTION OF ORDER  1, WHERE THE COMPONENTS ARE DEFINED TO BE --
         COMPONENT( 1) = X( 1) .P.     3.00000

TERM( 4) = INTERACTION OF ORDER  1, WHERE THE COMPONENTS ARE DEFINED TO BE --
         COMPONENT( 1) = X( 3) .P.     -.50000

TERM( 5) = INTERACTION OF ORDER  1, WHERE THE COMPONENTS ARE DEFINED TO BE --
         COMPONENT( 1) = X( 2) .P.     -.33333

TERM( 6) = INTERACTION OF ORDER  1, WHERE THE COMPONENTS ARE DEFINED TO BE --
         COMPONENT( 1) = X( 4) .P.      .33333

TERM( 7) = INTERACTION OF ORDER  3, WHERE THE COMPONENTS ARE DEFINED TO BE --
         COMPONENT( 1) = X( 2) .P.     -.33333
         COMPONENT( 2) = X( 3) .P.      .50000
         COMPONENT( 3) = X( 4) .P.    -2.00000

TERM( 8) = INTERACTION OF ORDER  4, WHERE THE COMPONENTS ARE DEFINED TO BE --
         COMPONENT( 1) = X( 1) .P.     2.00000
         COMPONENT( 2) = X( 2) .P.     2.00000
         COMPONENT( 3) = X( 3) .P.    -1.00000
         COMPONENT( 4) = X( 4) .P.      .33333

TERM( 9) = INTERACTION OF ORDER  4, WHERE THE COMPONENTS ARE DEFINED TO BE --
         COMPONENT( 1) = X( 1)
         COMPONENT( 2) = X( 2) .P.     2.00000
         COMPONENT( 3) = X( 3) .P.      .33333
         COMPONENT( 4) = X( 4) .P.     -.50000

TERM(10) = INTERACTION OF ORDER  1, WHERE THE COMPONENTS ARE DEFINED TO BE --
         COMPONENT( 1) = X( 1) .P.     -.33333

TERM(11) = INTERACTION OF ORDER  4, WHERE THE COMPONENTS ARE DEFINED TO BE --
         COMPONENT( 1) = X( 1) .P.      .50000
```

```
          COMPONENT( 2) = X( 2) .P.       .50000
          COMPONENT( 3) = X( 3) .P.      -.50000
          COMPONENT( 4) = X( 4) .P.     -2.00000

TERM(12) = INTERACTION OF ORDER  4, WHERE THE COMPONENTS ARE DEFINED TO BE --
          COMPONENT( 1) = X( 1) .P.     -3.00000
          COMPONENT( 2) = X( 2) .P.       .33333
          COMPONENT( 3) = X( 3) .P.     -2.00000
          COMPONENT( 4) = X( 4) .P.       .33333

TERM(13) = INTERACTION OF ORDER  2, WHERE THE COMPONENTS ARE DEFINED TO BE --
          COMPONENT( 1) = X( 2)
          COMPONENT( 2) = X( 4) .P.     -1.00000

TERM(14) = INTERACTION OF ORDER  1, WHERE THE COMPONENTS ARE DEFINED TO BE --
          COMPONENT( 1) = X( 1) .P.       .50000

TERM(15) = INTERACTION OF ORDER  1, WHERE THE COMPONENTS ARE DEFINED TO BE --
          COMPONENT( 1) = X( 2) .P.      -.50000

TERM(16) = INTERACTION OF ORDER  1, WHERE THE COMPONENTS ARE DEFINED TO BE --
          COMPONENT( 1) = X( 4) .P.      -.50000

TERM(17) = INTERACTION OF ORDER  3, WHERE THE COMPONENTS ARE DEFINED TO BE --
          COMPONENT( 1) = X( 2) .P.     -3.00000
          COMPONENT( 2) = X( 3) .P.     -2.00000
          COMPONENT( 3) = X( 4) .P.       .50000

TERM(18) = INTERACTION OF ORDER  3, WHERE THE COMPONENTS ARE DEFINED TO BE --
          COMPONENT( 1) = X( 1) .P.       .33333
          COMPONENT( 2) = X( 3) .P.      -.33333
          COMPONENT( 3) = X( 4) .P.      -.33333

TERM(19) = INTERACTION OF ORDER  2, WHERE THE COMPONENTS ARE DEFINED TO BE --
          COMPONENT( 1) = X( 2)
          COMPONENT( 2) = X( 3) .P.      2.00000

TERM(20) = INTERACTION OF ORDER  4, WHERE THE COMPONENTS ARE DEFINED TO BE --
          COMPONENT( 1) = X( 1) .P.      2.00000
          COMPONENT( 2) = X( 2) .P.       .33333
          COMPONENT( 3) = X( 3) .P.      -.50000
          COMPONENT( 4) = X( 4) .P.      3.00000

TERM(21) = INTERACTION OF ORDER  4, WHERE THE COMPONENTS ARE DEFINED TO BE --
          COMPONENT( 1) = X( 1) .P.      3.00000
          COMPONENT( 2) = X( 2) .P.     -2.00000
          COMPONENT( 3) = X( 3) .P.       .33333
          COMPONENT( 4) = X( 4)

TERM(22) = INTERACTION OF ORDER  4, WHERE THE COMPONENTS ARE DEFINED TO BE --
          COMPONENT( 1) = X( 1) .P.       .50000
```

```
          COMPONENT( 2) = X( 2) .P.     -2.00000
          COMPONENT( 3) = X( 3) .P.      -.50000
          COMPONENT( 4) = X( 4) .P.     -2.00000

  TERM(23) = INTERACTION OF ORDER  3, WHERE THE COMPONENTS ARE DEFINED TO BE --
          COMPONENT( 1) = X( 1) .P.      3.00000
          COMPONENT( 2) = X( 3) .P.       .33333
          COMPONENT( 3) = X( 4) .P.       .33333

  TERM(24) = INTERACTION OF ORDER  1, WHERE THE COMPONENTS ARE DEFINED TO BE --
          COMPONENT( 1) = X( 1) .P.     -2.00000

  TERM(25) = INTERACTION OF ORDER  4, WHERE THE COMPONENTS ARE DEFINED TO BE --
          COMPONENT( 1) = X( 1) .P.     -1.00000
          COMPONENT( 2) = X( 2) .P.     -3.00000
          COMPONENT( 3) = X( 3) .P.       .50000
          COMPONENT( 4) = X( 4)

  TERM(26) = INTERACTION OF ORDER  3, WHERE THE COMPONENTS ARE DEFINED TO BE --
          COMPONENT( 1) = X( 1)
          COMPONENT( 2) = X( 3) .P.       .33333
          COMPONENT( 3) = X( 4) .P.      -.33333

  TERM(27) = INTERACTION OF ORDER  2, WHERE THE COMPONENTS ARE DEFINED TO BE --
          COMPONENT( 1) = X( 2) .P.      2.00000
          COMPONENT( 2) = X( 3) .P.      -.50000

  TERM(28) = INTERACTION OF ORDER  2, WHERE THE COMPONENTS ARE DEFINED TO BE --
          COMPONENT( 1) = X( 3) .P.     -3.00000
          COMPONENT( 2) = X( 4) .P.      3.00000

  TERM(29) = INTERACTION OF ORDER  1, WHERE THE COMPONENTS ARE DEFINED TO BE --
          COMPONENT( 1) = X( 4) .P.     -2.00000

  TERM(30) = INTERACTION OF ORDER  2, WHERE THE COMPONENTS ARE DEFINED TO BE --
          COMPONENT( 1) = X( 1)
          COMPONENT( 2) = X( 3) .P.       .50000

  TERM(31) = INTERACTION OF ORDER  1, WHERE THE COMPONENTS ARE DEFINED TO BE --
          COMPONENT( 1) = X( 2) .P.     -3.00000

  TERM(32) = INTERACTION OF ORDER  2, WHERE THE COMPONENTS ARE DEFINED TO BE --
          COMPONENT( 1) = X( 1) .P.     -1.00000
          COMPONENT( 2) = X( 3) .P.     -1.00000

  TERM(33) = INTERACTION OF ORDER  4, WHERE THE COMPONENTS ARE DEFINED TO BE --
          COMPONENT( 1) = X( 1)
          COMPONENT( 2) = X( 2) .P.      -.50000
          COMPONENT( 3) = X( 3) .P.      3.00000
          COMPONENT( 4) = X( 4)
```

```
TERM(34) = INTERACTION OF ORDER  2, WHERE THE COMPONENTS ARE DEFINED TO BE --

          COMPONENT( 1) = X( 1)
          COMPONENT( 2) = X( 4)

TERM(35) = INTERACTION OF ORDER  1, WHERE THE COMPONENTS ARE DEFINED TO BE --
          COMPONENT( 1) = X( 1) .P.     -1.00000

TERM(36) = INTERACTION OF ORDER  4, WHERE THE COMPONENTS ARE DEFINED TO BE --
          COMPONENT( 1) = X( 1) .P.      -.50000
          COMPONENT( 2) = X( 2) .P.      2.00000
          COMPONENT( 3) = X( 3) .P.      -.50000
          COMPONENT( 4) = X( 4) .P.      -.50000

TERM(37) = INTERACTION OF ORDER  3, WHERE THE COMPONENTS ARE DEFINED TO BE --
          COMPONENT( 1) = X( 2) .P.       .50000
          COMPONENT( 2) = X( 3) .P.       .33333
          COMPONENT( 3) = X( 4) .P.     -3.00000

TERM(38) = INTERACTION OF ORDER  2, WHERE THE COMPONENTS ARE DEFINED TO BE --
          COMPONENT( 1) = X( 1) .P.     -1.00000
          COMPONENT( 2) = X( 4) .P.      3.00000

TERM(39) = INTERACTION OF ORDER  3, WHERE THE COMPONENTS ARE DEFINED TO BE --
          COMPONENT( 1) = X( 1) .P.     -1.00000
          COMPONENT( 2) = X( 3) .P.     -2.00000
          COMPONENT( 3) = X( 4)

TERM(40) = INTERACTION OF ORDER  4, WHERE THE COMPONENTS ARE DEFINED TO BE --
          COMPONENT( 1) = X( 1) .P.     -2.00000
          COMPONENT( 2) = X( 2) .P.      -.33333
          COMPONENT( 3) = X( 3) .P.      2.00000
          COMPONENT( 4) = X( 4) .P.       .33333

TERM(41) = X( 5), DEPENDENT VARIABLE.
```

STEPWISE REGRESSION

PROBLEM NO. 9

NO. OF DATA SETS = 67

NO. OF TERM CHOICES = 40

PROBABILITY OF
1) ERROR IN ENTERING TERM = 1.0000 0/0
2) ERROR IN DELETING TERM = 1.0000 0/0

WEIGHTED DEGREES OF FREEDOM = 153.00

STANDARD ERROR OF Y = 4.520168837E-02

STEP NO. 1
TERM ENTERED 1
F LEVEL = 2.760698297E+02
STANDARD ERROR OF Y = 2.696665040E-02
COEFF OF DETERMINATION = 6.464278451E-01
MULTIPLE CORLTN COEFF = 8.040073663E-01

CONSTANT TERM = 0.

TERM NO.	COEFFICIENT	STD ERR OF COEFF	F LEVEL
TERM- 1	3.622352941E-02	2.180124470E-03	-2.742415527E+02

STEP NO. 2
TERM ENTERED 2
F LEVEL = 3.950497630E+01
STANDARD ERROR OF Y = 2.407161170E-02
COEFF OF DETERMINATION = 7.201349312E-01
MULTIPLE CORLTN COEFF = 8.486076426E-01

CONSTANT TERM = 0.

TERM NO.	COEFFICIENT	STD ERR OF COEFF	F LEVEL
TERM- 1	2.946580434E-02	2.223326994E-03	-1.744716743E+02
TERM- 2	2.150504170E-01	3.421482997E-02	-3.924160979E+01

STEP NO. 3
TERM ENTERED 3
F LEVEL = 7.071688062E-03
STANDARD ERROR OF Y = 2.415168072E-02
COEFF OF DETERMINATION = 7.201482132E-01
MULTIPLE CORLTN COEFF = 8.486154684E-01

CONSTANT TERM = 0.

TERM NO.	COEFFICIENT	STD ERR OF COEFF	F LEVEL
TERM- 1	2.954288611E-02	2.411704339E-03	-1.490504042E+02
TERM- 2	2.145327551E-01	3.487619958E-02	-3.758411764E+01

STEP NO. 4
TERM ENTERED 4

```
  F LEVEL =                    1.426954461E-01
  STANDARD ERROR OF Y =        2.422146302E-02
  COEFF OF DETERMINATION =     7.204177748E-01
  MULTIPLE CORLTN COEFF =      8.487742779E-01

  CONSTANT TERM =              0.
      TERM NO.          COEFFICIENT          STD ERR  OF COEFF          F LEVEL
   TERM=  1          3.023966844E-02          3.041770436E-03    =9.816502928E+01
   TERM=  2          2.239504990E-01          4.295287141E-02    =2.700071623E+01
   TERM=  4         -1.276483826E-03          3.379171702E-03    =1.417312877E-01


STEP NO.     5
    TERM ENTERED    3
  F LEVEL =                    5.757298688E-04
  STANDARD ERROR OF Y =        2.430375690E-02
  COEFF OF DETERMINATION =     7.204166798E-01
  MULTIPLE CORLTN COEFF =      8.487736328E-01

  CONSTANT TERM =              0.
      TERM NO.          COEFFICIENT          STD ERR  OF COEFF          F LEVEL
   TERM=  1          3.024863211E-02          3.029156113E-03    =9.903841670E+01
   TERM=  2          2.236414031E-01          4.112857272E-02    =2.936653191E+01
   TERM=  4         -1.253946347E-03          3.257954565E-03    =1.471307280E-01


STEP NO.     6
    TERM ENTERED   33
  F LEVEL =                    1.741971064E+01
  STANDARD ERROR OF Y =        2.305047404E-02
  COEFF OF DETERMINATION =     7.502188408E-01
  MULTIPLE CORLTN COEFF =      8.661517424E-01

  CONSTANT TERM =              0.
      TERM NO.          COEFFICIENT          STD ERR  OF COEFF          F LEVEL
   TERM=  1          2.232314471E-02          3.443794573E-03    =4.173029175E+01
   TERM=  2          2.256800334E-01          3.901073496E-02    =3.323786782E+01
   TERM=  4          2.718752757E-03          3.233233135E-03    =7.022318675E-01
   TERM= 33          1.797375556E-04          4.306439623E-05    =1.730039755E+01


STEP NO.     7
    TERM REMOVED    4
  F LEVEL =                   -7.022318675E-01
  STANDARD ERROR OF Y =        2.318576283E-02
  COEFF OF DETERMINATION =     7.490091561E-01
  MULTIPLE CORLTN COEFF =      8.654531507E-01

  CONSTANT TERM =              0.
      TERM NO.          COEFFICIENT          STD ERR  OF COEFF          F LEVEL
   TERM=  1          2.434341229E-02          2.481741462E-03    =9.555299980E+01
   TERM=  2          2.425714050E-01          3.363753703E-02    =5.164464774E+01
   TERM= 33          1.690770147E-04          4.139752164E-05    =1.656589668E+01


STEP NO.     8
    TERM ENTERED   31
  F LEVEL =                    9.238797642E+00
  STANDARD ERROR OF Y =        2.255386738E-02
  COEFF OF DETERMINATION =     7.641414441E-01

  MULTIPLE CORLTN COEFF =      8.741518427E-01
```

CONSTANT TERM = 0.

TERM NO.	COEFFICIENT	STD ERR OF COEFF	F LEVEL
TERM- 1	2.069526590E-02	2.696007368E-03	-5.851583644E+01
TERM- 2	1.425038670E-01	4.641664333E-02	-9.360076168E+00
TERM- 31	5.365656863E-02	1.765286372E-02	-9.174639325E+00
TERM- 33	1.887468655E-04	4.078595112E-05	-2.126727529E+01

STEP NO. 9
TERM ENTERED 40
F LEVEL = 7.447402219E+00
STANDARD ERROR OF Y = 2.206530434E-02
COEFF OF DETERMINATION = 7.758168436E-01
MULTIPLE CORLTN COEFF = 8.808046569E-01

CONSTANT TERM = 0.

TERM NO.	COEFFICIENT	STD ERR OF COEFF	F LEVEL
TERM- 1	1.713341378E-02	2.942870367E-03	-3.365873967E+01
TERM- 2	1.529012948E-01	4.557071188E-02	-1.117900131E+01
TERM- 31	5.556429371E-02	1.728460860E-02	-1.026182972E+01
TERM- 33	1.962250132E-04	3.999642529E-05	-2.390114385E+01
TERM- 40	1.151095676E-03	4.218023721E-04	-7.395322483E+00

STEP NO. 10
TERM ENTERED 34
F LEVEL = 1.011783128E+01
STANDARD ERROR OF Y = 2.139379737E-02
COEFF OF DETERMINATION = 7.907279644E-01
MULTIPLE CORLTN COEFF = 8.892288594E-01

CONSTANT TERM = 0.

TERM NO.	COEFFICIENT	STD ERR OF COEFF	F LEVEL
TERM- 1	8.645618737E-03	3.906628866E-03	-4.863160670E+00
TERM- 2	6.097603143E-02	5.279582217E-02	-1.324493905E+00
TERM- 31	6.833089089E-02	1.723250318E-02	-1.561234716E+01
TERM- 33	2.171792698E-04	3.933478215E-05	-3.027011054E+01
TERM- 34	1.030738865E-02	3.240447095E-03	-1.004657895E+01
TERM- 40	1.744661764E-03	4.495272771E-04	-1.495688503E+01

STEP NO. 11
TERM REMOVED 2
F LEVEL = -1.324493905E+00
STANDARD ERROR OF Y = 2.157012996E-02
COEFF OF DETERMINATION = 7.887621521E-01
MULTIPLE CORLTN COEFF = 8.881228249E-01

CONSTANT TERM = 0.

TERM NO.	COEFFICIENT	STD ERR OF COEFF	F LEVEL
TERM- 1	7.076219509E-03	3.692872955E-03	-3.645715563E+00
TERM- 31	8.225265006E-02	1.241645375E-02	-4.357260962E+01
TERM- 33	2.201272670E-04	3.957539910E-05	-3.071892402E+01
TERM- 34	1.235598381E-02	2.734223620E-03	-2.027661815E+01
TERM- 40	1.829584869E-03	4.471279424E-04	-1.662456998E+01

STEP NO. 12
TERM REMOVED 1
F LEVEL = -3.645715563E+00
STANDARD ERROR OF Y = 2.192707090E-02

COEFF OF DETERMINATION = 7.832613441E-01
MULTIPLE CORLTN COEFF = 8.850205332E-01

CONSTANT TERM = 0.

TERM NO.	COEFFICIENT	STD ERR OF COEFF	F LEVEL
TERM- 31	8.977008756E-02	1.197532121E-02	-5.579248689E+01
TERM- 33	2.563466756E-04	3.534506730E-05	-5.222572988E+01
TERM- 34	1.564559439E-02	2.163299352E-03	-5.193231209E+01
TERM- 40	2.312518117E-03	3.754419631E-04	-3.766790169E+01

STEP NO. 13
TERM ENTERED 21
F LEVEL = 9.988935814E+00
STANDARD ERROR OF Y = 2.125531912E-02
COEFF OF DETERMINATION = 7.977925475E-01
MULTIPLE CORLTN COEFF = 8.931923351E-01

CONSTANT TERM = 0.

TERM NO.	COEFFICIENT	STD ERR OF COEFF	F LEVEL
TERM- 21	-2.041078354E-03	6.458030114E-04	-9.917072967E+00
TERM- 31	8.949233392E-02	1.160878117E-02	-5.900145279E+01
TERM- 33	2.310252471E-04	3.518650245E-05	-4.279873896E+01
TERM- 34	2.579828676E-02	3.836228330E-03	-4.489904685E+01
TERM- 40	2.172822617E-03	3.666142206E-04	-3.487339421E+01

REGRESSION TERMINATED AFTER 13 STEPS.

DIAGONAL ELEMENTS

VAR. NO.	VALUE
1	1.840499099E-01
2	2.862174955E-01
3	7.564781012E-01
4	1.094420447E-01
5	1.209600193E-01
6	1.051069576E-01
7	7.286519372E-01
8	8.462939066E-01
9	7.242610019E-01
10	1.738657141E-01
11	8.517885603E-01
12	7.404759474E-01
13	7.195664554E-01
14	2.482125128E-01
15	1.007836291E-01
16	4.112423017E-01
17	7.818752467E-01
18	2.930198234E-01
19	5.799484836E-01
20	5.636817328E-01
21	4.735142172E+00
22	5.939567278E-01
23	7.076040277E-01
24	2.140858949E-01
25	3.050298503E-01
26	5.496804763E-01
27	7.459085597E-01

28	7.989339884E-01
29	7.594975739E-01
30	4.469638133E-01
31	1.675030984E+00
32	4.115323042E-01
33	1.161433880E+00
34	5.633433234E+00
35	1.610299166E-01
36	7.593739901E-01
37	7.992169085E-01
38	5.126306648E-01
39	7.563706783E-01
40	1.110786159E+00

POSTULATED CRITERIA

STANDARD ERROR OF Y = -0.
COEFF OF DETERMINATION = 9.7000000E-01

FITTED CURVE PROPERTIES

STANDARD ERROR OF Y = 2.1255319E-02
COEFF OF DETERMINATION = 7.9779255E-01

FITTED CURVE MEETS NEITHER CRITERIA.

PASS NUMBER 2 BEGUN FOR PROBLEM NO. 9
2 TOTAL PASSES ALLOWED.

APPENDIX I

REGRESSION ANALYSIS OF DATA

The immediate problem that must be faced with an experimental program of the type reported here is the volume of data available for analysis. Therefore, one of the first steps to an adequate treatment is a systemization of the data. Because this study has as its purpose the correlation of the cavitation number with a group of broadly applicable (in fluid flow problems) dimensionless parameters, the data can be handled in much more general sets than is possible in correlations against limited parameters such as velocity or gas content. The general approach used here is to begin with the water cavitation studies for which there is ample reported data for comparison. The base line one-half inch diameter venturi results are treated first, and then we progress through the general correlations with all the water data. Mercury is treated in a similar manner and then the gross correlations combining the two fluids are presented. The key to whatever success has been enjoyed in this general approach is a computerized regression analysis, the essential features of which are discussed in Appendix H. The flexibility of this program, coupled with the statistical information it develops on the equation it generates provides a powerful assessment tool.

A. Single Parameter Correlations, Water Cavitation

1. One-half-inch-Throat-Diameter Plastic Venturi

Because the bulk of the data taken during the water portions of this study were from experiments in the 1/2 inch system; and, because

this has been the "standard" test system for cavitation damage studies at the University of Michigan, it was decided to first attempt a correlation with data from this system. The analysis was begun by examining the results of the correlation of the observed cavitation number with each of the possibly pertinent parameters previously discussed: Reynolds number, the three Weber numbers, the Prandtl number, the thermodynamic parameter, the exposure time parameter, and the gas-content parameter in turn. Based upon experience, it was not anticipated that this would produce a significant correlation because of the variations in velocity, temperature, and gas content from run to run. However, it was believed that because of the statistics available in this analysis, some insight could be gained as to the most profitable avenues to explore, and for the most probable parameters to use in combination. The results of these trials are shown in Table 6. In each instance, only a single term for the independent variable is reported. The regression analysis can and does provide polynominal equations. However, it was considered unlikely that one could attach real physical significance to equations that included these "standard" parameters in such form, particularly when considering possible combinations. The table therefore indicates the best equation involving the single variable. The standard error of estimate may be roughly interpreted as the standard error of the predicted dependent variable. The coefficient of determination is interpreted as the proportion of the total variation in the dependent variable that is explained by the predicting equation. A value of 1 is a perfect prediction, a value of 0, no prediction. In many cases it was necessary to reduce the magnitude of the independent parameter by arbitrary scale

TABLE 6

REGRESSION ANALYSIS RESULTS - SINGLE PARAMETER
VENTURI 412 WATER CAVITATION

Standard Error of Data = .0619

	Standard Error of Estimate	Coefficient of Determination	Remarks
1. $\sigma = -.0515 + .157 Re_n^{-0.250}$	.021	.889	$Re_n = Rex10^{-5}$
2. $\sigma = .128 - .0535 We_n^{0.200}$	.0226	.872	$We_n = Wex10^{-2}$ (Note 1)
3. $\sigma = .0350 + .0888 We_n^{-2.00}$	.0176	.926	$We_n = Wex10^{-2}$ (Note 1)
4. $\sigma = .0351 + .02230 We_n^{-2.00}$	.0172	.925	$We_n = Wex10^{-4}$ (Note 1)
5. $\sigma = .0602 - 3090\ Pr^{-10.00}$	.0257	.833	
6. $\sigma = .0536 + 6.11X10^{-15} B_n^{-10.0}$	.0275	.810	$B_n = Bx10^{-5}$
7. $\sigma = .0316 + .00191\ \tau_n^{3.000}$	.0172	.925	$\tau_n = \tau\ x10^{-10}$
8. $\sigma = .0301 + .105\beta$	.0184	.915	
9. $\sigma = .0317 + .0137\ V^{-3.00}$	.0172	.926	

NOTE: Weber numbers are based on three assumptions and use characteristic length based on those assumptions:
(1) Diameter of bubble is linear function of gas content
(2) Constant bubble diameter of 1 mil
(3) Diameter is that of venturi throat

factors (powers of ten) to avoid exceeding machine capacity when terms were raised to a power. These cases are also indicated in the table.

As indicated above, it was not expected that any single parameter would provide a conclusive correlation. However, the results of this analysis are quite encouraging. The "standard error" or "standard deviation" of the uncorrelated data is 0.0619 and there are several instances where the standard deviation of the predicted cavitation number is approximately 0.0172, or a factor of 3.6 improvement. And, because this is about the same order of magnitude as the minimum cavitation number measured, it indicates that the analysis will produce equations with standard deviations reasonably smaller than the parameter being predicted.

The correlation with Reynolds number indicates the same monotonically decreasing relationship that has been reported earlier for cavitation in the University of Michigan facilities[10]. However, the Reynolds number range covered is not large (1.89×10^5 to 17.9×10^5) and the Reynolds number variation arises only from changes in velocity and temperature. From the low-velocity, cold case (63.1 ft/sec, 58°F) to the high-velocity, hot case (217.5 ft/sec, 136°F) the variation in Reynolds number is nearly linear with velocity and temperature with the effects of the latter being reflected most in the viscosity (viscosity decreases by a factor of 2.8). Other reported correlations[9] against Reynolds indicate a monotonically increasing relationship for those situations where flow separations, (e.g., ogives, sharp edges) usually occur. Smooth shapes (hydrofoils) exhibit a decreasing σ_c

with increasing Reynolds number. Definite size effects are evidenced in the literature reports and Holl[14] also suggests that cavitation which is predominantly "gaseous" exhibits this decrease with Reynolds number, just as it does with velocity. This implies of course that until size variations are included, one is only really getting a $\frac{\rho V}{\mu}$ correlation as influenced by gas content.

In the Weber number correlations, it seems apparent that for a fixed linear dimension, whether an arbitrary bubble radius or the venturi diameter, and given the relative temperature insensitivity of surface tension (e.g., for a temperature increase by a factor of 2.6 the surface tension only varies by about 10%) over the test range, the correlation is with ρV^2; and, we find a much stronger dependence than that noted above for Reynolds number. In the case where an assumed linear relationship between gas content and the characteristic length was employed, the cavitation number is still an inverse function of the Weber number, although not nearly as strongly as that for the other two cases. The author has been unable to locate any other attempts at correlation of cavitation inception with Weber number except that of Kermeen and Parkin[21], which is mentioned by Holl[9]. Ivany[61] and Plesset[62] in their analytical studies of single bubble dynamics assert that surface tension effects are important for growth of small bubbles, such as are present at cavitation inception. Van der Walle[63] also presents some strong arguments for serious consideration of surface tension effects in cavitation studies particularly for cavitation near or on walls, such as occurs in this study.

The Prandtl number correlation provides a rather interesting situation which serves to illustrate the care that must be exercised in accepting and interpreting the results from a purely mathematical correlation of data. The Prandtl number is simply temperature dependent and decreases by a factor of 3 over the range 53°F to 136°F. It is quite difficult to make a case for a Prandtl relationship with such a large exponent and this underscores the fact that given two sets of numbers and sufficient latitude a "correlation" between them can be found.

The thermodynamic parameter also exhibits a large negative exponent for which it is quite difficult to establish physical significance. Garcia and Hammitt[40] show from damage data taken in a vibratory facility and also based on a modified parameter similar to that of Florschuetz and Chao[42] that water cavitation damage for relative warm water appears to be importantly affected by heat transfer process. However, no allowance is made for the presence and influence of permanent gases. The results from the other single parameter correlations suggest that the thermodynamic effects are not nearly as important in the present study as velocity and gas content effects. Seidel[64] and Kornhauser[65] in their studies of thermodynamic effects in water cavitation indicate that higher temperatures must be used to provide insight into thermodynamic effects, and they express concern over the potential interplay and masking effects of gas content.

The correlation with the exposure time parameter provides a surprisingly good correlation. Because the only variation that occurs is velocity, a check run was made by attempting a correlation with the

velocity. As expected, the results essentially agree and we find that the velocity provides good correlation. As stated above, Holl[14] has shown that for gaseous cavitation there is a strong inverse dependence on velocity when no size effects are involved.

The correlation with the gas-content parameter did provide the type of relationship expected from the experimental data, that is, cavitation number increases with gas content. Again, however, the degree of correlation achieved is somewhat surprising in light of the competing effects of velocity and temperature.

2. All Plastic Venturis

The next step was to repeat the above sequence of correlations using all the available water data. Based upon the discussions already presented it was assumed that in general the correlations would not be nearly as effective because of the increased number of variables now active (e.g., velocity, size, and temperature in Reynolds number). The results are presented on Table 7. The expectations concerning the quality of correlation attainable are borne out. The standard deviation does not show the improvement it did in the 1/2 inch case and none of the correlations approach the 90% prediction capability found in the single venturi.

The Reynolds number correlation indicates that the cavitation number decreases with increases in Reynolds number. However, there is a considerable difference in the nature of this change compared to that for the 1/2 inch venturi. For the 1/2 inch case, the value of σ_c drops from 0.105 to -.046 as Re_n varies from 1 to 100, and approaches a value of -0.051 asymptotically. When all venturis are

TABLE 7

REGRESSION ANALYSIS RESULTS - SINGLE PARAMETER
ALL PLASTIC VENTURIS - WATER CAVITATION

Standard Error of Data = 0.0447

	Standard Error of Estimate	Coefficient of Determination	Remarks
1. $\sigma_c = 0.0375 - 2.25X10^{-6}Re_n^{3.0}$	0.0256	0.677	$Re_n = R_eX10^{-5}$
2. $\sigma_c = 0.0643 - 0.162We_n^{1/3}$	0.0240	0.715	$We_n = W_eX10^{-2}$ (Note 1)
3. $\sigma_c = 0.0287 + 0.775We_n^{-10.0}$	0.0199	0.805	$We_n = W_eX10^{-2}$ (Note 1)
4. $\sigma_c = 0.0210 + 0.0585We_n^{-1/10}$	0.0251	0.689	$We_n = W_eX10^{-4}$ (Note 1)
5. $\sigma_c = 0.0294 + 8.26X10^{-12}Pr^{10}$	0.0227	0.745	
6. $\sigma_c = 0.0289 + 0.00896B_n^{-1/2}$	0.0249	0.695	$B_n = BX10^{-5}$
7. $\sigma_c = 0.0117 + 0.0432\tau_n$	0.0228	0.745	$\tau_n = \tau X10^{-10}$
8. $\sigma_c = 0.0199 + 0.072\beta$	0.0223	0.754	
9. $\sigma_c = 0.0281 + 0.000515V_n^{-10.0}$	0.0201	0.801	$V_n = VX10^{-2}$

NOTE: (1) Weber number uses characteristic length linearly proportional to gas content
(2) Weber number uses 1 mil as characteristic length
(3) Weber number uses D_t as the characteristic length

are considered, σ_c ranges from 0.0375 to -2.22 are Re_n varies from 1 to 100, and the asymptotic behavior is evidenced as Re_n decreases.

For the Weber number involving the assumed linear relationship between gas content and bubble diameter, the general form of the correlation is the same in both cases, in the 1/2 inch case a fifth root is involved. In both instances, this Weber number provides a better correlation than the Reynolds number, but still not as good as that provided by the Weber number which uses a fixed 1-mil bubble radius, although in this latter instance, it is difficult to explain such a large exponent. In the run that uses the venturi throat diameter as the characteristic length, we find a change in the predicted dependence. For the 1/2 inch venturi, an increase in cavitation number with increasing Weber number is predicted approaching a value of .035 as the limit, while in the case where the characteristic length is also varied decreases with increasing Weber number approaching -0.021 as a limit. This change in trend must reflect the influence of size.

The Prandtl number correlation shows a similarity in trend to that for the 1/2 inch case although the coefficients of the curve do differ from the earlier case and again the correlation is not very enlightening.

The cavitation number shows a similar behavior in both instances for the thermodynamic parameter. σ_c increases without bound as B decreases and approaches some limiting value as B increases. Because B decreases as temperature increases, the cavitation number trend is opposite to that predicted by the theory. But again it must be emphasized that the correlation is not conclusive and the thermodynamic

effects are apparently being overshadowed by other competing processes.

The exposure time parameter also shows a complete change in relationship compared with the 1/2 inch venturi case. When all the data is considered the cavitation number is a monotonically increasing function of the parameter as opposed to the decreasing nature previously observed. In contrast the correlation with velocity alone shows a function which asymptotically approaches a constant value as the velocity is allowed to increase.

Finally, we observe that the cavitation number does increase as a function of gas content just as was predicted for the 1/2 inch venturi. Of course, the competing effects have reduced the effectiveness of the correlation.

There is another point that should be borne in mind when examining the results of these correlation analyses. In this study, a venturi system is used to simulate to a limited extent the characteristics of a flowing system such as an impeller or turbine cascade. Therefore, the results are intended to guide in the selection of parameters to be considered in correlating large equipment tests and not be interpreted as "absolutes". Further, the correlations will perhaps be modified as they are extended and checked out increasing ranges of the variables.

B. Multiple Parameter Correlations, Water Cavitation

There are two options open at this point in the analysis and both of them have been exercised. The first step was to give the program free rein with the parameters available to it. The second step is to insist that the computer analyses consider terms such as have already been proven important. The results of these investigations are discussed

1. One-half-inch-Throat-Diameter Plastic Venturi

Table 8, Part I, equation 1. This is the equation which resulted when the analyses were applied to the 1/2 inch venturi data, using the Reynolds number, a Weber number, the Prandtl number, thermodynamic parameter, and gas-content parameter as the independent variables. The only restriction on the analysis was that the cubes and their reciprocals were the largest exponents the program was allowed to consider. It is interesting to note that the Reynolds number and the Prandtl number do not appear in the equation generated. According to the statistics generated in the analyses, the gas-content term was the most significant in explaining the data with the Weber number and the thermodynamic parameter being of the same importance. Comparing the coefficients of determination for equations (2) and (1), indicates only about a 2% improvement in the correlation by including the thermodynamic effects.

Equation (3) was generated in the same manner as equation (1) except that in this instance the Weber number using the venturi throat diameter as the characteristic length was employed. As would be expected from the earlier results (Table 7), the correlation and its effectiveness essentially repeated that of equation (1).

Equation (4) was generated by using the exponents for the four independent variables cited above, that were generated during the single parameter correlations. Again the coefficient of determination is only a percent or so less than for equation (1). The importance factors computed during the analysis rank the terms in the following descending order of importance, B, $We_n^{-2.0}$, B^{-10}; and $Re_n^{-1/4}$.

TABLE 8

REGRESSION ANALYSIS RESULTS - MULTIPLE PARAMETERS
VENTURI 412 WATER CAVITATION

Standard Error of Data - 0.0619

	Standard Error of Estimate	Coefficient of Determination	Remarks
Part I Additive Terms			
1. $\sigma_c = .0375-.00299B_n^{-1.0}+.0471We_n^{-2.0}+.149\beta^2$	.0123	.964	(1)(2)(3)
2. $\sigma_c = .0347+0631We_n^{-2.0}+.0690\beta^2$	.0157	.939	(2)(3)
3. $\sigma_c = .0376-.0029B_n^{-1.0}+1.21We_n^{-2.0}+.149\beta^2$	0.124	.963	(1)(2)(4)(7)
4. $\sigma_c = .00580+.0359Re_n^{-1/4}+.0100We_n^{-2.0}-5.85X10^{-5}B_n^{-10.0}+.0734\beta$	.0149	.947	(2)(3)(5)(6)
5. $\sigma_c = .0296+.0574We_n^{-2.0}+.0526\beta$	.0158	.939	(2)(3)(6)
6. $\sigma_c = .00677+.0469Re_n^{-1/4}+.0729We_n^{-2.0}$	.0169	.929	(2)(3)(5)
7. $\sigma_c =0.0432+0.0167Gas/We_n^{2.0}-3.52X10^{-6}Re_n^{3.0}$	.0143	.947	(2)(3)(5)(6)
8. $\sigma_c =0.0387+.0184Gas/We_n^{2.0}$	.0156	.939	(2)(3)
9. $\sigma_c = .00939+.0148Gas/We_n^{2.0}+.0756Re_n^{-1/4}$	.0137	.954	(2)(3)(5)(6)
10. $\sigma_c = .0515+0.0155Gas/We_n^{2.0}-.00159Re_n$	.0141	.951	(2)(3)(5)(6)

TABLE 8 (Con't)

	Standard Error of Estimate	Coefficient of Determination	Remarks
11. $\sigma_c = .0135+.0858\phi^2+.0557Re^{-1/2}+.0312We_n^{-2.0}$	.0147	.948	(2)(3)(5)
12. $\sigma_c = .0538+.189\,\phi/We_n^{2.0}-.0425B_n^{-.10}+0377Re_n^{-.25}$	.0128	.961	(1)(2)(3)(5)
Part II Multiplication Terms			
1. $\sigma_c = .0599-.000375Re_nWe_nB_n\phi$	.0264	.825	(1)(2)(3)(5)
2. $\sigma_c = .0489+\frac{.00926}{Re_nWe_nB_n\phi}$	.0264	.825	(1)(2)(3)(5)
3. $\sigma_c = .0536+2.56X10^{-14}Re_n^{-.25}We_n^{-2.0}B_n^{-10.}\phi$	.0275	.810	(1)(2)(3)(5)
4. $\sigma_c = .0429+1.097\,\frac{\phi}{Re_n^{-2.0}}$	.0157	.938	(1)(2)(3)(5)

REMARKS:
(1) $B_n = B \times 10^{-5}$
(2) $We_n = B \times 10^{-2}$
(3) Weber used assumes 1 mil characteristic length
(4) Weber number used assumes D_t as characteristic length
(5) $Re_n = Re \times 10^{-5}$
(6) Terms inserted without regard to statistics
(7) $We_n = We \times 10^{-5}$

Equations (5) and (6) resulted when an attempt was made to examine the statistics for an equation which essentially duplicated equation (4), with the thermodynamic parameter dropped. Using the partial equations generated, some useful observations are possible. The statistics for equations (2) and (5) are nearly identical, which implies that there is little change in the correlation regardless of whether one uses the first order or second order term, but it is clear that the gas content is important in the physical processes. Of course, the fact that equation (6) also has such good statistics implies that Weber number effects really dominate, and this, recalling the earlier arguments on single parameter analyses, is actually an inverse velocity correlation.

Equations (7) through (11) indicate the results from equations selected by the author with the gas content and Weber number combined into a single term according to the suggestion of Kermeen and Parkin[21]. Equation (7) uses the cubed Reynolds number since this was the exponent developed during the analysis with all the data. However, comparison with equation (8) indicates once again that the Reynolds number is not really a significant factor although an improved correlation results (equation (9)) when the Reynolds number is included as $Re_n^{-1/4}$. Equation (8) compared with equation (2) implies that the Weber number gas content combination is the significant factor and it really makes little difference whether these are additive or allowed to interact. Intuitively, a term which allows for interaction would seem to be the most logical because the surface tension effects would be related to the size and number of any permanent gas bubbles present. Equation

(9) provides the best correlation with the exceptions of equations (1) and (3), so it is extended in equation (12) to include the thermodynamic parameter as developed in equations (1) and (3). The result provides a correlation that is essentially equal to any other achieved to date and which includes all the relevant terms.

The difficulty with multiple correlations such as presented here is that a graphical presentation if the data is nearly impossible to provide, especially when it is impossible to "lump" or average one or more of the variables in order to observe the effects of variations in a single variable. However, a graphical presentation can be provided so that the goodness of fit can be seen. This is done by plotting the calculated value for σ_c (using experimentably determined values for the independent variables) against the observed σ_c. A perfect correlation would provide a single straight line with a slope of unity, therefore, the scatter of points about such a line provides a measure of the non-correlation. Such plots were generated for equations (9) and (12) from Table 4 and are presented as Figures 74 and 75.

In Figure 74, the correlation with gas content, Weber number, and Reynolds number is presented. In this instance, although 66% of the data does lie within the standard deviation bandwidth about the exact correlation line, there appears to be a systematic omission because all the noncorrelated data lie to the right of the correlation line. On Figure 75 the correlation is shown with the thermodynamic parameter included. The importance of this additional factor is emphasized by the fact that although we do not have a "perfect" correlation, the data points are now more equally distributed about

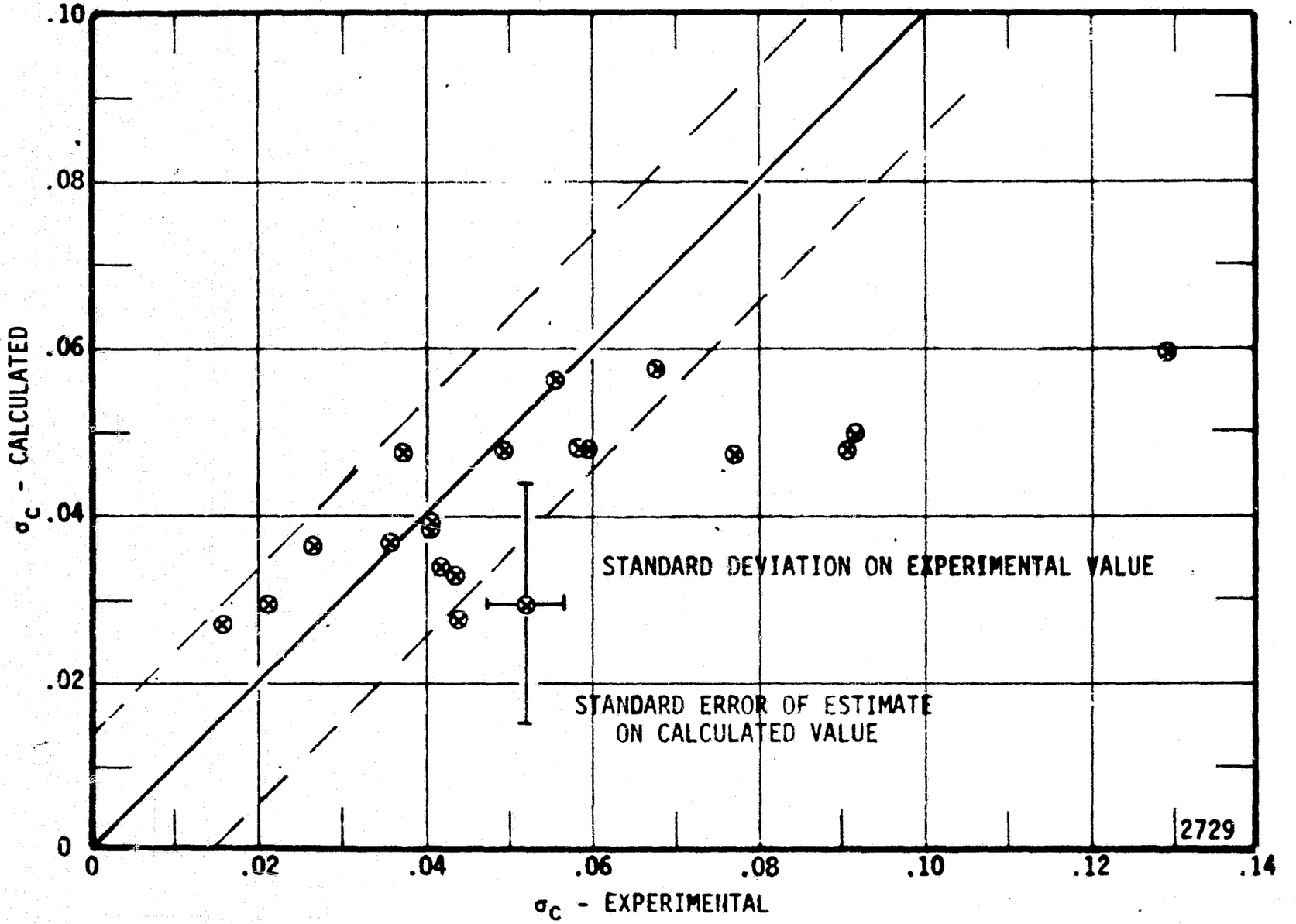

Figure 74. Calculated Cavitation Number versus Experimental Cavitation Number, Venturi 412, Water, Equation 9, Part I, Table 8.

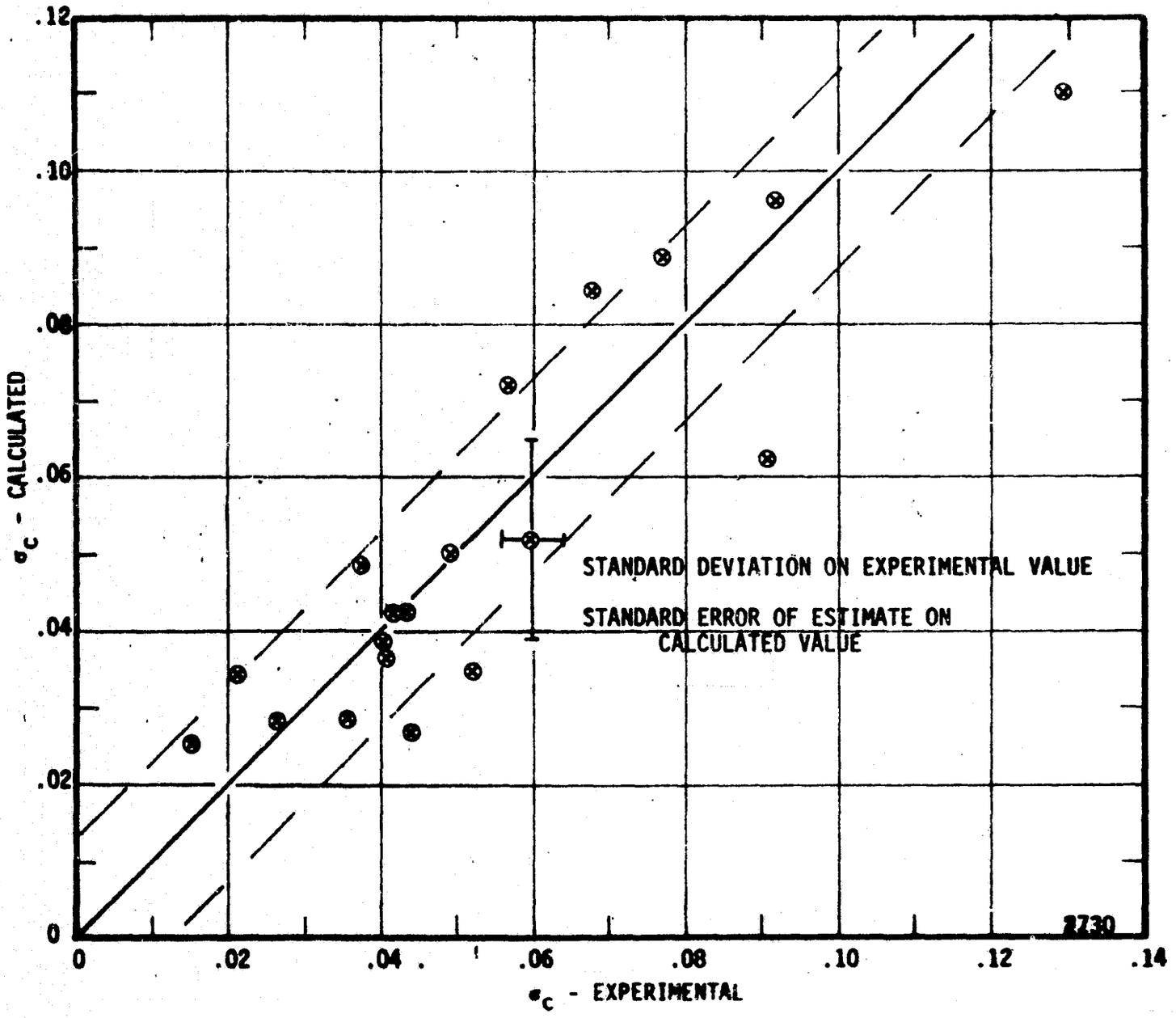

Figure 75. Calculated Cavitation Number versus Experimental Cavitation Number, Venturi 412, Water, Equation 12, Part I, Table 8.

the exact correlation line. Therefore, one can conclude that gas content, Weber number, Reynolds number, and thermodynamic effects are controlling in those cases where the geometry is exactly constant, including any surface roughness effects. In this case the cavitation number increases with gas content as expected; decreases with Reynolds number, and decreases with Weber number. Of course, as has been noted earlier, the correlation requires testing over larger ranges and the analyses will be significantly enhanced as experimental data over a wider range of variables become available.

In Part II of Table 8 we show the results obtained when an interaction between the independent variables is examined. That is, rather than say that cavitation is some function of the pressure field or pressure differentials and that such effects are additive and independent, the possibility of enhancement is allowed. In no single case examined, and again the analysis was constrained to a single grouping, did this approach provide a better correlation (as measured by the coefficient of determination) than did the additive approach. The quality of equation (4), coupled with earlier results, certainly leads to the conclusion that gas content and Reynolds number effects are predominant in the cavitation observed here.

2. All Plastic Venturis

The results from the regression analyses of all the water data are shown in Table 9. A procedure similar to that discussed earlier for the one-half-inch venturi was employed. Equations (1), (2) and (3) (Table 9) are the predictions when the program was allowed to consider the five variables: Reynolds number, Weber number, Prandtl number,

TABLE 9

REGRESSION ANALYSIS - MULTIPLE PARAMETERS
ALL PLASTIC VENTURI - WATER CAVITATION

Standard Error of Data = .0447

	Standard Error of Estimate	Coefficient of Determination	Remarks
Part I Additive Terms			
1. $\sigma_c = .0258+.0612We_n^{-2.0}$	.0236	.742	(2)(3)
2. $\sigma_c = .0278+.0839We_n^{-3.0}$	.0233	.748	(2)(3)
3. $\sigma_c = .0286-.00470We_n^{1/2}+.000147We_n^{3}+.0147We_n^{-1}-0.00125We_n^{-2}$	.0189	.832	(2)(7)
4. $\sigma_c = .0214+1.35X10^{-6}-7.23X10^{-9}We_n^{-10}-.00269B_n^{-1/2}+.0791\beta$	.0237	.744	(1)(2)(3)(5)
5. $\sigma_c = .0566+3.19X10^{-6}Re_n^{3.0}+.0935We_n^{-10}-.00199B_n^{-1/2}+.0508\beta$	.0235	.748	(1)(2)(3)(5)
6. $\sigma_c = .0254 +.152\beta/We_n^{2.}+9.15X10^{-3}Re_n^{3}$	.0211	.783	(2)(3)(5)
7. $\sigma_c = .0260+.150\beta/We_n^{2}$	.0210	.782	(2)(3)
8. $\sigma_c = .0265+6.95X10^{-7}Re_n^{3.0}+.315\beta/We_n^{4}$	.0199	.805	(2)(3)(5)
9. $\sigma_c = .0269+.312\beta/We_n^{4.0}$	.0202	.805	(2)(3)
10. $\sigma_c = .0276+2.19\beta/We_n^{10}+4.69X10^{-4}Re_n^{3}$	.0178	.844	(2)(3)(5)

TABLE 9 (Con't)

	Standard Error of Estimate	Coefficient of Determination	Remarks
11. $\sigma_c = -.0278+2.17\,\varepsilon/We_n^{10}$	.0178	.844	(2)(3)
12. $\sigma_c = .324+2.13\,\frac{\varepsilon}{We_n}10-.00112B_n^{-.5}$	.0199	.817	(1)(2)(3)
13. $\sigma_c = .0234+2.023\,\frac{\varepsilon}{We_n^{10}}-.00164B_n^{-.5}+7.84X10^{-7}Re_n^{3.0}+.0109We_n^{-.333}$	.0220	.817	
Part II Multiplicative Terms			
1. $\sigma_c = .0377-.000154Re_nWe_nB_n\varepsilon$	.0270	.649	(1)(2)(3)(5)
2. $\sigma_c = .0358+.00530Re_n^{3.0}We_n^{-10.0}B_n^{-.5}\varepsilon$	.0252	.704	(1)(2)(3)(5)
3. $\sigma_c = .035+.0940Re_nWe_n^{-3.0}B_n\varepsilon$	.0232	.741	(1)(2)(3)(5)
4. $\sigma_c = .036+.00115Re_nWe_n^{-1.0}B_n^{-10}\varepsilon$	.0257	.693	(1)(2)(3)(5)
5. $\sigma_c = .0305+.227\,\varepsilon^2/We_n^2$	.0241	.720	(1)(2)(3)(5)

TABLE 9 (Con't)

REMARKS: (1) $B_n = BX10^{-5}$

(2) $We_n = WeX10^{-2}$

(3) Weber number used assumes 1 mil characteristic length

(4) Weber number used assumes D_t as characteristic length

(5) $Re_n = ReX10^{-5}$

(6) Terms inserted without regard to statistics

(7) $We_n = WeX10^{-4}$

thermodynamic parameter, and the gas-content parameter. Again, the only restriction was that only terms with exponents no larger than the positive cube or its reciprocal or smaller than the negative cube and its reciprocal could be employed. In equations (1) and (2), which represent two trials with the data, only a single term appears. This Weber number is based upon a characteristic length of 1-mil. Equation (3) results when the throat diameter is used as the characteristic length. Although there are more terms in this equation, and the correlation is better, again only Weber number terms appear, which obviously provides an inadequate physical interpretation of the data.

Equations (4) and (5) result from forcing the analyses to consider terms with exponents as they were generated during the single parameter studies. The only difference between these two is the characteristic length in the Weber number. Because varying this length in the Weber number really had no clear influence upon the predicted equation, all subsequent analyses were accomplished using the 1-mil Weber number and thus forcing the size effects into the Reynolds number. Furthermore, the correlation achieved with these two equations is not very satisfactory.

Because it is quite difficult to provide some physical explanation for a tenth power relationship, several alternate solutions were tried. These analyses were all run using the β/We form, and the exponent on Weber number varied. Examining the sequence of equations (6), (8) and (10), it is immediately obvious that the larger exponent on the Weber number provides the best fit. The relatively small improvement in the correlation when the Reynolds number is included

indicates that such effects (mainly size) are not really significant, at least over the range available. Here of course, conclusions can only be tentative because it is impossible to evaluate the effects of surface imperfections on the cavitation initiation when various sizes of venturis are employed. Although the thermodynamic effects are not included in this particular set of equations, (6) through (11), calculations were performed by using equation (10), Table 5 and the results plotted on Figure 76. Here, as in the earlier case, although the data obeys the statistics there is a definite "skewing" of the data, predicting values of σ_c, much greater (approximately an order of magnitude) than those observed. The next step was to include the thermodynamic effect and examine the effect upon the correlation. Unfortunately, unexpected difficult with the regression analysis program arose and it was not possible to generate an equation that incorporated only a single term each for the gas content, Weber number, Reynolds number, and thermodynamic parameter in the desired fashion. Equation (12) resulted when Reynolds number terms were neglected. The results from a calculation using this equation are shown in Figure 77. Once again, although the statistics are correct, a systematic bias in the plot is apparent. In this instance, no size effects are included and so one finds a "clustering" of the data about a single predicted value. As noted above, it was impossible to produce the desired form of equation. However, when the analyses was retried, equation (13) was generated. Because the extra Weber number term is a relatively small contribution over the experimental range, a plot of the calculated values using this equation with the data was generated and this is shown in

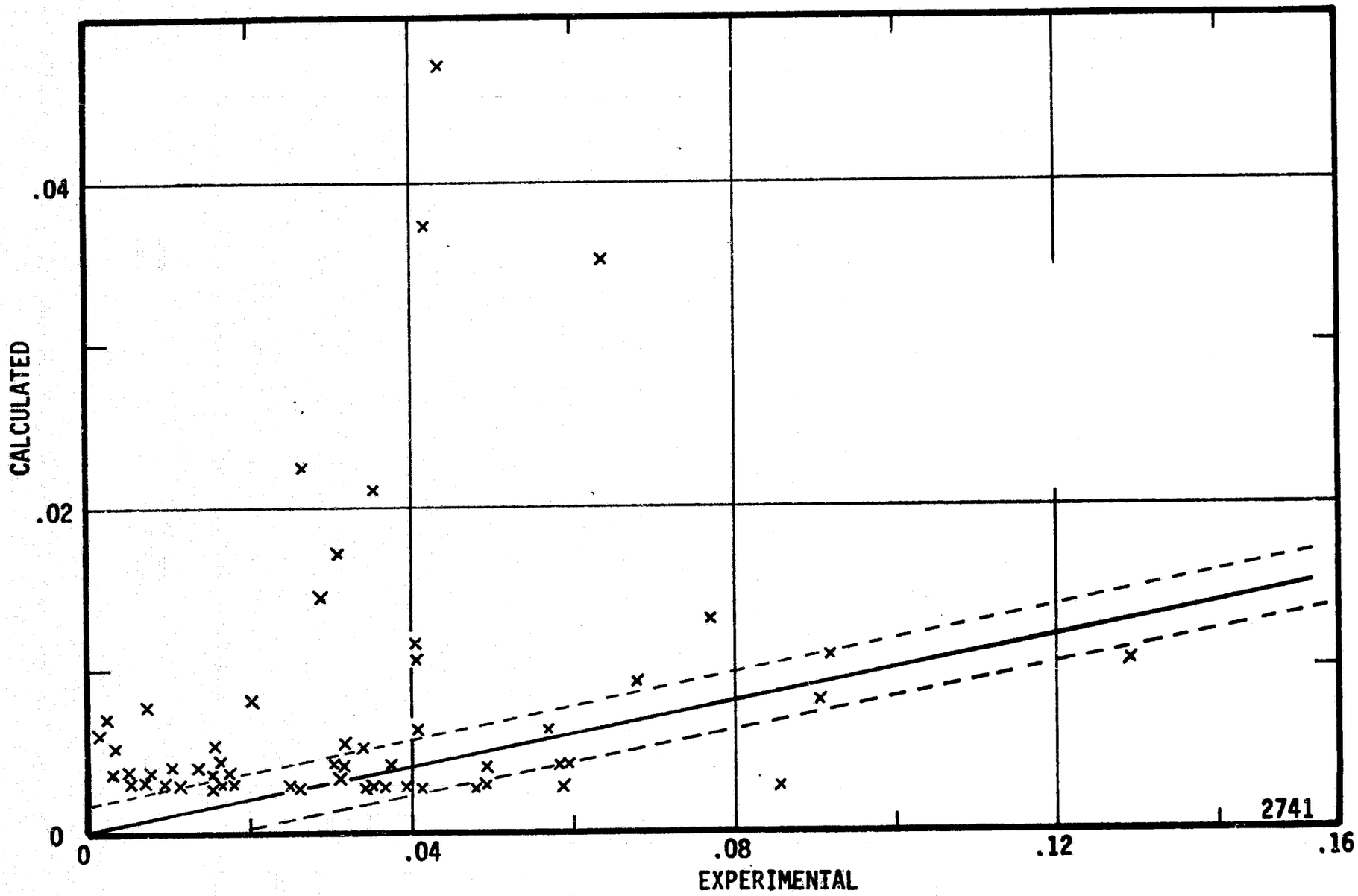

Figure 76. Calculated Cavitation Number versus Experimental Cavitation Number, All Plastic Venturis, Water, Equation 10, Part I, Table 9.

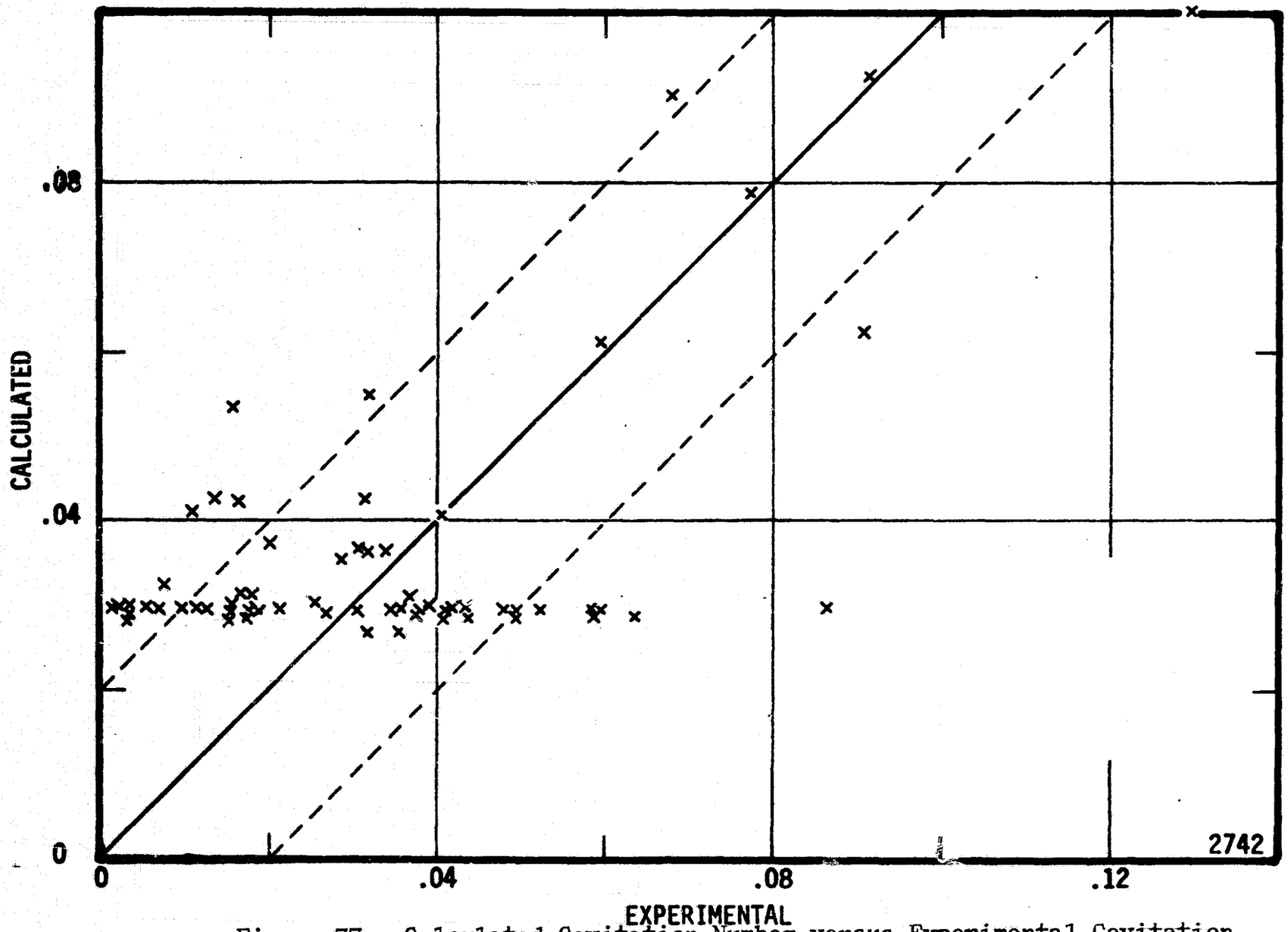

Figure 77. Calculated Cavitation Number versus Experimental Cavitation Number, All Plastic Venturis, Water, Equation 12, Part I, Table 9.

Figure 78. In this correlation of all of the water data, the cavitation number increases with gas content; decreases with temperature; and, decreases with Weber number as was observed in the one-half-inch case. However, now it is also observed that when the Reynolds number includes size effects, cavitation number increases with Reynolds number.

The correlations using cross-products were repeated using all the available data to provide a check on the results form the one-half-inch venturi trials. In Part II of Table 9 the results are presented. Equations 1 through 4 were generated using first just a first order value for each variable and then exponents that had proven successful in earlier correlation attempts. It is apparent that no unique improvement over the additive approach is afforded. Equation 5 is included because it appeared several times during these trials when the regression analysis was given access to a larger number, though not all, of the possible terms. This confirms the importance of the combined gas content and Weber number relationship.

C. Summary of Correlations, Water Cavitation

Based upon the correlations achieved and the previously presented experimental data the following statements can be made.

1. The cavitation observed here is heavily influenced by the permanent gas present. This obscures the details of any vaporous cavitation that occurs, although the cavitation number is dependent upon both. This is vased upon the fact that the air content could not be reduced below about 0.5 volume percent at STP and that the dominant term in correlating the data is a gas content parameter

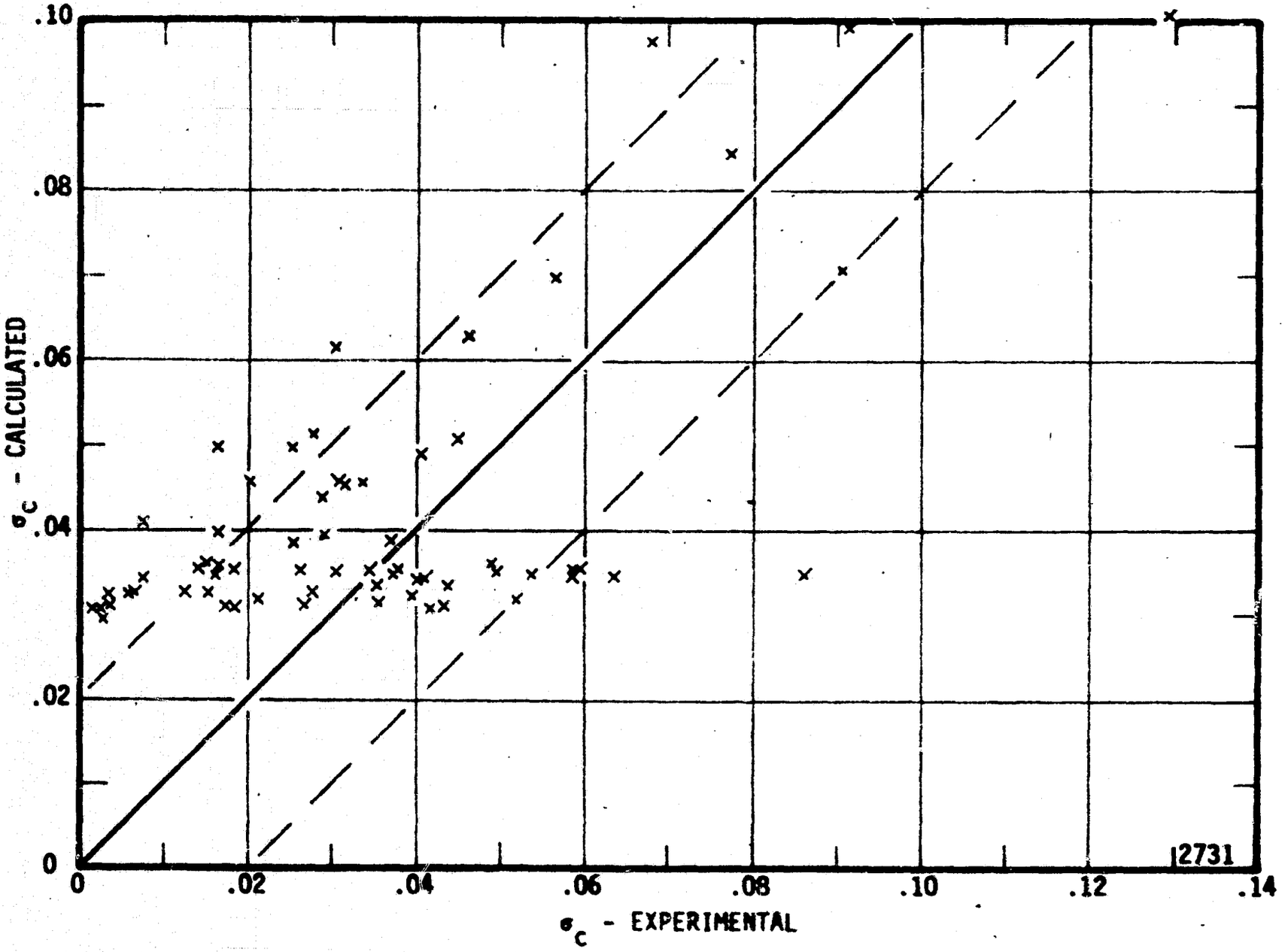

Figure 78. Calculated Cavitation Number versus Experimental Cavitation Number, All Plastic Venturis, Water, Equation 13, Part I, Table 9.

essentially modified by surface tension considerations.

2. Size effects are not controlling over the range of venturis tested. This is evidenced by the fact that the goodness of the correlation as indicated by the coefficient of determination is not changed dramatically by inclusion or deletion of the Reynolds number. However, it is clear from the improvement in the distribution of the "scatter diagrams" when the Reynolds number is included that there are significant Reynolds number influences.

3. Thermodynamic effects, although present and important, are, like size effects, not dominant. Again this is evidenced by the fact that inclusion or deletion of the thermodynamic parameter does not produce much change in the correlation statistics although the distribution is improved. Nevertheless, it is anticipated that in the absence of permanent gas, thermodynamic considerations will be important. However, the overwhelming importance of gas effects here, obscures the vaporous cavitation and any attendant thermodynamic effects.

4. Not included in analyses here are other effects that do seriously affect the cavitation. This is evidenced by our failure to achieve a complete correlation. Because the cavitation was frequently observed to occur in relatively isolated spots, it is concluded that the most likely factor not included in the analysis is surface roughness, or localized turbulence leading to severe, unmeasurable, and very localized pressure reductions that can initiate cavitation. Unfortunately, it is extremely difficult to quantify this effect and essentially impossible to scale it

geometrically across a range of venturi sizes.

D. Single Parameter Correlations, Mercury Cavitation

1. One-Half-Inch-Throat-Diameter Plastic Venturi

As was noted earlier, the one-half-inch venturi has been the baseline test system in the University of Michigan cavitation facilities so a correlation is first attempted with this data. The same "caveats" used with water must be applied here because no single variable is expected to provide a complete correlation. The analysis was simplified somewhat based on the earlier results with water by considering only the Reynolds number, the 1-mil and throat diameter Weber numbers, the thermodynamic parameter and the gas content. The results of this first set of trials is shown in Table 10. Comparing these results with those for water on Table 2 there are several parallels and several differences immediately apparent. The Reynolds number dependence is similar, although the mercury does exhibit a stronger dependency. The Weber number relationship is the same in both cases. For both water and mercury the cavitation number decreases with an increasing thermodynamic parameter but the mercury does exhibit a different form of equation. Finally, both water and mercury cavitation numbers exhibit an increase with increasing gas content, with the mercury exhibiting a much stronger dependence upon the gas content (fifth power) than does the water (first power). There is of course the difference in the two cases in that the gas in mercury is all entrained while the water has a significant portion in solution. Thus the important entrained gas portion may differ much more for a given change in total gas in

TABLE 10

REGRESSION ANALYSIS RESULTS - SINGLE PARAMETER
1/2" PLASTIC VENTURI - MERCURY CAVITATION

Standard Error of Data = .0613

	Standard Error of Estimate	Coefficient of Determination	Remarks
1. $\sigma_c = .318+2.07Re_n^{-2.0}$	.0366	.656	(1)
2. $\sigma_c = .0379+.00100We_n^{-2.0}$	.0362	.663	(2) (3)
3. $\sigma_c = .0378+.00386We_n^{-2.0}$	.0362	.663	(4) (5)
4. $\sigma_c = .0573-.00160B_n$	.0369	.650	(6)
5. $\sigma_c = .0417+16.8\beta^{5.0}$	.0245	.847	

REMARKS: (1) $Re_n = ReX10^{-5}$

(2) $We_n = WeX10^{-5}$

(3) Weber number is based upon throat diameter

(4) $We_n = WeX10^{-2}$

(5) Weber number is based upon 1 mil

(6) $B_n = BX10^{-10}$

the mercury than it does in the water tests. These factors may account for the significant differences in results. Also the mercury data include hydrogen and argon tests in addition to air tests, so that differences in interfacial tension with these gases may account for some of the otherwise unexplained scatter in results. In general however, the substantial agreement between the water and mercury results are encouraging, even though the correlations with mercury are generally not as "good" as those for water. No attempt was made to use cross-product correlations with mercury or in subsequent sections in light of the generally unsuccessful results with the water data.

2. All Venturis

The most immediate apparent conclusion from examining the results for all venturis shown in Table 11 is that single parameters are not at all effective in correlating these data. This is evidenced in the very low coefficients of determination reported. Nevertheless, some comparisons with the results for water (Table 7) are in order. The correlation with Reynolds number still indicates a decrease in cavitation number with an increase in Reynolds number, although the dependence in the case of mercury is not nearly as strong as with water; just the reverse of the observations made for the 1/2-inch venturi alone. In the case of Weber number, the water data consistently exhibited a decrease in cavitation number for an increase in Weber number as would be expected. In mercury, we find that when the 1-mil characteristic length is used, the cavitation number increases with Weber number, although when "size" effects are included, i.e.,

TABLE 11

REGRESSION ANALYSIS RESULTS - SINGLE PARAMETER
ALL VENTURIS - MERCURY CAVITATION

Standard Error of Data = .0980

	Standard Error of Estimate	Coefficient of Determination	Remarks
1. $\sigma_c = .1074-.0052Re_n$	.0770	.387	(1)
2. $\sigma_c = .0280+.000702We_n^{2.0}$	.0754	.381	(2) (3)
3. $\sigma_c = .0574-.00615We_n^{2.0}$	.0801	.311	(4) (5)
4. $\sigma_c = .0589-1.57\ X10^{-5}B_n^{-1/2}$	.0789	.323	(6)
5. $\sigma_c = .0180699+.111\beta^{1/2}$	.0793	.349	

REMARKS: (1) $Re_n = ReX10^{-5}$

(2) $We_n = WeX10^{-5}$

(3) Weber number based on throat diameter

(4) $We_n = WeX10^{-2}$

(5) Weber number based on 1 mil

(6) $B_n = BX10^{-12}$

venturi throat diameter, the reverse relationship holds. For the thermodynamic parameters, mercury again reverses the trend observed with water in that the cavitation number is increasing with B_n, which is counter to what theory predicts because B decreases with temperature. For both water and mercury the increasing value of cavitation number with increasing gas content is noted. In examining this data for mercury and comparing it with water data, several additional points need to be kept in mind. First, in water there were four different size venturis used, although all were made of plastic. In mercury only two sizes were used, 1/2-inch and 1/8-inch, but one set was plastic and the other stainless steel. In the latter the cavitation could not of course be observed visually. Second, the plastic venturis consistently evidenced damage, i.e., surface roughening, after exposure to mercury cavitation so that there is an increasing perturbation of the flow pattern and consequently conditions may not remain significantly constant throughout the test.

E. Multiple Parameter Correlation, Mercury Cavitation

The approach used with the water cavitation data was repeated in the case of mercury. That is the analysis was first attempted giving the program free rein to choose terms as it would, and then preselected terms were employed.

1. One-half-Inch-Throat-Diameter Plastic Venturi

The results of the attempts to correlate the data are shown on Table 12, Part I. Equation (1) is the predicting equation generated when no constraints (except limitations on exponent size) are applied

TABLE 12

REGRESSION ANALYSIS RESULTS - MULTIPLE PARAMETER MERCURY CAVITATION

I. 1/2" Plastic Venturi Standard Error Data = .0613

	Standard Error of Estimate	Coefficient of Determination	Remarks
1. $\sigma_c = .0400+1.02X10^{6}\beta^{2}-78.7\beta$	.026	.808	
2. $\sigma_c = .0259+6.42X10^{10}Re^{-2.0}-121We^{2.0}-.00161B_n+9.08X10^{5}\beta^{2}$	.0271	.822	
3. $\sigma_c = .0518-7.63X10^{9}Re^{-2.0}+1.00X10^{9}\beta^{2}/We^{2}-.00103B_n$	.0294	.787	

II. All Venturis Standard Error of Data = .0956

	Standard Error of Estimate	Coefficient of Determination	Remarks
1. $\sigma_c = .662+5.92X10^{5}Re^{-1.}+2.43X10^{-7}Re-2.46X10^{-4}B_n^{2}-3.74X10^{-5}B_n^{-1/2}+3.24X10^{5}\beta^{2}-1220X10^{11}Re^{-2.0}$	.0640	.562	
2. $\sigma_c = .0530-4.86X10Re^{-8}+1.69X10^{-6}We^{2.0}-1.16X10^{-5}B_n^{-1/2}+4.05\beta^{1/2}$	.0729	.428	
3. $\sigma_c = .278-3.71X10^{-4}B+4.45X10^{9}Re^{-2.0}+3.51X10^{5}X\beta^{2}$	.0761	.376	
4. $\sigma_c = .0849-5.61X10^{-8}Re-9.39X10^{-6}B^{-1/2}+4.42X10^{5}\beta^{2}+2.04X10^{-6}We^{2}$	.0725	.434	

TABLE 12 (Con't)

	Standard Error of Estimate	Coefficient of Determination	Remarks
5. $\sigma_c = .0102-1.85X10^{3}\beta/We^{2.0}-4.42X10^{-6}B^{-1/2}-4.67X10^{-8}Re$	.0758	.379	
6. $\sigma_c = .0102-4.66X10^{-8}Re-1.11X10^{7}\beta^{2}/We^{2}-4.35X10^{-6}B_n^{-1/2}$	.0759	.378	

to the analyses. Comparing these results with those for water (Table 8, it may be noted that no parameters other than gas content have been inserted in the mercury case; while in the case of water, other parameters were included. Because a single parameter does not seem sufficient to interpret the data, two additional trials were attempted. Equation (2) results when the forms of the variables indicated by the single variable trials are inserted. The correlation is improved over the unconstrained trial, although the effects of Weber number and thermodynamic parameter are in the opposite direction to those for water. In these trials, because the values of the exponents were limited, the Reynolds number and Weber number were used as calculated without any reduction in magnitude to allow for machine limitations. This condition is maintained throughout the balance of the analysis. However, the thermodynamic parameter continued to be used in a reduced or normalized manner. When a β/We relationship is attempted (Equation (3)), the correlation is not as complete, although the cavitation number is decreasing with increasing B as theory requires, but this trend is counter to those in the water test. In order to graphically portray the results from these latter two equations, "scatter" diagrams were plotted and are shown as Figure 79 and 80. In both instances, the distribution is reasonably uniform, however, there is a severe clustering of the data because a sufficiently wide variation in velocity, temperature, and gas content was not achievable in this venturi.

2. All Venturis

Once again the analysis was started by allowing the program

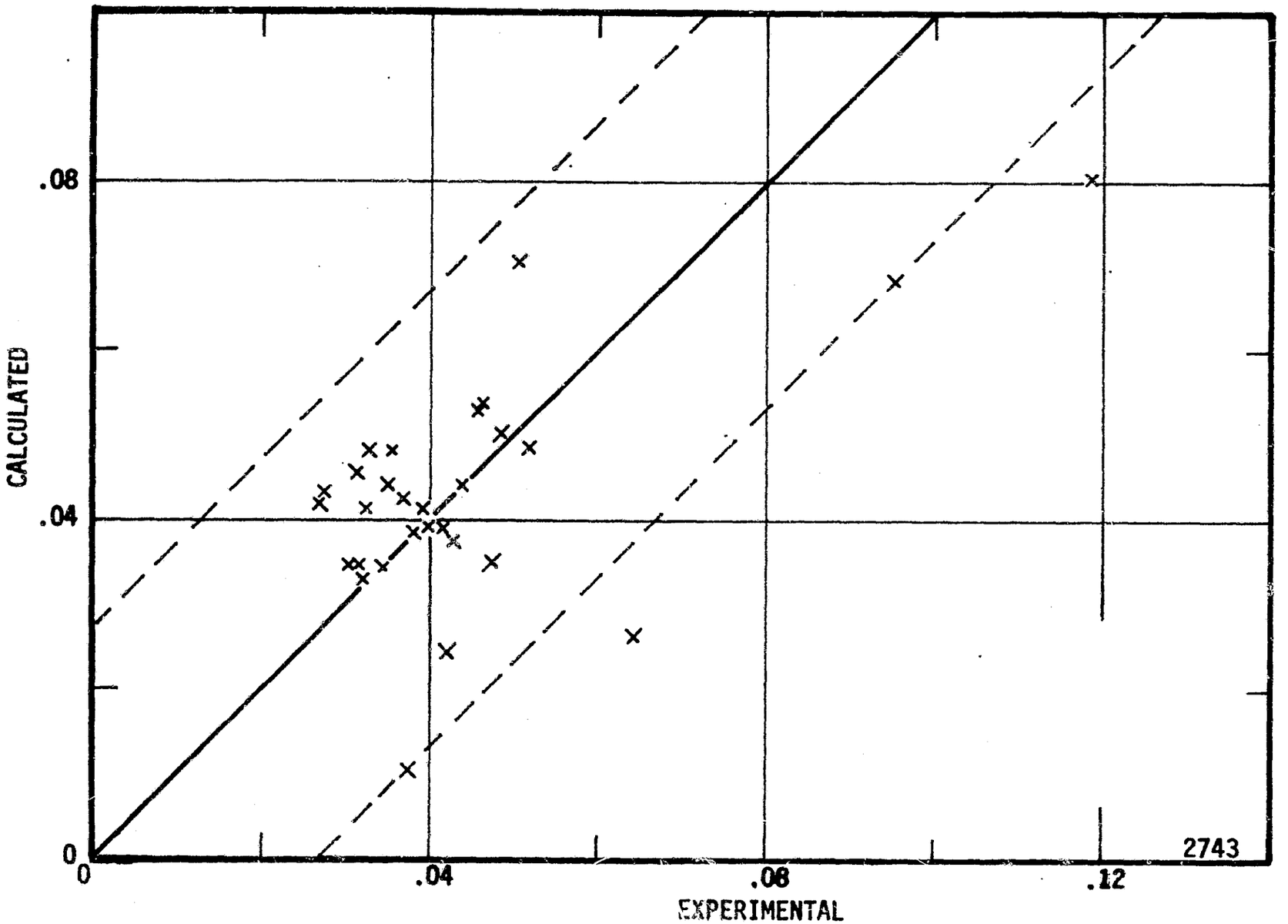

Figure 79. Calculated Cavitation Number versus Experimental Cavitation Number, Venturi 412, Mercury, Equation 2, Part I, Table 12.

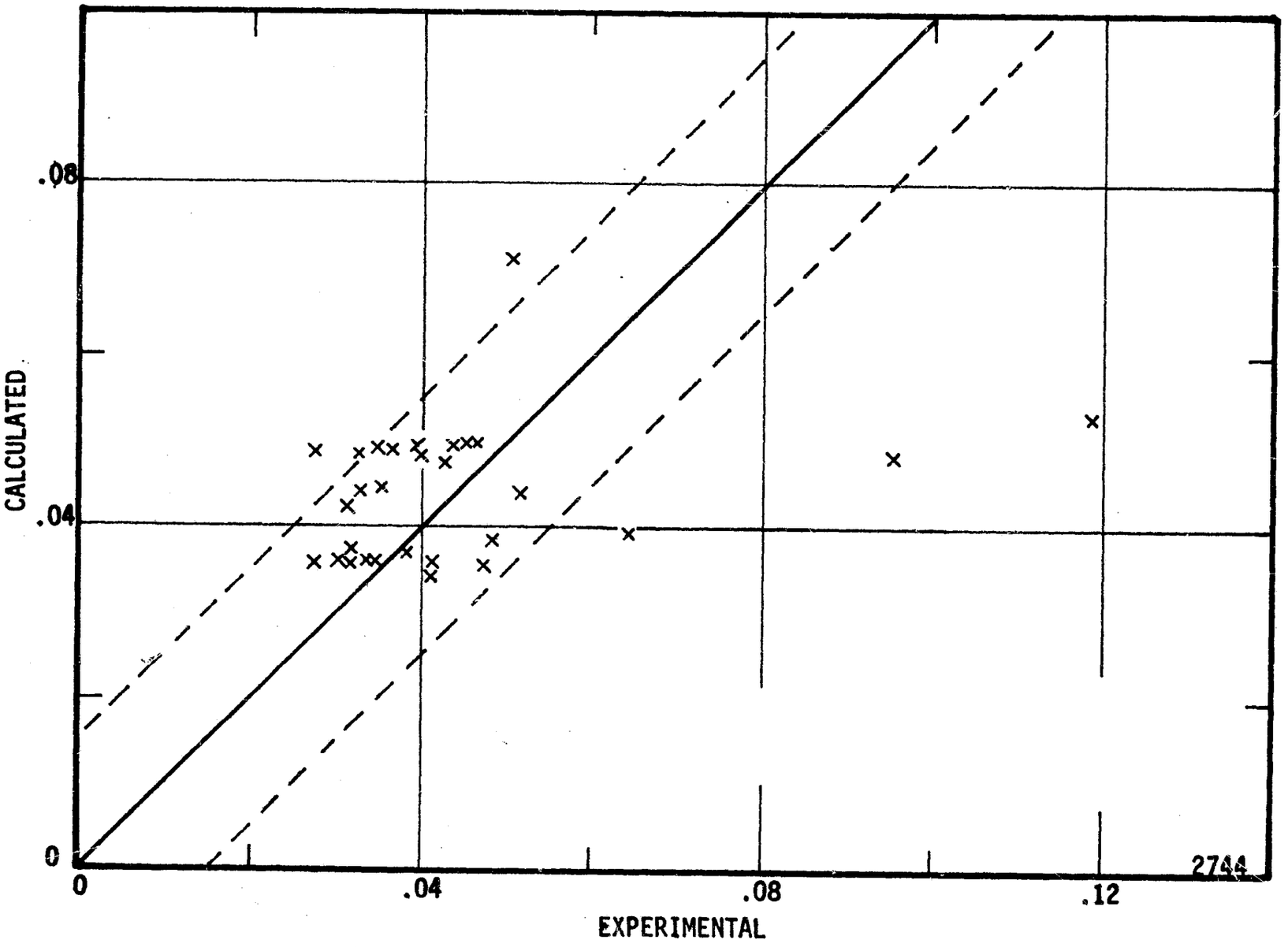

Figure 80. Calculated Cavitation Number versus Experimental Cavitation Number, Venturi 412, Mercury, Equation 3, Part I, Table 12.

free rein on terms selected. For this multiple venturi case, the results are presented in Table 12, Part II. In general the results continue to exhibit a poorer correlation than the water data. The inclusion of several terms of a single parameter, as in Equation (1), is typical when no constraints are applied. Equation (2) was generated by again using the forms from the single term analysis and we find a degradation in the correlation. Several other combinations were attempted and are presented for comparison. None were very successful in providing improvement to the correlation. Equation (4) used the single parameter results modified by the knowledge that in Equation (1) a Reynolds number first order term was the most significant. A "scatter" diagram for Equation (4) not included here indicated a clustering of the plotted values and again the equation does not adequately explain the data.

F. Summary of Correlations, Mercury Cavitation

The conclusions for the mercury correlations are nearly self evident, but they may be stated as follows:

1. As was the case with water, the gas content is the variable or parameter of predominant importance, and therefore some effects, such as the temperature related thermodynamic effects are masked.

2. Since the water data from several different venturis did correlate reasonably well as compared with the mercury data, it must be assumed that the cavitation in the stainless steel and plastic venturis is different, even though the designs have the same geometry. For instance, this could be the result of different degrees of cavita-

tion being compared due to the different methods of or variations in surface roughness.

G. Multiple Parameter Correlations, Water and Mercury Cavitation

In spite of the generally unsatisfactory correlations obtained with the mercury data, a general correlation of all the data for both fluids together was attempted. The results are shown in Table 13. For the base line case of the 1/2-inch plastic venturi, a fairly good correlation is achieved using Reynolds number, Weber number, gas content, and the thermodynamic parameter. The "scatter" diagram (Figure 81) indicates a good distribution of the data, considering the limitation on the number and range of experimental data points. This correlation is encouraging because of the large differences in properties of the two fluids and the extreme difference in the way the gas appears (that is, mostly dissolved in water, mostly entrained in mercury). On the other hand, it must be noted that no size effects are included. Unfortunately, the very promising results from the base line case are not substantiated when all the data is treated. Equation (1) (Part II of Table 13) results when the analysis is run with no constraints, and the balance of the equations when various options were considered. No scatter diagram was attempted with this data because the correlations were generally inconclusive.

TABLE 13

REGRESSION ANALYSIS RESULTS - MULTIPLE PARAMETERS
WATER AND MERCURY CAVITATION

I. 1/2" Plastic Venturi Standard Error of Data = .0613

	Standard Error of Estimate	Coefficient of Determination	Remarks
1. $\sigma_c = .0404 - 3.62X10^{-10}B^{-1.} + 34.8We^{-2.0} + .22^2$	.0279	.801	
2. $\sigma_c = .0377 + 7.18X10^{8}Re^{-2.0} + 38.5We^{-2.0} - 2.66X10^{-10}B^{-1} + .181^2$	.0279	.805	

II. All Venturis Standard Error of Data = .0829

1. $\sigma_c = .101 - 1.23X10^{-4}\beta^{-1/2} - .291\beta^{1/2} - 1.75X10^{-4}B_n^{2.0} + .319\beta - 1.96X10^{-14}Re^2$	.0642	.409	
2. $\sigma_c = .0825 - 1.92X10^{-14}Re^{2.0} - 1.14X10^{-8}We - 1.75X10^{-3}B_n - .065\beta^{1/2}$	.0654	.384	
3. $\sigma_c = .0484 - 8.802X10^{7}Re^{-2.0} - .095We^{-2.0} - 8.42X10^{-11}B_n^{-1} + .0347\beta^2$	.0681	.333	
4. $\sigma_c = .0412 - 9.15X10^{-15}Re^2 + 1352\beta^2/We^2 - .0138B_n + .049B_n^{1/2}$	.0644	.408	

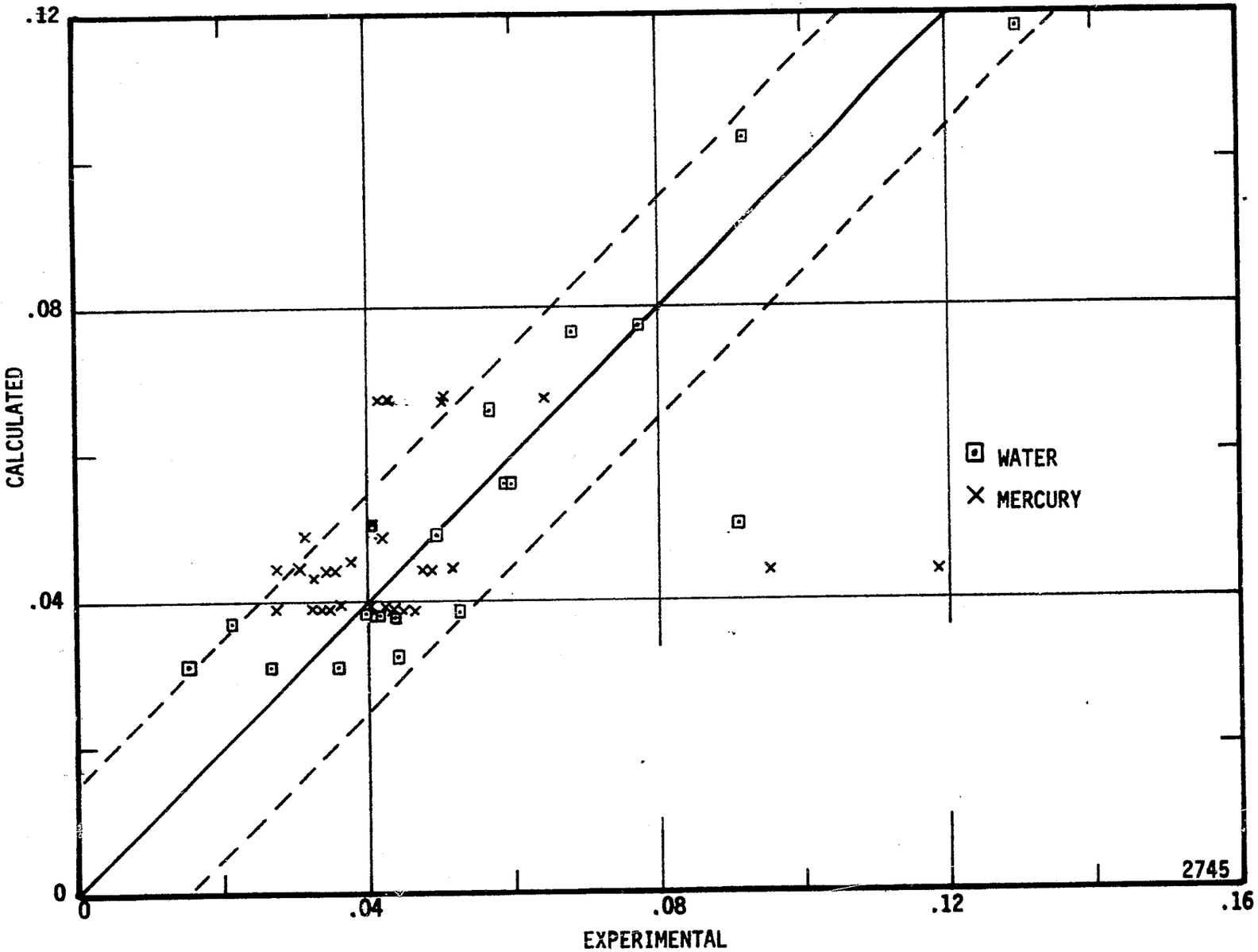

Figure 81. Calculated Cavitation Number versus Experimental Cavitation Number, Water and Mercury, Equation 3, Part I, Table 13.

REFERENCES

1. Euler, Leonhard, "Theorie Plus Complete des Machines, qui sont mises en Mouvement Par La Reaction de l'eau," Historic de l' - Academic Royale des Sciences et Belles Lettres, Classe de Philosophic Experimentale, pp 227 - 295, Mem 10, 1754, Berline, 1756.

2. Thornycroft, Sir John, and Barnaby, S.W., "Torpedo-boat Destroyers," Proc. Inst. Civ. Eng., 122, (1895) 51 - 103.

3. Reynolds, Osborne, "Experiments Showing the Boiling of Water in an Open Tube at Ordinary Temperatures," Scientific Papers, 2, (1901) 578 - 587.

4. Besant, W., A Treatise on Hydrodynamics, Cambridge University Press, Cambridge, (1895), Dover Reprint

5. Lord Rayleigh, "On the Pressure Developed in a Liquid During the Collapse of a Spherical Cavity," Phil. Mag., 34, (1917) 94 - 98.

6. Hammitt, F.G., "Observations of Cavitation Damage in a Flowing System," ASME, J. Basic Engr, 85, (Sept 1963) 347 - 359.

7. Robinson, M. John, "On the Detailed Flow Structure and the Corresponding Damage to Test Specimens in a Cavitating Venturi," PhD. Thesis, Department of Nuclear Engineering, University of Michigan, 1965.

8. Kelly, R.W., et al., "Rotating Disc Approach for Cavitation Damage Studies in High Temperature Liquid Metal," ASME Paper No. 63 - AHGT - 26.

9. Holl, J. William, and Wislicenus, George F., "Scale Effects on Cavitation," ASME, J. Basic Engr., Series D, 83, (Sept 1961) 385 - 398.

10. Hammitt, F.G., "Observations of Cavitation Scale and Thermodynamic Effects in Stationary and Rotating Components, " Trans ASME, J. Basic Engr. (March 1963) 1 - 16.

11. Oshima, R., "Theory of Scale Effects on Cavitation Inception on Axially Symmetric Bodies," ASME J. Basic Engr., Series D, 83, (Sept 1961) 379 - 384.

12. Jekat, W. "A New Approach to Reduction of Pump Cavitation - Hubless Inducer," Trans ASME J. Basic Engr., 89, (March 1967) 137 - 139.

13. Kermeen, R.W., et al., "Mechanism of Cavitation Inception and the Related Scale Effects Problem., Trans ASME J. Basic Engr., 77 (1955) 533 - 541.

14. Holl, J.W., "An Effect of Air Content on the Occurrence of Cavitation," Trans ASME J. Basic Engr. Paper No. 69-Hyd-8, 1960.

15. Ripken, J.R., and Killen, J.M., "Gas Bubbles: Their Occurrence, Measurement, and Influence on Cavitation Testing," Proceedings of IAHR Symposium, Sendal, Japan, 1962.

16. Holl, J.W., "The Inception of Cavitation on Isolated Surface Irregularities," Trans ASME J. Basic Engr., 82, (1960) 169 - 183.

17. Gavrilenko, T.P., and Topchryan, M. Ye, "Investigation of the Dynamic Rupture Strength of Water," Zhurnal prekladnoy mekhaniki i lekhnickeskoy fiziki, 4 (1966) 172 - 174.

18. Fisher, John C., "The Fracture of Liquids," Jour. Applied Physics, 19 (1948) 1062 - 1067.

19. Ruggeri, R.S., and Gelder, T.F., Effects of Air Content and Water Purity on Liquid Tension at Incipient Cavitation in Venturi Flow, NASA TN D-1459, March 1963.

20. Lehman, A.F. and Young, J.O., "Experimental Investigation of Incepreent and Desinent Cavitation," Trans ASME Jr. Basic Engr., Page No. 63-AHGT-20, December 1962.

21. Kermeen, R.W., and Parkin, B.R., Incipient Cavitation and Wake Flow Behind Sharp-Edged Desks, Report 85-4, Hydrodynamics Labroatory, California Institute of Technology, August 1957.

22. Frenkel, J., Kinetic Theory of Liquids, The Clarendon Press, Oxford, 1946, Dover Press 1955.

23. Stahl, H.A., and Stepanoff, A.J., "Thermodynamic Aspects of Cavitation in Centrifugal Pumps," Trans ASME, J. Basic Engr., 78, (1956) 1691 - 1693.

24. Hammitt, F.G., "Liquid Metal Cavitation - Problems and Desired Research," Trans ASME, J. Basic Engr., Paper No. 69-HYD-13, 1960.

25. Wislicenus, G.F., Fluid Mechanics of Turbomachinery, Dover Press 1965.

26. Streeter, V.L., Fluid Mechanics, Chapter 5, McGraw-Hill, 1958.

27. Rouse, H., and McNown, J.S., Cavitation and Pressure Distribution-Head Forms at Zero Angle of Yaw, Bulletin 32, University of Iowa, 1948.

28. Parkin, B.R., and Holl, J.W., Incipient - Cavitation Scaling Experiments for Hemispherical and 1.5 Caliber Ogive - Nosed Bodies, Report NOrd 7958-264, Ordnance Research Laboratory, The Pennsylvania State University, May 1954.

29. Parkin, B.R., Scale Effects in Cavitation Flow, PhD. Thesis, California Institute of Technology, 1952.

30. Calehuff, G.L., and Wislicenus, G.F., ORI Investigations of Scale Effects on Hydrofoil Cavitation, TM 19.4212-03, Ordnance Research Laboratory, the Pennsylvania State University, February 1956.

31. Plesset, M.S., "The Dynamics of Cavitation Bubbles," Trans ASME, J. Appl Mech, (Sept 1949) 277 - 282.

32. Harvey, E.N., et al., "On Cavity Formation in Water," Journal of Applied Physics, 18, (1947) 162.

33. Olson, R.M., Cavitation Testing in Water Tunnels, St Anthony Falls Hydraulic Laboratory, University ofMinnesota, Project Report No. 42, (Dec 1954).

34. Ripken, J.F. and Olson, R.M., A Study of the Influence of Gas on Cavitation Scale Effects in Water-Tunnel Tests, St Anthony Falls Hydraulic Laboratory, University of Minnesota, Project Report No. 58, (Feb 1968).

35. Narayanan, R., "The Effect of Air Injection on the Cavitation Limits of the Centrifugal Pump," Paper at the First Asian Conference at Bangalore, May 1963.

36. Silverleaf, A., and Berry, L.W., "Propeller Cavitation as Influenced by the Air Content of the Water," Proceedings of IAHR-Symposium, Sendai, Japan, 1962.

37. Hammitt, F.G., Lafferty, J.F., Ericson, D.M., and Robinson, M.J., "Gas Content, Size, Temperature and Velocity Effects on Cavitation Inception in a Venturi," ASME Paper 67-WA/FE-22, Nov 1967.

38. Karplus, H.B., "The Velocity of Sound in a Liquid Containing Gas Bubbles," Armour Research Foundation Report COO-248, June 1958.

39. Hammitt, F.G., Robinson, M.J., and Lafferty, J.F., "Choked-Flow Analogy for Very Low Quality Two-Phase Flows," Nuc. Sci and Engr., 29, No. 1 July 1967.

40. Garcia, R., and Hammitt, F.G., "Cavitation Damage and Correlations with Material and Fluid Properties," Trans ASME, J. Basic Engr, D, 89, 4, 753 - 763, 1967.

41. Holl, J.W., and Treaster, A.L., "Cavitation Hysteresis," Trans ASME, J. Basic Engr., 88, No. 1 (March 1966).

42. Van Wyngaarden, L., "On the Growth of Small Cavitation Bubbles by convective Diffusion," I. J. Heat and Mass Transfer, 10, (1967), 127 - 134.

43. Stepanoff, A.J., "Cavitation in Centrifugal Pumps with Liquids Other than Water," Trans ASME Jr. Basic Engr., 83, (1961) 79 - 90.

44. Saleman, V., "Cavitation and NPSH Requirements of Various Liquids," Trans ASME, Jr. Basic Engr., 81, No. 2, (1959) 167 - 180.

45. Florschuetz, L.W., and Chas, B.T., On the Mechanics of Vapor Bubble Collapse - A Theoretical and Experimental Investigation, Report ME-TN-1069-2, Department of Mechanical and Industrial Engineering, The University of Illinois, Urbana, Illinois, Oct 1963 (Also, ASME Paper 64-HT-23, Aug 1964).

46. Hammitt, F.G., "Cavitation Damage and Performance Research Facilities," Sym. on Cavit. Resch Facilities and Techniques, ASME, May 1964, pp 175 - 184.

47. Hammitt, F.G., et al., Feasibility Investigation of Cavitation Number Measurements in Mercury and Water with Gas Injection, U-M OAR Report 06110-2-T, July 1964.

48. Peters and Van Slyke, "Quantitative Clinical Chemistry," Volume II, Williams and Wilkins.

49. Killen, J.M., and Ripken, J.F., A Water Tunnel Air Content Meter, St Anthony Falls Hydraulic Laboratory, University of Minnesota, Project Report No. 70, Feb 1964.

50. Knapp, R.T., "Cavitation and Nuclei," Trans ASME, 80, No. 6, (Aug 1958) 1315.

51. Gelder, T.F., Moore, R.D., and Ruggeri, R.S., Incipient Cavitation of Freon - 114 in a Tunnel Venturi, NASA TN-D-2662, Lewis Research Center, Feb 1965.

52. Gelder, T.F., Moore, R.D., and Ruggeri, R.S., Incipient Cavitation of Ethylene Glycol in a Tunnel Venturi, NASA TN-D-2722, Lewis Research Center, March 1965.

53. Gelder, T.F., Moore, R.D., and Ruggeri, R.S., Effects of Wall Pressure Distribution and Liquid Temperature on Incipient Cavitation of Freon - 114 and Water in Venturi Flow, NASA TN-D-4340, Lewis Research Center, Jan 1968.

54. Westervelt, F.H., Automatic System Simulation Programming, PhD Thesis, University of Michigan, November 1969.

55. Crandall, R.L., The Mathematical and Logical Procedure of the Stepwise Regression Program with Learning, Internal Memo, UM Computer Center, 1965.

56. Hammitt, F.G., et al, Measuring Instrument for High Vapor-Pressure Component Content, Record of Invention, UM Office of Research Administration, 1964.

57. Hodgeman, C.D., et al, Handbook of Chemistry and Physics, 44th Edition, Chemical Rubber Publishing Co., Cleveland, Ohio, 1967.

58. Lyon, R.N. Ed., Liquid Metals Handbook, Second Edition, 1962.

59. Weatherford, W.D., Jr., et al, Properties of Inorganic Energy-Conversion and Heat Transfer Fluids for Space Applications, WADD TR 61-96, November 1961.

60. Handbook of Heat Transfer Media

61. Ivany, R.D., Collapse of a Cavitation Bubble in Viscous, Compressible Liquid - Numerical and Experimental Analyses, PhD Dissertation, University of Michigan, 1965. (Also, Ivany, R.D., and Hammitt, F.G., J. Basic Engr., Dec 1965, pp 977 - 985.)

62. Plesset, M.S., Bubble Dynamics, Division of Engineering and Applied Science, Californis Institute of Technology, Report No. 85 - 23 Feb 1963.

63. Van der Walle, F., "On the Growth of Nuclear and the Related Scaling Factors in Cavitation Inception," International Shipbuilding Progress, Vol 10, 106 (1963) 195 - 204.

64. Seidel, G.S., An Investigation of Thermodynamic Effects on Cavitation in Water from 80°F to 180°F on Hemispherical - Nosed Bodies, M.S. Thesis, Department of Aeronautical Engr., Pennsylvania State University, June 1966.

65. Korhauser, A.L., Thermodynamic Effects on Desinent Cavitation in Water, MS Thesis, Department of Aeronautical Engineering, Pennsylvanis State University, June 1967.

SELECTED BIBLIOGRAPHY

1. Arndt, R.E. and Ippen, A.T., "Rough Surface Effects on Cavitation Inception," Trans ASME, J. Basic Engr, Paper 68-FE-6, 1968.

2. Birkhoff, G. and Zarantonello, E.H., Jets, Wakes and Cavities, Academic Press, New York, 1957.

3. Brand, R.S., The Shock Wave Produced by Collapse of a Shperical Cavity, University of Cincinnati, School of Engr, Technical Report No 1, June 1962.

4. Dean, R.B., "The Formation of Bubbles," Journ of App Phys, 15:5, May 1944, pp 446-451.

5. Fox, F.E. and Herzfeld, K.F., "Gas Bubbles with Organic Skin as Cavitation Nuclei," J. of the Acoustical Society of America, 26:6, Nov 1954.

6. Gelder, T.F., et al, Cavitation Similarity Considerations Based on Measured Pressure and Temperature Depressions in Cavitated Regions of Freon 114, NASA TN-D-3509, July 1966.

7. Jakobsen, J.K., "On the Mechanism of Head Breakdown in Cavitating Inducers," Trans of the ASME, J of Basic Engr, Paper 63-AHGT-29, 1963.

8. Holl, J.W., et al, "On Several Laws of Cavitation Scaling," La Houille Blanche, No 4, September 1957.

9. Lecher, W., "Another 15 Years of Applied Research on Turbomachines," Escher Wyss News, Vol 33, 1960.

10. Lienhard, J.H., A Study of the Dynamic and Thermodynamics of Liquid-Gas-Vapor Bubbles, Div of Ind Rsch, Wash State Univ, Bulletin No. 266.

11. Numachi, F., Editor, Cavitation and Hydraulic Machinery, Proc of IAHR Symposium, Sendai, Japan 1962.

12. Moore, R.D., and Ruggeri, R.S., Venturi Scaling Studies on Thermodynamic Effects of Developed Cavitation in Freon 114, NASA TN D-4387, Feb 1968.